

THE RADIATION TOLERANCE OF *IGNICOCCUS* SPECIES

THEIR ASTROBIOLOGICAL RELEVANCE
AND IMPLICATIONS TO DNA REPAIR PROCESSES



DISSERTATION

ZUR ERLANGUNG DES DOKTORGRADES
DER NATURWISSENSCHAFTEN (DR. RER. NAT.)
DER FAKULTÄT FÜR BIOLOGIE UND VORKLINISCHE MEDIZIN

DER UNIVERSITÄT REGENSBURG

VORGELEGT VON

DAGMAR KOSCHNITZKI

AUS DORMAGEN

IM JAHR 2016

Das Promotionsgesuch wurde eingereicht am

- **29.06.2016**

Die Arbeit wurde angeleitet von

- **Prof. Dr. Reinhard Wirth** (Universität Regensburg)

in Zusammenarbeit mit

- **Dr. Petra Rettberg** (Deutsches Zentrum für Luft- und Raumfahrt in Köln).

Prüfungsausschuss:

Vorsitzender: **Prof. Dr. Björn Brembs**

1. Gutachter: **Prof. Dr. Reinhard Wirth**

2. Gutachter: **PD Dr. Ruth Hemmersbach**

3. Prüfer: **Prof. Dr. Reinhard Rachel**

—Für Vadda—

“We will now discuss in a little more detail the Struggle for Existence!”

—Charles Darwin—

Table of Contents

Table of Contents	I
List of Figures	V
List of Tables	VII
Abbreviations	VIII
Abstract	X
Zusammenfassung	XII

1 Introduction 1

1.1	Life on early Earth	1
1.1.1	Environmental conditions on early Earth	1
1.1.2	Radiation levels on early Earth	3
1.1.3	Where LUCA may have felt at home	4
1.1.4	LUCA's potential mode of life	5
1.1.5	LUCA's descendants	6
1.2	Hydrothermal vents	9
1.3	The genus <i>Ignicoccus</i>	10
1.3.1	<i>Ignicoccus islandicus</i> and <i>Ignicoccus pacificus</i>	10
1.3.2	<i>Ignicoccus hospitalis</i>	11
1.3.3	" <i>Ignicoccus morulus</i> "	13
1.3.4	Tolerance of (hyper-) thermophilic archaea to radiation	14
1.4	Radiation and its effects	14
1.4.1	Non-ionizing radiation	14
1.4.2	Ionizing radiation	16
1.4.3	Effects on biological systems	16
1.4.4	Effects on DNA	17
1.5	DNA repair pathways in Archaea	18
1.6	Aim of this work	19

2 Material and Methods 21

2.1	Sources of supply	21
2.1.1	Chemicals	21
2.1.2	Standards	22
2.1.3	PCR reagents and cDNA synthesis	22
2.1.4	Oligonucleotides	23
2.1.4.1	RAPD primer	23
2.1.4.2	qRT-PCR primers for gene expression and qPCR primers for DNA damage detection after ⁶⁰ Co radiation exposure	23
2.1.5	Buffers	26
2.1.6	Gas mixtures	26
2.2	Strains and cultivation	26

2.2.1	Strains	26
2.2.2	Media	27
2.2.2.1	SME medium (Synthetisches Meerwasser/synthetic sea water)	27
2.2.2.2	½ SME+S ⁰ medium for all <i>Ignicoccus</i> representatives	27
2.2.3	Cultivation	29
2.2.3.1	Stock cultures	29
2.2.3.2	Anaerobic cultivation	29
2.2.3.3	Phase contrast microscopy of cultures	29
2.3	Determination of viable (culturable) and total cell numbers	30
2.3.1	Total cell number	30
2.3.2	Most probable number (MPN) technique to determine growth and reproduction	30
2.3.3	Detection of metabolic activity by detecting metabolically produced hydrogen sulfide (H ₂ S)	30
2.3.4	Determination of survival after stress exposure	31
2.4	Exposure to radiation	31
2.4.1	Non-ionizing radiation	31
2.4.1.1	UV-C source and determination of fluence rates	31
2.4.1.2	Measuring the absorption of medium	32
2.4.1.3	UV-C irradiation in liquid suspension	32
2.4.1.4	DNA damage repair by photoreactivation	33
2.4.2	Ionizing radiation	35
2.4.2.1	Heavy ions	35
2.4.2.2	X-ray source and determination of dose rates	36
2.4.2.3	X-ray irradiation in liquid suspension	37
2.4.2.4	Hot exposure	38
2.4.2.5	The impact of cultivation temperature on X-ray tolerance	39
2.4.2.6	Sample preparation for gene expression studies after X-ray exposure (qRT-PCR)	39
2.4.2.7	Gamma ray (⁶⁰ Co radiation) source and dosimetry for Death by Radiation (DbR #1, #2, #3)	41
2.4.2.8	⁶⁰ Co irradiation in liquid suspension	41
2.4.2.9	⁶⁰ Co irradiation of single ½ SME medium components	43
2.4.2.10	Exposure of sulfur	44
2.4.2.11	Quorum sensing	44
2.5	Molecular biological methods	45
2.5.1	Extraction of genomic DNA	45
2.5.1.1	Qubit® Fluorometric Quantitation of double stranded DNA for RAPD assays	46
2.5.1.2	Agarose gel electrophoresis to determine the quality of extracted genomic DNA	47
2.5.1.3	Agarose gel electrophoresis for RAPD band pattern analyses	47
2.5.2	RNA extraction for qRT-PCR	47
2.5.2.1	Determination of total RNA concentrations using NanoDrop™	48
2.5.2.2	Agarose gel electrophoresis to determine RNA quality	49
2.5.3	First strand cDNA synthesis for qRT-PCR	49
2.5.3.1	Removal of genomic DNA from RNA preparations	49
2.5.3.2	First strand cDNA synthesis	49
2.5.4	Analytical methods	50
2.5.4.1	RAPD (randomly amplified polymorphic DNA) to determine genomic DNA integrity	50
2.5.4.2	qPCR (quantitative real-time PCR) to detect relative amounts of DNA lesions	51
2.5.5	DNA repair	52

2.5.5.1	RAPD for DNA repair determination after 12.6 kGy exposure	52
2.5.5.2	Determination of gray-levels	53
2.5.6	Gene expression by qRT-PCR (quantitative Reverse Transcription-PCR)	53
2.5.6.1	Absolute C _t value and molecule number	54
3	Results	56
3.1	Non-ionizing radiation (UV-C)	56
3.1.1	Measuring the absorption of the medium	56
3.1.2	Survival of <i>Ignicoccus</i> (0-300 J/m ²)	57
3.1.3	Survival of <i>Ignicoccus</i> (0-3000 J/m ²)	58
3.1.4	UV-C leveling	59
3.1.5	Extraction of genomic DNA	59
3.1.6	Relative amount of DNA lesions, and genomic DNA integrity after UV-C exposure of <i>I. hospitalis</i>	60
3.2	Ionizing radiation	62
3.2.1	Heavy ions	62
3.2.2	Electromagnetic radiation	64
3.2.2.1	⁶⁰ Co irradiation in liquid suspension	64
3.2.2.2	Survival of <i>I. hospitalis</i> and " <i>I. morulus</i> " after ⁶⁰ Co radiation exposure	64
3.2.2.3	Comparing the impact of ⁶⁰ Co radiation exposed ½ SME+S ⁰ medium to <i>I. hospitalis</i> stationary phase cells which were serial diluted prior to exposure	71
3.2.2.4	⁶⁰ Co radiation exposure of elemental sulfur (dry and wet)	72
3.2.2.5	⁶⁰ Co irradiation of single ½ SME medium components	73
3.2.2.6	Quorum sensing	75
3.2.2.7	DNA integrity after gamma ray (⁶⁰ Co radiation) exposure	77
3.2.2.8	X-ray exposure of <i>I. hospitalis</i> with and without soft X-rays	80
3.2.2.9	Survival of <i>I. hospitalis</i> after X-ray exposure	81
3.2.2.10	Influence of the cultivation temperature on X-ray tolerance	81
3.2.2.11	Hot exposure	82
3.2.2.12	DNA integrity after X-ray exposure	83
3.3	DNA repair	84
3.3.1	DNA repair of <i>I. hospitalis</i> after X-ray exposure	84
3.3.2	RNA extraction for qRT-PCR	85
3.3.3	Gene expression studies by qRT-PCR	86
3.3.3.1	Test of experimental setup	86
3.3.3.2	RNA transcription levels of potential housekeeping genes tested under various experimental conditions	87
3.3.3.3	RNA transcription levels of DNA damage repair genes tested under various experimental conditions	89
3.3.3.4	Determination of molecule numbers of putative DNA damage repair genes	91
3.3.3.5	RNA transcription levels of genes involved in DNA replication	92
3.3.3.6	DNA damage repair by photoreactivation	93
4	Discussion	96
4.1	Non-ionizing radiation	96
4.2	Ionizing radiation tolerance	100

4.3	DNA integrity and DNA repair of <i>I. hospitalis</i> after ionizing radiation exposure	109
5	Conclusion and Outlook	114
6	References	122
7	Appendix	136
	Primer design	136
	Metabolic activity of " <i>I. morulus</i> " after ^{60}Co radiation exposure	152
	^{60}Co irradiation of single $\frac{1}{2}$ SME medium compounds	153
	Certified dosimetry data for DbR #1, #2, #3	154
	Acknowledgement	158

List of Figures

Introduction

Figure 1: Schematic representation of environmental conditions present on early Earth.....	3
Figure 2: Phylogenetic tree based on 16S rRNA sequence comparisons.	7
Figure 3: Main energy-yielding reactions used by chemolithoautotrophic hyperthermophiles.	8
Figure 4: Black smoker.....	10
Figure 5: Transmission electron micrograph from <i>I. hospitalis</i> and <i>N. equitans</i> (ultrathin sections).	11
Figure 6: <i>Ignicoccus</i> and the mode of life.	12
Figure 7: Ultrathin section from an <i>I. hospitalis</i> cell shown as transmission electron micrograph.	13
Figure 8: Solar radiation spectrum reaching Earth's surface compared to the action spectrum predominating on early Earth.	15
Figure 9: Schematic representation of ionizations caused by radiation with low, or high LET	16
Figure 10: Damages on cellular level caused by ionizing radiation following direct or indirect interactions	17
Figure 11: Different types of DNA damages caused by either radiation or chemical agents.	18

Material and Methods

Figure 12: Exemplaric illustration of $\frac{1}{2}$ SME+S ⁰ medium preparation.	28
Figure 13: Serum bottle containing 20 ml $\frac{1}{2}$ SME+S ⁰ medium, and syringe with 0.6 x 30 mm needle used for inoculation.	29
Figure 14: Experimental setup for UV-C exposure in liquid suspension.....	33
Figure 15: Experimental setup for photoreactivation.....	34
Figure 16: Schematic representation of photoreactivation experiment.....	35
Figure 17: Experimental setup for X-ray exposure in liquid suspension.....	37
Figure 18: Schematic representation of exposure/reference bucket.	38
Figure 19: Dose rate determination for hot exposure experiment.....	39
Figure 20: Schematic representation and comparison of experimental setups designed for the first and second radiation campaign.	42
Figure 21: Determination of gray-levels.	53

Results

Figure 22: Absorption spectrum of different $\frac{1}{2}$ SME medium combinations.....	56
Figure 23: Survival curve of all <i>Ignicoccus</i> representatives after UV-C exposure (0-300 J/m ²).	57
Figure 24: Survival curves of all <i>Ignicoccus</i> representatives after UV-C exposure (0-3000 J/m ²). .	58
Figure 25: Survival curve of UV-C exposed <i>I. hospitalis</i> cells compared to <i>E. coli</i> cells exposed in either cuvettes or petri dishes.....	59
Figure 26: Agarose gel of extracted genomic DNA from <i>I. hospitalis</i> and " <i>I. morulus</i> ".	60
Figure 27: Relative amount of DNA lesions vs. survival, and genomic DNA integrity of <i>I. hospitalis</i> after UV-C exposure.....	61
Figure 28: Analysis of heavy ion exposed samples (<i>I. hospitalis</i>) on agarose gels.....	63
Figure 29: ⁶⁰ Co radiation exposed stationary phase cultures of <i>I. hospitalis</i>	65
Figure 30: Metabolic activity of <i>I. hospitalis</i> (IH1, IH2, IH3) after ⁶⁰ Co radiation exposure monitored on lead acetate paper.	66
Figure 31: Survival curve of <i>I. hospitalis</i> and " <i>I. morulus</i> " after ⁶⁰ Co radiation exposure.....	67
Figure 32: Discrimination between culturable, and viable but nonculturable (VBNC) state.	69
Figure 33: Microscopic images of <i>I. hospitalis</i> cells at 1000-fold magnification.....	69

Figure 34: Metabolic activity of three independent <i>I. hospitalis</i> stationary phase cultures (IH1, 2, 3) after gamma ray exposure monitored on lead acetate tape.	70
Figure 35: Impact of ^{60}Co radiation exposed $\frac{1}{2}$ SME+S ⁰ medium on the survival of <i>I. hospitalis</i>	72
Figure 36: Relative survival of <i>I. hospitalis</i> when cultivated in ^{60}Co radiation exposed or unexposed $\frac{1}{2}$ SME medium supplemented by elemental sulfur.	73
Figure 37: Aliquots of substances needed for $\frac{1}{2}$ SME-S ⁰ medium preparations.	74
Figure 38: Quorum sensing with ^{60}Co radiation exposed stationary phase cells of <i>I. hospitalis</i>	76
Figure 39: Quorum sensing with samples from the last bottle giving a positive signal within the serial dilution after ^{60}Co radiation exposure.	76
Figure 40: Analysis of the genomic DNA integrity of <i>I. hospitalis</i> after ^{60}Co radiation exposure.	78
Figure 41: Analysis of the genomic DNA integrity of " <i>I. morulus</i> " after ^{60}Co radiation exposure.	78
Figure 42: Survival of <i>I. hospitalis</i> after X-ray exposure with and without the use of a 0.1 mm Al filter.	80
Figure 43: HPLC vials.	80
Figure 44: Survival curve of <i>I. hospitalis</i> after X-ray exposure.	81
Figure 45: Survival curve of <i>I. hospitalis</i> after X-ray exposure when cultivated below/above T _{opt} ...	82
Figure 46: Survival curve of <i>I. hospitalis</i> after X-ray exposure at ~88 °C.	83
Figure 47: DNA repair of <i>I. hospitalis</i> after X-ray exposure.	84
Figure 48: Agarose gel of extracted total RNA.	86
Figure 49: qRT-PCR of X-ray (1500 Gy) exposed <i>I. hospitalis</i> cells using the sequence specific recB primer.	87
Figure 50: Recorded melting curves for gene specific primers (16S rRNA, Pol E', Mips, Thermosome) using cDNA from experimental condition A	88
Figure 51: RNA transcription levels represented by absolute C _t values for different experimental conditions.	90
Figure 52: Standard curve generated with genomic DNA of <i>I. hospitalis</i> using the gene specific primer recB.	91
Figure 53: Calculated molecule or copy numbers for <i>rad2</i> , <i>rad50</i> , <i>recB</i> , and <i>radA</i>	92
Figure 54: RNA transcription levels for genes involved in replication are represented by absolute C _t values using cDNA from experimental condition E.	93

Discussion

Figure 55: Bacterial survival curve after UV-C exposure.	96
Figure 56: Different types of membranes used for sterile filtration.	106
Figure 57: Chemical substances with strongest color change after ^{60}Co radiation exposure (117.1 kGy).	106
Figure 58: Colloidal sulfur.	108
Figure 59: Potential scenario for the origin and early evolution of life.	119

Appendix

Figure 60: Test of primers	151
Figure 61: Metabolic activity of " <i>I. morulus</i> " (IM1, IM2, IM3) monitored on lead acetate paper.	152
Figure 62: Aliquots of substances needed for $\frac{1}{2}$ SME-S ⁰ medium preparations.	153
Figure 63: Certificate of irradiation for DbR #1.	154
Figure 64: Certificate of irradiation for DbR #2.	155
Figure 65: Certificate of irradiation for DbR #3.	156

List of Tables

Material and Methods

Table 1: Chemicals used for experimentation.....	21
Table 2: Primer used for RAPD analysis.....	23
Table 3: <i>Ignicoccus hospitalis</i> specific primers used for qRT-PCR (housekeeping, DNA repair) .	24
Table 4: <i>Ignicoccus hospitalis</i> specific primers used for qRT-PCR (replication)	25
Table 5: <i>Ignicoccus hospitalis</i> specific primers used for qPCR to detect DNA damages after ^{60}Co radiatin exposure	25
Table 6: Impact of 0.1 mm Al filter vs. filter-less exposure on the dose rate in dependence of an additional HPLC filter (here: glass).	36
Table 7: X-ray dose applied with or without 0.1 mm Al filter.	37
Table 8: Different experimental setups for qRT-PCR gene expression studies after X-ray exposure.	41
Table 9: Preparation of $\frac{1}{2}$ SME medium from single components which were exposed to increasing ^{60}Co radiation dose.	43
Table 10: Preparation of $\frac{1}{2}$ SME medium from unexposed single components.....	43
Table 11: Preparation of $\frac{1}{2}$ SME medium (^{60}Co radiation exposed or unexposed) which was supplemented by different sulfur combinations (dry/wet, exposed/unexposed).	44
Table 12: Scheme of steps needed for genomic DNA extraction.	46
Table 13: Scheme of steps needed for total RNA extraction.	48
Table 14: RAPD cycles.	51
Table 15: qPCR program for DNA damage detection.....	51

Results

Table 16: qRT-PCR program for gene expression studies after stress exposure.	54
Table 17: Calculated F_{10} -values for different <i>Ignicoccus</i> representatives.....	58
Table 18: F_{10} -values for model organisms.	58
Table 19: Calculated D_{10} -values (^{60}Co radiation) for different <i>Ignicoccus</i> representatives.....	67
Table 20: D_{10} -values (^{60}Co radiation) for model organisms	67
Table 21: D_{10} -values (^{60}Co radiation) for <i>I. hospitalis</i> , serial diluted in exposed $\frac{1}{2}$ SME+S 0 medium or serial diluted prior to exposure in (unexposed) $\frac{1}{2}$ SME+S 0	72
Table 22: Preparation of $\frac{1}{2}$ SME medium from single components which were exposed to increasing ^{60}Co radiation dose.	74
Table 23: Gray-levels of RAPD bands.	85
Table 24: RNA transcription levels of tested housekeeping genes listed as absolute C_t values for different experimental conditions.	88
Table 25: RNA transcription levels of Pol E' (potential housekeeping gene), and photolyase listed as absolute C_t values.	94

Abbreviations

(6-4)PPs	pyrimidine(6-4)pyrimidone photoproducts
" <i>I. morulus</i> "	<i>Ignicoccus morulus</i>
°C	degree centigrade
½ SME	½ synthetic sea water
½ SME+S ⁰ medium	½ SME medium supplemented with elemental sulfur
½ SME-S ⁰ medium	sulfur-free ½ SME medium
<i>A. fulgidus</i>	<i>Archaeoglobus fulgidus</i>
Al	aluminum
AP site	apurinic/apyrimidinic site
BER	base excision repair
BGS	Beta Gamma Service
bp	base pair
CFU	colony forming unit
CPDs	cyclobutane-pyrimidine dimer
C _t	threshold cycle
<i>D. radiodurans</i>	<i>Deinococcus radiodurans</i>
DbR	Death by Radiation
ddH ₂ O	double distilled water
DLR	Deutsches Zentrum für Luft- und Raumfahrt (German Aerospace Center)
DNA	deoxyribonucleic acid
dsDNA	double-strand DNA (breaks)
<i>E. coli</i>	<i>Escherichia coli</i>
Fe	iron
for	forward primer
Ga	billion years
Gy	gray
<i>H. salinarum</i>	<i>Halobacterium salinarum</i>
HR	homologous recombination
<i>I. hospitalis</i>	<i>Ignicoccus hospitalis</i>
<i>I. islandicus</i>	<i>Ignicoccus islandicus</i>
<i>I. pacificus</i>	<i>Ignicoccus pacificus</i>

ICP-MS	inductively coupled plasma mass spectrometry
J/m ²	joule per square meter
kGy	kilo gray
kV	kilo volt
LET	linear energy transfer
LUCA	last universal common ancestor
Mn	manganese
MPN	most probable number (technique)
NCBI	National Center for Biotechnology Information
NER	nucleotide excision repair
NHEJ	non-homologous end joining
O/N	over night
<i>P. furiosus</i>	<i>Pyrococcus furiosus</i>
PBS	phosphate-buffered saline
PCR	polymerase chain reaction
PFGE	pulsed-field gel electrophoresis
qPCR	quantitative real-time PCR
qRT-PCR	quantitative Reverse Transcription-PCR
RAPD	randomly amplified polymorphic DNA
RBE	relative biological effectiveness
rev	reverse primer
RIN	RNA integrity number
RNA	ribonucleic acid
ROS	reactive oxygen species
RT	room temperature
<i>S. solfataricus</i>	<i>Sulfolobus solfataricus</i>
ssDNA	single-strand DNA (breaks)
<i>T. gammatolerans</i>	<i>Thermococcus gammatolerans</i>
T _{opt}	optimal growth temperature
UV	ultraviolet
v/v	volume per volume
VBNC	viable but nonculturable

Abstract

The environmental conditions on early Earth were harsh and hostile for life compared to environmental conditions prevailing on present Earth. The atmosphere during the Archaean Age (3.8-2.5 Ga ago) was essentially anoxic and the lack of an UV-absorbing ozone layer enabled the solar ultraviolet radiation spectrum to penetrate Earth's surface increasing the overall terrestrial UV stress. In addition, elevated radiation levels in terms of ionizing radiation contributed to this rugged terrestrial environment. The Late Heavy Bombardment of the planet took place heaviest until about 3.8 Ga and may have heated up the ocean partially over 100 °C. Nevertheless, life has evolved during the Archaean under these circumstances inhabiting our planet since about 3.8 Ga. The potential setting under which life has evolved fascinates and still encourages humans to think about it. Different ideas, hypothesis and opinions about the Last Universal Common Ancessor (LUCA) and essential abilities needed for the propagation of life are still under debate. The underlying work emphasizes a hot origin of life and focuses on representatives of the genus *Ignicoccus* isolated from (deep-sea) hydrothermal vents. All representatives of this genus belong to the crenarchaeal branch and follow a hyperthermophilic, chemolithoautotrophic mode of life, living as obligate anaerobes growing by sulfur reduction. *Ignicoccus* species are promising candidates for early Earth inhabitants because they combine several abilities which may have been advantageous to withstand early Earth's harsh environmental conditions including elevated levels of radiation. Results of this work show that *Ignicoccus* species tend to survive high doses of ionizing radiation. This observation was the starting point to investigate the resistance of all four representatives of this genus with respect to different radiation types, ionizing radiation (X-rays, γ -rays) and non-ionizing radiation (UV-C). All tested species demonstrated similar inactivation tendencies after non-ionizing radiation exposure resulting in a F_{10} -value of $\sim 300 \text{ J/m}^2$. Additionally, *I. hospitalis* and "*I. morulus*" showed a high tolerance to ionizing radiation exposure with a D_{10} -value of $\sim 5 \text{ kGy}$. Besides this impressive radiation tolerance, it was possible to demonstrate for the first time, that a so called VBNC (viable but nonculturable) state may also exist for Archaea after ionizing radiation exposure. Viable and culturable cells were microscopically observed after exposure to ^{60}Co radiation doses of $<19 \text{ kGy}$, passing a transition state, and reaching the VBNC state after doses of $>27.2 \text{ kGy}$. This observed VBNC state was ascribed to the ongoing metabolic activity, thus H_2S production could be monitored. Additional experiments showed that the ionizing radiation tolerance of *I. hospitalis* seemed to be unaffected by pre-cultivation temperature and the temperature during radiation exposure. However, the tolerance of *I. hospitalis* to ionizing radiation accompanied by active repair of radiation induced DNA damages was

investigated in more detail. It was shown that the PCR-based randomly amplified polymorphic DNA (RAPD) analysis method was a powerful tool to visualize radiation induced DNA damages thus inferring genomic DNA integrity. This method allowed monitoring the DNA repair over time. It was demonstrated that the overall genome integrity was highly affected by both types of radiation and that RAPD analysis represents an attractive alternative for the commonly used and time consuming pulse-field gel electrophoresis (PFGE). *I. hospitalis* showed fast DNA repair after ionizing radiation exposure; the repair seemed to be completed within one hour. Due to the fact that *I. hospitalis* was able to withstand these high radiation doses, it was of great interest to investigate whether classical genes involved in DNA repair (e.g. *rad2*, *rad50*, *recB* and *radA*) were up- or down-regulated upon irradiation. Gene specific primers were designed for qRT-PCR studies and tested under varying experimental conditions. An upregulation of gene expression was detected for the genes mentioned above after 1500 Gy with *I. hospitalis* cells, when exposed in their early exponential phase. These promising results gave the first indication in regards to its radiation resistance capabilities and further investigation in terms of transcriptomics is definitely warranted. It is very likely that additional mechanisms may support this unusual high radiotolerance. Post-translational modifications for example would point to a completely new way of thinking in terms of the radiation tolerance of *I. hospitalis* and would allow the regulation of potentially high levels of repair proteins present due to its hot lifestyle. The surprisingly high radiotolerance may also be supported by a potential polyploidy, an increased genome copy number resulting in an enhanced resistance against DNA-damaging conditions. Nevertheless, *I. hospitalis* has not yet been observed in terms of post-translational modifications or polyploidy; these are promising experiments for follow-up studies. All underlying results obtained with these studies add new pieces to the puzzle how life on Earth may have evolved and the successful propagation under harsh and life hostile conditions.

Zusammenfassung

Die Umweltbedingungen der frühen Erde, vor 3,8-2,5 Milliarden Jahren, waren im Vergleich zu den heutigen Umweltbedingungen hart und lebensfeindlich. Die Atmosphäre während des Archaikums war nahezu sauerstofflos und die UV-absorbierende Ozonschicht fehlte. Das solare ultraviolette Strahlenspektrum konnte ungehindert in die Erdoberfläche eindringen. Dieses hohe Strahlungsniveau wurde begleitet von einem ebenfalls erhöhten Anteil an ionisierender Strahlung, welche zu diesen schwierigen Umweltbedingungen maßgeblich beitrugen. Zudem führte das große Bombardement, das vor ca. 3,8 Milliarden Jahren sein Maximum erreichte, dazu, dass der Ozean durch die Meteoriteneinschläge teilweise auf über 100 °C erhitzt wurde. Dennoch hat sich das Leben unter den oben genannten Bedingungen während dieses Erdzeitalters entwickelt und besiedelt bis heute erfolgreich unseren Planeten. Diese Tatsache fasziniert Menschen noch immer und ermutigt sie, über die möglichen Umstände nachzudenken, unter denen sich das Leben entwickelt hat. Unterschiedliche Ideen, Hypothesen und Meinungen über den letzten gemeinsamen Vorfahren (LUCA) und seiner notwendigen Fähigkeiten, damit sich das Leben verbreiten konnte, werden noch immer kontrovers diskutiert.

Die zu Grunde liegende Arbeit stützt sich auf die Theorie eines heißen Ursprungs des Lebens. Die Stellvertreter der Gattung *Ignicoccus*, die von hydrothermalen Quellen isoliert wurden, werden im Nachfolgenden als mögliche Bewohner der frühen Erde betrachtet. Alle Vertreter dieser Gattung gehören der crenarchaeellen Abzweigung des phylogenetischen Stammbaums an. Sie folgen als obligate Anaerobier einer hyperthermophilen, chemolithoautotrophen Lebensweise und gewinnen ihre Energie mit Hilfe der Schwefelreduktion. Diese Mikroorganismen vereinen mehrere Fähigkeiten, die vorteilhaft waren, um den damals vorherrschenden Umweltbedingungen, insbesondere der erhöhten Strahlungsintensitäten, zu trotzen. In dieser Arbeit wurde gezeigt, dass *Ignicoccus* Spezies hohe Dosen ionisierender Strahlung überleben können. Diese Beobachtung war ausschlaggebend für nachfolgende Untersuchungen mit allen bisher bekannten Vertretern dieser Gattung in Bezug auf ihre Toleranz gegenüber unterschiedlicher Strahlungsarten. Alle untersuchten Spezies zeigten vergleichbare Inaktivierungstendenzen gegenüber nicht ionisierender Strahlung resultierend in F_{10} -Werten von $\sim 300 \text{ J/m}^2$. Zudem zeigten *I. hospitalis* und "*I. morulus*" eine hohe Strahlungstoleranz gegenüber ionisierender Strahlung resultierend in D_{10} -Werten von $\sim 5 \text{ kGy}$. Neben dieser beeindruckenden Strahlentoleranz war es zudem möglich zu zeigen, dass ein sogenannter VBNC Status (viable but nonculturable) nach Exposition gegenüber ionisierender Strahlung auch für

Archaeen zu existieren scheint. Lebensfähige und damit kultivierbare Zellen konnten nach ^{60}Co Exposition mit Dosen $<19\text{ kGy}$ beobachtet werden. Dem als Übergangszustand definierten Bereich folgte der VBNC Status nach Exposition mit Dosen $>27,2\text{ kGy}$. In diesem VBNC Status konnte eine fortlaufende metabolische Aktivität in Form von H_2S Produktion verfolgt werden. Zusätzliche Experimente konnten zeigen, dass die Toleranz von *I. hospitalis* gegenüber ionisierender Strahlung unbeeinträchtigt von der Temperatur während der Anzucht und der Temperatur während des Experiments war.

Die Toleranz von *I. hospitalis* gegenüber ionisierender Strahlung einhergehend mit aktiver Reparatur von strahleninduzierten DNS-Schäden wurde im Detail untersucht. Es konnte gezeigt werden, dass die PCR-basierte RAPD (randomly amplified polymorphic DNA)-Methode sehr gut geeignet ist, um strahleninduzierte DNS-Schäden zu veranschaulichen und erlaubt den Verlauf der Reparatur zu verfolgen. Somit stellt diese Methode eine attraktive Alternative zu der häufig verwendeten und zeitintensiven Puls-Feld-Gelelektrophorese (PFGE) dar. Es wurde demonstriert, dass die gesamte Integrität des Genoms stark durch beide Arten von Strahlung negativ beeinflusst wurde. *I. hospitalis* zeigte indes eine schnelle DNS-Reparatur nach ionisierender Strahlung. Basierend auf vorliegenden Experimenten wurde demonstriert, dass diese Reparatur binnen einer Stunde vollzogen war. Da gezeigt werden konnte, dass *I. hospitalis* fähig ist, hohe Dosen ionisierender Strahlung zu überleben, war es von besonderem Interesse, die Regulierung von klassischen Reparaturgenen wie bspw. *rad2*, *rad50*, *recB* und *radA* nach Bestrahlung zu betrachten. Gen spezifische Primer wurden für diesen Zweck entworfen, um qRT-PCR Studien durchführen zu können und die Expression dieser Gene unter variierenden experimentellen Bedingungen zu untersuchen. Eine leichte Hochregulierung wurde nach Exposition mit 1500 Gy in *I. hospitalis* Zellen gesehen, die sich in ihrer frühen exponentiellen Phase befanden. Diese vielversprechenden Ergebnisse geben einen ersten Eindruck auf die Strahlentoleranz von *I. hospitalis* und der Expression von Reparaturgenen. Sie ermutigen dazu, weitere Untersuchungen in Bezug auf das Transkriptom durchzuführen. Es ist anzunehmen, dass zusätzliche Mechanismen diese Strahlentoleranz unterstützen. Posttranslationale Modifizierungen würden auf eine komplett neue Denkweise in Bezug auf die Strahlungstoleranz von *I. hospitalis* hinweisen. Diese Modifizierungen würden eine Regulation von Reparaturgenen, die potenziell bereits in hohem Maße aufgrund der heißen Lebensweise vorliegen, erlauben. Diese überraschend hohe Strahlentoleranz dürfte auch eine mögliche Polyploidie unterstützen, da eine erhöhte Genomkopienzahl bei einer erhöhten Toleranz gegenüber DNS zerstörenden Bedingungen von Vorteil sein könnte. Nichtsdestotrotz, bis jetzt wurden weder eine mögliche Polyploidie noch posttranslationale Modifizierungen

untersucht. Diese Untersuchungen wären äußerst interessant für Folgestudien. Alle zu Grunde liegenden Ergebnisse fügen dem Gesamtbild, wie das Leben auf der Erde entstanden sein könnte, neue Puzzleteile hinzu. Dies führt zu potenziellen Antworten auf die Frage warum eine erfolgreiche Verbreitung unter den vorherrschenden harten und lebensfeindlichen Bedingungen auf der frühen Erde möglich war.

1 Introduction

1.1 Life on early Earth

Earth has been inhabited since the Archaean Age, and terrestrial life has been represented since about 3.8 Ga or earlier. The main biochemical carbon cycle developed around 3.5 Ga ago and is in use to present day (according to Nisbet & Sleep, 2001). The prevailing conditions on early Earth, the circumstances and potential settings under which life has evolved, fascinates and still encourages humans to think about it. A vast number of possible scenarios has been developed over the past decades, resulting in enduring debates and discussions, supported or disproved by e.g. geochemical and isotopic evidence. A commonly accepted hypothesis concerning life's origin and evolution has not been established yet; the debate is still ongoing. Several ideas and hypotheses in regards to how life could have evolved are shortly described in the following few Sections, strongly emphasizing a "hot origin" of life on our "Blue Planet".

1.1.1 Environmental conditions on early Earth

The environmental conditions as they prevailed on early Earth were harsh and hostile for life as compared to environmental conditions on present Earth. The atmosphere during the Archaean Age (approx. 3.8-2.5 Ga ago) was essentially anoxic which can be deduced from several geochemical and isotopic studies (Grenfell *et al.*, 2010; Holland, 1999). As a consequence, the UV-absorbing ozone layer was absent, enabling the solar ultraviolet radiation spectrum to penetrate to Earth's surface, and thus increased as a result the overall UV stress on the Earth's surface (Cockell & Horneck, 2001; according to Margulis *et al.*, 1976) (Figure 1). Environmental conditions did not only influence early Earth's atmosphere but the prevailing ocean was significantly affected as well. The Late Heavy Bombardment of the planet during the early Archaean, heaviest until about 3.8 Ga, may have heated up the ocean partially over 100 °C (according to Nisbet & Sleep, 2001). Sleep reviewed the Hadean-Archaean environment on early Earth in more detail, and discussed three well-known scenarios in which life may have evolved (Sleep, 2010). These scenarios are described below:

1) In the 1st hypothesis, he assumed that the Hadean climate, including the Late Heavy Bombardment, (according to Sleep, 2010), was clement or icy after the early warm greenhouse ceased. Life originated and colonized the planet by e.g. adapting to a thermophilic mode of life at hydrothermal events and in the kilometer-deep surface. Such

an adaptation would have been beneficial after large asteroid impacts have boiled much of the ocean. Descendants of these thermophilic survivors may have adaptively colonized low-temperature environments as well. Proteins adapted to high temperatures may have also been lost over the course of time in the low-temperature branch (according to Sleep, 2010).

2) The 2nd hypothesis describes a scenario in which a comparable phylogeny occurred except that the thermophilic organisms may have outcompeted their low-temperature relatives. This event may have resulted in an apparent LUCA (Last Universal Common Ancessor) bottleneck without a sudden mass extinction (according to Miller and Lazcano, 1995; according to Sleep, 2010).

3) Finally, the 3rd hypothesis was focused at the end of the Hadean Age (~3.3 Ga) in which the climate cooled slowly when the CO₂ greenhouse was ended leaving an overall temperature of approximately 50-70 °C. Only thermophiles therefore were able to exist (Gaucher *et al.*, 2008, 2010).

Sleep inferred that the first two possibilities had similar genetic and geologic implications until recent evidence of a Hadean massive impact has been found. But the accessible Archaean geologic record seems to support the third scenario, potentially eliminating the other two (according to Sleep, 2010). The discussion about early Earth's harsh environmental conditions, including the divergent opinions about the last universal common ancestor, allows the assumption of LUCA preferring a thermophilic lifestyle (Gaucher *et al.*, 2010; Sleep, 2010; Stetter, 2006). Based on this idea, one can think about microbial communities that inhabited the mid-ocean ridges, volcanic ocean islands and island-arc volcanoes, a chain of volcanoes being arranged in an arc-shaped manner (Nisbet, 2000). These microbial communities may have been dependent upon igneous activity, hydrothermal circulations and systems to provide chemical disequilibria (Sleep, 2010). Living in a sufficient depth of water may have been advantageous for the evolution and propagation of these communities by preventing them from solar ultraviolet light and its harmful effects.

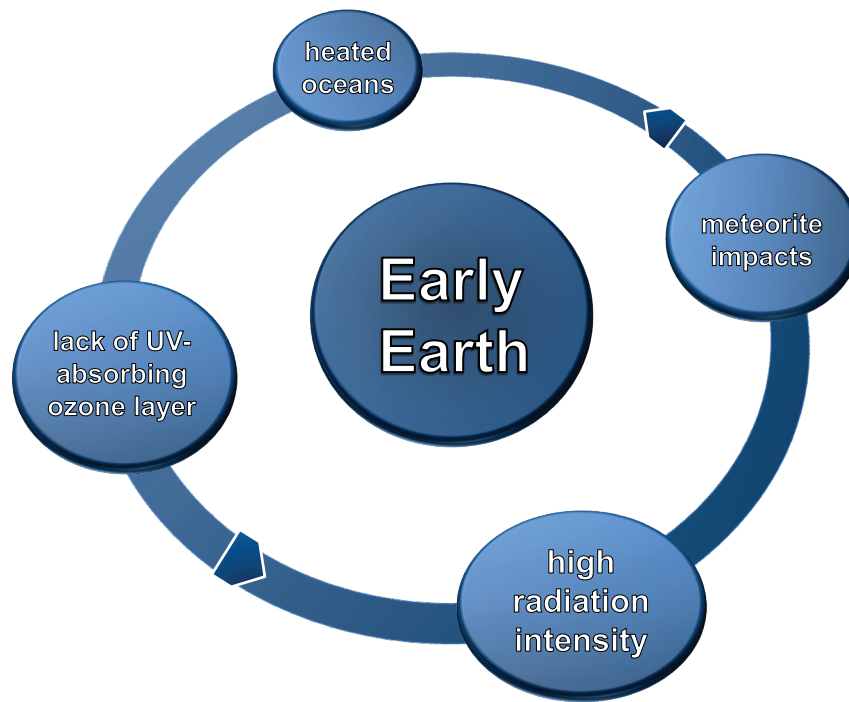


Figure 1: Schematic representation of environmental conditions present on early Earth.

1.1.2 Radiation levels on early Earth

Solar ultraviolet radiation, harmful to all biological material, is absorbed in the modern terrestrial atmosphere by ozone, which is photochemically produced from atmospheric oxygen. This ozone layer has gradually developed as oxygen accumulated over the course of history (first Great Oxidation Event, 2.45 Ga), and by the later development of photosynthesis, which enabled the organisms to directly use the Sun's energy for their own purposes (according to Sessions *et al.*, 2009; according to Margulis, 1976). Early Earth's surface has not only been subjected to the solar ultraviolet radiation spectrum (referred as non-ionizing radiation), naturally occurring ionizing background radiation has been present since its formation. But, overall radiation levels in terms of UV-light and ionizing background radiation have decreased over time, while the oxygen concentration has increased (Kasting, 1993; Holland, 1994; Karam *et al.*, 2001). Background beta and gamma radiation levels including radiation doses from geologic material and internal emitters have changed significantly over time with an maximal ambient radiation level of about 6 mGy y^{-1} 4 Ga ago (Karam & Leslie, 1999; Karam *et al.*, 2001); ambient radiation levels have decreased steadily resulting in a present average exposure due to natural background radiation of around 3 mGy y^{-1} (Karam *et al.*, 2001). Sources for background radiation include radioactive elements and their decay in Earth's crust such as uranium, thorium, potassium, radium, radon, and others. Radiation from the sun and other stars or cosmogenic nuclides formed through the interaction of cosmic rays with atmosphere and

surface rocks take an important role, too. Internal radionuclides, primarily represented by ^{40}K , are another source of radiation exposure within organisms through biochemical reactions (Karam *et al.*, 2001).

Karam *et al.* hypothesized in 2001 that mutation rates may not necessarily be in direct proportion to rates of DNA damage at low exposure rates; with long intervals between damaging events, cells may have had the capacity to respond. In general, mutations can have several distinct effects for an organism and its potential offspring. They may be beneficial for an organisms' survival or remain silent, being without any consequence. Unfavorable or lethal effects are possible as well, if undetected by the organism. Nevertheless, the type of response would be on a cellular level by mechanisms being able to fully repair caused DNA damages with unfavorable consequences (see Paragraph 5); prevention from being mutagenic, and transmitted to the next generation (Karam *et al.*, 2001). Therefore, life relies on mutation repair mechanisms, assuming that DNA repair pathways may have evolved very early in the history of life (Mackinodan & James, 1990), because of similarities in disparate modern organisms. Repair mechanisms may have retained the ability to efficiently and accurately repair higher rates of DNA damages than exist at present day (Karam *et al.*, 2001). Summarizing, the rise of prevailing oxygen levels, the formation of the ozone layer in the upper atmosphere, the resulting absorption of harmful UV radiation, and the overall decrease in background radiation enabled life to further evolve and to colonize this planet. So far, Earth is the best known example to study how life modified and still modifies a planet's atmosphere over time resulting in a co-evolution of life, atmosphere, and the terrestrial climate (Grenfell *et al.*, 2010).

1.1.3 Where LUCA may have felt at home

The idea that life may have emerged in hydrothermal environments is quite attractive (according to Nisbet & Sleep, 2001) while controversially discussed to the present day. Deamer and Georgiou compared conditions and properties of deep-sea hydrothermal vents and hydrothermal fields of volcanic origin above sea level in respect to their ability to support the evolution of early life (Deamer & Georgiou, 2015). As an example, alkaline vents last up to 30,000 years, providing a constant supply of chemical energy at temperatures of 50-90 °C, whereas light energy is abundant in hydrothermal fields allowing the development of photosynthesis. The hydrothermal field theory would suggest that early life quickly evolved mechanisms to capture this light-driven chemiosmotic energy for reactions (according to Deamer, 1997; Deamer & Weber, 2010), but life in alkaline vents would depend on chemotrophic reactions (Deamer & Georgiou, 2015).

Deamer and Georgiou criticized that none of the predictions mentioned above have ever been tested *in situ* by experiments and laboratory simulations. The plausibility of these two potential sites for the origin of life requires testing; the ensuing discussion about the setting of life's evolution will remain ongoing (for detailed review see Gaucher *et al.*, 2010).

1.1.4 LUCA's potential mode of life

The discussion whether the first organisms on early Earth were (at least) hyperthermophiles is still ongoing. Di Giulio discussed in 2000 whether LUCA was a progenote or a cenancestor. A progenote is described as primitive entity being still in process of evolving its relationship between phenotype and genotype (according to Woese & Fox, 1977; Di Giulio, 2000), whereas a cenancestor would be an organism with cellular complexity which still had to solve the problem of the genotype-phenotype relationship (Di Giulio, 2000). A correspondence between the physical setting in which life originated and LUCA's first speciation took place has to be considered when thinking about a progenote. Di Giulio worked on estimations of the G+C content in ancestral rRNA sequences of the LUCA and decided, if LUCA lived in a high-temperature setting, the origin of life may have taken place at high temperature in relation to a progenote (Di Giulio, 2000). Taking a thermophily index into consideration when analyzing the propensity of amino acids to enter thermophile/hyperthermophile proteins, Di Giulio described the last universal common ancestor as "hot LUCA" (Di Giulio, 2001). Seven years later he tried to reconstruct the ancestral sequences of proteins in regard to an oxyphobic index and concluded based on his observations that the origin of life and the main phase of the evolution of the first organisms on early Earth may have taken place in an anaerobic environment (Di Giulio, 2007). Nevertheless, the methods for reconstructing ancestral sequences have to be improved/perfected to give "definite" answers to these questions (Di Giulio, 2001, 2010, 2011).

Another topic controversially discussed is the evolution of the sulfur cycle. Nisbet and Sleep discussed in 2001 that the microbial fraction of sulfur was limited during the Archaean based on isotopic evidence resulting in potentially low sulfate concentrations (supported by Habicht & Canfield, 1996; Canfield & Teske, 1996). Isotopic evidence in 2.7 Ga rocks of the Belingwe belt in Zimbabwe may have inferred however that the full sulfur cycle evolved earlier than originally predicted (Grassineau *et al.*, 2001). Woese suggested in 1987 that the ancestral archaebacterium (today: archaeon) was an extremely thermophilic, anaerobic living microorganism that probably thrived from sulfur

reduction. It is conceivable that a microbial diversity of sulfur consumers was present quite early in Earth's history, but a global distribution subsequently took place later on (Canfield *et al.*, 2000). Rasmussen reported in a Nature article published in 2000 that there is evidence for life in a 3,235-million-year-old deep-sea volcanogenic massive sulfide deposit from the Pilbara Craton of Australia (Rasmussen, 2000). He presented pyritic filaments as probable fossil remains of thread-like microorganisms, and assumed that these fossils represented the first evidence for life in a Precambrian submarine thermal spring system. Rasmussen suggested that these microorganisms were probably thermophilic chemotrophic prokaryotes. Thus, recent microorganisms found in close proximity to modern hydrothermal vent systems are reasonable candidates for being potential early Earth inhabitants.

1.1.5 LUCA's descendants

The universal phylogenetic tree (exemplarily depicted in Figure 2) and the standard model of microbial descent is based on small-subunit ribosomal RNA, positioning LUCA at the root of this tree (according to Nisbet & Sleep, 2001; Woese, 1987; Doolittle, 2000). One appealing idea, shared by e. g. Woese, Graham and colleagues, is of an early population of simple, replicating organisms within a community sharing mutually information instead of a single cell representing LUCA (Woese, 1987; Graham *et al.*, 2000). An organism's genes were exchanged with others and were in effect shared communally. This proposed model of genomic evolution is based on the successive "crystallization" of differentiated cellular subsystems (Graham *et al.*, 2000; Woese, 1998). Evolution enabled continuing divergence making genes less interchangeable later on (Graham *et al.*, 2000). Based on this idea of LUCA, being part of an early community, most scientists have one common opinion ("standard view") (according to Nisbet & Sleep, 2001; Zuckerkandl & Pauling, 1965; according to Pace, 1991) concerning the three domains of life. Both domains, Bacteria and Archaea, arose from LUCA, whereas the domain Eukarya evolved slowly from a parental stem that symbiotically incorporated chloroplasts (cyanobacterial descendants) and mitochondria (α -proteobacterial descendants) (Figure 2) (according to Nisbet & Sleep, 2001; Woese *et al.*, 1990; Margulis, 1971).

Two popular hypotheses include the assumption of a hot environment, and are nicely reviewed by Nisbet and Sleep (2001), although evidence for a hyperthermophile ancestry was challenged (Galtier *et al.*, 1999). There is the "hyperthermophile Eden" theory implying an early microbial community hosting the last common ancestor, in which life was hot and chemotrophic (according to Nisbet & Sleep, 2001; Stetter, 1996). An alternative

version would be the “hyperthermophile Noah” theory describing a not necessarily hyperthermophilic universal ancestor. But this version of LUCA may have diversified from an unknown Eden into an early population that included some hyperthermophiles near hydrothermal systems (according to Nisbet & Sleep, 2001).

Keeping a potential hot origin in mind, the shortest branches within the universal phylogenetic tree as depicted in Figure 2 are exclusively covered by hyperthermophilic prokaryotes (red branches) and cluster around the phylogenetic root (Figure 2). Deep branches give evidence for an early separation, whereas short phylogenetic branches indicate a slow rate of evolution. One has to keep in mind that the constructed phylogenetic trees tend to give ideas of the phylogenetic distance between recent organisms (e.g. Figure 2) rather than their evolutionary development (Hug *et al.*, 2016).

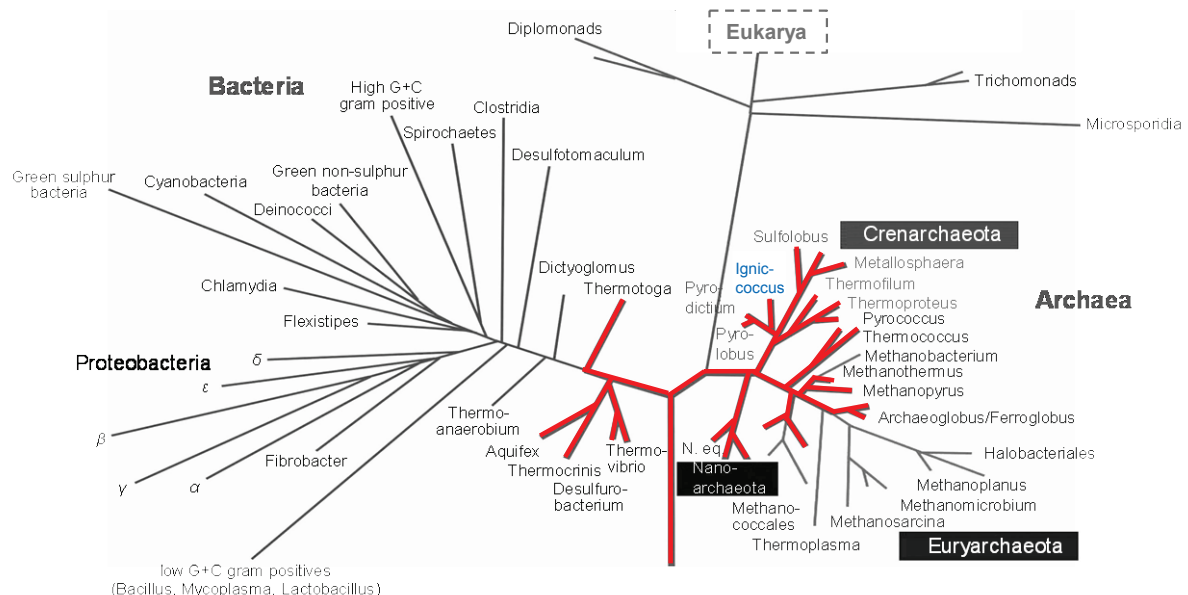


Figure 2: Phylogenetic tree based on 16S rRNA sequence comparisons. The phylogenetic tree was constructed based on sequence comparisons of small subunit ribosomal RNA of cultivable microorganisms. The red branches represent hyperthermophiles. The eukaryal branch has subsequently been reduced (adapted from Stetter, 2006; credit Dr. Harald Huber). *Ignicoccus* is highlighted in blue. The two recently proposed archaeal phyla Thaumarchaeota (Brochier-Armanet *et al.*, 2008) and Lokiarchaeota (Spang *et al.*, 2015) have not been taken into account.

The energy source of hyperthermophiles is quite simple as most gain their energy chemolithoautotrophically by fixation of CO₂ serving as carbon source for organic cell material (Figure 3; Stetter, 2006).

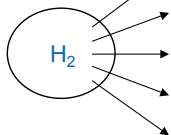
energy-yielding reactions of hyperthermophiles		
electron donor	electron acceptor	product
	• CO ₂	methane
	• Fe(OH) ₃	magnetite
	• S ⁰ ; SO ₄ ²⁻	hydrogen sulfide (H ₂ S)
	• NO ₃ ⁻	nitrogen (NH ₃)
	• O ₂ traces	water
S ⁰ (pyrite) →	• O ₂	H ₂ SO ₄ (+FeSO ₄)
source of cell carbon:	CO ₂	
additional growth requirements:	heat	
	trace minerals	
	liquid water	

Figure 3: Main energy-yielding reactions used by chemolithoautotrophic hyperthermophiles. Highlighted in blue: Donor, acceptor, product and other sources used by *Ignicoccus* (adapted from Stetter, 2006).

A detailed description of the anaerobic, chemolithoautotrophic, hyperthermophilic lifestyle will be described in detail within Section 1.3.2 using the example of *Ignicoccus hospitalis*. Pace proposed in 1991 that modern representatives of these evolutionary primitive organisms (he used examples from the genera *Pyrodictium*, *Thermoproteus*, *Pyrobaculum* (according to Stetter *et al.*, 1990)) have similar requirements. They need high temperatures in their natural habitat besides geochemical energy sources such as sulfur and hydrogen to live mainly anaerobic in their geothermal environment (according to Pace, 1991). Common properties of modern organisms were properties of the ancestor, meaning that least-evolved Archaea might share similar properties with their ancestors (earliest Archaea) (according to Pace, 1991). The conclusion of Karam and colleagues in 2001 was that direct evidence concerning the conditions under which life evolved was nearly absent, and that the indirect evidence we currently possess is strongly dependent upon varying interpretations. The ancient radiation environment may have caused an evolutionary selection, and modern organisms may have acquired characteristics advantageous for this selection process (Karam *et al.*, 2001). These properties might have pertained to the most recent common ancestor of all modern life (according to Pace, 1991; Woese, 1987). So, it is reasonable to investigate a modern organism's ability to tolerate harsh environmental conditions as they occurred on early Earth.

Hydrothermal systems are promising sites where the evolution of life may have started. Modern hydrothermal vents are a good starting point to look for appropriate early Earth inhabitants. Interesting candidates represented by the genus *Ignicoccus* were found in

submarine hydrothermal systems and were described in 2000 by Huber and colleagues. Members of the genus are a focus of attention and their tolerance to different environmental parameters of astrobiological relevance will be presented in the underlying work.

1.2 Hydrothermal vents

Hydrothermal vent systems were discovered during the early 1980s (according to Martin *et al.*, 2008), and identified as chemically reactive environments, with thermal and chemical gradients composed of reactive gases and dissolved elements (Baross & Hoffmann, 1985). Deep-sea hydrothermal vent deposits are formed by precipitations of these minerals present in hot, reduced, metal-rich fluids, accumulating on the seafloor (Pagé *et al.*, 2008; Haymon, 1983). These reactive environments were recognized as potential sites for prebiotic syntheses (Baross & Hoffmann, 1985).

The Faulty Towers complex in Figure 4 can be seen as an imposing example of a black smoker complex (according to Martin *et al.*, 2008). This black smoker complex, and others, can be found directly above magma chambers 1-3 km under sea level (for detailed explanation see review article by Kelley *et al.*, 2002). Black smoker chimneys emit mineral enriched sea water with temperatures of up to 405 °C (Von Damm *et al.*, 2003). Escaping water comes into close contact with the magma chamber, and re-emerges at the vents after circulating from the ocean floor through the crust resulting in black smoker fluids rich in dissolved transition metals (according to Martin *et al.*, 2008; Von Damm, 2013). Besides high concentrations of Fe(II) and Mn(II), fluids contain high concentrations of dissolved gasses such as magmatic CO₂ (4-215 mmol/kg), H₂S (3-110 mmol/kg), H₂ (0.1-50 mmol/kg), and CH₄ (0.05-4.5 mmol/kg) formed by biotic and abiotic processes (Kelley *et al.*, 2002). Microbial communities including chemolithoautotrophic microorganisms thrive on these metal enriched black smoker fluids. Temperature gradients between the hot interior of the smoker and the surrounding sea water enable them to adapt to specific environmental regions (Figure 4, according to Martin *et al.*, 2008; Schrenk *et al.*, 2003). These chemolithoautotrophic species can gain their energy by distinct oxidation-reduction reactions under a wide range of temperature, caused by physical gradients and chemical disequilibria occurring in the (deep-sea) hydrothermal vent fields (McCollom & Shock, 1997). All four *Ignicoccus* species were isolated from such submarine hydrothermal fields or systems in the Atlantic and in the Pacific (Huber *et al.*, 2000; Paper *et al.*, 2007). Detailed information on the places of isolation and the organisms themselves will be given in the following Sections.

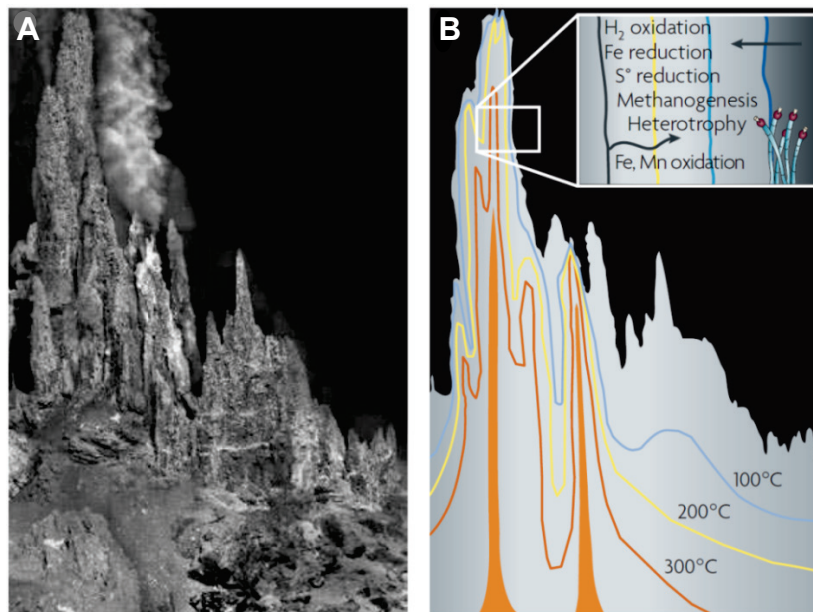


Figure 4: Black smoker. (A) This black smoker was found in the Faulty Towers complex in the Mothra hydrothermal field on the Endeavour Segment of the Juan de Fuca Ridge and serves as general example for black smokers from which *Ignicoccus* was isolated (adapted from Martin *et al.*, 2008). (B) Schematic representation of a black smoker chimney. The chimney is surrounded by 2 °C cold sea water and warm fluids escaping from the vent itself. Up-flow fluids can have temperatures exceeding 300 °C, but intermediate conditions exist as indicated by lines. Due to this temperature gradient, a diverse microbial community can be uncovered within the chimney walls (adapted from Martin *et al.*, 2008; Pagé *et al.*, 2008; Schrenk *et al.*, 2003).

1.3 The genus *Ignicoccus*

The genus *Ignicoccus* was first described in 2000 by Huber *et al.* and consists of three described type species. All of them are members of the crenarchaeal branch within the domain of Archaea which was revealed by 16S rRNA sequence comparisons. Taxonomically, *Ignicoccus* belongs to the order of *Desulfurococcales* and represents a deeply branching lineage within the family of the *Desulfurococcaceae* (Huber *et al.*, 2000; Huber & Stetter, 2001). Members of this genus are the only ones within this family gaining their energy as obligate chemolithotrophic sulfur reducers (Huber *et al.*, 2000).

1.3.1 *Ignicoccus islandicus* and *Ignicoccus pacificus*

Two species of this new genus were isolated from submarine hydrothermal systems in the Atlantic and in the Pacific in 2000 (Huber *et al.*, 2000). *I. islandicus* (Kol8^T), the type species of this genus, was isolated from hot sediments at the Kolbeinsey Ridge (North of Iceland) in a depth of 103-106 m, whereas rocky black smoker material from the East Pacific Rise (9 °N, 104 °W; Depth: 2500 m) was used to enrich *I. pacificus* (LPC33^T, LPC37). Their names were devoted to the places of isolation. Morphological and physiological characteristics which are exceptional for this genus will be explained using the example of *Ignicoccus hospitalis*.

1.3.2 *Ignicoccus hospitalis*

Seven years later, in 2007, Paper *et al.* isolated and described a new *Ignicoccus* species, KIN4/I^T (now described as *Ignicoccus hospitalis* sp. nov.). This new *Ignicoccus* representative was isolated from rocky material from hydrothermal vents at Kolbeinsey Ridge, to the north of Iceland in a depth of 106 m. An unusual morphological feature was observed for this new species; tiny cocci covered the surface which were later designated as *Nanoarchaeum equitans*, the first identified representative of the novel archaeal phylum Nanoarchaeota (Huber *et al.*, 2002; according to Huber *et al.*, 2003; Waters *et al.*, 2003) (Figure 5). *Nanoarchaeum equitans* cells have a coccoid shape with a diameter of 350-500 nm, which are attached to the cell surface of *I. hospitalis* (Figure 5) (Huber *et al.*, 2002). *I. hospitalis* is the only representative able to host these tiny cocci (according to Huber *et al.*, 2003; Paper *et al.*, 2007; Huber *et al.*, 2002). All attempts to co-cultivate *N. equitans* with other members of the genus *Ignicoccus* failed (according to Huber *et al.*, 2003). Genomic analysis revealed that *N. equitans* has, with ~490 kb, one of the smallest genomes known so far (Waters *et al.*, 2003). Only few genes crucial for distinct metabolic and biosynthetic pathways have been identified. The majority of information for lipid, cofactor, amino acid, and nucleotide biosynthesis is lacking (Waters *et al.*, 2003) ascribed to its highly reduced genome size. A direct contact of *N. equitans* to its host is obligatory for its growth (Huber *et al.*, 2002). In contrast, *I. hospitalis* is able to grow axenic or in co-culture with *N. equitans*.

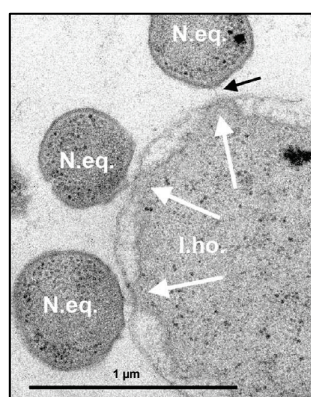


Figure 5: Transmission electron micrograph from *I. hospitalis* and *N. equitans* (ultrathin sections). White arrows (contact sites of the outer cellular membrane of *I. hospitalis* with its inner membrane), black arrow (fibrous material in the gap between *I. hospitalis* and *N. equitans*) (adapted from Jahn *et al.*, 2008).

All members of the genus *Ignicoccus* share common morphological and physiological properties (Figure 6). They have an irregular coccoid cell shape with a cell diameter of 1-4 μm (Huber *et al.*, 2012; Huber *et al.*, 2000), stain Gram-negative, and have an optimal growth temperature at 90 °C, classifying them as hyperthermophiles. All isolated representatives live as obligate anaerobes, growing by sulfur reduction of elemental sulfur

using hydrogen as electron donor producing H_2S . No other electron donor and acceptor can be utilized (Huber *et al.*, 2000), and CO_2 is the sole carbon source fixed via a new CO_2 fixation pathway (Paper *et al.*, 2007; Jahn *et al.*, 2007). This mode of life is described as chemolithoautotrophic (Huber *et al.*, 2012, Huber *et al.*, 2000) (Figure 6).

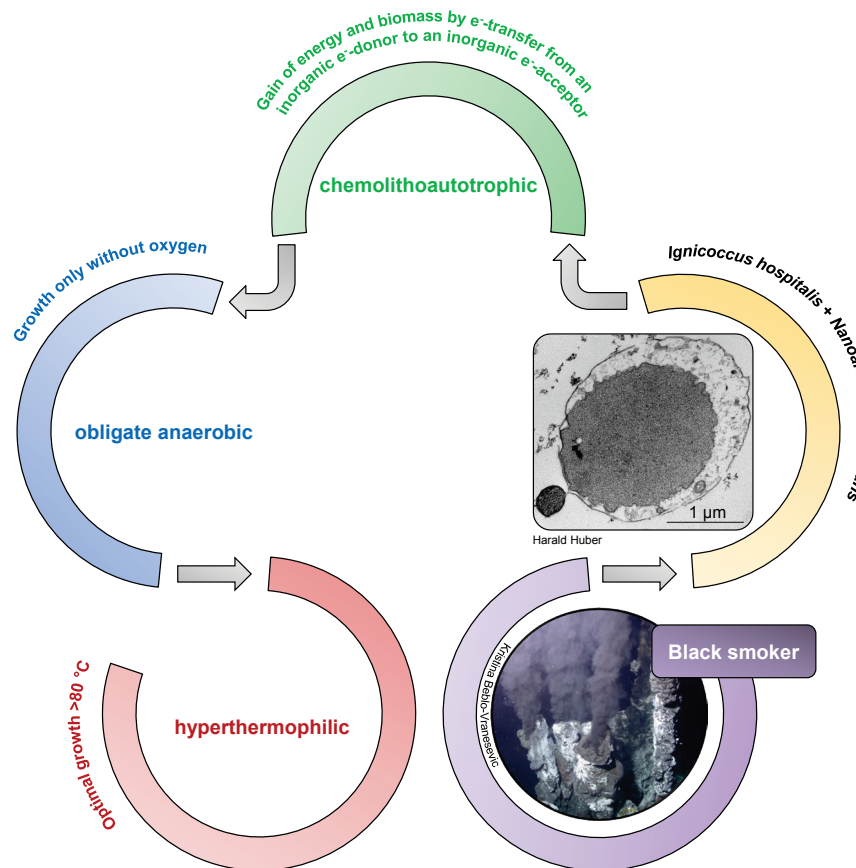


Figure 6: *Ignicoccus* and the mode of life. All *Ignicoccus* representatives, known to date, share a common mode of life. The already mentioned species were isolated from submarine hydrothermal systems including sandy sediments and venting water at depths between 103-106 m, and from black smoker material at a depth of 2500 m.

The unique cell envelope, which is common for all strains within the genus *Ignicoccus*, is exceptional among Archaea. It is composed of two membranes, the cytoplasmic/inner membrane and the outer cellular membrane (Rachel *et al.*, 2002, Huber *et al.*, 2012), defining two compartments, namely the cytoplasm and the intermembrane compartment (Figure 7). The intermembrane compartment between these membranes has a variable width of 20 to 500 nm (Rachel *et al.*, 2002). Model calculations demonstrated, that the volume of this compartment exceeds that of the cytoplasm by 1.8-3.3 times (Rachel *et al.*, 2002). An asymmetrical organization is characteristic due to the presence of up to nine flagella-like appendages (Rachel *et al.*, 2002; Huber *et al.*, 2000) anchored at one pole into the cell (Paper *et al.*, 2007). Membrane-coated vesicles of varying size (~50 nm in diameter, ≤300 nm in length) were seen to be released from the cytoplasmic membrane,

and can be found within the intermembrane compartment where they come in close proximity with the outer cellular membrane (Paper *et al.*, 2007; Näther & Rachel, 2004) (Figure 7). In point of fact, the great majority of these vesicles are tubular structures originating from the cytoplasm (see dissertation Thomas Heimerl, 2014).

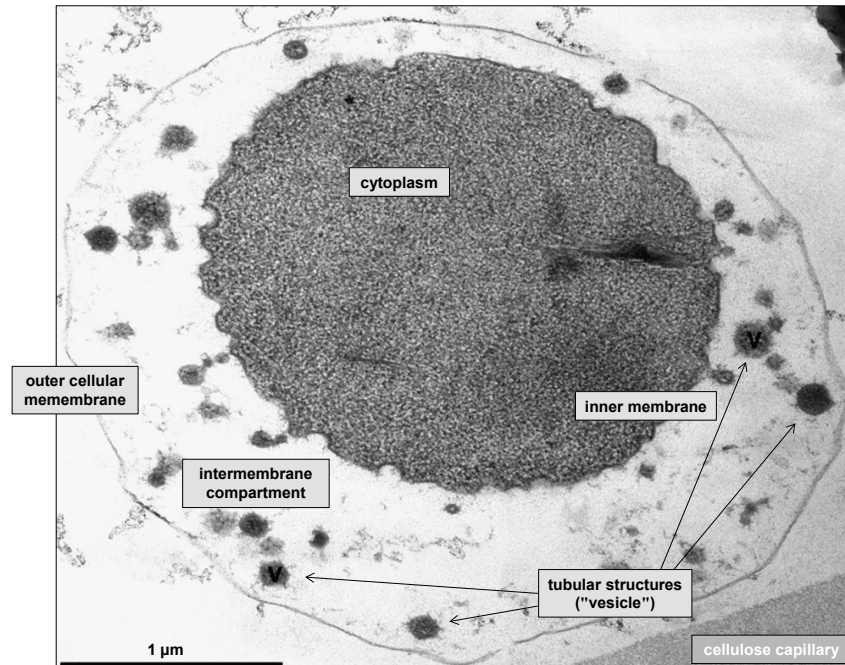


Figure 7: Ultrathin section from an *I. hospitalis* cell shown as transmission electron micrograph. (Adapted from Huber *et al.*, 2012; Rachel *et al.*, 2010; Heimerl, 2014).

One of the most surprising physiological properties of *Ignicoccus* species was detected in 2010 by Küper and colleagues. They have shown on the basis of immune-EM analyses with ultrathin sections that the outer cellular membrane of *Ignicoccus* is energized, and that ATP synthesis is locally separated from information processing and protein biosynthesis (Küper *et al.*, 2010). The outer cellular membrane contains both the H_2 :sulfur oxidoreductase complex acting as primary proton pump for the A_1A_0 ATP synthase, and the A_1A_0 ATP synthase itself. As a result, energy conservation happens in the intermembrane compartment, whereas transcription, translation and DNA replication occurs in the cytoplasm (Küper *et al.*, 2010); ribosomes and DNA were exclusively found in this compartment.

1.3.3 “*Ignicoccus morulus*”

“*Ignicoccus morulus*” is the fourth member of the genus *Ignicoccus* known so far. A detailed characterization in terms of physiology and morphology has not been published yet. In this study, this representative was tested in terms of its ionizing and non-ionizing radiation tolerance and compared to other members of this genus.

1.3.4 Tolerance of (hyper-) thermophilic archaea to radiation

Several thermophilic, and hyperthermophilic archaea have been tested with respect to their tolerance against ionizing, and non-ionizing radiation (Beblo *et al.*, 2011). One of the tested microorganisms was *I. hospitalis* in axenic culture, as well as in co-culture with *N. equitans*. Viable cells of *I. hospitalis* have been detected after an applied dose of 20 kGy (^{60}Co radiation exposure), independent from (co-) cultivation (Beblo *et al.*, 2011). All tested organisms showed comparable tolerances to non-ionizing radiation (Beblo *et al.*, 2011).

1.4 Radiation and its effects

Radiation can be divided into two types, ionizing and non-ionizing radiation. Both types can cause severe damages to biological systems. The damages caused by radiation and the ways to cope with them will be discussed in the following Sections.

1.4.1 Non-ionizing radiation

Solar electromagnetic radiation consists of visible light with wavelengths in the range of 400-700 nm and of a large proportion of short, more energetic wavelengths. These highly energetic wavelengths (100-400 nm) are covered by the ultraviolet (UV) spectrum. This spectrum is composed of UV-C (100-280 nm), which is essentially absorbed by atmospheric oxygen and the ozone layer of today's Earth. Large quantities of UV-B (280-315 nm) are efficiently absorbed by ozone as well, while UV-A (315-400 nm) are easily transmitted to Earth's surface (Figure 8) (according to Madronich *et al.*, 1998).

All biological systems are rich in UV-absorbing molecules like nucleic acids and proteins. DNA is one of the key targets, and UV-induced damages can result in both cytotoxic and genotoxic effects (according to Sinha & Häder, 2002). The two major photoproducts caused by high-energy short-wavelength UV-C radiation (190-290 nm), resulting in mutagenic DNA lesions, are cyclobutane-pyrimidine dimers (CPDs) between adjacent thymine or cytosine residues and pyrimidine(6-4)pyrimidone photoproducts ((6-4)PPs) (Yoon *et al.*, 2000; Rolfsmeier *et al.*, 2010; reviewed in Sage, 1993; according to Pfeifer, 1997). For the variety of additional DNA damages induced by radiation see Figure 11. To conduct experiments with microorganisms most researchers use a low pressure mercury lamp, emitting its energy mainly at 254 nm, the wavelength near the peak of DNA absorption, and assessed satisfying organismic sensitivity (according to Coohill & Sagripanti, 2008; Jagger, 1967; Taghipour, 2004).

Several DNA repair mechanisms have evolved to repair DNA damages, including UV-C induced DNA lesions, and are distributed along the tree of life. There are e.g. two excision repair pathways represented by base excision repair (BER) and nucleotide excision repair (NER) and two recombinational repair mechanisms, namely homologous recombination (HR) and non-homologous end-joining (NHEJ). The latter one is known to be present e.g. in *Bacillus subtilis* (De Vega, 2013), and photoreactivation is used by several organisms including halophilic archaea (Leuko *et al.*, 2011). For more information and detailed review see Rastogi *et al.*, 2010.

To repair UV-C induced DNA lesions two repair mechanisms are of particular importance and are present in all three domains of life. One is the light-independent (“dark repair”), NER (e.g. Rastogi *et al.*, 2010; Kelman & White, 2005), whereas photoreactivation by the enzyme photolyase is driven by light (“light repair”) (Roflsmeier *et al.*, 2010; for detailed reviews see Sancar, 1996 and Sancar, 2003), and can be found within Archaea (e. g. Leuko *et al.*, 2011). The latter one uses light with a wavelength of 350-450 nm as an energy source or as a cosubstrate (Sancar, 2003; Rupert *et al.*, 1958). This photolyase dependent light repair has been found in several Archaea (e. g. Leuko *et al.*, 2011; Kiontke *et al.*, 2011), and this enzyme is considered to be an ancient repair enzyme, which may have helped in organismic evolution on primordial Earth (according to Sinha & Häder, 2002; according to Carell & Epple, 1998; Woese *et al.*, 1978).

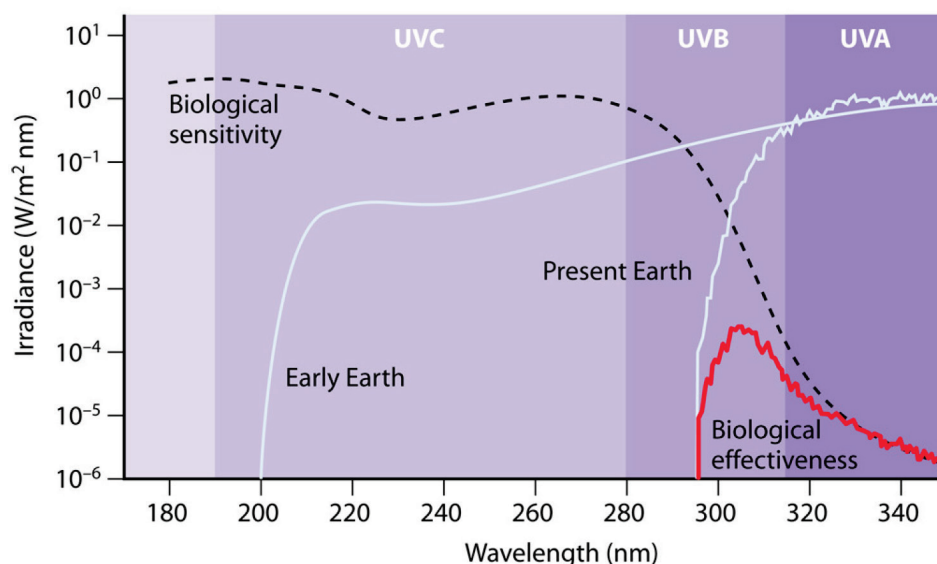


Figure 8: Solar radiation spectrum reaching Earth’s surface compared to the action spectrum predominating on early Earth. Dashed line: DNA damage action spectrum as example for biological sensitivity. Red line: Biological effectiveness (according to Horneck *et al.*, 2010).

1.4.2 Ionizing radiation

Life has always been exposed to radiation until today. Natural background radiation, in terms of ionizing beta and gamma rays, from geologic sources caused by e.g. decay of radioactive elements in Earth's crust, or ^{40}K acting as internal emitter within cells, and cosmic radiation are only some examples (Karam *et al.*, 2001). Life was and still is able to cope with different types of radiation and radiation induced damages, which will be discussed in the following Sections.

Different types of ionizing radiation, such as X- and γ -rays, α - and β -particles, neutrons and heavy ions have differing biological effects. The relative biological effectiveness (RBE) of a particular type of ionizing radiation describes the relative amount of biological damages given by the same amount of absorbed energy. RBE depends on the spatial density of ionizing events per unit of absorbed dose in the biological system (according to Baumstark-Khan & Facius, 2001; according to Powell, 1959; Goodhead, 1999). Ionization events caused by e.g. γ -rays are homogeneously distributed within the cell (low Linear Energy Transfer (LET)), whereas particles with high LET produce clusters of ionization (Figure 9) (according to Baumstark-Khan & Facius, 2001; according to Powell, 1959; Goodhead, 1999). The damage caused by energetic charged particles is normally higher compared to the same dose of energetic photons (X-rays, γ -rays) (according to Baumstark-Khan & Facius, 2001) due to more complex types of damage in a small volume.

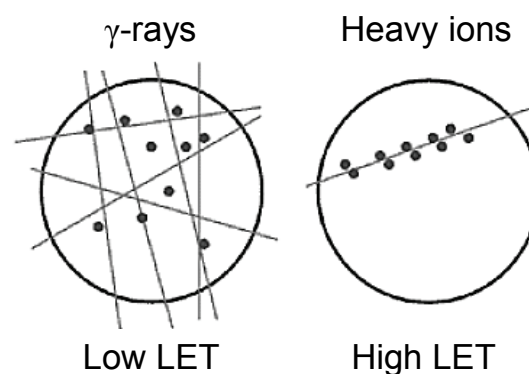


Figure 9: Schematic representation of ionizations caused by radiation with low, or high LET (adapted from Baumstark-Khan & Facius, 2001; according to Powell, 1959).

1.4.3 Effects on biological systems

The impact of ionizing radiation on biological systems is characterized by direct and indirect effects (Figure 10). The inactivation of molecules by direct radiation effects is

proportional to the applied dose, whereas indirect radiation effects on molecules depend on the dose and their concentration (according to Baumstark-Khan & Facius, 2001). As described in the upper Section, clusters formed by sparsely ionizing radiation (low LET) are spatially more distributed compared to clusters produced by densely ionizing radiation (high LET). The ionization increases with increasing LET, with the result that the number of changed molecules, and radiation effects increases as well (according to Baumstark-Khan & Facius, 2001). The radiolysis of water or the surrounding solution forms highly reactive radicals being the reason for indirect radiation effects on e.g. DNA (Jones *et al.*, 1994). Other targets of these indirect radiation effects are proteins and RNA. These biological molecules, which are essential for life, can additionally be damaged by direct energy absorption (direct energy effects) (Michaels & Hunt, 1978; Jones, *et al.*, 1994). Not only radiation effects on the surrounding medium can produce reactive damaging radicals, direct effects on intracellular water can result in indirect effects on target molecules (Michaels & Hunt, 1978).

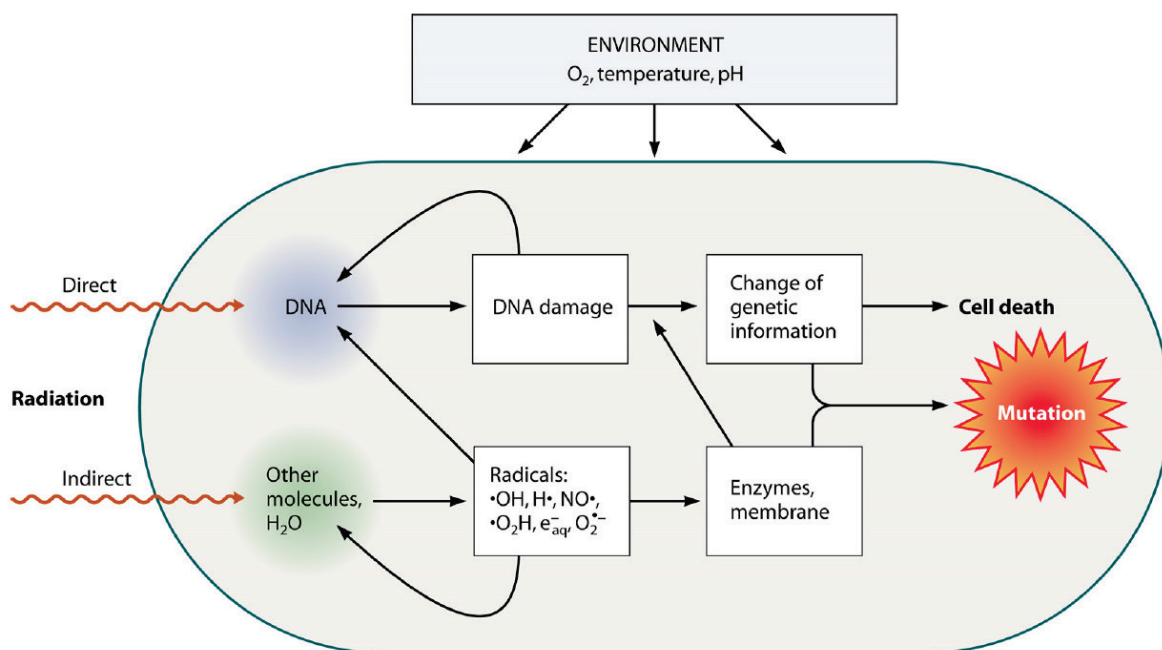


Figure 10: Damages on cellular level caused by ionizing radiation following direct or indirect interactions (according to Horneck *et al.*, 2010).

1.4.4 Effects on DNA

Radiation, either of ionizing or non-ionizing nature, has adverse effects on DNA integrity; the effect of chemicals will not be considered in the following. DNA is the most important biological molecule for cellular organisms. It contains all genetic information for a cell's structure and function, and all information needed for maintenance. The process of DNA

replication ensures an accurate transfer of the same genetic information from a parental cell to the progeny (according to Baumstark-Khan & Facius, 2001). The damage of this molecule by physical and chemical agents is therefore severe for an organism's survivability. Figure 11 gives an impression on the diversity of DNA damages that can be caused by radiation.

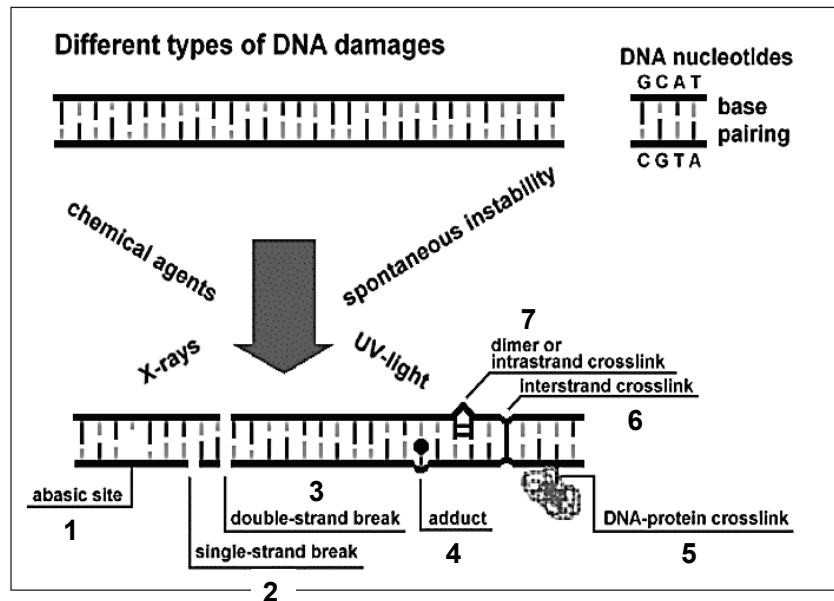


Figure 11: Different types of DNA damages caused by either radiation or chemical agents. The numbers indicate repair mechanisms involved in the reversal of these damages. (1) Base excision repair, (2) ligation, (3) ligation, recombination, (4) direct repair, base excision repair, nucleotide excision repair, (5) direct repair, nucleotide excision repair, (6) nucleotide excision repair, recombination, (7) direct repair, nucleotide excision repair (adapted from Baumstark-Khan & Facius, 2001).

1.5 DNA repair pathways in Archaea

Since the beginning of the evolution of life, organisms have to guarantee their DNA integrity. The environmental conditions as they prevailed on early Earth were harsh and hostile for life. Life had to cope with higher radiation intensities in terms of non-ionizing and ionizing radiation compared to present Earth. Efficient repair mechanisms have evolved to repair radiation induced damages besides damages caused by other environmental parameters e.g. temperature. Hyperthermophilic organisms, which are in the focus of this work, and thermophilic microorganisms have developed several repair mechanisms allowing them an adaptation to their hot environment (reviewed in Grogan, 1998 and Grogan, 2000) and allow them to withstand periods of high radiation intensities (Beblo *et al.*, 2011). In terms of DNA repair pathways, Archaea seem to combine universal bacterial and eukaryal-like repair proteins and pathways (according to Grogan, 2004 and Kelman & White, 2005) that include the direct reversal of the DNA damage, the excision of bases or whole nucleotides, and recombination (according to Seitz *et al.*, 2001 and

Friedberg *et al.*, 1995). Several DNA repair pathways have evolved to cope with different types of damage (Figure 11). Besides direct reversal of DNA damages, numerous repair mechanisms can be found among all living cells (according to Lindahl & Wood, 1999) which are universally distributed in all three domains of life. Seitz *et al.* extensively reviewed in 2001 three repair pathways relevant for Archaea whereof photoreactivation found in e.g. halophilic archaea (Leuko *et al.* 2011) is not taken into account (see paragraph 1.4.1.). Additional information will be given in the following.

DNA double strand breaks or single strand breaks are repaired by (homologous) recombination. For this, the damaged DNA is paired with a homologous partner to copy the lost information for accurate repair (Seitz *et al.*, 2001). Base excision repair (BER), the removal of nonbulky DNA lesions, is accomplished by DNA glycosylases which cleave the glycosidic bond between the base and the deoxyribose. An AP site (apurinic/apyrimidinic site) is generated by AP lyases and endonucleases which finally release the abasic sugar moiety (according to Friedberg *et al.*, 1995, according to Sancar, 1996; Wood *et al.*, 1997); the DNA is prepared for excision, repair synthesis, and ligation (Seitz *et al.*, 2001). Nucleotide excision repair (NER), describes the enzymatic removal of oligonucleotides especially pyrimidine dimers and (6-4) photoproducts as whole nucleotides within an oligonucleotide fragment (Seitz *et al.*, 2001). Seitz *et al.* concluded that Archaea possess proteins involved in DNA repair which are related to both Bacteria and Eukarya and others that are more distantly related. Therefore, a clear classification of (hyperthermophilic) archaea in terms of mechanisms to maintain genome integrity, and DNA repair mechanisms cannot clearly be made (according to Seitz *et al.*, 2001 and Grogan, 2015).

1.6 Aim of this work

Earth has been inhabited since the Archaean Age, and terrestrial life has been present since about 3.8 Ga or earlier. The prevailing environmental conditions during that time were harsh and hostile for life compared to present day's environmental conditions. The UV-absorbing ozone layer was lacking due to the essentially anoxic atmosphere (Grenfell *et al.*, 2010; Holland, 1999), enabling solar ultraviolet radiation composed of short wavelengths to penetrate Earth's surface increasing the overall terrestrial UV stress (Cockell and Horneck, 2001; Margulis *et al.*, 1976). The circumstances and potential settings under which life evolved fascinated and encouraged me to investigate hyperthermophilic microorganisms in terms of their tolerance against radiation of different types. Interesting candidates for early Earth inhabitants are phylogenetic deep-branching, strictly anaerobic living, stress-tolerant organisms from the genus *Ignicoccus* (Paper *et al.*, 2007; Huber *et al.*, 2000; Beblo *et al.*, 2011). Experiments with non-ionizing radiation (UV-

C) were conducted with all four known representatives to test their tolerance against this type of radiation. Whereas, experiments with ionizing radiation were solely conducted with the radiation-tolerant *I. hospitalis* and “*I. morulus*”; genomic DNA extractions of untreated “*I. morulus*” cells showed additional plasmids besides its genomic DNA making it interesting for further studies. All experiments dealing with DNA repair and coherent expression of genes playing an important role in these repair processes were exclusively conducted with *I. hospitalis*.

Subsequent experiments were designed to find answers to the following questions:

- Which fluence intensity and ionizing radiation dose can be survived by *I. hospitalis* and the other representatives?
- Does active enzymatic repair influence the radiation tolerance of *I. hospitalis*?
- Is it possible to determine the boundaries for life as we know it with subsequent experimentation?
- What is the definition of survivability by the example *I. hospitalis*?
- Does the environment play a role in radiation tolerance and cell survivability of an organism?
- Does “quorum sensing” exist for *I. hospitalis* and can cells be revived?
- How does radiation impact the genomic DNA integrity of *I. hospitalis*?
- Is *I. hospitalis* able to repair radiation induced DNA damages?
- What mechanisms are involved in DNA repair?

A hot origin of life is assumed in this work and *Ignicoccus* is seen as a potential candidate for an early Earth inhabitant. The underlying experiments were designed to support this assumption and will give reasonable explanations.

2 Material and Methods

2.1 Sources of supply

2.1.1 Chemicals

All chemicals were of analytical grade or better and were purchased either from Serva Electrophoresis GmbH (Heidelberg, Germany), VWR International GmbH (Darmstadt, Germany), Sigma-Aldrich Chemie GmbH (Steinheim, Germany), Alfa Aesar GmbH & Co. KG (Karlsruhe, Germany), Carl Roth GmbH & Co. KG (Karlsruhe, Germany), or AppliChem GmbH (Darmstadt, Germany).

Table 1: Chemicals used for experimentation.

Substance	Chemical formula	Manufacturer
1-Bromo-3-chloropropane	C_3H_6BrCl	VWR
2-Propanol	$CH_3CH(OH)CH_3$	VWR
8-Hydroxyquinoline	C_9H_7NO	VWR
Agarose for DNA electrophoresis	-	Serva
Agarose low melting for nucleic acid electrophoresis of DNA/RNA	-	Serva
Ammonium acetate	$CH_3CO_2NH_4$	Sigma-Aldrich
Ammonium sulfate	$(NH_4)_2SO_4$	Roth
Boric acid	H_3BO_3	VWR
Bromphenol blue sodium salt	$C_{19}H_9Br_4NaO_5S$	Sigma-Aldrich
Calcium chloride dihydrate	$CaCl_2 \times 2 H_2O$	VWR
Diethyl dicarbonate (DEPC)	$C_6H_{10}O_5$	AppliChem
EMSURE [®] ethanol, absolute	C_2H_5OH	VWR
Ethidium bromide solution (EtBr) (10 mg/ml)	$C_{21}H_{20}BrN_3$	Roth
Ethylenediaminetetraacetic acid (EDTA)	$C_{10}H_{16}N_2O_8$	Sigma-Aldrich
Ethylenediaminetetraacetic acid disodium salt (Na_2EDTA)	$C_{10}H_{14}N_2Na_2O_8$	Sigma
Glacial acetic acid	CH_3COOH	VWR
Glycerol	$C_3H_8O_3$	Sigma-Aldrich
Guanidine thiocyanate	$C_2H_6N_4S$	VWR
Guanidinium chloride	CH_6ClN_3	VWR
Hydrochloric acid fuming 37 %	HCl	VWR
Magnesium chloride hexahydrate	$MgCl_2 \times 6 H_2O$	VWR
Magnesium sulfate heptahydrate	$MgSO_4 \times 7 H_2O$	VWR
Phenol	C_6H_6O	VWR
Phenol/Chloroform/Isoamylalcohol (25:24:1)	-	Applichem
Potassium acetate	CH_3COOK	VWR
Potassium chloride	KCl	Sigma-Aldrich
Potassium dihydrogen orthophosphate	KH_2PO_4	VWR
Potassium ethyl xanthogenate, 96%	$C_2H_5OCS_2K$	Sigma-Aldrich
Potassium iodide	KI	Sigma-Aldrich
Resazurin Na-salt	$C_{12}H_6NO_4 \cdot Na$	Serva
Sodium acetate	CH_3COONa	VWR
Sodium bromide	NaBr	AppliChem
Sodium chloride	NaCl	VWR
Sodium dodecyl sulfate (SDS)	$C_{12}H_{25}NaO_4S$	Sigma-Aldrich
Sodium hydrogen carbonate	$NaHCO_3$	VWR

Table 1: Chemicals used for experimentation (continued).

Substance	Chemical formula	Manufacturer
Sodium hydroxide pellets extra pure	NaOH	VWR
Sodium sulfide nonahydrate	Na ₂ S x 9 H ₂ O	Sigma-Aldrich
Strontium chloride hexahydrate	SrCl ₂ x 6 H ₂ O	Alfa Aesar
Sulfur	S ⁰	Sigma-Aldrich
Tris ultrapure	C ₄ H ₁₁ NO ₃	AppliChem
Triton™ X-100	-	Sigma-Aldrich

2.1.2 Standards

DNA standard

- GeneRuler 1 kb DNA Ladder Thermo Scientific (Waltham, USA)
- GeneRuler 1kb Plus DNA Ladder Thermo Scientific (Waltham, USA)

RNA standard

- RiboRuler High Range RNA Ladder Thermo Scientific (Waltham, USA)

2.1.3 PCR reagents and cDNA synthesis

RAPD

- Platinum® Taq DNA Polymerase Invitrogen (Carlsbad, USA)
- 100 mM dTTP, dGTP, dATP, dCTP Invitrogen (Carlsbad, USA)

qRT-PCR

- KAPA SYBR® FAST qPCR Kit Master Mix (2x) Universal Kapa Biosystems (Wilmington, USA)

DNase I digestion

- peqGOLD DNase I Peqlab (Erlangen, Germany)

cDNA synthesis

- peqGOLD cDNA Synthesis Kit H Minus Peqlab (Erlangen, Germany)

2.1.4 Oligonucleotides

All oligonucleotides were purchased from Sigma-Aldrich (Sigma-Aldrich Biochemie GmbH, Hamburg, Germany).

2.1.4.1 RAPD primer

The single decameric primer used for RAPD (randomly amplified polymorphic DNA) was designed according to the sequence published by Lepage *et al.*, 2004 (Table 2). The primer sequence was used as a nucleotide query to search for potential binding sites in *Ignicoccus hospitalis* KIN4/l complete genome (NCBI Reference Sequence NC_009776.1) using NCBI/blastn.

Table 2: Primer used for RAPD analysis. This primer was used to analyze the genomic DNA integrity of *Ignicoccus hospitalis* and "*Ignicoccus morulus*". *(Number of matches in the annotated genome of *I. hospitalis*).

Type	Name	Sequence (5'→3')	Length	Number of matches*	Source
RAPD	P2	GGGGCCCTAC	10	1211	Lepage <i>et al.</i> , 2004

2.1.4.2 qRT-PCR primers for gene expression and qPCR primers for DNA damage detection after ^{60}Co radiation exposure

Primers were designed based on the *I. hospitalis* complete genome sequence available on the NCBI Reference Sequence NC_009776.1 (see Appendix). They were designed using the web-based program Primer3web Version 4.0.0 (<http://primer3.ut.ee/>) and checked for primer dimer formation using the online platform OligoCalc (<http://biotools.nubic.northwestern.edu/OligoCalc.html>).

The presence of each gene in *I. hospitalis* strain was verified by PCR amplification using the specific primer pair. The resulting products were analyzed by agarose gel electrophoresis (see Appendix). The primers were used for gene expression studies by qRT-PCR (Table 3, 4).

The relative amount of DNA lesions after ^{60}Co radiation exposure was determined using the primer pair listed in Table 5.

Table 3: *Ignicoccus hospitalis* specific primers used for qRT-PCR. In light gray: Primers specific for potential housekeeping genes; Others: Primers specific for DNA repair genes. The primer binding site (Start*) refers to the nucleotide position in the specific sequence (Sequence*).

Name of primer	Gene description (NCBI)	Locus tag	Sequence (5'→3')	Length (bp)	for/rev	Binding (Start*)	Product (bp)	Sequence*
16S rRNA	16S ribosomal RNA	IGNI_RS04235	GTAGTCCCGGCTGTAAACGAT	21	for	741	224	NC_009776.1 (728379..729800)
			CTTCAGCCTGACCTTCATCCT	21	rev	964		
Mips	myo-inositol-1-phosphate synthase	IGNI_RS04495	GGCTATAGGGACAGGAAGT	20	for	864	104	NC_009776.1 (771144..772307)
			CGGGCGAGTCATTAATCCTC	20	rev	967		
Thermosome	thermosome subunit	IGNI_RS00515	AGGGTAGGCAAGGACAAAGAT	20	for	1069	126	NC_009776.1 (89714..91390)
			GAGAGCGTCGGTTATGTTCC	20	rev	1194		
znuC	hypothetical protein	IGNI_RS00620	CGTAGTGATGATGGGCTCA	20	for	261	151	NC_009776.1 (107253..108068)
			CACCCCTCTGCTTTTGTCTC	20	rev	411		
pol E'	DNA-directed RNA polymerase subunit E'	IGNI_RS00455	AGGAGCTCGGATAATTCTG	20	for	198	201	NC_009776.1 (81589..82122)
			TACCGTCTATGGGGCCATG	20	rev	398		
rad2	endonuclease	IGNI_RS03580	TCTCCTCGCTGGTTAGGAA	20	for	553	122	NC_009776.1 (624002..625054)
			CCTCCAGCACACACTTCAA	20	rev	664		
rad50	hypothetical protein	IGNI_RS07180	CGAGTTGGTGGAGTTGAGTC	20	for	2478	110	NC_009776.1 (1245174..1247795)
			TGGGGTGCCCTTATAGTAGT	20	rev	2587		
recB	recombinase B	IGNI_RS02490	GGGGTCAAGAGAGGTTTATG	20	for	360	216	NC_009776.1 (430537..431124)
			CCCTTCAAGAGCTTCCACAA	20	rev	575		
radA	DNA repair and recombination protein RadA	IGNI_RS05180	CAAGCTGGCGAAGTTTACA	20	for	732	174	NC_009776.1 (896102..897085)
			ACCCTCGCTATCCTCTTTGTT	20	rev	905		
Photolyase	radical SAM protein	IGNI_RS04065	AAGTACAGCTCCCAACCGTA	20	for	64	113	NC_009776.1 (699797..700654)
			TCGAGCCTCTCCAAGAGTT	20	rev	176		

Table 4: *Ignicoccus hospitalis* specific primers used for qRT-PCR. Primers specific for genes involved in replication. The primer binding site (Start*) refers to the nucleotide position in the specific sequence (Sequence*).

Name of primer	Gene description (NCBI)	Locus tag	Sequence (5'→3')	Length (bp)	for/rev	Binding (Start*)	Product (bp)	Sequence*
ccrB	chromosome condensation protein CcrB	IGNI_RS04740	TCCACCTTCGCTGCTGATA	19	for	232	109	NC_009776.1 (816604..816975)
			CCAGACGACCGAGACTAT	19	rev	340		
cdc6	cell division control protein Cdc6	IGNI_RS01295	GTATAGGGTCTAGCGAGGA	20	for	327	207	NC_009776.1 (216447..217658)
			ACGTCTCGTTTATCCTGGT	20	rev	533		
cdc6-orc1	ORC complex protein Cdc6/Orc1	IGNI_RS06675	GGCCACGGTATTAAACAGCA	20	for	333	225	NC_009776.1 (1150318..1151592)
			ACGTGACCCCTCTCTTCTT	20	rev	557		
dbp1	DNA-binding protein	IGNI_RS00915	GTTAGGGTCGGTAAAGACC	20	for	31	120	NC_009776.1 (156959..157252)
			GTCTACCGCCTTGCTATGG	20	rev	150		
ber	base excision DNA repair protein	IGNI_RS04460	TCCAGAACACACACAGAGAA	20	for	118	221	NC_009776.1 (765361..765999)
			ACGCCTTGTCTCCCTTTTC	20	rev	338		
poll	DNA polymerase I	IGNI_RS03575	GTTGTGGGGGAGAAAGAGG	20	for	2258	239	NC_009776.1 (621184..623928)
			CGCGGATGTTCTTAGTGT	20	rev	2496		
mcm	replicative DNA helicase Mcm	IGNI_RS06685	AGAGTACGTGCGCAAGTTA	20	for	335	152	NC_009776.1 (1151795..1153864)
			GGTAGGGCTTGTTAGTACT	20	rev	486		
tfb	transcription initiation factor IIB	IGNI_RS07105	CTCTGAACCTCCCGAAAC	19	for	393	206	NC_009776.1 (1227915..1228865)
			AACACTGGCCACTCTTTC	20	rev	598		
fen-1	endonuclease	IGNI_RS03580	GCAAAGCTGACGAGGAGAT	20	for	385	200	NC_009776.1 (624002..625054)
			CTCACGGCCAAAGTTCCTAAC	20	rev	584		
rg	reverse gyrase	IGNI_RS02665	TTCGACGGCTTCCTCTTAGT	20	for	3256	226	NC_009776.1 (457134..460913)
			CCACCTTGCTCAGAGTTACG	20	rev	3481		

Table 5: *Ignicoccus hospitalis* specific primers used for qPCR to detect genomic DNA damages after ⁶⁰Co radiation exposure. The primer binding site (Start*) refers to the specific sequence (Sequence*). "*Ignicoccus morulus*" genomic DNA integrity was analyzed by qPCR after gamma ray (⁶⁰Co radiation) exposure using this primer (Dbr) as well.

Name of primer	Gene description (NCBI)	Locus tag	Sequence (5'→3')	Length (bp)	for/rev	Binding (Start*)	Product (bp)	Sequence*
Dbr	16S ribosomal RNA	IGNI_RS04235	CTAAGCCATGGGAGTCGAAC	20	for	27	1368	NC_009776.1 (728379..729800)
			ACGGTACCTTGTTACGACT	20	rev	1394		

2.1.5 Buffers

<u>50x TAE (stock solution):</u>	242 g	Tris (solved in 500 ml ddH ₂ O)
	100 ml	0.5 M Na ₂ EDTA (pH 8.0)
	57.1 ml	Glacial acetic acid
	ad 1000 ml	ddH ₂ O
<u>1x TAE (working solution):</u>	20 ml	50x TAE
	ad 1000 ml	ddH ₂ O
<u>DNA Loading dye (6x):</u>	3 ml	Glycerol
	25 mg	Bromphenol blue Na-salt
	ad 10 ml	ddH ₂ O

RNase-free ddH₂O (DEPC treated water)

One ml of 0.1 % DEPC were added to 1000 ml ddH₂O, placed on a magnetic stirrer and stirred over night at room temperature, followed by autoclaving (121 °C, 20 min) to inactivate the remaining DEPC.

2.1.6 Gas mixtures

- | | |
|--|-------------------------|
| • Forming gas (N ₂ /H ₂ , 95:5, v/v) | Linde (Munich, Germany) |
| • N ₂ /CO ₂ (80:20, v/v) | Linde (Munich, Germany) |
| • H ₂ /CO ₂ (80:20, v/v) | Linde (Munich, Germany) |

2.2 Strains and cultivation

2.2.1 Strains

All strains were obtained from the culture collection of the Lehrstuhl für Mikrobiologie & Archaeenzentrum, University Regensburg.

- | | |
|---------------------------------|--------------------------------|
| • <i>Ignicoccus hospitalis</i> | KIN4/I, DSM 18386 ^T |
| • “ <i>Ignicoccus morulus</i> ” | (provided by Dr. Harald Huber) |
| • <i>Ignicoccus pacificus</i> | LPC33, DSM 13166 ^T |
| • <i>Ignicoccus islandicus</i> | Kol8, DSM 13165 ^T |

2.2.2 Media

2.2.2.1 SME medium (Synthetisches Meerwasser/synthetic sea water) (Stetter *et al.*, 1983, Pley *et al.*, 1991, modified by Huber *et al.*, 2006)

<u>Substance</u>	<u>Amount</u>	<u>Concentration</u>
NaCl	27.7 g	473.99 mM
MgSO ₄ x 7 H ₂ O	7.0 g	28.4 mM
MgCl ₂ x 6 H ₂ O	5.5 g	27.1 mM
CaCl ₂ x 2 H ₂ O	0.75 g	5.1 mM
KCl	0.65 g	8.7 mM
NaBr	0.1 g	0.97 mM
H ₃ BO ₃	0.03 g	0.49 mM
SrCl ₂ x 6 H ₂ O	0.015 g	0.056 mM
KI	0.5 g	3 mM
ddH ₂ O	ad 1000 ml	

The components were dissolved in ~800 ml ddH₂O in the order listed. The volume was adjusted to 1000 ml with ddH₂O.

2.2.2.2 ½ SME+S⁰ medium for all *Ignicoccus* representatives (Paper *et al.*, 2007)

<u>Substance</u>	<u>Amount</u>	<u>Concentration</u>
SME	500 ml	½ x
KH ₂ PO ₄	0.5 g	3.7 mM
(NH ₄) ₂ SO ₄	0.25 g	1.9 mM
NaHCO ₃	0.16 g	1.9 mM
Resazurin (0.1 %)	1 ml	0.0001 %
Na ₂ S x 7-9 H ₂ O	0.5 g	2.1 mM
ddH ₂ O	ad 1000 ml	

All components (except Na₂S x 7-9 H₂O) were dissolved in ~800 ml ddH₂O. The final volume was adjusted to 1000 ml with ddH₂O. The following preparatory steps to obtain the anaerobic ½ SME medium followed the protocols by Hungate (1950), Miller and Wolin (1974) and were performed according to Balch and Wolfe (1976). The preparation is illustrated in Figure 12. One half SME medium was transferred in a 1l Duran[®] glass bottle (DURAN Group GmbH, Wertheim, Germany), closed with a rubber plug and secured by a

pierced screw cap **(1)**. Dissolved oxygen was removed by purging N_2/CO_2 gas (80:20 v/v, Linde) for 20 min, 0.5 bar, with pressure compensation **(2)**. The remaining oxygen was removed by adding the reducing agent $\text{Na}_2\text{S} \times 7-9 \text{ H}_2\text{O}$ (0.5 g dissolved in 2 ml dd H_2O) resulting in the discoloring of the redox indicator Resazurin **(3)**. The resultant pH was 5.5-6.0. Anoxic medium was then dispensed under N_2/H_2 (95:5, v/v) atmosphere in the anaerobic chamber (COY chamber, COY Laboratory Products Inc., Arbor, USA), with 20 ml per 120 ml serum bottle (Glasgerätebau Ochs, Bovenden, Germany), and one spatula of elemental sulfur added (resulting in $\frac{1}{2} \text{SME}+\text{S}^0$ medium, unless otherwise indicated) **(4)**. All bottles were closed with butyl rubber septa (Glasgerätebau Ochs, Bovenden, Germany), and sealed with 20 mm aluminum rings (WICOM, Heppenheim, Germany) **(5)**. Gas exchange (evacuation and re-fill with the respective gas mixture) occurred with H_2/CO_2 (80:20, v/v) at 1.5 bar repeating this cycle three times with a final pressure of 1.5 bar/bottle **(6)**. Prepared serum bottles containing the sulfur containing $\frac{1}{2} \text{SME}$ medium were sterilized by autoclaving for 60 min at 110°C.



Figure 12: Exemplaric illustration of $\frac{1}{2} \text{SME}+\text{S}^0$ medium preparation. **(1)** $\frac{1}{2} \text{SME}$ medium in 1 l Duran® glass bottle. The blue color is caused by Resazurin. **(2)** Removing the dissolved oxygen by purging N_2/CO_2 gas with pressure compensation. **(3)** Discoloring of Resazurin by addition of $\text{Na}_2\text{S} \times 7-9 \text{ H}_2\text{O}$. **(4)** Dispersion of medium in COY chamber and addition of sulfur. **(5)** Serum bottles containing the $\frac{1}{2} \text{SME}+\text{S}^0$ medium were sealed with aluminum rings. **(6)** Gas exchange with H_2/CO_2 .

2.2.3 Cultivation

2.2.3.1 Stock cultures

Stock cultures of *I. hospitalis*, "*I. morulus*", *I. pacificus*, and *I. islandicus* were continuously maintained, and stored at room temperature. Fresh cultures were inoculated with 0.2 ml of original stock (provided by Dr. Harald Huber) every ~6 months to ensure continued viability.

2.2.3.2 Anaerobic cultivation

Twenty ml of $\frac{1}{2}$ SME+S⁰ medium were inoculated with 0.2 ml of a stationary phase *Ignicoccus* culture ($\sim 1 \times 10^7$ cells/ml) using a 1 ml SOFT-JECT[®] syringe (Henke-Sass Wolf GmbH, Tuttlingen, Germany) with a 0.6 x 30 mm NEOLUS needle (TERUMO[®], Eschborn, Germany) (Figure 13). Incubation temperature was set to 90 °C and incubator speed adjusted to 60 rpm in a Thermotron (Infors HT, Bottmingen, Switzerland) over night.



Figure 13: Serum bottle containing 20 ml $\frac{1}{2}$ SME+S⁰ medium, and syringe with 0.6 x 30 mm needle used for inoculation.

2.2.3.3 Phase contrast microscopy of cultures

Cells were routinely observed using a phase contrast microscope (Standard 16, Carl Zeiss, Göttingen, Germany) at 400-fold or 1000-fold magnification.

A Zeiss Axio Imager M2 microscope (Carl Zeiss AG, Oberkochen, Germany) equipped with a Zeiss AxioCam MRm camera was used for microscopic documentation.

2.3 Determination of viable (culturable) and total cell numbers

2.3.1 Total cell number

Total cell numbers were determined microscopically with a 400-fold magnification using a Thoma counting chamber (Depth: 0.02 mm x 0.0025 mm² per small square, Brand GmbH, Wertheim, Germany) and calculated according to the following formulas

$$(1) \quad \text{Cells/ml} = \frac{\text{Total number of cells counted}}{\text{Number of small squares counted}} * \text{Volume of small squares in ml}$$

$$(2) \quad \text{Cells/ml} = \frac{\text{Cells}}{160} * (2 \times 10^7 \text{ ml})$$

2.3.2 Most probable number (MPN) technique to determine growth and reproduction

The e.g. colony forming unit (CFU) method on agar plates was not applicable due to the optimal growth temperature of *Ignicoccus* (T_{opt} 90 °C) and the lack of a plating method. Therefore, the most probable number technique (MPN; Franson, 1985) was used to estimate the concentration of reproducible cells in growth medium in ten-fold dilution steps; potential outliers are within the frame of +/- one log phase.

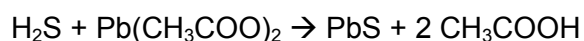
The cultivable cell number of *Ignicoccus* representatives was determined before and after stress exposure by MPN in anoxic serum bottles containing 20 ml ½ SME+S⁰ medium. Serial 1:10 dilutions (2 ml sample transferred to 20 ml ½ SME+S⁰ medium/serum bottle) were conducted and the bottles then incubated at 90 °C, and agitated at 60 rpm for up to six days. Cultivable cells were detected by phase-contrast microscopy as described in paragraph 2.2.3.3.

2.3.3 Detection of metabolic activity by detecting metabolically produced hydrogen sulfide (H₂S)

Ignicoccus hospitalis gains energy from the reduction of elemental sulfur using molecular hydrogen as electron donor, producing H₂S (Huber *et al.*, 2000). This is also true for all other representatives of this genus.

Metabolic activity in terms of H₂S production was qualitatively monitored by dripping a small volume (~10 µl) of the culture onto lead acetate paper (Macherey-Nagel, Düren, Germany). The sulfide ion from metabolically produced H₂S reacts with lead acetate to

insoluble lead sulfide which can be seen as dark brown spots on the paper (Paper *et al.*, 2007).



2.3.4 Determination of survival after stress exposure

The cultivable cell number was determined by MPN to calculate the survival of stress exposed cells using the following formula

$$(3) \quad S = \frac{N}{N_0}$$

with (N) number of cultivable cells after stress exposure, and (N_0) number of cultivable cells before stress exposure (control). Single experiments were performed at least in triplicates. Means and standard deviations were determined. The survival (S) was plotted semi-logarithmically over the applied fluence (UV-C), and dose (X-rays or gamma rays), respectively. The Fluence/Dose (F_{10}/D_{10}) needed to inactivate the population by 90 % were determined by linear regression from the linear parts of the semi-logarithmically plotted survival curves using SigmaPlot 13.0 (Systat Software Inc., San Jose, USA).

2.4 Exposure to radiation

The tolerance of *Ignicoccus* to radiation of different quality has extensively been studied in this work. Genomic DNA integrity was analyzed after heavy ion exposure, whereas survival/inactivation after non-ionizing radiation (UV-C), and ionizing radiation (X-rays, gamma rays) was investigated in more detail. DNA repair, DNA integrity, and gene expression studies after ionizing radiation exposure were conducted as well. All experimental setups are described in the proceeding Sections.

2.4.1 Non-ionizing radiation

2.4.1.1 UV-C source and determination of fluence rates

The impact of non-ionizing radiation on the survival of *Ignicoccus* was tested using a low pressure mercury lamp (NN 8/15, Heraeus, Hanau, Germany) with a main emission line of 254 nm serving as source for monochromatic UV-C radiation. The experiments were conducted in a black painted laboratory (German Aerospace Center, Institute of Aerospace Medicine, Department of Radiation Biology, Cologne, Germany) to avoid any undesirable reflections. The UV-C lamp was switched on 60 min prior to experimentation

to ensure a homogenous fluence during exposure. The samples were placed in the center of the irradiation field with an irradiance of $\sim 148 \mu\text{W}/\text{cm}^2$ for “low dose” (up to $300 \text{ J}/\text{m}^2$) and of $\sim 169 \mu\text{W}/\text{cm}^2$ for “high dose” (up to $3000 \text{ J}/\text{m}^2$). The precise fluence rates were measured with a UV-X radiometer (UVP Ultra-Violet Products, Cambridge, UK) with UV-sensor for 254 nm (UVX-25), and the irradiation time calculated according to the following formula

$$(4) \quad \text{Fluence } (\text{J}/\text{m}^2) = \text{Irradiance } (\text{W}/\text{m}^2) * \text{Irradiation time } (\text{s})$$

The irradiation time varied between 30 seconds and 30 minutes.

2.4.1.2 Measuring the absorption of medium

Before testing the impact of non-ionizing radiation on the survival of *Ignicoccus*, the absorption of different medium combinations with and without cells (see below) was determined photometrically using a spectrophotometer (Hitachi U-3310, Hitachi High-Technologies Europe GmbH, Krefeld, Germany) performing a wavelength scan from 200-400 nm in UV-C transmissible screw-capped quartz cuvettes (Thickness: 10 mm; Volume: 3.5 ml) (Starna, Pfungstadt, Germany). The quartz cuvettes were filled under anoxic conditions and closed airtight to prevent any disturbing impact of oxygen and to simulate the later experimental setup.

- $\frac{1}{2}$ SME medium + sulfur
- $\frac{1}{2}$ SME medium – sulfur
- Stationary phase culture of *Ignicoccus* (different representatives) with $\sim 1 \times 10^7$ cells/ml grown in $\frac{1}{2}$ SME medium + sulfur
- Stationary phase culture of *Ignicoccus* (different representatives) diluted 1:10 (1×10^6 cells/ml) in $\frac{1}{2}$ SME medium + sulfur
- Stationary phase culture of *Ignicoccus* (different representatives) diluted 1:10 (1×10^6 cells/ml) in $\frac{1}{2}$ SME medium - sulfur

2.4.1.3 UV-C irradiation in liquid suspension

The tolerance of *Ignicoccus* to non-ionizing radiation was tested with stationary phase cells which were diluted 1:10 in sulfur-free $\frac{1}{2}$ SME medium. A final cell concentration of 1×10^6 cells/ml was required to exclude any shadowing effects. The exposure to monochromatic UV-C radiation was conducted with all four *Ignicoccus* representatives (namely *I. hospitalis*, “*I. morulus*”, *I. islandicus*, *I. pacificus*) under anoxic conditions in UV-

C transmissible quartz cuvettes while stirring. The cuvettes were placed in the center of the irradiated area on a magnetic stirrer to provide a homogenous irradiation procedure. The experiment was conducted at room temperature and the samples exposed to monochromatic UV-C for increasing periods of time. To exclude any mechanical influence due to stirring, a reference sample (no irradiation) was identically treated and stirred as long as the sample irradiated with the highest fluence intensity. Two ml of stress exposed cells were transferred under anoxic conditions into serum bottles containing 20 ml of $\frac{1}{2}$ SME+S⁰ medium (Figure 14). The dose dependent survivability of *Ignicoccus* after stress exposure was determined by the MPN technique (see 2.3.2), and their growth followed microscopically with a 400-fold magnification (see 2.2.3.3) (Beblo *et al.*, 2011). The survival (S) was plotted semi-logarithmically (see 2.3.4).

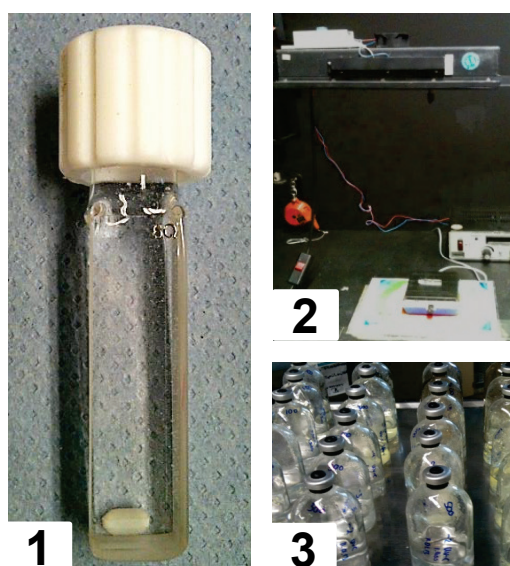


Figure 14: Experimental setup for UV-C exposure in liquid suspension. (1) UV-C transmissible quartz cuvette (Starna, Pfungstadt, Germany) with magnetic stir bar. (2) Low pressure mercury lamp and magnetic stirrer. (3) Serial dilutions conducted after exposure.

2.4.1.4 DNA damage repair by photoreactivation

Photoreactivation, the repair of UV-C induced DNA damages by the enzyme photolyase, is known for e.g. the halophilic archaeon *Halococcus hamelinensis* (Leuko *et al.*, 2011). To test whether *I. hospitalis* has a light-induced photolyase, able to repair non-ionizing radiation induced DNA damages, the following experiment was conducted:

Five *I. hospitalis* stationary phase cultures ($\sim 1 \times 10^7$ cells/ml) were pooled and anaerobically enriched by centrifugation (2 min, 12,000 x g, room temperature). This process was repeated for three cuvettes in total. The cuvettes were placed in the center of the irradiated area on a magnetic stirrer to provide a homogenous irradiation procedure. The experiment was conducted at room temperature and the samples exposed to

150 J/m² monochromatic UV-C. To exclude any mechanical influence due to stirring, a reference sample (no irradiation) was treated identically, and stirred as long as the irradiated samples. Two cuvettes, namely “Darkness” and the unexposed sample (“No UV-C”) were wrapped in aluminum foil directly after UV-C exposure to avoid the activation of a potential photolyase by ambient light. Samples were transferred anaerobically and in darkness into 10 ml preheated $\frac{1}{2}$ SME+S⁰ medium, and were incubated at 90 °C for up to 90 min under light exposure (see Figure 15 (4)). Two ml sample were taken as indicted in Figure 16 and subjected to total RNA extraction. To see whether a potential photolyase was activated due to UV-C induced DNA damages, and following exposure to white light (polychromatic light), qRT-PCR was conducted as described in 2.5.6.

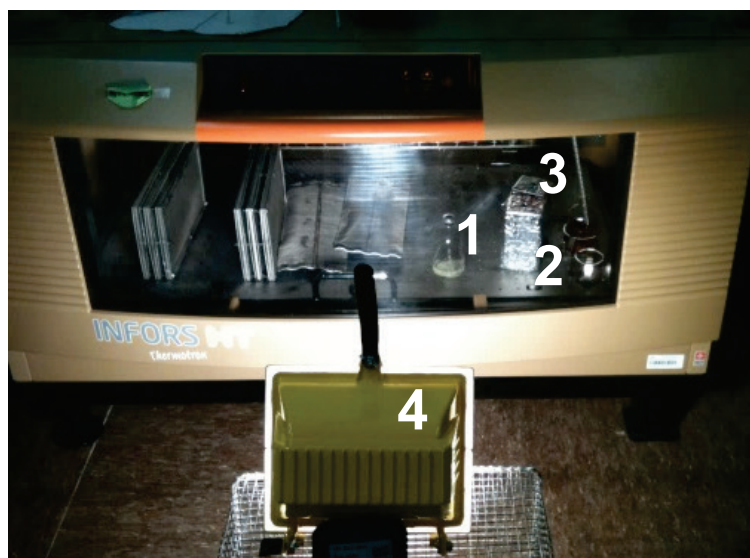


Figure 15: Experimental setup for photoreactivation. The exposed samples were incubated at 90 °C for photolyase activation, and repair. (1) Light (UV-C (150 J/m²), followed by white light exposure), (2) Darkness (UV-C (150 J/m²), no white light exposure) and (3) Control (no UV-C, no white light exposure) were wrapped in aluminum foil to avoid light exposure (4).

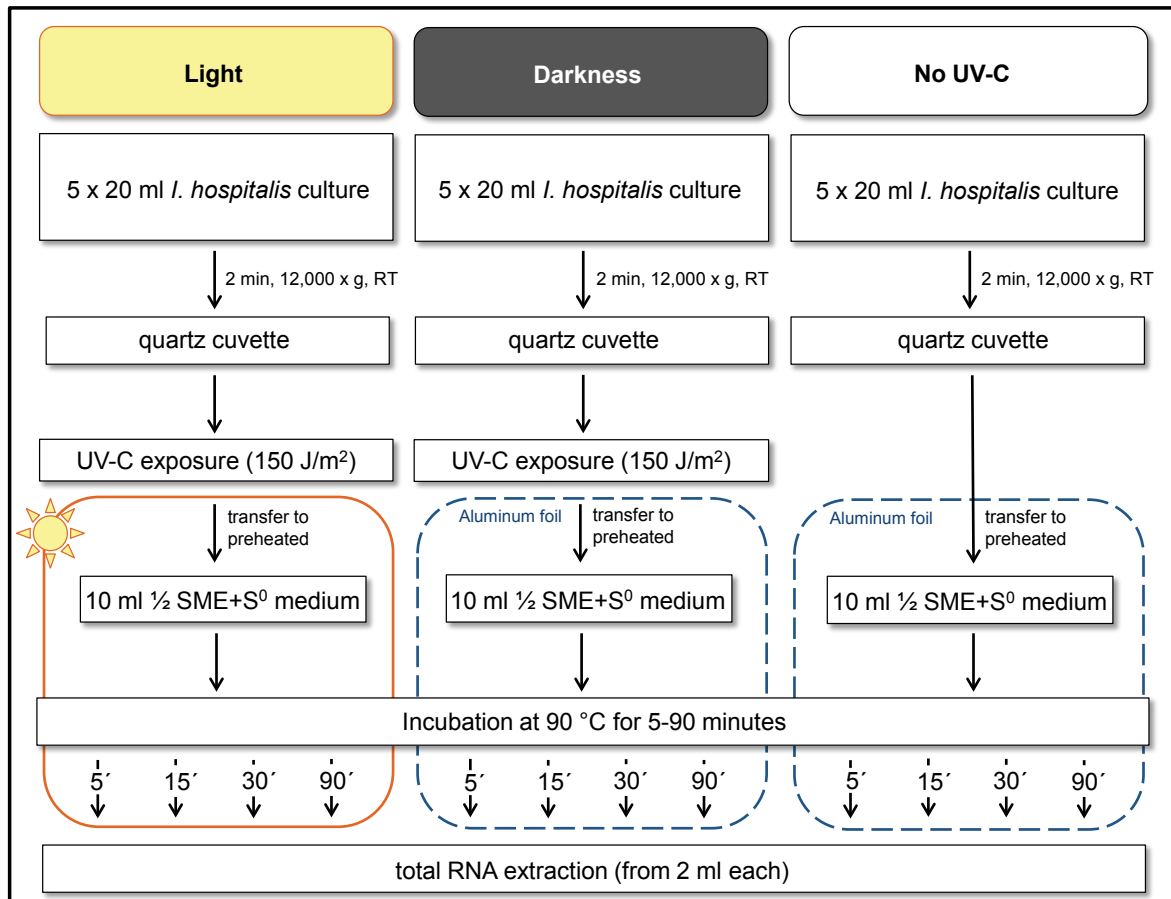


Figure 16: Schematic representation of photoreactivation experiment. Abbreviations: ' (minutes).

2.4.2 Ionizing radiation

2.4.2.1 Heavy ions

Heavy ion experiments, with low and high energy charged particles, were conducted at the HIMAC facility (Heavy Ion Medical Accelerator in Chiba) at the National Institute of Radiological Science (NIRS, Chiba, Japan) to study the biological effects of radiation fields as they occur in space. X-ray experiments were conducted at the DLR (German Aerospace Center, Cologne, Germany), whereas gamma ray exposure was carried out at BGS (Beta-Gamma-Service GmbH, Wiehl, Germany).

I. hospitalis and "*I. morulus*" cells were exposed to heavy ions with low, intermediate and high LET ranges between 2-200 keV/μm. The following ions were chosen: Helium with 150 MeV/n (LET 2.2 keV/μm), the medium LET ion Argon with 500 MeV/n (LET 90 keV/μm) and the high Let ion Iron with 500 MeV/n (LET 200 keV/μm).

For exposure, 200 μl aliquots in 0.2 ml PCR tubes were aerobically prepared with stationary phase *I. hospitalis* and "*I. morulus*" cells (final concentration: 1×10^9 cells/ml).

The aerobic preparation implicated on the one hand a change in color (colorless to pink indicating the presence of oxygen), and on the other hand the death of the strictly anaerobic living *Ignicoccus*. Genomic DNA from each specimen at each dose applied for each selected heavy ion was extracted using XS-buffer. The impact of heavy ions on genomic DNA integrity was analyzed by RAPD band pattern profile comparison. A detailed description for XS-buffer extraction, RAPD, and subsequent horizontal agarose gel electrophoresis can be found in Paragraph 2.5 and following.

2.4.2.2 X-ray source and determination of dose rates

The impact of ionizing radiation (X-rays) on the survivability of *I. hospitalis* was investigated as follows. *I. hospitalis* stationary phase cells were exposed to X-rays in anoxic HPLC vials at the German Aerospace Center (Cologne, Germany). The X-ray dose was applied using a Gulmay RS225A radiation source from Gulmay Medical Limited (Camberley, England). Initial radiation experiments were conducted at 200 kV, and 15 mA using a 0.1 mm Al filter to filter out soft X-rays leaving mainly hard X-rays (higher energy) to penetrate the sample. A dosimeter (PTW Freiburg TM30013, and PTW UNIDOS^{webline} T121-0277, PTW-Freiburg, Germany) was used to determine the dose rate (Gy/min) prior to experimentation. The dose rate for experiments with 0.1 mm Al filter was ~32 Gy/min in a distance of ~10 cm to the X-ray tube assembly.

A similar experiment was conducted without any filter to check whether the use of a 0.1 mm Al filter has any impact on the X-ray tolerance and survival of *I. hospitalis*. The irradiation took place from a distance of ~10 cm to the X-ray tube assembly at a dose rate of ~40 Gy/min.

I. hospitalis cells were exposed in HPLC vials to maintain anoxic conditions during exposure. It should be noted that the HPLC vial itself absorbed between 30-40 % of the applied dose, meaning that the actual dose rate was rather 25 Gy/min than 32 Gy/min by using a 0.1 mm Al filter during exposure, and 28 Gy/min than 40 Gy/min in the case of a filter-less exposure (Table 6). Comparable dose rates were obtained during filter-less exposure (only “HPLC vial filter”) and exposure using a 0.1 mm Al filter + “HPLC vial filter” (Table 6).

Table 6: Impact of 0.1 mm Al filter vs. filter-less exposure on the dose rate in dependence of an additional HPLC filter (here: glass). The distance of the irradiated sample to the X-ray source was ~10 cm for both experimental set ups. The dosimeter used to determine the dose rate was placed at the same height.

	0.1 mm Alu filter	No filter
- HPLC filter	32.11 Gy/min	40.40 Gy/min
+ HPLC filter	24.78 Gy/min	27.69 Gy/min

The applied dose plotted in the following graphs has already been reduced by 40 % (Table 7).

Table 7: X-ray dose applied with or without 0.1 mm Al filter. Abbreviations: x (applied dose), - (no exposure).

	Dose [kGy]											
	1	2	2.5	3	4	5	7.5	10	12.5	15	17.5	20
0.1 mm Al	x	x	-	x	x	x	-	-	-	-	-	-
No filter	x	x	x	x	x	x	x	x	x	x	x	x
-40 % [kGy]	0.6	1.2	1.5	1.8	2.4	3	4.5	6	7.5	9	10.5	12

2.4.2.3 X-ray irradiation in liquid suspension

The irradiation of *I. hospitalis* cells was performed in HPLC vials (Figure 17). Several bottles of stationary phase cultures were pooled anaerobically and transferred into HPLC vials. The vials were placed in the center of the irradiated area, and exposed to X-rays. The experiment was performed at room temperature, and 2 ml of stress exposed cells were transferred into serum bottles containing 20 ml of $\frac{1}{2}$ SME+S⁰ medium. The dose dependent survivability of *I. hospitalis* after stress exposure was determined by the MPN technique (see 2.3.2). The survival (S) was plotted semi-logarithmically (see 2.3.4).



Figure 17: Experimental setup for X-ray exposure in liquid suspension. (1) HPLC vial with sample. **(2)** Gulmay RS225A radiation source from Gulmay Medical Limited. **(3)** Serial dilutions conducted after exposure.

2.4.2.4 Hot exposure

The hot exposure experiment was designed to test whether the incubation of *I. hospitalis* at 90 °C during X-ray exposure had an influence on its survival in comparison to an exposure at room temperature.

Two bottles of 20 ml $\frac{1}{2}$ SME+S⁰ medium were inoculated each with 0.2 ml *I. hospitalis* cells and incubated in the exposure bucket, and in the reference bucket (same setup) at ~90 °C overnight (see Figure 18). This test was conducted to ensure a consistent temperature during exposure. The overnight cultures were anaerobically enriched by centrifugation (2 min, 13,000 x g, RT), split and transferred into two serum bottles containing fresh $\frac{1}{2}$ SME+ S⁰ medium (washing of cells). The cells were counted with a Thoma counting chamber (6×10^6 cells/ml), and incubated for 30 min at 90 °C prior to exposure. One bottle was transferred to the exposure bucket, the other to the reference bucket. The dose rate was determined as described in 2.4.2.2 and the exposure was conducted with ~25 Gy/min at an average temperature of ~88 °C (Figure 19). Four samples à 2 ml were taken from the exposed as well as the reference samples, following exposure to 3, 6, 9, 12 kGy, and transferred into serum bottles containing 20 ml of $\frac{1}{2}$ SME+ S⁰ medium. The dose dependent survival of *I. hospitalis* was determined by the MPN technique (see 2.3.2). The survival (S) was plotted semi-logarithmically (see 2.3.4).

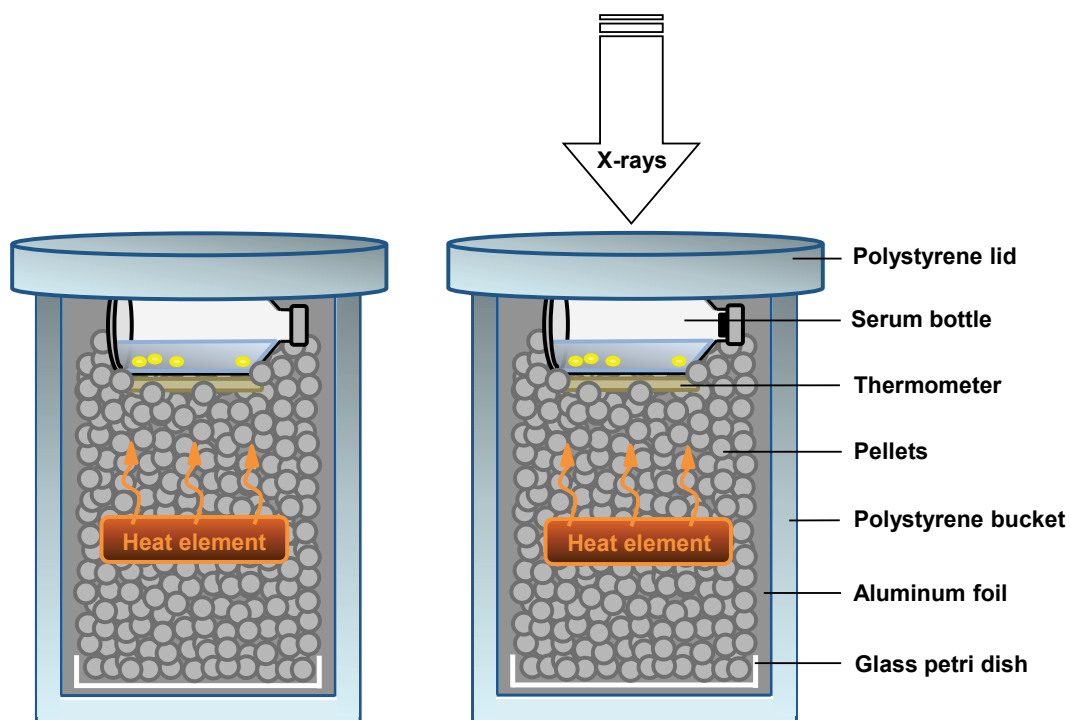


Figure 18: Schematic representation of exposure/reference bucket. Both buckets were used for O/N incubation, and X-ray exposure. *I. hospitalis* was exposed in fresh $\frac{1}{2}$ SME+S⁰ medium to increasing dose of ionizing radiation. Samples were taken at different points in time. The pellets (Lab Armor™ beads) were provided by Lab Armor (Cornelius, Oregon, USA).

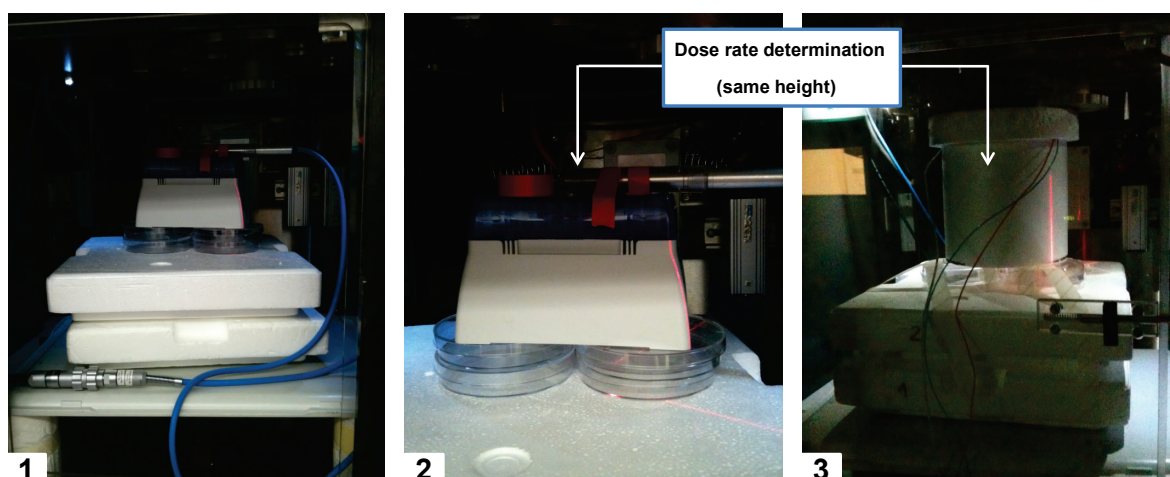


Figure 19: Dose rate determination for hot exposure experiment. The dosimeter was positioned at the height of 20 ml $\frac{1}{2}$ SME+S⁰ in a serum bottle. (1) Setup for dose rate determination, and position of dosimeter. (2) Dosimeter. (3) Exposure bucket.

2.4.2.5 The impact of cultivation temperature on X-ray tolerance

To test whether the pre-cultivation temperature of *I. hospitalis* impacts its tolerance to ionizing radiation, cells were cultivated at three different temperatures, i.e. at 75 °C (below optimum), at 95 °C (above optimum), and compared to cells grown at 90 °C (T_{opt}) (Paper *et al.*, 2007).

Several bottles of $\frac{1}{2}$ SME+S⁰ medium were inoculated each with ~0.1 ml of *I. hospitalis* stationary phase culture. Inoculated bottles were transferred either to 75 °C, 90 °C or 95 °C, and incubated for 1-2 days. After incubation, cells from the bottles incubated at the same temperature were pooled and combined anaerobically in HPLC vials for X-ray irradiation. The vials were placed on the irradiation table and exposed at room temperature to 0, 1.5, 3, 4.5, 6, 7.5, 9 kGy. Two ml of stress exposed cells were transferred to serum bottles containing 20 ml of $\frac{1}{2}$ SME+S⁰ medium. The dose dependent survivability of *I. hospitalis* after stress exposure was determined by the MPN technique (see 2.3.2). The survival (S) was plotted semi-logarithmically (see 2.3.4).

2.4.2.6 Sample preparation for gene expression studies after X-ray exposure (qRT-PCR)

Several gene specific primers (Table 3, 4) were designed to see whether *I. hospitalis* up- or down-regulates these genes of interest after X-ray exposure.

X-ray exposure was conducted in HPLC vials as described in 2.4.2.3. Three well grown *I. hospitalis* stationary phase cultures were pooled and enriched (evacuation with N₂/CO₂ to remove produced H₂S; enrichment in anaerobic chamber by centrifugation (12,000 x g,

2 min, RT)) for one sample/HPLC vial. Both exposed and unexposed samples were transferred into 10 ml preheated $\frac{1}{2}$ SME+S⁰ medium afterwards, and incubated for 5, 15, 30, (60) or 90 min at 90 °C. The samples were cooled down as fast as possible (cold water, ice). Total RNA was extracted, subjected to horizontal agarose gel electrophoresis, and finally qRT-PCR for gene expression studies.

Several distinct experimental setups were tested, and are additionally listed in Table 8.

A) *I. hospitalis* stationary phase cultures (90 °C, 15 hours) were prepared for X-ray exposure as described above. The cells were exposed to 1500 Gy, to reduce their survival by less than one order of magnitude but to induce their DNA repair mechanisms due to the degree of damaged DNA. The first experiments were designed to expose cells to 1500 Gy following repair for 5 min at 90 °C. The additional repair points (15, 30, 90 min) were conducted on following days.

B) The experimental setup was slightly changed by increasing the applied dose from 1500 Gy to 3000 Gy. An additional modification in the experimental set up was to conduct all repair points within one day, i.e. the samples were exposed to 3000 Gy, and the repair for 5, 15, 30, 90 min conducted in parallel.

C) To test whether cultivation at 90 °C increases the expression of the classical repair genes, *I. hospitalis* cultures were cultivated at only 75 °C for 2 days to obtain cells in their stationary phase (previous experiments showed a decreased cell concentration, therefore slower reproduction). The cells were exposed to 3000 Gy, and the repair conducted in parallel for every point in time.

D) Due to low total RNA concentrations *I. hospitalis* cells were incubated at 75 °C for 4 days to increase cell density, thus, their total RNA concentrations after extraction. The cells were exposed to 3000 Gy, and the repair conducted in parallel for every point in time.

E) The previous experiments were conducted with cells in stationary phase in which they already reached their protein level essential for survival. To bypass this circumstance, *I. hospitalis* cells were incubated at 90 °C for only 8 hours. The cells were exposed to 3000 Gy, and the repair for every point in time conducted in parallel.

F) *I. hospitalis* cells were incubated at 90 °C for only 4.5 hours. The dose was reduced to 1500 Gy, and the repair for every point in time conducted in parallel.

Table 8: Different experimental setups for qRT-PCR gene expression studies after X-ray exposure.

Description	Volume for inoculation [ml]	Incubation [°C]	Duration	Phase	Dose [Gy]
A	0.2	90	O/N (~15 h)	stationary	1500
B	0.2	90	O/N (~15 h)	stationary	3000
C	0.2	75	2 days	stationary	3000
D	0.2	75	4 days	stationary	3000
E	0.2	90	8 h	exponential	3000
F	0.4	90	4.5	early exponential	1500

2.4.2.7 Gamma ray (^{60}Co radiation) source and dosimetry for Death by Radiation (DbR #1, #2, #3)

Radiation experiments with gamma rays were conducted using the ^{60}Co source at BGS (Beta Gamma Service, Wiehl, Germany) by three radiation campaigns with slightly differing dose. The doses applied are mentioned in the following Sections. Certified dosimetry data were provided by the company for each radiation campaign (see Appendix).

2.4.2.8 ^{60}Co irradiation in liquid suspension

The impact of ionizing radiation in terms of γ -rays on the survivability of *I. hospitalis* and “*I. morulus*” was investigated as follows. The first radiation campaign was exclusively conducted with *I. hospitalis*. Several bottles of well grown *I. hospitalis* stationary phase cells ($\sim 1 \times 10^7$ cells/ml) were exposed to 6.2, 11.6, 17.5, 23.9, 46.9, 72.2, and 113.3 kGy at room temperature. Unexposed laboratory and transport control samples were kept at room temperature as well. Two ml of stress exposed cells were transferred into serum bottles containing 20 ml of $\frac{1}{2}$ SME+S⁰ medium. Additionally, *I. hospitalis* stationary phase cells were serial diluted (1:10) in $\frac{1}{2}$ SME+S⁰ medium prior to exposure (Figure 20). Serial diluted *I. hospitalis* cells were exposed to the same doses as mentioned above. The dose dependent survival after stress exposure was determined by direct incubation at 90 °C. The growth was followed microscopically with a 400x magnification (see 2.2.3.3) (Beblo *et al.*, 2011), and the survival (S) plotted semi-logarithmically (see 2.3.4).

For the second campaign, serum bottles containing 20 ml *I. hospitalis* or “*I. morulus*” stationary phase cultures as well as serum bottles containing 20 ml strictly anaerobic $\frac{1}{2}$ SME+S⁰ medium were exposed to ^{60}Co radiation with doses of 6.7, 12.7, 19.0, 27.2, 55.8, 81.1, and 117.1 kGy at room temperature. In addition, unexposed laboratory and transport control samples were kept at room temperature as well. Two ml of each exposed and unexposed samples were transferred into 20 ml culture medium followed by serial

dilution with tenfold dilution steps, respectively. The survival was determined by the most probable number technique (see 2.3.2). The metabolic activity was monitored on lead acetate paper (see 2.3.3). Samples, which were exposed in parallel, were used for DNA extraction (see 2.5.1).

To see whether exposed medium has an effect on the survivability of *I. hospitalis*, exposed serum bottles containing 20 ml $\frac{1}{2}$ SME+S⁰ medium were used for serial dilutions with untreated *I. hospitalis* cells for every applied ⁶⁰Co radiation dose (Figure 20). For that, *I. hospitalis* stationary phase cells were serial diluted (1:10) in this exposed $\frac{1}{2}$ SME+S⁰ medium, and the survival determined by the most probable number technique (see 2.3.2). The growth was followed microscopically with a 400-fold magnification (see 2.2.3.3) (Beblo *et al.*, 2011), and the survival (S) plotted semi-logarithmically (see 2.3.4). The results of ⁶⁰Co radiation exposed medium were compared to the results obtained for *I. hospitalis* cells which were serial diluted prior to exposure.

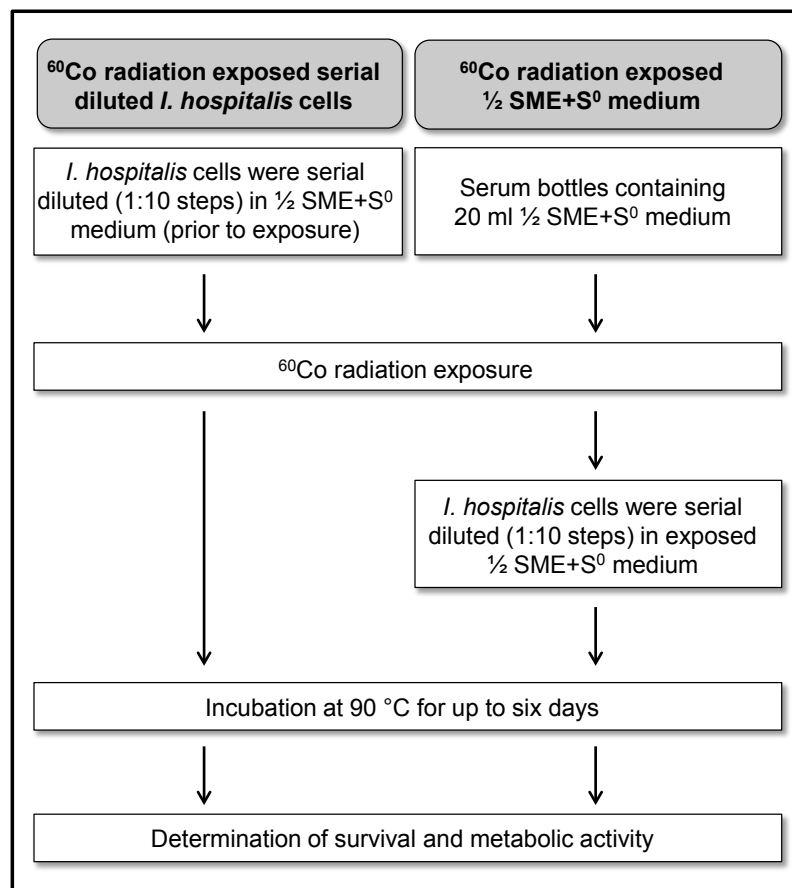


Figure 20: Schematic representation and comparison of experimental setups designed for the first and second radiation campaign. The effect of ⁶⁰Co radiation on cell survivability of *I. hospitalis* cells, serial diluted prior to exposure (DbR #1), and ⁶⁰Co radiation exposed $\frac{1}{2}$ SME+S⁰ medium (DbR #2) used for serial dilutions with untreated *I. hospitalis* cells was investigated in the following.

The effect of ^{60}Co radiation exposed sulfur on cell survivability was investigated during the third radiation campaign. A detailed description of the experimental set up will be given in Section 2.4.2.10.

2.4.2.9 ^{60}Co irradiation of single $\frac{1}{2}$ SME medium components

To test whether exposed single components needed for $\frac{1}{2}$ SME medium preparation have an effect on the growth of *I. hospitalis*, small amounts of every substance were exposed to ^{60}Co radiation (DbR #2: 27.2, 55.8, 117.1 kGy) in either Falcon® or Eppendorf tubes®. Dose specific $\frac{1}{2}$ SME medium was prepared from these components using sterile ddH₂O as described in 2.2.2 and following, except autoclaving. The prepared $\frac{1}{2}$ SME media were either supplemented with exposed or unexposed sulfur (Table 9). To test whether sulfur, crucial for the gain of energy, plays a special role, $\frac{1}{2}$ SME medium was prepared from unexposed single components either supplemented with unexposed or exposed sulfur (Table 10), too.

Table 9: Preparation of $\frac{1}{2}$ SME medium from single components which were exposed to increasing ^{60}Co radiation dose. The prepared media were supplemented either with exposed or unexposed sulfur.

$\frac{1}{2}$ SME components (-sulfur)	Sulfur	
^{60}Co radiation exposure [kGy]	No ^{60}Co radiation exposure	^{60}Co radiation exposure [kGy]
27.2	X	-
	-	27.2
55.8	X	-
	-	55.8
117.1	X	-
	-	117.1

Table 10: Preparation of $\frac{1}{2}$ SME medium from unexposed single components. The medium was either supplemented with exposed or unexposed sulfur.

$\frac{1}{2}$ SME components (-sulfur)	Sulfur	
No ^{60}Co radiation exposure	No ^{60}Co radiation exposure	^{60}Co radiation exposure [kGy]
X	X	-
X	-	27.2
X	-	55.8
X	-	117.1

These different $\frac{1}{2}$ SME media were inoculated with untreated *I. hospitalis* cells and serial dilutions with 1:10 dilution steps conducted followed by incubation at 90 °C for up to six days. The survival was determined according to the most probable number technique (see 2.3.2), and plotted semi-logarithmically (see 2.3.4).

2.4.2.10 Exposure of sulfur

Based on the idea that ionizing radiation (here ^{60}Co radiation) changes the natural conformation of elemental sulfur (S_8) in liquid solution, it was tried to investigate this supposed effect with an independent experiment during the third radiation campaign (DbR #3). Elemental sulfur was transferred anaerobically into serum bottles containing 20 ml of ddH₂O; the amount of sulfur per bottle was sufficient to prepare at least 10 serum bottles of sulfur containing $\frac{1}{2}$ SME medium after ^{60}Co radiation exposure. Additional serum bottles were prepared containing dry elemental sulfur to test whether its natural conformation is changed upon ^{60}Co radiation exposure as well. Serum bottles containing 20 ml sulfur-free $\frac{1}{2}$ SME medium were additionally prepared. All serum bottles were purged with H₂/CO₂ (80:20, v/v) and autoclaved for 60 min at 110 °C prior to exposure. The exposure was conducted with 0, 6.5, 24.2, 50.3, 117.3 kGy.

After ^{60}Co radiation exposure, bottles containing 20 ml sulfur-free $\frac{1}{2}$ SME medium (^{60}Co radiation exposed or unexposed) were opened within the anaerobic chamber and supplemented by either dry/wet exposed or unexposed sulfur which was transferred with a spatula (Table 11). The bottles were closed with butyl rubber plugs, sealed with aluminum rings, and purged with H₂/CO₂ (80:20, v/v) (no autoclaving!). Serial dilutions were conducted with untreated *I. hospitalis* stationary phase cultures, and the growth followed either microscopically (see 2.2.3.3) (Beblo *et al.*, 2011) or indirectly on lead acetate paper (see 2.3.3). The relative survival was plotted semi-logarithmically (see 2.3.4).

Table 11: Preparation of $\frac{1}{2}$ SME medium (^{60}Co radiation exposed or unexposed) which was supplemented by different sulfur combinations (dry/wet, exposed/unexposed).

Sulfur			$\frac{1}{2}$ SME(-S)				
			0 kGy	6.5 kGy	24.2 kGy	50.3 kGy	117.3 kGy
dry	^{60}Co radiation exposed [kGy]	0	x	x	x	x	x
		6.5	x	x			
		24.2	x		x		
		50.3	x			x	
		117.3	x				x
in ddH ₂ O	^{60}Co radiation exposed [kGy]	0	x	x	x	x	x
		6.5	x	x			
		24.2	x		x		
		50.3	x			x	
		117.3	x				x

2.4.2.11 Quorum sensing

The idea of this experiment was to check whether compounds in the supernatant of a well grown stationary phase *I. hospitalis* culture may be able to rescue cells which were exposed to high doses of ^{60}Co radiation (DbR #2: 19.0, 27.2, 55.8, 81.1, 117.1 kGy).

Several *I. hospitalis* cultures (evacuated with N_2/CO_2 to remove produced H_2S) were anaerobically sterile filtered using a 0.2 μm Whatman® filter unit and the filtrate transferred into anoxic sulfur-containing serum bottles. Gas exchange (evacuation and re-fill with H_2/CO_2) occurred at 1.5 bar repeating this cycle three times with a final pressure of 1.5 bar/bottle (no autoclaving afterwards).

Several control steps were performed on lead acetate paper by dripping a small volume on it:

- Stationary phase culture
- Evacuation (15 min, N_2/CO_2) to remove metabolically produced H_2S
- Sterile filtration (0.2 μm)
- Inoculation of sterile filtrate with 2 ml of sample (1:10)

The bottles were inoculated with 2 ml of sample, meaning 2 ml of exposed stationary phase cultures, and 2 ml of the last positive bottle within the serial dilution (Figure 30), respectively; metabolic production of H_2S was followed on lead acetate paper:

- Incubation for 2 days @ 90 °C
- Incubation for up to 6 days @ 90 °C

The obtained results were supported by microscopic observation. It turned out that using a 0.2 μm Whatman® filter unit was not sufficient for sterile filtration. The experiment was repeated by using Whatman® Nuclepore™ track-etched Membranes with 0.1 μm pore size.

2.5 Molecular biological methods

2.5.1 Extraction of genomic DNA

Genomic DNA from either *I. hospitalis* or “*I. morulus*” cells was extracted according to Tillet and Neilan (2000) before and after stress exposure. The cells were transferred from their exposure vessel (quartz cuvette, HPLC vial, serum bottle) into 15 or 50 ml Falcon tubes® using a 10 ml syringe with a 0.6 x 30 mm needle. The main reason for taking out the sample using a syringe was to reduce the amount of sulfur present in the medium to avoid potential disadvantageous interactions with the extraction buffer. The samples were centrifuged (60 min, 4,500 x g, 4 °C) in a Heraeus® Multifuge® 3 S-R centrifuge (Thermo Scientific, Waltham, USA). The supernatant was discarded and the cells resuspended in freshly prepared XS-buffer (700 μl /sample). The procedures are listed in Table 12.

<u>Stock concentration</u>	<u>concentration</u>	<u>Volume from stock</u>	<u>Final</u>
10 % Potassium ethyl xanthogenate		0.5 ml	1 %
0.5 M EDTA		0.2 ml	20 mM
10 % Sodium dodecyl sulfate		0.5 ml	1%
4 M Ammonium acetate		1.0 ml	800 mM
1 M Tris-HCl, pH 7.4		0.5 ml	100 mM
ddH ₂ O		ad 5 ml	

Table 12: Scheme of steps needed for genomic DNA extraction.

Genomic DNA Extraction		
1	Solve cell pellet in 700 µl freshly prepared XS-buffer, vortex	Homogenization
2	Incubate the suspension for 2 hours at 65 °C	
3	Vortex every 30 min	
4	Incubate for 10 min on ice	
5	Centrifuge (5 min, 12,000 x g, 4 °C)*	
6	Transfer supernatant into fresh Eppendorf Tube®, add 1 volume of Phenol/Chloroform/Isoamylalcohol (25:24:1), invert tubes several times	Extraction
7	Centrifuge (5 min, 12,000 x g, 4 °C)*	
8	Transfer upper phase (aqueous phase containing DNA) to a DNA LoBind Tube**	Precipitation
9	Add 1 volume of ice-cold 2-Propanol, and 1/10 volume of 4 M Potassium acetate, mix carefully	
10	Incubate over night at -20°C	
11	Centrifuge (10 min, 12,000 x g, 4 °C)*	
12	Discard the supernatant	Wash
13	Wash the DNA pellet twice with 70 % ice-cold ethanol, and centrifuge after each washing step (10 min, 12,000 x g, 4 °C)*	
14	Discard supernatant	Solubilization
15	Air-dry the DNA pellet (~ 15 min)	
16	Dissolve the DNA pellet in an appropriate volume of ddH ₂ O	Storage
17	Determine the dsDNA concentration by Qubit® fluorometric quantitation	
18	Store the DNA at 4 °C	

* Hermle Z216 MK (Hermle Labortechnik GmbH, Wehingen, Germany)

** (Eppendorf, Hamburg, Germany)

2.5.1.1 Qubit® Fluorometric Quantitation of double stranded DNA for RAPD assays

Double stranded DNA (dsDNA) was determined by fluorometric quantitation. The concentration of XS-buffer extracted genomic dsDNA of *I. hospitalis* and "*I. morulus*" was determined by Qubit™ dsDNA HS Assay (Thermo Scientific, Waltham, USA) using a Qubit® 2.0 Fluorometer (Thermo Scientific, Waltham, USA) for all following RAPD analyses. The concentration of dsDNA was determined as described in the user's manual.

2.5.1.2 Agarose gel electrophoresis to determine the quality of extracted genomic DNA

To check the quality of the extracted genomic DNA, agarose gel electrophoresis was conducted for visualization. One gram agarose for DNA electrophoresis per 100 ml of 1x TAE buffer was melted in a microwave to obtain a 1% agarose gel. The gel was mixed with SYBR® safe DNA gel stain (1 µl of 10,000x SYBR® safe in DMSO per 100 ml gel) from Invitrogen. Samples were mixed with 6x loading dye, loaded into the agarose gel slots and subjected to 7 V/cm for ~45 min in a horizontal gel electrophoresis system (PerfectBlue™ Gel System Mini M, Peqlab, Erlangen, Germany). A DNA standard was electrophoresed in a lane next to the samples allowing band size comparison. The DNA bands were visualized using ImageQuant LAS 4000 digital imaging system (GE Healthcare, Little Chalfont, UK).

2.5.1.3 Agarose gel electrophoresis for RAPD band pattern analyses

To determine the gain or loss of RAPD bands after stress exposure, the RAPD band pattern profiles were visualized under standardized agarose gel electrophoresis conditions. A 2 % agarose gel was prepared as described above, 20 µl of PCR product were mixed with 6x loading dye, loaded into the agarose gel slots and separated. The same occurred with an appropriate DNA standard in a lane next to the samples allowing band size comparison. The agarose gel was run in a horizontal gel electrophoresis system (PerfectBlue™ Gel System Maxi S Plus, Peqlab, Erlangen, Germany) with 176 Volt (7 V/cm) for 2.5 hours. The band patterns were visualized using ImageQuant LAS 4000 digital imaging system (GE Healthcare, Little Chalfont, UK). This standardized agarose gel electrophoresis allowed comparison also between separate gels after varying stress exposures.

2.5.2 RNA extraction for qRT-PCR

The total RNA of *I. hospitalis* was extracted for gene expression studies using the “Hot phenol extraction” according to the protocol of Pinto *et al.*, 2009. Total RNA was extracted from *I. hospitalis* cells before and after stress exposure. The cells were transferred from their exposure vessel (Figure 17 (1)) into 2 ml Eppendorf Tubes® using a 10 ml syringe with a 0.6 x 30 mm needle to reduce the amount of elemental sulfur present in the medium to a minimum preventing potential disadvantageous interactions with the extraction buffer. The cells were pelleted by centrifugation (13,000 x g, 5 min, RT) in a MiniSpin™ centrifuge (Eppendorf, Hamburg, Germany). The supernatant was discarded

and replaced by 1 ml freshly prepared PGTX-buffer. The following procedures (Pinto *et al.*, 2009) are described in Table 13.

<u>Substance</u>	<u>Amount</u>	<u>Concentration</u>
Phenol	39.6 g	4.21 M
Glycerol	6.9 ml	6.9%
8-Hydroxychinoline	0.1 g	7 mM
EDTA	0.58 g	20 mM
Sodium acetate	0.8 g	100 mM
Guanidine thiocyanate	9.5 g	800 mM
Guanidinium chloride	4.6 g	480 mM
Triton™ X-100	2.0 ml	2 %
RNase-free ddH ₂ O	ad 100 ml	

Table 13: Scheme of steps needed for total RNA extraction.

Total RNA Extraction		
1	Solve cell pellet in 1 ml freshly prepared PGTX-buffer	Homogenization
2	Incubate the suspension for 5 min at 95 °C	
3	Incubate for 5 min on ice	
4	Add 100 µl of 1-Bromo-3-chloropropane, mix vigorously	Extraction
5	Incubate samples for 10 min at room temperature	
6	Centrifuge (15 min, 12,000 x g, 4 °C)*	
7	Transfer upper phase (containing the RNA) to a DNA LoBind Tube**	Precipitation
8	Add equal volume of ice-cold 2-Propanol	
9	Incubate for 8 min at room temperature	
10	Centrifuge (10 min, 12,000 x g, 4 °C)*	
11	Discard the supernatant, and add 1 ml 75 % ethanol	Wash
12	Centrifuge (5 min, 8,000 x g, 4 °C)*	
13	Discard the supernatant	Solubilization
14	Air-dry the RNA pellet (~ 15 min)	
15	Dissolve the RNA pellet in an appropriate volume of DEPC-treated ddH ₂ O	
16	Determine the concentration spectrophotometrically	Storage
17	Prepare aliquots à 10 µl, and store at -80 °C	

* Hermle Z216 MK (Hermle Labortechnik GmbH, Wehingen, Germany)

** (Eppendorf, Hamburg, Germany)

2.5.2.1 Determination of total RNA concentrations using NanoDrop™

The concentration of extracted RNA was spectrophotometrically determined by using 1 µl of sample for each NanoDrop™ 2000c (Thermo Scientific, Waltham, USA) measurement.

2.5.2.2 Agarose gel electrophoresis to determine RNA quality

To check the quality of the extracted RNA, an agarose gel electrophoresis was conducted for visualization. Two gram of low melting Agarose for DNA/RNA electrophoresis per 100 ml of 1x TAE buffer was melted in a microwave to obtain a 2 % agarose gel, adding EtBr (0.5 µg/ml) after leaving to cool (hand-warm). Samples were mixed with 2x RNA loading dye (Thermo Scientific, Waltham, USA), loaded into the agarose gel slots and subjected to 7 V/cm for ~45 min in a horizontal gel electrophoresis system (PerfectBlue™ Gel System Mini M, Peqlab, Erlangen, Germany). A RNA standard was electrophoresed in a lane next to the samples allowing band size comparison. The RNA bands were visualized using ImageQuant LAS 4000 digital imaging system (GE Healthcare, Little Chalfont, UK).

2.5.3 First strand cDNA synthesis for qRT-PCR

2.5.3.1 Removal of genomic DNA from RNA preparations

To remove DNA contaminations, a DNase I digestion was conducted prior to cDNA synthesis. The removal of genomic DNA from total RNA preparations occurred by using pegGOLD DNase I (Peqlab, Erlangen, Germany)

1 µg	total RNA
2 µl	10x Digestion Buffer for DNase I
3 µl	pegGOLD DNaseI
ad 10 µl	RNase-free ddH ₂ O

The mix was incubated in a peqSTAR Thermocycler (Peqlab, Erlangen, Germany) for 45 min at 37 °C. The reaction was stopped by adding 1µl 50 mM EDTA and incubation for 10 min at 65 °C.

2.5.3.2 First strand cDNA synthesis

The following cDNA synthesis was performed using a peqSTAR Thermocycler (Peqlab, Erlangen, Germany) and the cDNA Synthesis Kit H Minus purchased from Peqlab (Erlangen, Germany). The first-strand cDNA synthesis was conducted using a random hexameric primer to give an equal representation of all targets in real-time PCR applications. Two setups were prepared in parallel, one containing the enzyme reverse transcriptase resulting in cDNA synthesis, the other without enzyme (negative control).

+ reverse transcriptase

5 µl DNase I digested RNA template (500 ng)
 1 µl Random Hexamer Primer
 4 µl 5x Reaction buffer
 1 µl RiboLock RI
 2 µl 10 mM dNTP Mix
 1 µl peqGold Reverse Transcriptase
 ad 20 µl with nuclease-free ddH₂O

- reverse transcriptase

5 µl RNA template (500 ng)
 1 µl Random Hexamer Primer
 4 µl 5x Reaction buffer
 1 µl RiboLock RI
 2 µl 10 mM dNTP Mix
 -
 ad 20 µl with nuclease-free ddH₂O

The mix was incubated in a peqSTAR Thermocycler (PepLab, Erlangen, Germany) for 5 min at 25 °C, 60 min at 42 °C, 5 min at 70 °C.

2.5.4 Analytical methods

2.5.4.1 RAPD (randomly amplified polymorphic DNA) to determine genomic DNA integrity

The RAPD (randomly amplified polymorphic DNA) band pattern profiles of *I. hospitalis* and "*I. morulus*" were analyzed for differences in band intensity as well as gain/loss of RAPD bands after varying stress conditions. The impact of non-ionizing radiation (UV-C), and ionizing radiation (X-rays, γ -rays, heavy ions) on genome integrity was analyzed by comparing the band pattern of exposed to patterns of non-treated cells.

Genomic DNA was extracted by XS-buffer extraction (see 2.5.1) and the concentration of dsDNA determined by Qubit[®] fluorometric quantitation (see 2.5.1.1). For one reaction (0.2 ml PCR tube), 25 ng of genomic DNA was used as template for primer P2 (sequence given in Table 2). One reaction was composed of

25 ng genomic DNA template
 2 µl 10 mM dNTPs mix
 2 µl 10 x PCR Rxn Buffer (-MgCl₂)
 1.5 µl 50 mM MgCl₂
 0.1 µl Platinum[®] Taq DNA Polymerase
 1 µl 10 µM P2
 ad 20 µl with ddH₂O

The cycles were run in a peqSTAR Thermocycler (Peqlab, Erlangen, Germany) (Table 14). The PCR products were subjected to horizontal agarose gel electrophoresis for analysis (see 2.5.1.3).

Table 14: RAPD cycles. Abbreviations: ' (minutes).

Steps	Temperature [°C]	Duration	Number of cycles
Initial denaturation	94	10'	40x
Denaturation	94	1'	
Annealing	42	1'	
Extension	72	2'	
Final extension	72	10'	
Store	4	∞	

2.5.4.2 qPCR (quantitative real-time PCR) to detect relative amounts of DNA lesions

The qPCR method was used to detect the relative amount of DNA lesion in a 1.3 kb fragment after ionizing radiation exposure (^{60}Co radiation exposure). Primers for the 16S rRNA gene sequence were designed to amplify between the positions 27-1394, resulting in an amplification product of 1368 bp (Table 5). The same primer set was used to amplify the 16S rRNA sequence in "*I. morulus*".

Genomic DNA was extracted by XS-buffer extraction (see 2.5.1) and the concentration of dsDNA determined by Qubit[®] fluorometric quantitation (see 2.5.1.1). For one reaction, 5 ng of genomic DNA was used as template. One reaction was composed of

5 ng	genomic DNA in 2.5 µl ddH ₂ O
0.25 µl	10 µM DbR for
0.25 µl	10 µM DbR rev
5 µl	2 x KAPA SYBR [®] FAST qPCR Master Mix
ad 10 µl	ddH ₂ O

Table 15: qPCR program for DNA damage detection. Abbreviations: ' (minutes), '' (seconds).

Temperature [°C]	Duration	Number of cycles
95	3'	35x
95	20''	
60	20''	
72	90''	

The cycles were carried out in 96-well plates (Brand, Wertheim, Germany) in a DNA Engine Opticon[®] 2 cycler (CFD-3220, MJ Research Inc., St. Bruno, Canada) utilizing the Opticon Monitor[™] software (MJ Research) (Table 15). The C_t value is the average of

results obtained from one experiment performed in triplicates. Relative amplification rates were calculated according to the normalized C_t values by

$$(5) \quad C_t \text{ normalized the minimum} = \frac{(Max-value)}{(Max-Min)}$$

where Max represents the highest and Min the lowest C_t value within the experiment, and $value$ is the C_t value to be normalized; the relative amplification rates were plotted against the applied dose (kGy).

Alternatively, the relative lesion frequency per 1.3 kb DNA was calculated by

$$(6) \quad \frac{lesions}{amplicon} = -\ln \left(\frac{A_t}{A_0} \right)$$

where A_t represents the C_t value of treated sample and A_0 the C_t value obtained for the untreated control (Hunter *et al.*, 2010).

2.5.5 DNA repair

2.5.5.1 RAPD for DNA repair determination after 12.6 kGy exposure

To get an impression on how fast *I. hospitalis* is able to repair its ionizing radiation induced DNA damages, cells were exposed to 12.6 kGy (X-rays) and incubated at 90 °C for increasing periods of time. Samples were taken for RAPD analysis. Based on these results qRT-PCR experiments and repair points were designed as described in 2.4.2.6.

Five bottles containing each 20 ml of *I. hospitalis* stationary phase cultures were pooled, and combined in one anoxic 120 ml serum bottle. 10 ml of this mix were transferred into a serum bottle containing only 10 ml $\frac{1}{2}$ SME+S⁰ medium. This bottle served as negative control and was incubated at 90 °C for 90 min without stress exposure. The remaining 90 ml were exposed to X-rays up to ~12.6 kGy. After exposure, 10 ml were transferred in serum bottles containing 10 ml fresh $\frac{1}{2}$ SME+S⁰ medium (preheated at 90 °C), seven times in total. These bottles were incubated at 90 °C for 5, 10, 15, 20, 25, 30, and 60 min, respectively, and the incubation stopped by cooling down. The DNA was extracted using XS-buffer as described in 2.5.1, and the concentration of extracted dsDNA determined by Qubit® fluorometric quantitation (see 2.5.1.1). A RAPD analysis was conducted with primer P2 as described in 2.5.4.1.

2.5.5.2 Determination of gray-levels

The gray-levels of the upper most bands were determined using ImageJ (Gel Analyzer). A histogram was generated for every selected lane (Figure 21). The valleys correspond to the band intensities within the lane of interest. Lines were drawn to determine the areas of the valleys. The values of these areas are described as gray-levels in the following.

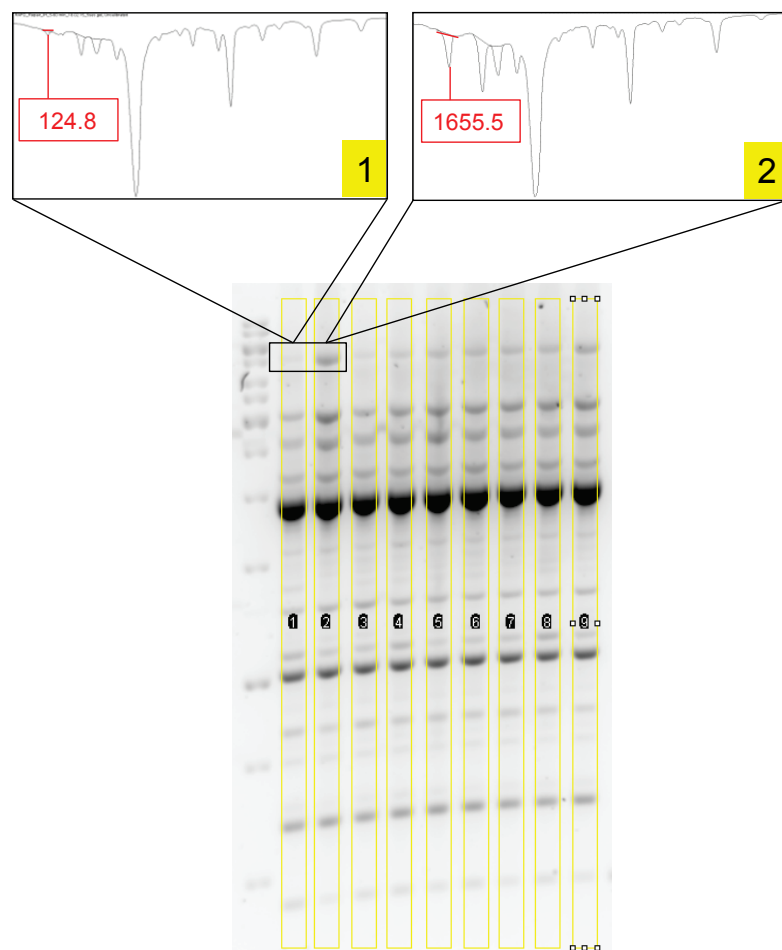


Figure 21: Determination of gray-levels. The valleys correspond to the band intensities within the lane of interest. (1) Exposed sample (12.6 kGy). (2) Unexposed sample (control). Red lines: Lines were drawn to determine the areas of the valleys. The values for the areas are highlighted in red.

2.5.6 Gene expression by qRT-PCR (quantitative Reverse Transcription-PCR)

qRT-PCR was conducted for gene expression studies with *I. hospitalis* after stress exposure (X-rays). It is based on real time measurement of products generated, and accumulated during each cycle of the PCR process by plotting the products' fluorescent signal as a function of cycle number. Two different types of qRT-PCR analysis can be used. There is "relative quantitation" by comparing the gene of interest to that of a control

gene within a sample. The so-called “standard-curve quantitation” quantifies an unknown sample by deriving the value from a standard curve generated with a known sample (Ginzinger, 2002). A detailed explanation on analysis will be given in the following.

The qRT-PCR was conducted according to the program listed in Table 16.

One reaction was composed of

5 ng	cDNA template in 2.5 µl ddH ₂ O
0.25 µl	10 µM Primer for
0.25 µl	10 µM Primer rev
5 µl	2 x KAPA SYBR® FAST qPCR Master Mix
ad 10 µl	ddH ₂ O

The quantitative RT-PCR cycles were carried out in triplicates in 96-well plates (Brand, Wertheim, Germany) in a DNA Engine Opticon® 2 cycler (CFD-3220, MJ Research Inc., St. Bruno, Canada) utilizing the Opticon Monitor™ software (MJ Research).

Table 16: qRT-PCR program for gene expression studies after stress exposure. Abbreviations: ' (minutes), '' (seconds).

Step	Temperature [°C]	Duration	Number of cycles
Enzyme activation	95	3'	hold
Denaturation	95	15''	40x
Annealing/Extension/Data acquisition	60	45''	

Fluorescence was detected, and a melting curve recorded from 65 °C to 95 °C every 0.5 °C. Analyzing the melting curve indicated a specifically amplified product. The amplification of the PCR products was additionally analyzed on a 2 % agarose gel (see 2.5.1.2).

2.5.6.1 Absolute C_t value and molecule number

Data obtained from qRT-PCR were depicted in two different ways. On the one hand, results were shown as absolute C_t values (Radonić *et al.*, 2004) where the C_t value is the average of results obtained from one experiment performed in triplicates. On the other hand, the molecule numbers were exclusively calculated for rad2, rad50, recB, and radA resulting from experimental condition F (4.5 hours at 90 °C, 1500 Gy; see 2.4.2.6). A primer specific standard curve was generated by using *I. hospitalis* genomic DNA with 4-5 1:10-dilution steps. A slope of -3.32 indicated a 100 % efficient PCR reaction; deviations were then calculated by the following formula (according to Ginzinger, 2002).

$$(7) \quad PCR \text{ efficiency } [\%] = \left(\left(10^{\left(\frac{1}{-slope} \right)} - 1 \right) * 100 \right)$$

The amount of primer specific amplicon for a specific sample was determined according to the linear regression of the appropriate standard curve. Molecule numbers were calculated using the following formula

$$(8) \quad \text{number of molecules} = \frac{X \text{ ng} * 6.0221 \times 10^{23} \text{ molecules/mole}}{(N * 660 \text{ g/mole}) * 1 \times 10^9 \text{ ng/g}}$$

with X (amount of amplicon in ng), N (length of dsDNA amplicon), Avogadro constant (6.0221×10^{23} molecules/mole), and 660 g/mole as average mass of 1 base pair of dsDNA (adapted from Whelan *et al.*, 2003). The molecule number was plotted against the repair in minutes.

3 Results

3.1 Non-ionizing radiation (UV-C)

3.1.1 Measuring the absorption of the medium

Before testing the impact of non-ionizing radiation on the survivability of *Ignicoccus* the absorption of ½ SME medium in different combinations was photometrically determined by performing a wavelength scan from 200-400 nm. UV-C transmissible quartz cuvettes were filled with samples to be tested under anoxic conditions, and closed airtight to simulate the later experimental setup. The absorption at 254 nm (corresponding to monochromatic UV-C, applied in the following experiments), the influence of sulfur particles, varying cell concentrations of *Ignicoccus hospitalis*, the combination of both, and the absorption of ½ SME medium itself was of special interest. The wavelength scans in Figure 22 are an example for all other scans conducted with other *Ignicoccus* representatives. No significant differences in absorption were detected between these specimens.

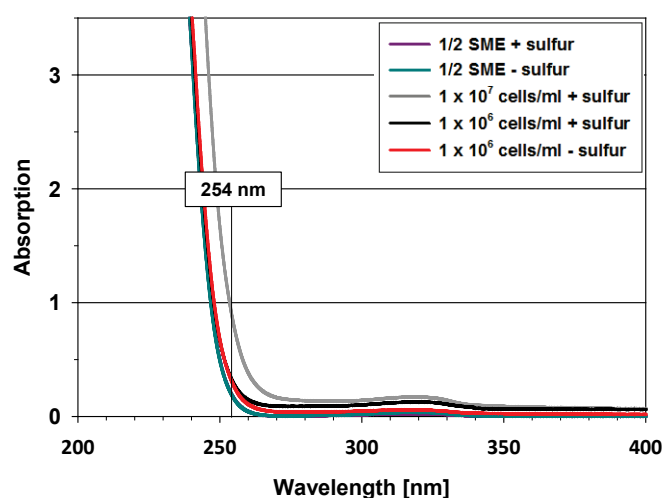


Figure 22: Absorption spectrum of different ½ SME medium combinations. A wavelength scan was conducted from 200-400 nm in UV-C transmissible quartz cuvettes. Different combinations were tested. Purple line: ½ SME medium supplemented with sulfur. Petrol blue: ½ SME without sulfur. Gray line: Stationary phase culture of *I. hospitalis*. Black line: *I. hospitalis* stationary phase culture 10-fold diluted in sulfur containing ½ SME medium. Red line: *I. hospitalis* stationary phase culture 10-fold diluted in sulfur-free ½ SME medium.

The wavelength scan with stationary phase *I. hospitalis* culture (gray line) resulted in the strongest absorption compared to all other tested conditions. ½ SME medium with or without sulfur did not influence the absorption at all. To make sure that the radiation was homogeneously absorbed by the cells, *Ignicoccus* cells were 10-fold diluted (1×10^6 cells/ml) in sulfur-free ½ SME medium (red line) for all following experiments.

3.1.2 Survival of *Ignicoccus* (0-300 J/m²)

The impact of non-ionizing radiation (UV-C) on the survival of *Ignicoccus* strains was studied using a low pressure mercury lamp with a main emission line of 254 nm serving as source for monochromatic UV-C radiation. The experiment was conducted in UV-C transmissible quartz cuvettes under anoxic conditions and vigorous stirring at room temperature.

The range between 0 and 300 J/m² (see Figure 24) was analyzed in detail (Figure 23) to see which fluence intensity initiates the linear part of the survival curve. *Ignicoccus islandicus* showed the strongest inactivation after 300 J/m², whereas *Ignicoccus hospitalis*, "*Ignicoccus morulus*", *Ignicoccus pacificus* showed very similar tendencies. The fluence required to inactivate the population by 90% (F_{10}) was determined by linear regression from the linear parts of the semi-logarithmically plotted survival curves (Figure 24, Table 17). F_{10} -values for different model organisms (Bacteria or Achaea) are listed in Table 18, and were obtained from the literature.

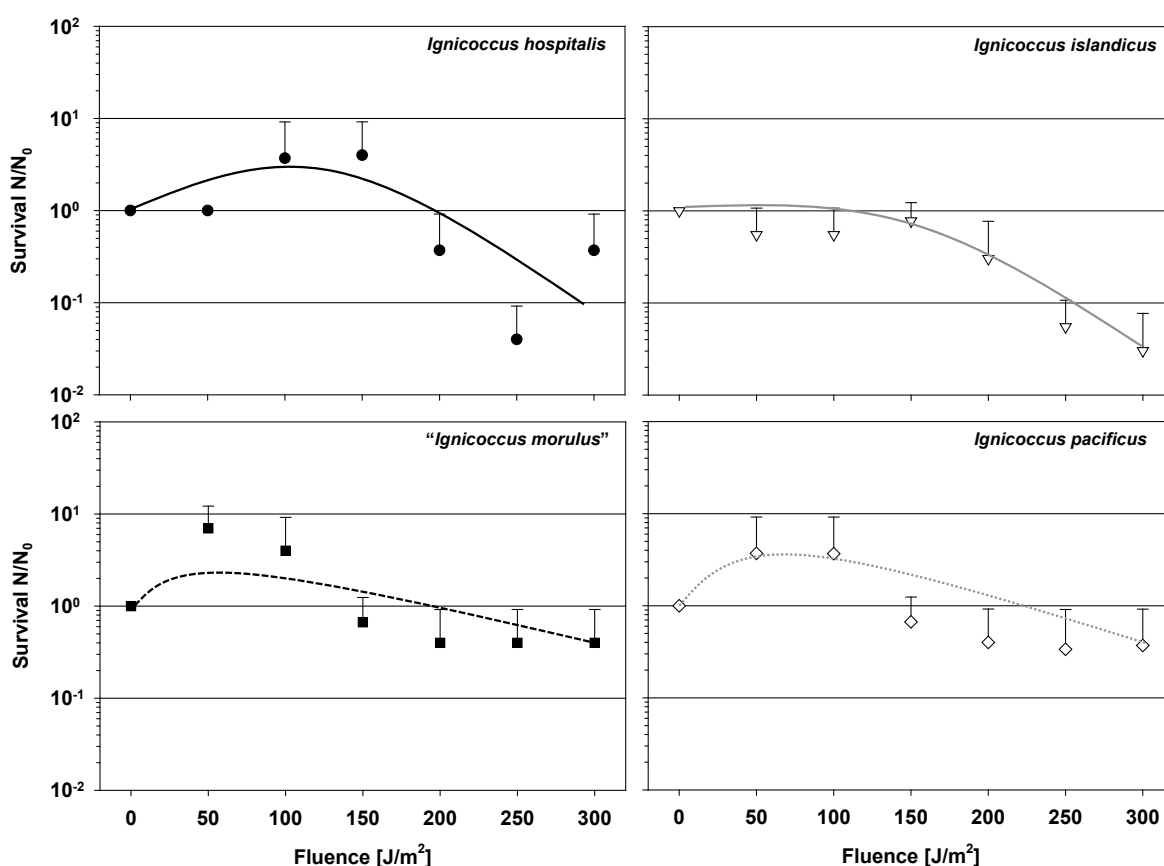


Figure 23: Survival curve of all *Ignicoccus* representatives after UV-C exposure (0-300 J/m²). The survival was plotted semi-logarithmically against the fluence (up to 300 J/m²). The experiments were conducted with $n=3$ for each representative. The trendlines were fitted by hand.

3.1.3 Survival of *Ignicoccus* (0-3000 J/m²)

All tested specimens showed fluence-dependent inactivation after UV-C exposure with increasing fluence intensities. An inactivation of three orders of magnitude was observed after an exposure of 1000 J/m² (Figure 24). Potential outliers occurred in the frame of experimental errors. An inactivation of 4-5 orders of magnitude was observed after an exposure of 1500 J/m², as well as after 3000 J/m².

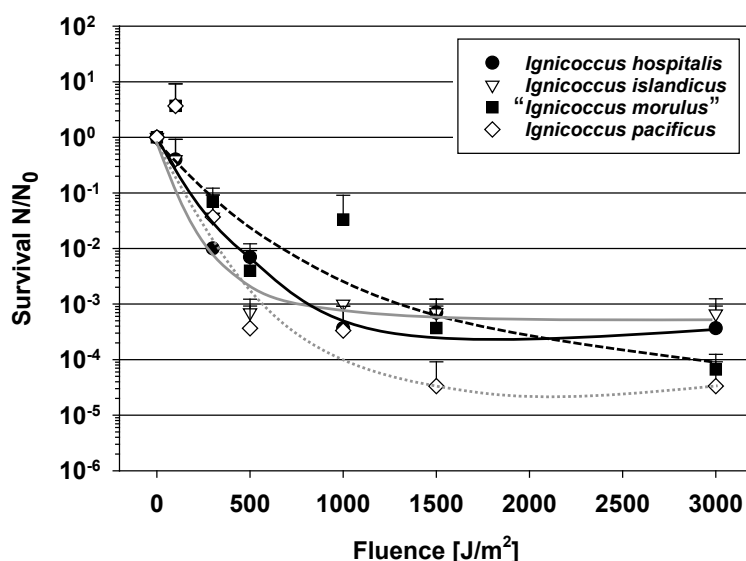


Figure 24: Survival curves of all *Ignicoccus* representatives after UV-C exposure (0-3000 J/m²). The survival was plotted semi-logarithmically against the fluence (up to 3000 J/m²). The experiments were conducted with $n \geq 3$ for each representative. The trendlines were fitted by hand.

Table 17: Calculated F₁₀-values for different *Ignicoccus* representatives.

Organism	F ₁₀ -value [J/m ²]
<i>Ignicoccus hospitalis</i>	337
<i>Ignicoccus islandicus</i>	245
" <i>Ignicoccus morulus</i> "	400
<i>Ignicoccus pacificus</i>	256

Table 18: F₁₀-values for model organisms (from Beblo *et al.*, 2011).

Model organism	F ₁₀ -value [J/m ²]	Source
<i>Bacillus subtilis</i> (vegetative cell)	40	Newcombe <i>et al.</i> , 2005
<i>Bacillus subtilis</i> (spore)	102	Riesenman and Nicholson, 2000
<i>Escherichia coli</i>	40	Arrage <i>et al.</i> , 1993
<i>Deinococcus radiodurans</i>	660	Bauermeister <i>et al.</i> , 2009
<i>Archaeoglobus fulgidus</i>	108	Beblo <i>et al.</i> , 2011
<i>Sulfolobus solfataricus</i>	37	Beblo <i>et al.</i> , 2011

3.1.4 UV-C leveling

To see whether irradiation in UV-C transmissible quartz cuvettes has any impact on organismic UV-C tolerance, *Escherichia coli*, known to be UV-C sensitive (F_{10} -value: 40 J/m^2 , Arrage *et al.*, 1993), was tested once under comparable experimental conditions as they were designed for *Ignicoccus*. Around 1×10^7 cells/ml were exposed at room temperature to increasing fluence intensities under oxic conditions in UV-C transmissible quartz cuvettes containing organic-free buffer (PBS). A comparable cell concentration was irradiated in an open petri dish under oxic conditions at room temperature. The most striking inactivation effect can be seen by comparing *E. coli* cells exposed in cuvettes to cells exposed in a petri dish. An “open” exposure reduced the survival of *E. coli* by five orders of magnitude, whereas both *E. coli* and *I. hospitalis* exposed in cuvettes showed similar inactivation tendencies (Figure 25). This effect will further be discussed in Section 4.1.

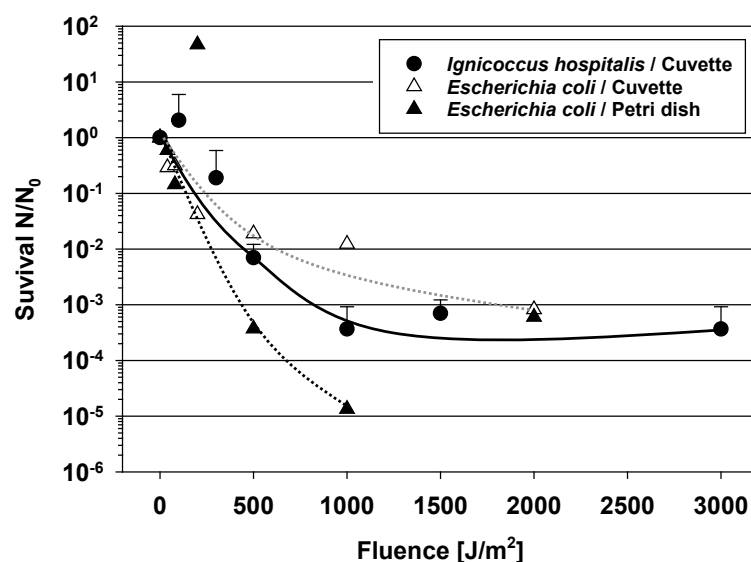


Figure 25: Survival curve of UV-C exposed *I. hospitalis* cells compared to *E. coli* cells exposed in either cuvettes or petri dishes. The survival was plotted semi-logarithmically against the fluence (up to 3000 J/m^2). The experiments with *E. coli* were performed only once. The trendlines were fitted by hand.

3.1.5 Extraction of genomic DNA

To investigate the molecular damage caused by radiation (non- and ionizing radiation), genomic DNA from either “*I. morulus*” or *I. hospitalis* cells was extracted before and after stress exposure. The extracted genomic DNA from untreated cells is exemplarily shown in Figure 26. The apparent difference between *I. hospitalis*, and “*I. morulus*” extracted

genomic DNA are two additional plasmids (~3000-3500 bp) in the case of "*I. morulus*", and shown for the first time.

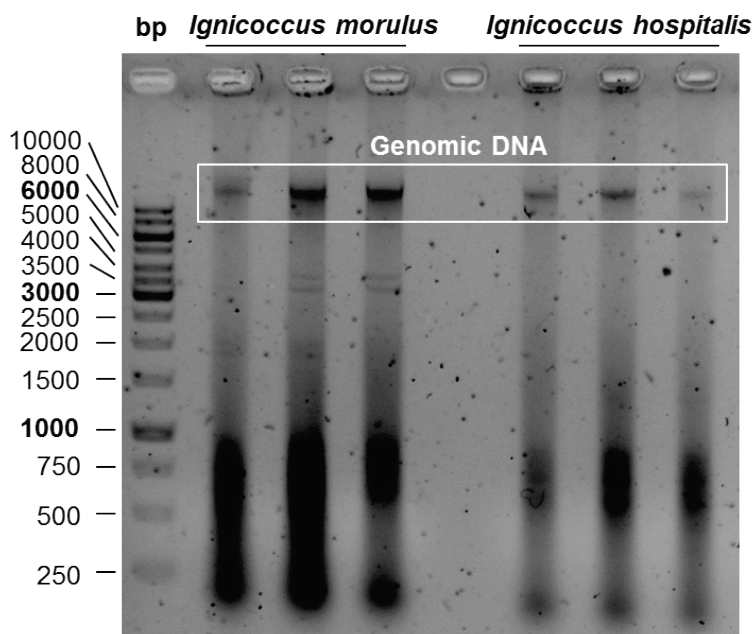


Figure 26: Agarose gel of extracted genomic DNA from *I. hospitalis* and "*I. morulus*". The quality of genomic DNA from three independent DNA extractions per species was checked on a 1 % agarose gel.

3.1.6 Relative amount of DNA lesions, and genomic DNA integrity after UV-C exposure of *I. hospitalis*

The relative amount of DNA lesions per 1.3 kb fragment were determined by quantitative real-time PCR (qPCR) using the 16S rRNA gene amplicon (see 2.1.4.2). The genome integrity of *I. hospitalis* after UV-C exposure was analyzed by RAPD (Randomly Amplified Polymorphic DNA) (see 2.5.4.1). The relative amount of DNA lesions increased with increasing fluence intensity, whereas the survival decreased (Figure 27A). The maximum amount of lesions (~0.4/1.3 kb fragment) was reached after an exposure to 3000 J/m² compared to the untreated control sample (0 J/m², lesions: 0). A similar effect was observed by RAPD, where the resulting band pattern profiles were analyzed with respect to changes such as differences in band intensity as well as gain/loss of RAPD bands. The distinct impact of non-ionizing radiation on the genome integrity of *I. hospitalis* is shown in Figure 27B. After irradiation with 100 J/m², the majority of bands were lost which were present in the unexposed sample (0 J/m²) except of the most prominent ones at e.g. 2000 bp, and 750 bp. The loss of bands increased with increasing fluence intensity.

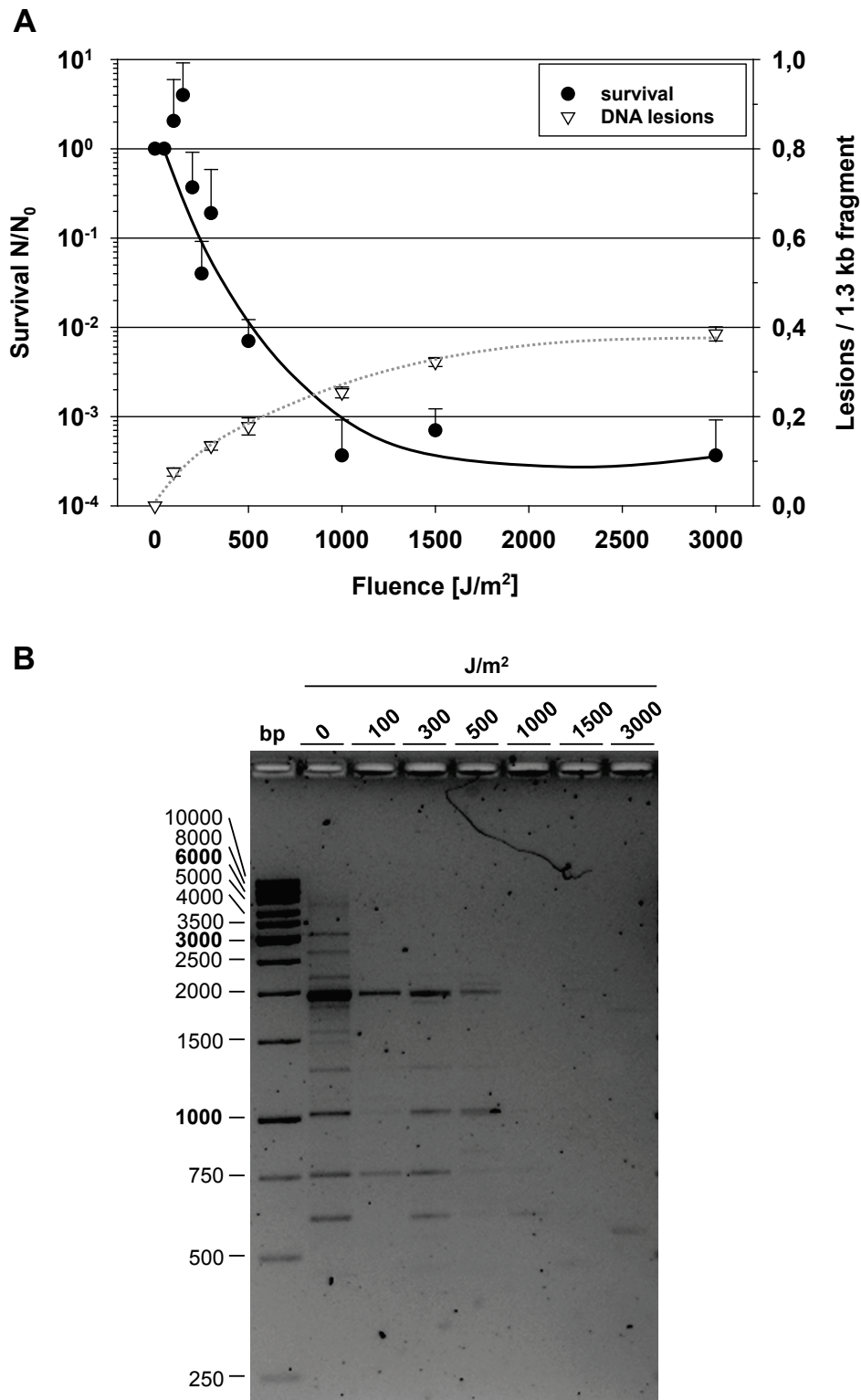


Figure 27: Relative amount of DNA lesions vs. survival, and genomic DNA integrity of *I. hospitalis* after UV-C exposure. (A) qPCR was conducted to determine the relative amount of DNA lesions per 1.3 kb fragment after UV-C exposure; the amount of lesions was plotted against the survival (as shown in Figure 24). The trendlines were fitted by hand. **(B)** RAPD band pattern profile of genomic DNA after UV-C exposure. *I. hospitalis* cells were exposed to increasing fluence intensities, and the resulting RAPD band pattern analyzed on a 2 % agarose gel.

Summary:

- All tested specimens showed an inactivation of three orders of magnitude after an exposure of 1000 J/m² (Figure 24). The fluence intensity to inactivate the population by 90% was 337 J/m² for *I. hospitalis*, and 245 J/m² in the case of *I. islandicus*. A fluence of 400 J/m² inactivated "*I. morulus*", and 256 J/m² *I. pacificus* by 90 %. All F₁₀-values are very similar within the accuracy of measurement (Table 17).
- *I. hospitalis* and *E. coli* showed comparable inactivation tendencies when exposed in cuvettes. Tailing (>1000 J/m²) was observed for both specimens (Figure 25).
- The impact of non-ionizing radiation on the genomic DNA integrity of *I. hospitalis* can be visualized by RAPD band pattern analysis (Figure 27B). The loss of bands increased with increasing fluence intensity. The maximum amount of lesions (~0.4/1.3 kp fragment) determined by qPCR was reached after an exposure to 3000 J/m² compared to the untreated control sample (0 J/m², lesions: 0) (Figure 27A).

3.2 Ionizing radiation

3.2.1 Heavy ions

The aim of the STARLIFE consortium was to compare the response of different model systems of astrobiological relevance to radiation as it is present in the interplanetary space; organisms would be exposed to bombardment by high-energy charged particle radiation from galactic sources and from the Sun. This interplanetary space radiation spectrum consists of photons (X-rays, γ -rays), protons, electrons and heavy ions (Möller *et al.*, 2010). The different types of ionizing radiation with different radiation qualities tested in the underlying studies were X-rays, γ -rays and heavy ions. Heavy ion experiments, with low and high energy charged particles known to induce damages within biological samples, were conducted at the HIMAC facility, whereas X-ray experiments were conducted at DLR, and the exposures to γ -rays at BGS.

I. hospitalis and "*I. morulus*" cells were exposed to low- and high-energy heavy ions with LETs in the range of 2-200 keV/ μ m. The following ions were chosen: Helium with 150 MeV/n (LET 2.2 keV/ μ m), the medium LET ion Argon with 500 MeV/n (LET 90 keV/ μ m) and the high LET ion Iron with 500 MeV/n (LET 200 keV/ μ m). Helium for

example comprises together with Hydrogen (H) more than 98 % of all cosmic rays (Mewaldt, 1994). Heavier nuclei like Iron are of greater importance due to their higher rate of energy loss, resulting in an enhanced relative biological effectiveness (RBE) (Mewaldt, 1994). The overall impact of heavy ion exposure on genomic DNA integrity was investigated with aerobically prepared and exposed *I. hospitalis*, and “*I. morulus*” cells for technical reasons. The results shown for *I. hospitalis* (Figure 28) are exemplarily for both specimens. Extracted genomic DNA was subjected to horizontal agarose gel electrophoresis as shown in Figure 28A. Varying genomic DNA band intensities (above 10,000 bp) can be seen, but no fragmentation can be observed after exposure to heavy ions regardless the dose and appearance (low/high energy charged particle). To get additional information about genomic DNA integrity, RAPD analysis was conducted. The same extracted genomic DNA (Figure 28B) was used as template. No gain or loss of bands can be seen after heavy ion exposure in comparison to the untreated sample (0 Gy). The doses applied were not sufficient to detect any changes in the RAPD band pattern profile. Therefore, no further experiments were carried out with heavy ions.

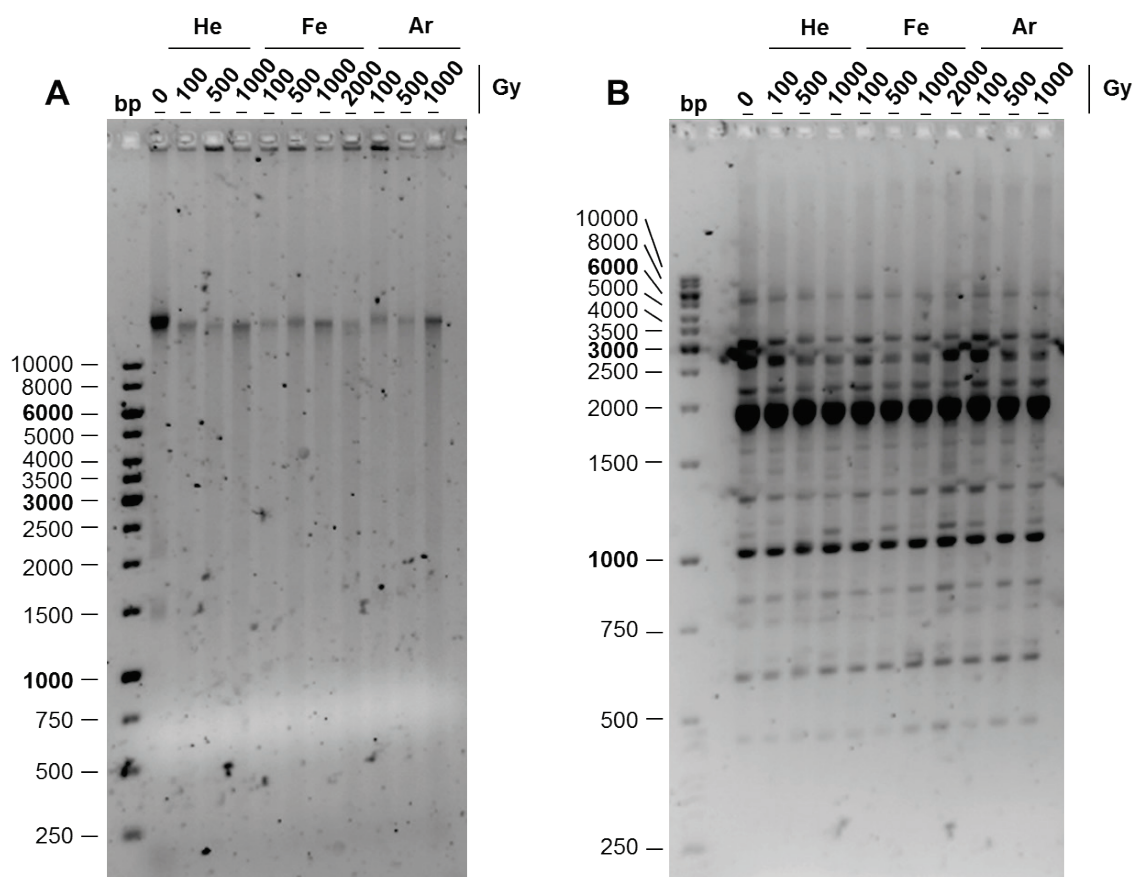


Figure 28: Analysis of heavy ion exposed samples (*I. hospitalis*) on agarose gels. (A) Genomic DNA was extracted from *I. hospitalis* cells which were exposed to either Helium (He), Argon (Ar), or Iron (Fe) ions by using XS-buffer. Extracted DNA was RNaseA digested prior to horizontal agarose gel electrophoresis. Around 300 ng of genomic DNA was loaded per lane on a 1% agarose gel. **(B)** RAPD band pattern profiles of heavy ion exposed *I. hospitalis* cells to determine genomic DNA integrity. 25 ng of DNA from the same extraction was used as template.

3.2.2 Electromagnetic radiation

Both, X-rays and gamma rays (γ -rays) are part of the electromagnetic spectrum. There are two ways to produce this ionizing radiation. X-rays are generated by interaction of accelerated electrons with matter, whereas gamma rays (γ -rays) are emitted as part of nuclear disintegration (Kiefer, 1990). The following experiments were either conducted with X-rays or γ -rays, depending on the question to be addressed. For example, experiments dealing with DNA repair were exclusively conducted with X-ray exposed cells, whereas gamma rays were used to determine the potential limits for the reproduction of *I. hospitalis*. The following experiments are grouped according to their radiation quality.

3.2.2.1 ^{60}Co irradiation in liquid suspension

The tolerance of *I. hospitalis* and "*I. morulus*" to ionizing radiation in terms of gamma radiation was investigated. Doses of up to ~100 kGy were applied, which were about ten times higher than the D_{10} -value of the extremely radiation-tolerant *Deinococcus radiodurans* (D_{10} -value: 10 kGy; Daly, 2009). The idea was to find the ultimate limit of life in terms of ionizing radiation. Survival, and DNA integrity was determined for both specimens. *I. hospitalis* was studied in more detail regarding its metabolic activity, and reproducibility to discriminate between viability and metabolic activity. The impact of the environment (here: $\frac{1}{2}$ SME+S⁰ medium) on radiation tolerance, and "quorum sensing" experiments were conducted as well. Two radiation campaigns (Death by Radiation (DbR) #1, and #2) were performed using the ^{60}Co source at BGS (Beta Gamma Service, Wiehl, Germany) with slightly diverging dose for technical reasons. The doses applied are subsequently mentioned for each experiment.

3.2.2.2 Survival of *I. hospitalis* and "*I. morulus*" after ^{60}Co radiation exposure

The first radiation campaign (DbR #1) was exclusively conducted with *I. hospitalis*, whereas the second campaign was carried out with "*I. morulus*" as well. Several bottles of well grown stationary phase cultures were anaerobically exposed in serum bottles to 6.2, 11.6, 17.5, 23.9, 46.9, 72.2, 113.3 kGy (DbR #1), and to 6.7, 12.7, 19.0, 27.2, 55.8, 81.1, 117.1 kGy (DbR #2).

The conditions of ionizing radiation exposed *I. hospitalis* stationary phase cultures were microscopically controlled (Figure 29). *I. hospitalis* cells can be seen as dark cocci with a diameter of around 3 μm independent of exposure. Cells were transferred into Falcon[®] tubes (lower left corner) for subsequent DNA extraction. Interestingly, the turbidity of the

culture increased with increasing radiation dose. The same effect was seen for “*I. morulus*”, and cell-free exposed $\frac{1}{2}$ SME+S⁰ medium. The increasing amount of bright particles, ascribed to sulfur particles attenuated by radiation, correlated with increasing turbidity (Figure 29).

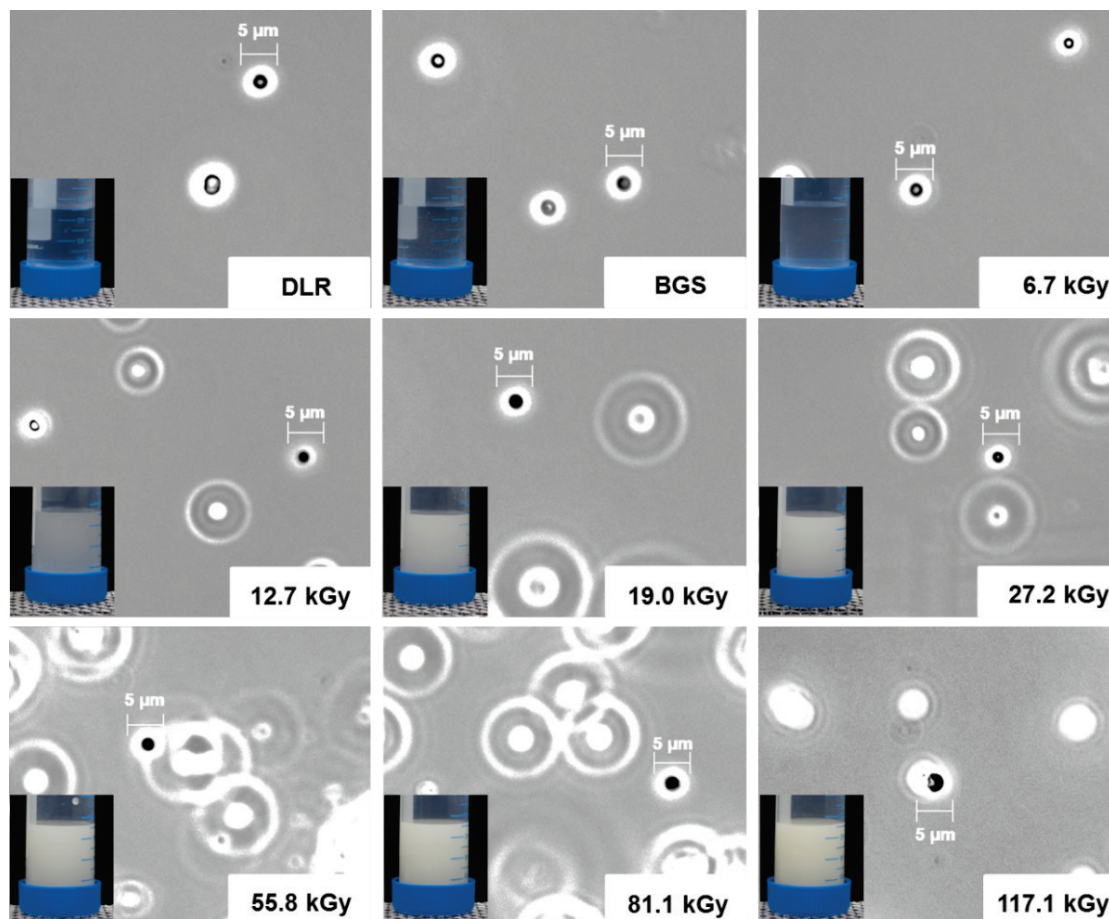


Figure 29: ⁶⁰Co radiation exposed stationary phase cultures of *I. hospitalis*. *I. hospitalis* stationary phase cultures were anaerobically exposed, and transferred into Falcon[®] tubes (lower left images). Their condition after exposure was microscopically controlled under 1000x magnification. *I. hospitalis* cells can be seen as black spots (scale bar=5 µm), whereas the strong refractive particles are ascribed to sulfur. The numbers in the lower right corner represent the applied dose (kGy). DLR represents the lab control, whereas BGS stands for the transport control.

Three independent *I. hospitalis* stationary phase cultures (here IH1, IH2, IH3) were exposed to ⁶⁰Co radiation as mentioned above (DbR #2). Survival was determined by MPN and evaluated under the microscope. To measure the metabolic activity following exposure to ⁶⁰Co radiation, the production of H₂S was monitored as previously described (see 2.3.3) (Figure 30). The documentation of “*I. morulus*” metabolic activity can be found in the Appendix. Small volumes (approximately 5 µl) of exposed *I. hospitalis* cells were dripped on lead acetate paper resulting in strong signals (brown spots) for every exposed sample (Figure 30). $\frac{1}{2}$ SME+S⁰ medium which was incubated at 90 °C for six days as well, did not lead to any positive signal. Signals which were obtained for every single step within the serial dilution were assessed as positive signal due to metabolic activity.

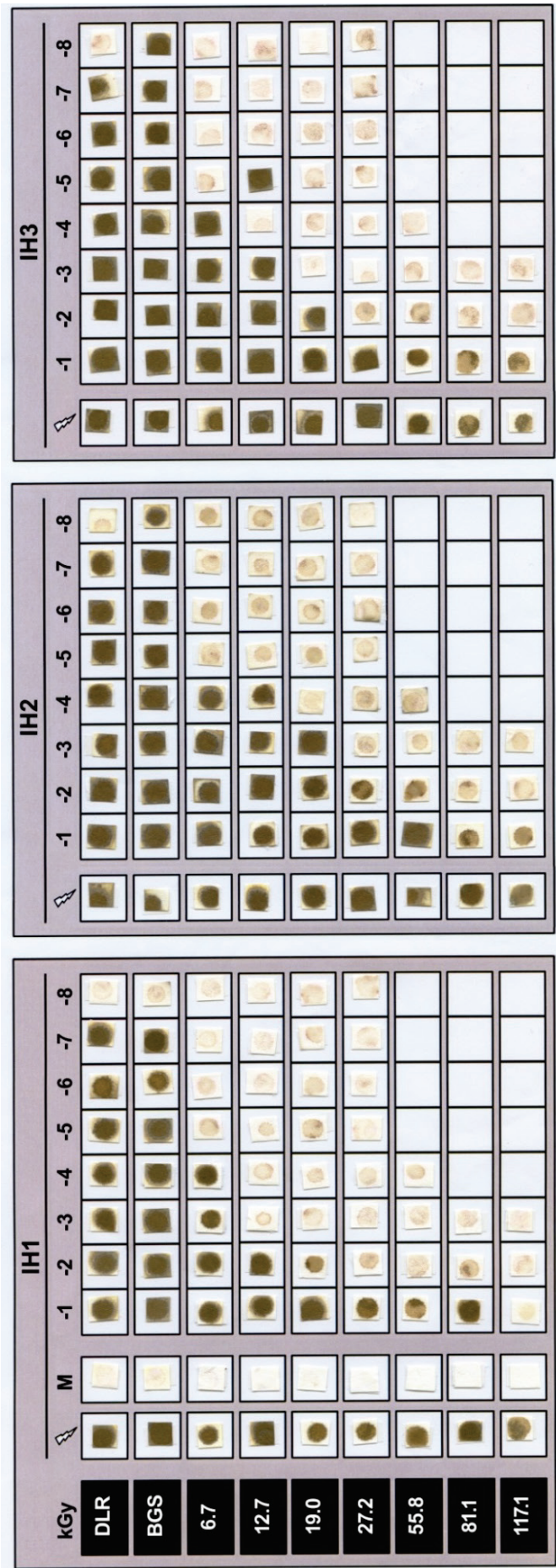


Figure 30: Metabolic activity of *I. hospitalis* (IH1, IH2, IH3) after ^{60}Co radiation exposure monitored on lead acetate paper. The metabolically produced H_2S reacts with lead acetate to lead sulfide, visible as dark brown spots. Abbreviations: Flash (^{60}Co radiation exposed stationary phase cultures), M ($\frac{1}{2}$ SME+S₀ medium incubated at 90 °C for up to six days), DLR (lab control), BGS (transport control). Serial dilutions with 1:10 dilution steps (10^{-1} to 10^{-8}) are represented by the exponent (-1 to -8).

The resulting survival was plotted semi-logarithmically (Figure 31). The overall results obtained for *I. hospitalis* during the first radiation campaign (DbR #1) joined the ranks of the second (DbR #2), although slightly differing radiation doses were applied. “*I. morulus*” showed comparable survival after ^{60}Co radiation exposure. An exposure to ~25 kGy inactivated the cultures by 5 orders of magnitude in all three cases. The dose needed to inactivate the population by 90 % (D_{10}) was determined by linear regression from the linear parts of the semi-logarithmically plotted survival curves (Table 19). For comparison, D_{10} -values for different model organisms (Bacteria or Achaea) are listed in Table 20.

Conspicuously, the exposure of *I. hospitalis* to 55.8, 81.8, and 117.1 kGy (DbR #2) gave positive lead acetate tape signals which can clearly be seen in Figure 30, indicating some metabolic activity although no survival occurred. This effect was further investigated by additional controls.

Table 19: Calculated D_{10} -values (^{60}Co radiation) for different *Ignicoccus* representatives.

Organism	D_{10} -value [kGy]
<i>Ignicoccus hospitalis</i>	4.7
“ <i>Ignicoccus morulus</i> ”	4.5

Table 20: D_{10} -values (^{60}Co radiation) for model organisms (from Beblo *et al.*, 2011).

Model organism	D_{10} -value [Gy]	Source
<i>Ignicoccus hospitalis</i>	1482	Beblo <i>et al.</i> , 2011
<i>Bacillus subtilis</i> (spore)	838	Möller <i>et al.</i> , 2007
<i>Escherichia coli</i>	250	Clavero <i>et al.</i> , 1994
<i>Deinococcus radiodurans</i>	10,000	Daly, 2009
<i>Archaeoglobus fulgidus</i>	1087	Beblo <i>et al.</i> , 2011

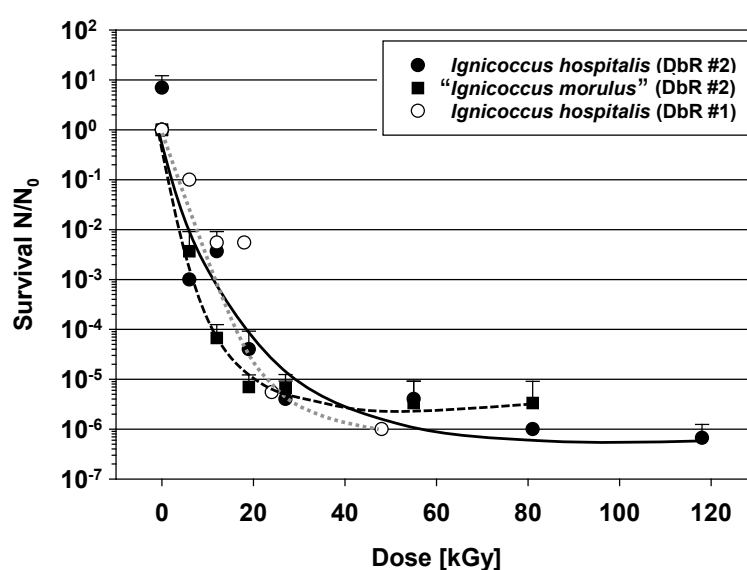


Figure 31: Survival curve of *I. hospitalis* and “*I. morulus*” after ^{60}Co radiation exposure. The survival was plotted semi-logarithmically against the dose. The experiments were conducted with $n=3$ (DbR #2). The trendlines were fitted by hand.

Additional experiments were carried out to discriminate between the viable/culturable state (ability to reproduce), and the viable/nonculturable state (loss of ability to reproduce; VBNC). Exposed $\frac{1}{2}$ SME+S⁰ medium was incubated at 90 °C for 6 days to test, whether H₂S can autonomously be produced by chemical/thermal reactions in absence of any cells giving a false positive signal on lead acetate tape. As shown in Figure 34, no insoluble lead sulfide was detected, therefore no H₂S was produced. A dilution (1:10) of ⁶⁰Co radiation exposed *I. hospitalis* stationary phase cultures in fresh $\frac{1}{2}$ SME+S⁰ medium resulted in only light brown spots before incubation. The signal was caused due to dissolved H₂S which was produced prior to exposure (compare to Figure 30). In the case of IH1 (Figure 34, rows 3, 4), the 1:10 diluted samples (27.2-117.1 kGy) were incubated at 90 °C for up to six days. The same positive signals were obtained after 27.2, and 81.1 kGy as shown in Figure 30. To increase sensitivity, freshly prepared $\frac{1}{2}$ SME+S⁰ medium was inoculated with only 0.2 ml from the serum bottle giving the last positive lead acetate tape signal within the serial dilution. This was conducted for all three independently exposed *I. hospitalis* stationary phase cultures (Figure 34, IH1, IH2, IH3). A dose <19.0 kGy inactivated the survival by ~3 orders of magnitude (Figure 34, 31), and can be seen as viable, and culturable. An applied dose in the range of 19.0-27.2 kGy (Figure 34, IH2, IH3), represented by gray circles in Figure 32, is defined as transition state. Within three independently exposed *I. hospitalis* stationary phase cultures, only two (IH2, IH3) were able to give positive results on lead acetate paper when diluted 1:100 (0.2 ml in 20 ml $\frac{1}{2}$ SME+S⁰ medium). Additionally, cells were detected by microscopic observation (1000-fold) in the case of IH2/19.0 kGy/10⁻³-dilution, and IH3/27.2 kGy/10⁻¹-dilution (Figure 33). The ability of reproduction/cell division ended with an applied dose >27.2 kGy (Figure 34, IH3), and is represented by open circles. This state is denoted as VBNC (viable but nonculturable) and describes here an ongoing metabolic activity in terms of H₂S production, although the ability for cell division was lost. It was not possible to detect any cell under the microscope.

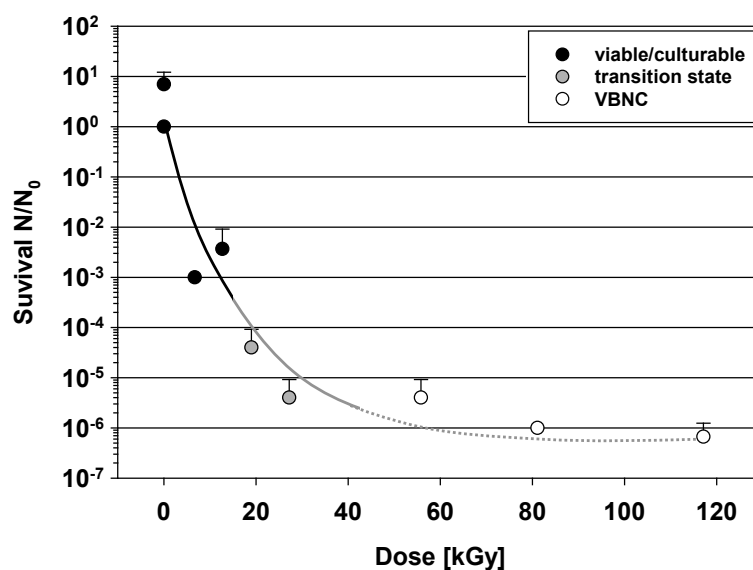


Figure 32: Discrimination between culturable, and viable but nonculturable (VBNC) state. The survival of *I. hospitalis* was analyzed in respect to its reproduction ability (culturable), and its viable but nonculturable (VBNC) state. Filled circles (black): Clearly viable and replication-competent, hence culturable. Filled circles (gray): Transition state between culturable, and viable but nonculturable (VBNC). Open circles: Viable but nonculturable (VBNC). The experiment was conducted with $n=3$. Trendlines were fitted by hand.

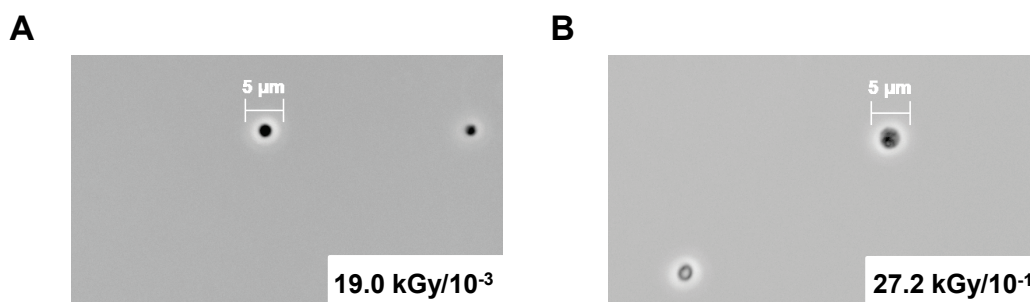


Figure 33: Microscopic images of *I. hospitalis* cells at 1000-fold magnification. Fresh $\frac{1}{2}$ SME+S⁰ medium was inoculated with 2 ml of the last bottle giving a positive signal on lead acetate tape within the serial dilution after irradiation. The microscopic picture was taken after 6 days incubation at 90 °C. *I. hospitalis* cells can be seen as black cocci (scale bar=5 µm). (A) IH2, (B) IH3. The numbers in the lower right corner represent the applied dose (kGy), and the dilution step.

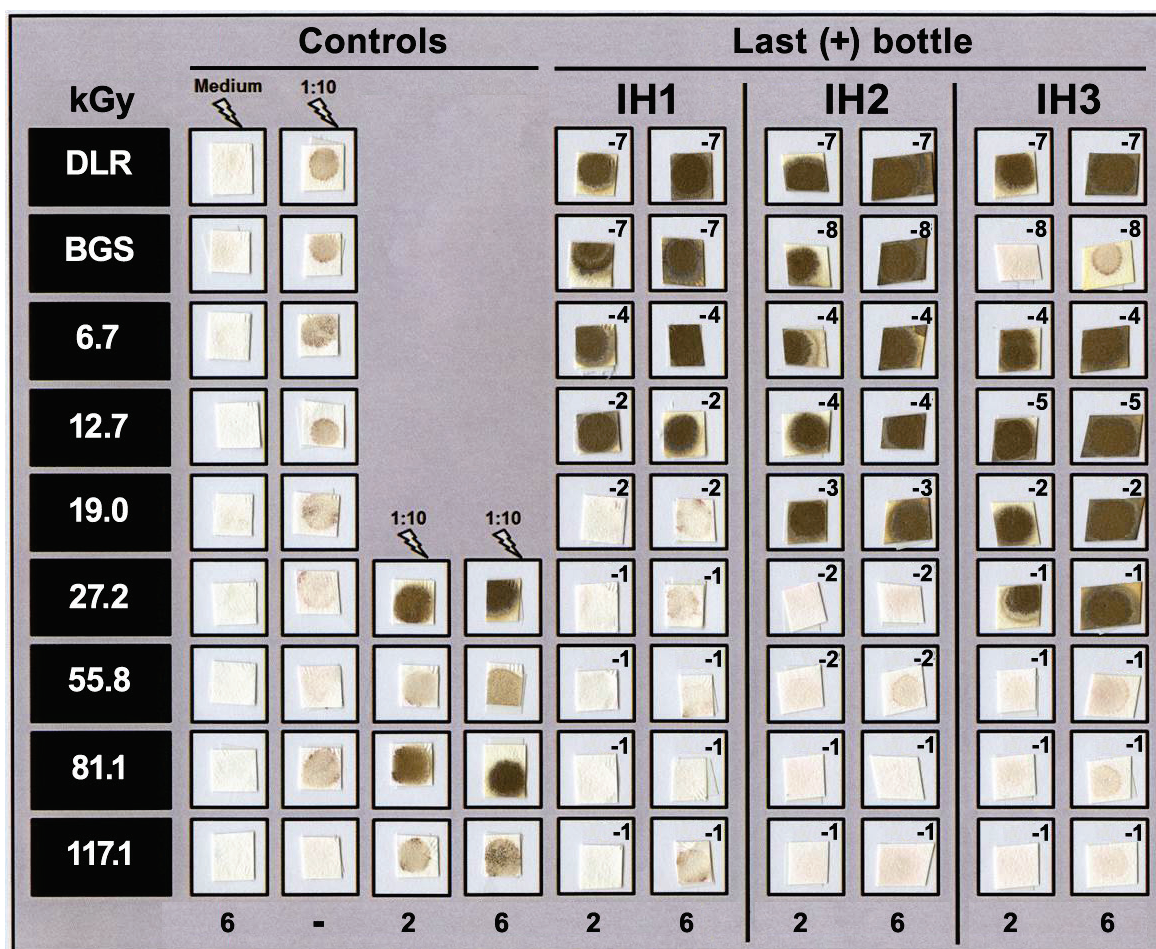


Figure 34: Metabolic activity of three independent *I. hospitalis* stationary phase cultures (IH1, 2, 3) after gamma ray exposure monitored on lead acetate paper. Exposed $\frac{1}{2}$ SME+S⁰ medium, and exposed stationary phase cultures (1:10 diluted in fresh $\frac{1}{2}$ SME+S⁰ medium) were incubated at 90 °C for up to six days (rows 1, 3, 4). Exposed IH1 stationary phase cultures 10-fold diluted in fresh medium before incubation (row 2). For higher sensitivity, 0.2 ml of the last positive IH1 bottle within a serial dilution (see Figure 30) were transferred into fresh $\frac{1}{2}$ SME+S⁰ medium, and incubated at 90 °C for up to 6 days (rows 5, 6). The same was conducted with IH2 (rows 7, 8), and IH3 (rows 9, 10). The metabolically produced H₂S was monitored on lead acetate paper. Abbreviations: DLR (laboratory control), BGS (transport control), 2 (2 days incubation at 90 °C), 6 (6 days incubation at 90 °C). Bottles giving the last positive lead acetate signal within the serial dilution (see Figure 30) are represented by the exponent (-1 to -8).

Summary:

- The turbidity of the culture increased with increasing radiation dose, and the increasing amount of bright particles, ascribed to sulfur particles, correlates with that (Figure 29). $\frac{1}{2}$ SME+S⁰ medium was incubated at 90 °C for up to 6 days, to make sure that all following signals on lead acetate tape were due to metabolically produced H₂S. No signals were detected in cell-free medium. Signals which were obtained for every single step within the serial dilution were assessed as positive signal due to metabolic activity (Figure 30).
- The first radiation campaign (DbR #1) joined the ranks of the second (DbR #2), although slightly differing radiation doses were applied. “*I. morulus*” showed comparable survival after ⁶⁰Co radiation exposure as shown for *I. hospitalis*. An exposure to ~25 kGy inactivated the cultures by 5 orders of magnitude in all three cases (Figure 31).
- To discriminate between the viable/culturable, and VBNC state of *I. hospitalis* additional controls were introduced. A dose of <19.0 kGy reduced the survival by ~3 orders of magnitude (Figure 32), and can be seen as viable and culturable. An applied dose in the range of 19.0-27.2 kGy was defined as transition state. The ability of reproduction/cell division ended with an applied dose >27.2 kGy, when no cells were detected with a 1000-fold magnification, while the metabolic activity was monitored on lead acetate tape. This state was described as VBNC.

3.2.2.3 Comparing the impact of ⁶⁰Co radiation exposed $\frac{1}{2}$ SME+S⁰ medium to *I. hospitalis* stationary phase cells which were serial diluted prior to exposure

I. hospitalis showed reduced tolerance to ionizing radiation (⁶⁰Co radiation) when serial diluted in $\frac{1}{2}$ SME+S⁰ medium prior to exposure (DbR #1; Figure 35) compared to stationary phase cultures which were serial diluted in $\frac{1}{2}$ SME+S⁰ medium after exposure (Figure 31). To test whether the exposure of $\frac{1}{2}$ SME+S⁰ medium itself has a negative or inhibitory effect on cell survivability, $\frac{1}{2}$ SME+S⁰ medium was exposed to ⁶⁰Co radiation (DbR #2), and used for serial dilutions with untreated *I. hospitalis* cells (Figure 35). The dose dependent survivability of *I. hospitalis* in ⁶⁰Co radiation exposed medium was determined by the most probable number technique. As shown in Figure 35, $\frac{1}{2}$ SME+S⁰ medium which was exposed to ⁶⁰Co radiation has a comparable inhibitory effect on cell survivability compared to cells which were serial diluted prior to exposure.

The inhibitory effect of ^{60}Co radiation exposed $\frac{1}{2}$ SME+S 0 medium on cell survivability can be compared to the results obtained for *I. hospitalis* cultures, which were serial diluted prior to exposure. An exposure of ~20 kGy reduced the survival by around 5 orders of magnitude in both cases (Figure 35). Interestingly, the log reduction does not increase with gamma ray doses >20 kGy.

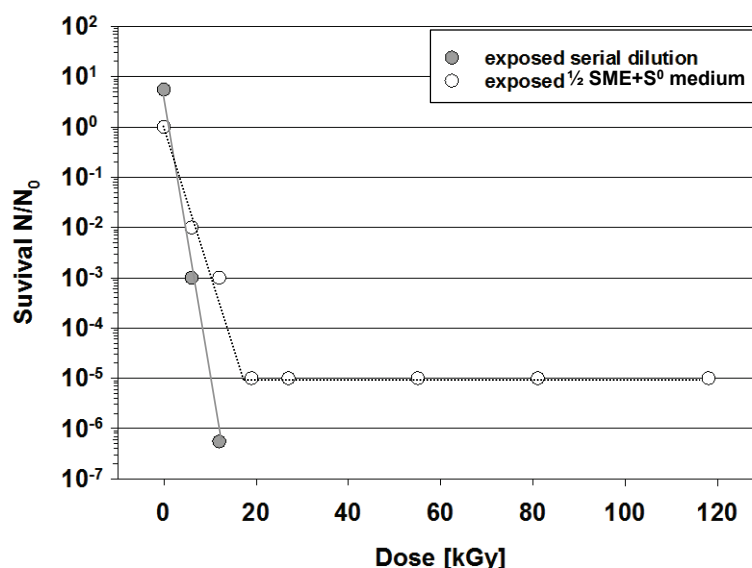


Figure 35: Impact of ^{60}Co radiation exposed $\frac{1}{2}$ SME+S 0 medium on the survival of *I. hospitalis*. The survival was plotted semi-logarithmically against the dose (up to 117.1 kGy). The experiments were conducted with $n \geq 1$. Open circles: Exposed $\frac{1}{2}$ SME+S 0 medium. The exposed medium was used for serial dilutions with untreated *I. hospitalis* cells. Filled circles: *I. hospitalis* cells were serial diluted in $\frac{1}{2}$ SME+S 0 medium prior to exposure. The diluted samples were exposed to ^{60}Co radiation. Trendlines were fitted by hand.

The doses needed to inactivate the population by 90 % (D_{10}) were deduced from the linear parts of the semi-logarithmically plotted survival curves (Figure 35), and are listed in Table 21.

Table 21: D_{10} -values (^{60}Co radiation) for *I. hospitalis*, serial diluted in exposed $\frac{1}{2}$ SME+S 0 medium or serial diluted prior to exposure in (unexposed) $\frac{1}{2}$ SME+S 0 .

Condition	D_{10} -value [kGy]
Exposed $\frac{1}{2}$ SME+S 0 medium	~3.5
Serial dilution prior to exposure	~2.5

3.2.2.4 ^{60}Co radiation exposure of elemental sulfur (dry and wet)

Based on the idea that ionizing radiation changes the natural conformation of elemental sulfur (S_8) in liquid solution, the potential reason for turbidity (Figure 29), several sulfur combinations were independently exposed to increasing ^{60}Co radiation dose and used to supplement sulfur-free $\frac{1}{2}$ SME medium after exposure. Therefore, elemental sulfur was anaerobically exposed (dry or wet) to 6.5, 24.2, 50.3, 114.3 kGy. Unexposed sulfur-free $\frac{1}{2}$ SME medium supplemented by unexposed sulfur served as control sample (N_0). Sulfur-free $\frac{1}{2}$ SME medium, which was exposed to ^{60}Co radiation, was completed by untreated

or treated sulfur. *I. hospitalis* stationary phase cultures were used to inoculate these prepared serum bottles, and serial dilutions were performed to determine the relative survival.

As shown in Figure 36A, the most prominent effect was obtained for ^{60}Co radiation exposed $\frac{1}{2}$ SME- S^0 medium which was supplemented by either unexposed (light gray bars) or exposed dry elemental sulfur (dark gray bars). An inactivation tendency in the range of 6-orders of magnitude was shown in both cases. The relative survival of *I. hospitalis* cells which were serial diluted in exposed $\frac{1}{2}$ SME- S^0 medium completed by wet unexposed sulfur (light gray bars) showed a similar inactivation (Figure 36B). The same effect was obtained for irradiated $\frac{1}{2}$ SME- S^0 medium supplemented by wet exposed elemental sulfur (dark gray bars). An exposure of sulfur-free $\frac{1}{2}$ SME medium to >6.5 kGy ^{60}Co radiation resulted in a 6-fold log reduction of *I. hospitalis*' relative survival independent from sulfur supplementation (Figure 36).

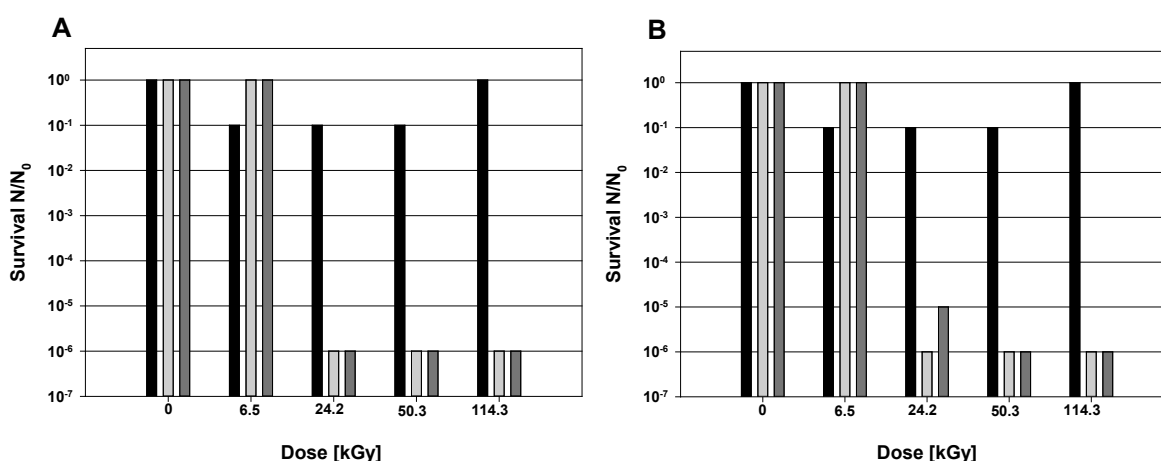


Figure 36: Relative survival of *I. hospitalis* when cultivated in ^{60}Co radiation exposed or unexposed $\frac{1}{2}$ SME medium supplemented by elemental sulfur. (A) Dry exposed elemental sulfur. (B) Wet exposed elemental sulfur. Black bars: $\frac{1}{2}$ SME medium (unexposed) + sulfur (^{60}Co radiation exposed). Light gray bars: $\frac{1}{2}$ SME medium (^{60}Co radiation exposed) + sulfur (unexposed). Dark gray bars: $\frac{1}{2}$ SME medium (^{60}Co radiation exposed) + sulfur (^{60}Co radiation exposed). The experiment was conducted with $n=1$.

3.2.2.5 ^{60}Co irradiation of single $\frac{1}{2}$ SME medium components

Aliquots of every substance needed for $\frac{1}{2}$ SME medium preparation were exposed to ^{60}Co radiation (27.2, 55.8, 117.1 kGy) as they were provided by the manufacturer. The strongest color changes after 117.1 kGy was achieved with substances containing sodium or bromide (Figure 37, substances 1 (sodium chloride), 6 (sodium bromide), 12 (sodium hydrogen carbonate), 13 (sodium sulfide nonahydrate)) or iodide (substance 9 (potassium iodide)). Dose specific $\frac{1}{2}$ SME- S^0 medium was prepared from these substances using sterile ddH₂O as described in 2.2.2. The prepared $\frac{1}{2}$ SME- S^0 media were either supplemented with exposed or unexposed sulfur (Table 22). Additionally, to test whether

sulfur plays a special role, $\frac{1}{2}$ SME-S⁰ medium was prepared from unexposed single substances and supplemented with either unexposed or exposed sulfur. Medium which was prepared from exposed single $\frac{1}{2}$ SME medium substances has no inhibitory effect, independent of the supplied sulfur variant (+/- ⁶⁰Co radiation exposure). The preparation of $\frac{1}{2}$ SME-S⁰ medium from unexposed single substances completed by unexposed sulfur served as reference sample. One half SME-S⁰ medium prepared from unexposed substances has no inhibitory effect when exposed sulfur was added. No inhibitory effect was observed at all independently of all different variants tested (Table 22).

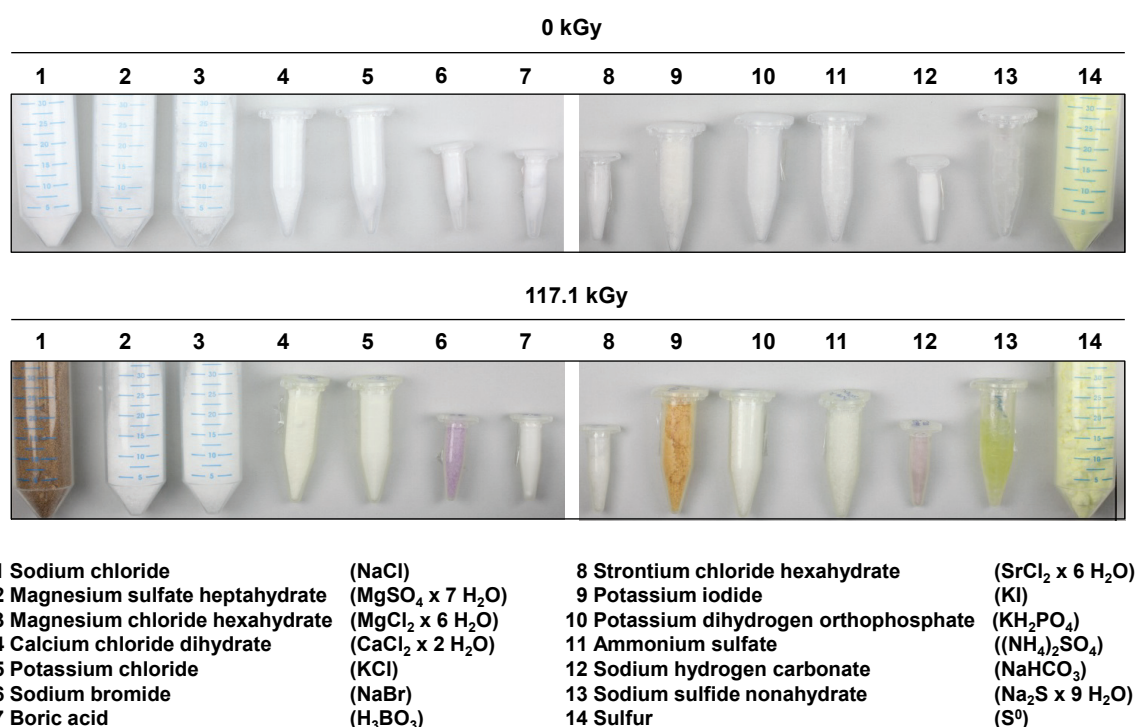


Figure 37: Aliquots of substances needed for $\frac{1}{2}$ SME-S⁰ medium preparations. The exposure was conducted in either Falcon® or Eppendorf Tubes®. Pictures were taken before (0 kGy) and after ⁶⁰Co radiation exposure (117.1 kGy). Illustrated documentation for 27.2 kGy, and 55.8 kGy can be found in the Appendix.

Table 22: Preparation of $\frac{1}{2}$ SME medium from single components which were exposed to increasing ⁶⁰Co radiation dose. The prepared media were supplemented either with exposed or unexposed sulfur, and inoculated with *I. hospitalis* cells. The log reductions (*) refer to the respective medium supplemented with unexposed sulfur (No ⁶⁰Co radiation exposure*). The experiment was conducted with n=1.

$\frac{1}{2}$ SME components (-sulfur)	Sulfur		log reduction*
⁶⁰ Co exposure [kGy]	No ⁶⁰ Co exposure*	⁶⁰ Co exposure [kGy]	
27.2	x	-	0
	-	27.2	0
55.8	x	-	0
	-	55.8	1
117.1	x	-	0
	-	117.1	1

3.2.2.6 Quorum sensing

Quorum sensing, meaning the production, release, and detection of signaling molecules, and the subsequent response to them at high cell population densities, is known for Gram-negative, and Gram-positive bacteria (according to Bassler, 2002). To test whether secreted compounds in the supernatant of an *I. hospitalis* stationary phase culture are able to rescue cells which were exposed to high doses of ^{60}Co radiation (19.0, 27.2, 55.8, 81.1, 117.1 kGy), several cultures were sterile filtered (0.2 μm Whatman[®] filter unit) to obtain a cell-free supernatant. The filtrates were inoculated with ^{60}Co radiation exposed stationary phase cultures, followed by incubation. Several control steps were performed on lead acetate paper by dripping a small volume on it (Figure 38). All stationary phase cultures gave positive signals indicating the presence of metabolically produced H_2S . The produced H_2S was removed by N_2/CO_2 evacuation. No positive signal was obtained after sterile filtration. The filtrates were inoculated (1:10) with ionizing radiation exposed *I. hospitalis* stationary phase cultures. No signal was detected. Incubation at 90 °C for up to 6 days indicated an active production of H_2S regardless the applied ^{60}Co radiation dose (Figure 38). The negative control (M) meaning sterile filtrate inoculated with fresh $\frac{1}{2}$ SME+S⁰ medium resulted in a positive signal as well. Sterile filtrates were inoculated (1:10) in parallel with samples from the last bottles giving a positive signal within the serial dilution (Figure 39). Strong signals were obtained for the negative control (M), the positive control (DLR), and the 55.8 kGy sample.

Due to the fact that negative control samples (sterile filtrates inoculated with medium) gave positive signals on lead acetate paper in both cases, and cells were detected by microscopic observation, the experiments were repeated using Whatman[®] Nuclepore[™] Track-Etched Membranes with 0.1 μm pore size. Similar results were obtained for the negative controls; a sterile filtration was not possible. A definite statement cannot be made whether *I. hospitalis* secretes compounds which are able to rescue cells exposed to high doses of ionizing radiation.

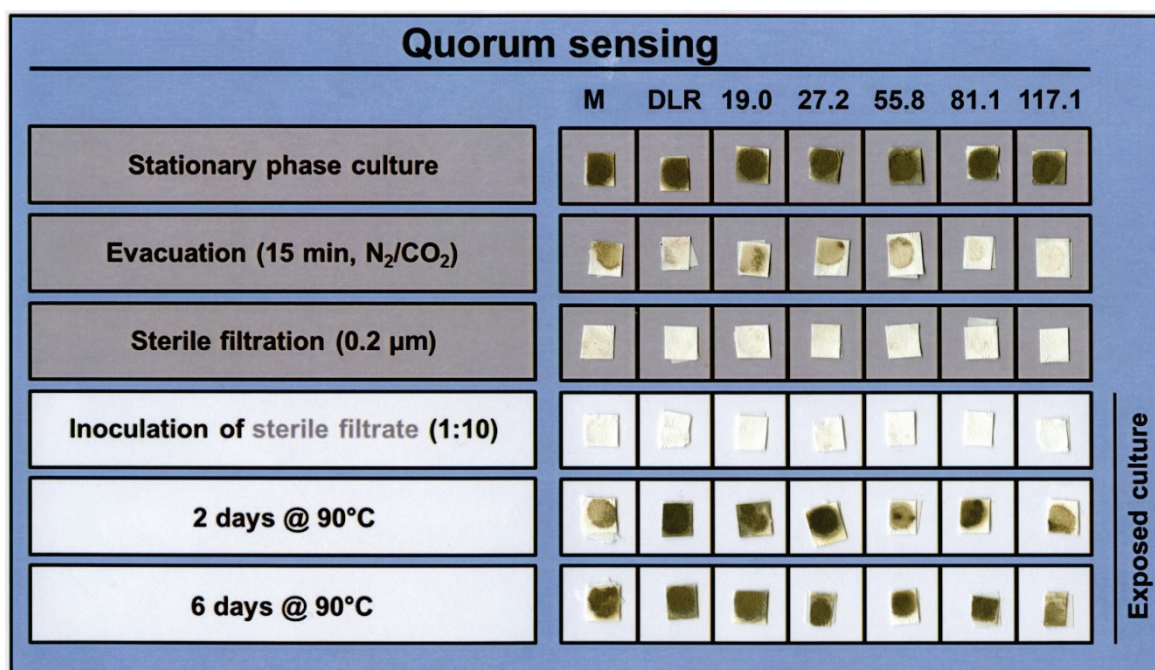


Figure 38: Quorum sensing with ^{60}Co radiation exposed stationary phase cells of *I. hospitalis*. The metabolically produced H_2S was visualized on lead acetate paper. Abbreviations: M (fresh $\frac{1}{2}$ SME+S⁰ medium was used to inoculate the sterile filtrate), DLR (laboratory control). The applied dose is given in kGy.

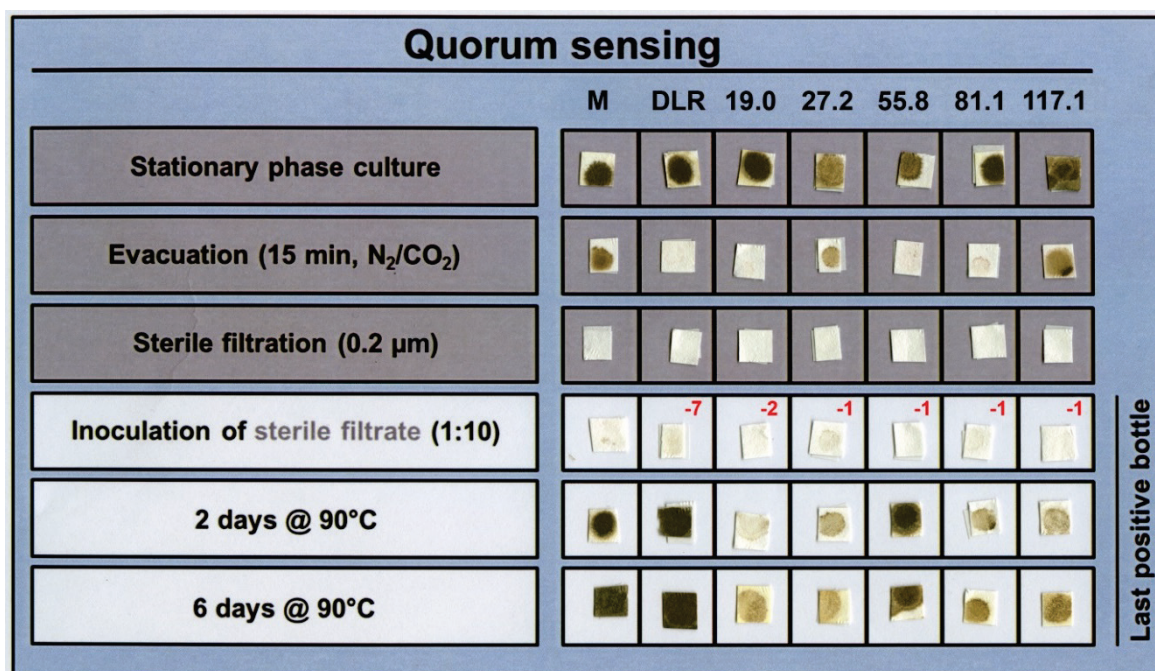


Figure 39: Quorum sensing with samples from the last bottle giving a positive signal within the serial dilution after ^{60}Co radiation exposure. The metabolically produced H_2S was visualized on lead acetate paper. Abbreviations: M (fresh $\frac{1}{2}$ SME+S⁰ medium was used to inoculate the sterile filtrate), DLR (laboratory control), red numbers (serial dilutions with 1:10 dilution steps (10^{-1} to 10^{-7}) are represented by the exponent (-1 to -7)). The applied dose is given in kGy.

3.2.2.7 DNA integrity after gamma ray (^{60}Co radiation) exposure

The genome integrity of *I. hospitalis* and “*I. morulus*” was analyzed after ^{60}Co radiation exposure. The DNA was extracted from three independently exposed stationary phase cultures (*I. hospitalis*, “*I. morulus*”), pooled and used as template for both RAPD and qPCR analysis. RAPD analysis was conducted with a single decameric primer, the resulting band pattern profiles were analyzed with respect to changes such as differences in band intensity as well as gain/loss of RAPD bands.

Figure 40A shows, that the overall band pattern of *I. hospitalis* is severely impacted by ionizing radiation comparing to untreated control sample (DLR, BGS). The loss of bands increased with increasing dose (Figure 40A). An exposure to 19.0 kGy resulted in the absence of the band with a length of >2000 bp, and ~1400 bp. Similar results were obtained for “*I. morulus*”. A dose of 12.7 kGy produced no bands above ~1300 bp (Figure 41A).

A supportive result was obtained by qPCR. The 16S rRNA primer set, specific for *I. hospitalis*, was used to amplify a 1.3 kb fragment of the 16S rRNA sequence from pooled genomic DNA mentioned above. The same primer set was used to amplify “*I. morulus*” 16S rRNA sequence, too. The relative amplification rates were calculated according to the normalized C_t values. The C_t value is the average from one experiment performed in triplicates conducted with pooled genomic DNA. The overall amplification rate decreased with increasing radiation dose compared to the untreated transport control (BGS) (Figure 40C). The agarose gel (Figure 40C) of qPCR amplified 16S rRNA fragments emphasized the result; an exposure to 117.1 kGy prevented amplification. A comparable result was obtained for “*I. morulus*”; the amplification was inhibited at doses above 55.8 kGy (Figure 41B, C).

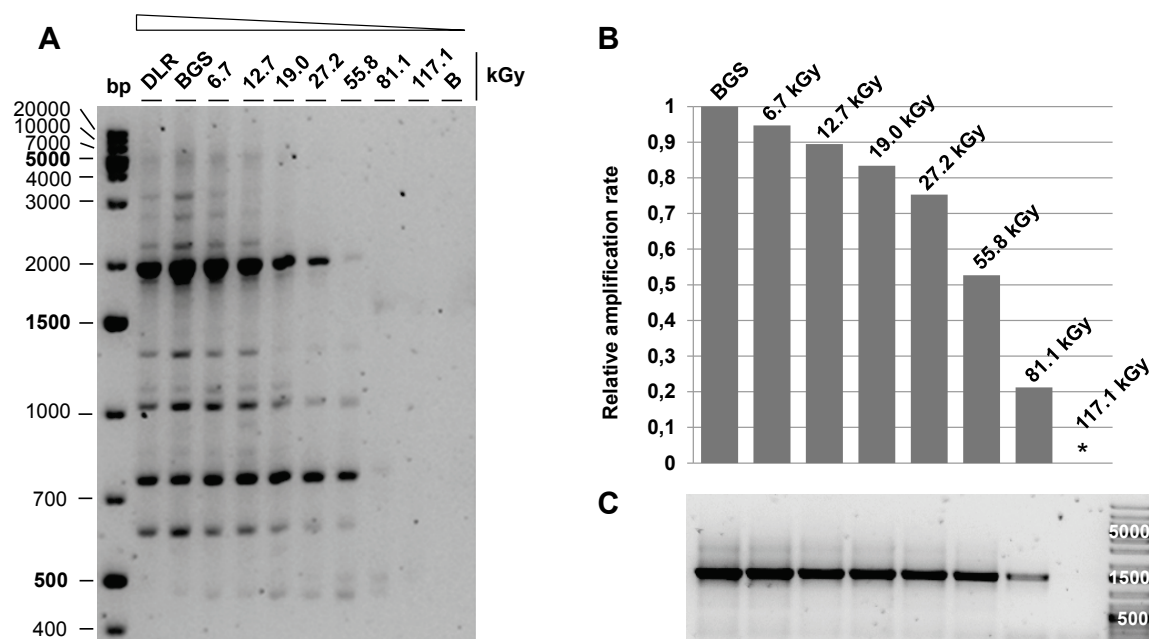


Figure 40: Analysis of the genomic DNA integrity of *I. hospitalis* after ^{60}Co radiation exposure. Pooled DNA from three independently exposed stationary phase cultures were used as template for RAPD analysis and qPCR. **(A)** RAPD profile of genomic DNA analyzed on a 2 % agarose gel. The numbers indicate the applied dose. **(B)** qPCR with 16S rRNA primer. The C_t values were normalized to the minimum with DLR acting as untreated reference sample. **(C)** Primer specific amplicon analyzed on a 2 % agarose gel, 2 μl were loaded per lane. Abbreviations: * (no signal obtained), DLR (laboratory control), BGS (transport control).

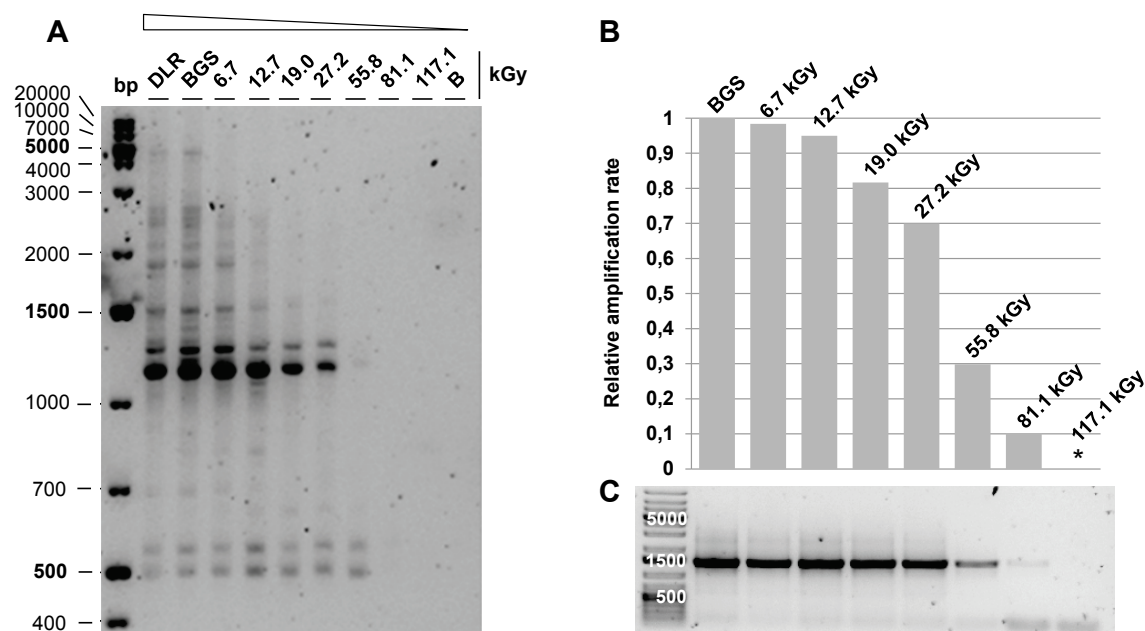


Figure 41: Analysis of the genomic DNA integrity of *I. morulus* after ^{60}Co radiation exposure. Pooled DNA from three independently exposed stationary phase cultures were used as template for RAPD analysis and qPCR. **(A)** RAPD profile of genomic DNA analyzed on a 2 % agarose gel. The numbers indicate the applied dose. **(B)** qPCR with 16S rRNA primer. The C_t values were normalized to the minimum with DLR acting as untreated reference sample. **(C)** Primer specific amplicon analyzed on a 2 % agarose gel, 2 μl were loaded per lane. Abbreviations: * (no signal obtained), DLR (laboratory control), BGS (transport control).

Summary:

- *I. hospitalis* showed reduced tolerance to ionizing radiation (^{60}Co radiation) when serially diluted in $\frac{1}{2}$ SME+S⁰ medium prior to exposure (DbR #1; Figure 35) compared to stationary phase cultures which were serially diluted in $\frac{1}{2}$ SME+S⁰ medium after exposure (Figure 31). The exposed (cell-free) $\frac{1}{2}$ SME+S⁰ medium showed a comparable inhibitory effect on cell survivability as shown for cells which were serially diluted prior to exposure.
- Elemental sulfur which was exposed in $\frac{1}{2}$ SME medium may have changed its natural conformation (S₈); a changed conformation could also be the reason for turbidity. An exposure of sulfur-free $\frac{1}{2}$ SME medium to >6.5 kGy ^{60}Co radiation resulted in a 6-fold log reduction of the relative survival of *I. hospitalis* independent from sulfur supplementation (Figure 36).
- Dry exposed single substances were used to prepare dose specific $\frac{1}{2}$ SME+S⁰ medium. To test whether sulfur plays a special role, $\frac{1}{2}$ SME medium was also prepared from unexposed single substances either supplemented with un- or exposed sulfur. No inhibitory effect was observed independently of all different variants tested (Table 22).
- To elucidate a possible quorum sensing effect, and to test whether *I. hospitalis* stationary phase cultures may be able to rescue cells which were exposed to high doses of ^{60}Co (19.0, 27.2, 55.8, 81.1, 117.1 kGy), several cultures were sterile filtered to obtain a cell-free supernatant. The negative control (M) meaning sterile filtrate inoculated with fresh $\frac{1}{2}$ SME+S⁰ medium resulted in a positive signal, on lead acetate tape, and by microscopic observation (Figure 38, 39).
- The genome integrity of *I. hospitalis* and "*I. morulus*" was analyzed by RAPD and qPCR after ^{60}Co radiation exposure. The overall RAPD band pattern profile of both specimens were severely impacted by ionizing radiation comparing to untreated control samples indicating that numerous DNA damages (e.g. strand breaks) were induced by radiation (Figure 40A, 41A). These results were supported by qPCR. An exposure of *I. hospitalis* to 117.1 kGy prevented amplification, whereas the amplification in the case of "*I. morulus*" was already inhibited at doses >55.8 kGy (Figure 40B, 41B).

3.2.2.8 X-ray exposure of *I. hospitalis* with and without soft X-rays

All following experiments concerning X-ray exposure, and DNA repair were exclusively conducted with *I. hospitalis* due to its already known high ionizing radiation tolerance (Beblo *et al.*, 2011). *I. hospitalis* stationary phase cells were exposed to X-rays under anoxic conditions in HPLC vials. The X-ray dose was applied using a Gulmay RS225A radiation source from Gulmay Medical Limited (Camberley, England).

Initial irradiation experiments were performed at 200 kV, and 15 mA using a 0.1 mm Aluminum filter. Filters are commonly used during the experiment to filter out soft X-rays leaving mainly hard X-rays with higher energy to penetrate the sample. As a result, no differences in survival of *I. hospitalis* were detected after X-ray exposure with/without a 0.1 mm Al filter (Figure 42).

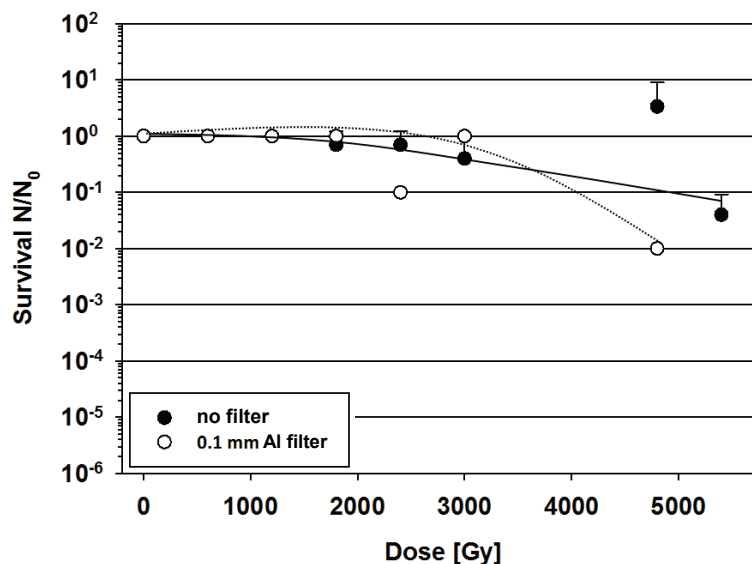


Figure 42: Survival of *I. hospitalis* after X-ray exposure with and without the use of a 0.1 mm Al filter. The experiments were conducted with $n=3$, except for 0.1 mm Al filtered exposure ($n=1$). The trendlines were fitted by hand.

The use of an additional 0.1 mm Al filter was neglected; all HPLC vials turned from colorless to brownish during exposure (Figure 43) indicating a homogenous irradiation.



Figure 43: HPLC vials. Left side: unexposed vial; right side: X-ray exposed vial.

It was concluded that comparable amounts of hard X-rays were able to penetrate the sample based on comparable dose rates. All experiments were conducted without an additional 0.1 mm Al filter. Potential outliers occurred in the frame of experimental errors and due to a limited number of repetitions. All values plotted in the following graphs have already been corrected accordingly.

3.2.2.9 Survival of *I. hospitalis* after X-ray exposure

The dose dependent survival of *I. hospitalis* after X-ray exposure was determined as described in the following. *I. hospitalis* stationary phase cells were anaerobically exposed to increasing doses of ionizing radiation. The survival was determined by the most probable number technique. As shown in Figure 44, the overall survival decreases with increasing radiation dose. The survival curve shows a broad shoulder region up to approximately 4000 Gy. Almost no difference in survival can be seen between unexposed cells, and cells exposed to 3000 Gy. Inactivation starts with doses >3000 Gy, and results in a reduction of 3-4 orders of magnitude after exposure to 12000 Gy.

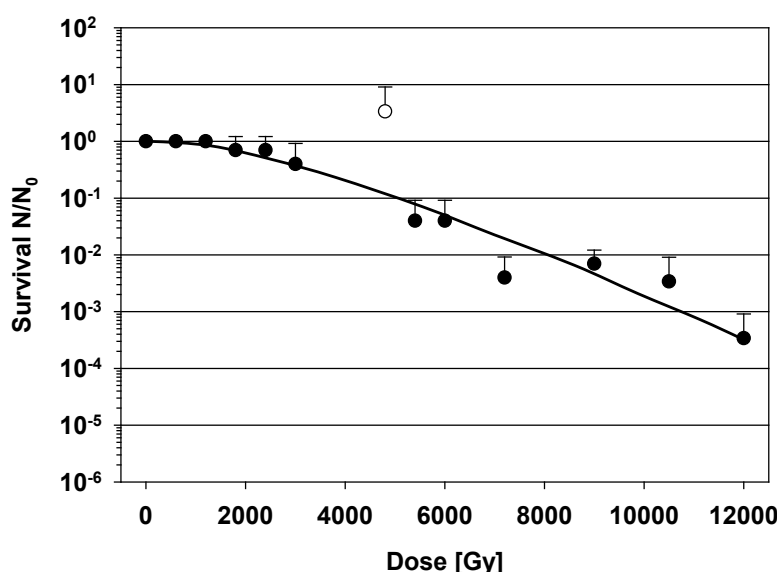


Figure 44: Survival curve of *I. hospitalis* after X-ray exposure. The survival was plotted semi-logarithmically against the dose (up to 12000 Gy). Open circle: Outlier, not taken into account. The experiments were conducted with $n=3$. A trendline was fitted by hand.

The dose needed to inactivate the population by 90 % (D_{10}) was deduced from the linear parts of the semi-logarithmically plotted survival curve (Figure 44), and turned out to be in the range of 5 kGy.

3.2.2.10 Influence of the cultivation temperature on X-ray tolerance

To test whether the cultivation temperature influences the tolerance of *I. hospitalis* to ionizing radiation, cells were cultivated at three different temperatures prior to exposure.

Cells were grown at 75 °C ($<T_{\text{opt}}$), at 95 °C ($>T_{\text{opt}}$), and at their T_{opt} (90 °C; Paper *et al.*, 2007). The samples were exposed to increasing doses of ionizing radiation, and recovered at 90 °C. The survival was plotted semi-logarithmically (Figure 45). The radiotolerance of *I. hospitalis* seemed to be unaffected by cultivation temperature (Figure 45). An exposure to 9000 Gy reduces the survival by approximately two orders of magnitude independently from cultivation temperature.

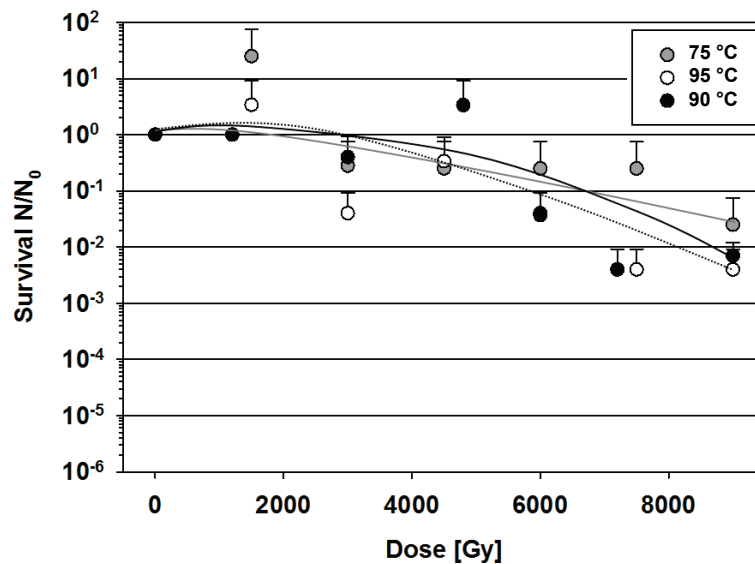


Figure 45: Survival curve of *I. hospitalis* after X-ray exposure when cultivated below/above T_{opt} . The survival was plotted semi-logarithmically against the dose (up to 9000 Gy). The experiments were conducted with $n=3$. The graph was completed with data obtained for X-ray exposed *I. hospitalis* cells cultivated at 90 °C (T_{opt}) (see Figure 44). The trendlines were fitted by hand.

3.2.2.11 Hot exposure

The hot exposure experiment was designed to test whether the incubation of *I. hospitalis* at 90 °C (T_{opt}) during X-ray exposure has an influence on its survival in comparison to an exposure at room temperature. It is assumed that *I. hospitalis* is metabolically inactive at RT due to the temperature difference of ~70 °C, meaning neither reproduction nor repair may take place during exposure. Two serum bottles containing *I. hospitalis* stationary phase cells in fresh $\frac{1}{2}$ SME+S⁰ medium were either transferred to the exposure bucket, or the reference bucket (Figure 18). Both setups were run in parallel at ~88 °C during the whole experiment. It was necessary to incubate the reference sample as well, to be able to follow the potential increase in cell concentration. Samples were taken from both setups as indicated in Figure 46. The survival of hot exposed cells is almost identical to the survival of cells exposed at RT. An incubation at T_{opt} does not influence the X-ray tolerance of *I. hospitalis*.

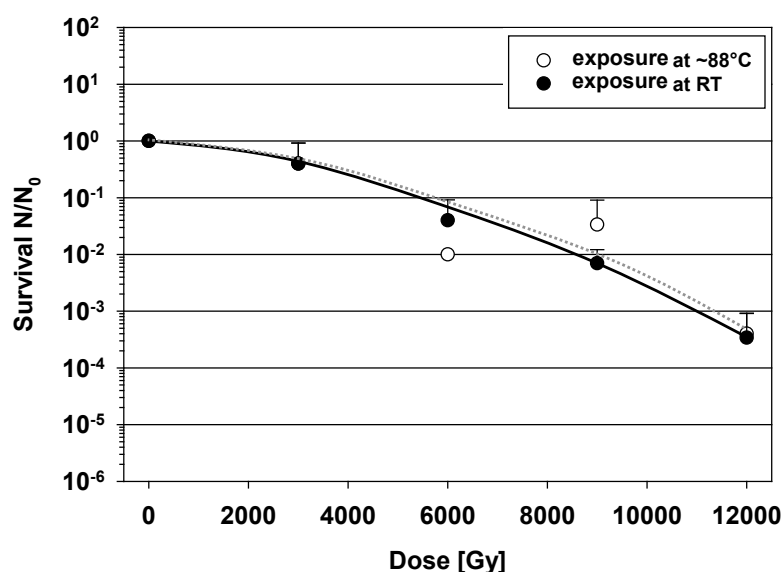


Figure 46: Survival curve of *I. hospitalis* after X-ray exposure at ~88 °C. The survival was plotted semi-logarithmically against the dose (up to 12 kGy). The experiments were conducted with $n=3$. The graph was completed with data presented in Figure 44. Trendlines were fitted by hand.

3.2.2.12 DNA integrity after X-ray exposure

The relative amount of DNA lesions per 1.3 kb fragment (16S rRNA gene, Table 5), and the genome integrity of *I. hospitalis* after X-ray exposure was analyzed by qPCR and RAPD assay (data not shown). Similar tendencies were obtained as already presented for γ -ray exposed cells (Figure 40). The relative amount of DNA lesions increased with increasing dose, whereas the survival decreased (Figure 44); the loss of RAPD bands increased with increasing ionizing radiation dose.

Summary:

- No differences in the survival of *I. hospitalis* were detected after X-ray exposure with/without a 0.1 mm Al filter (Figure 42). The inactivation started with doses >3000 Gy, and resulted in a reduction of 3-4 orders of magnitude after exposure to 12000 Gy (Figure 44). The dose needed to inactivate the population by 90% (D_{10}) was ~5 kGy.
- The ionizing radiation tolerance of *I. hospitalis* seemed to be unaffected by varying pre-cultivation temperatures (Figure 45); an exposure to 9000 Gy reduced the survival by ~2 orders of magnitude independently from cultivation temperature. Additionally, the survival of hot exposed cells was almost identical to the survival of cells exposed at RT. Incubation at T_{opt} did not influence the X-ray tolerance of *I. hospitalis* (Figure 46).

- The genome integrity of *I. hospitalis* was analyzed by RAPD, and qPCR after X-ray exposure. A decreased genome integrity was detected with increasing radiation dose, concomitantly with an increase in the relative amount of induced DNA lesions.

3.3 DNA repair

3.3.1 DNA repair of *I. hospitalis* after X-ray exposure

RAPD analysis was conducted to get an impression on how fast *I. hospitalis* is able to repair its ionizing radiation induced DNA damages. Cells were exposed to 12.6 kGy and incubated afterwards at 90 °C for increasing periods of time. Samples were taken at times indicated in Figure 47. Bands with an amplicon size >2000 bp were most sensitive to ionizing radiation. No band pattern differences were detected after 5 min incubation at 90 °C when comparing to the 12.6 kGy exposed unrepaired sample.

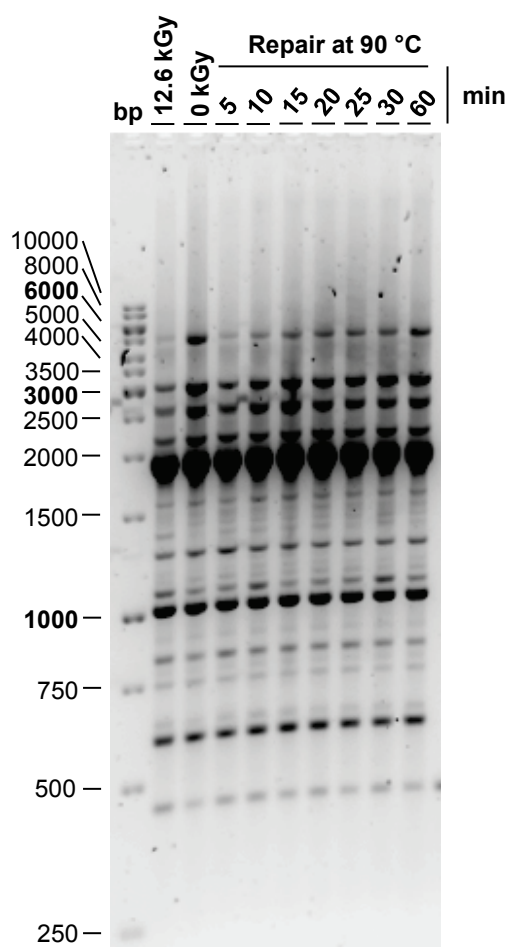


Figure 47: DNA repair of *I. hospitalis* after X-ray exposure. *I. hospitalis* cells were exposed to 12.6 kGy at room temperature, and transferred at 90 °C for DNA repair. The repair process was followed over time, and analyzed by RAPD. The sample indicated as 12.6 kGy served as positive control (no repair), whereas the sampled indicated as control was not exposed.

The gray-levels of the upper most bands were determined by using ImageJ (Table 23). Gray-levels of the upper most bands, representing the areas of the valleys in the histogram which correspond to the intensity of the band at a height of ~5000 bp, are listed in Table 23. The uppermost band of the unexposed sample has a gray-level of 1655.5 whereas the value of the X-ray expose sample was 124.8. The repair for 60 min at 90 °C resulted in a gray-level of 1178.8, which is comparable to the value obtained for the unexposed sample.

Table 23: Gray-levels of RAPD bands. The gray-levels were determined for the uppermost band (~5000 bp).

X-ray [Gy]	Band size [bp]	Repair [min]	Gray-level
12.6	5000	-	124.8
0		-	1655.5
12.6		5	170.0
		10	344.0
		15	543.2
		20	606.1
		25	619.9
		30	636.7
		60	1178.8

Subsequent experiments elucidating possible DNA repair mechanisms were based on the information given by RAPD (Figure 47), and the gray-levels of the upper most bands (Table 23). Gene expression studies were conducted with varying experimental set ups, but with incubations at 90 °C for 5, 15, 30, (60), and 90 minutes after X-ray exposure. The repair related gene regulation was investigated by means of qRT-PCR as follows.

3.3.2 RNA extraction for qRT-PCR

The quality of total RNA (see 2.5.2 and following), extracted from *I. hospitalis* stress exposed cells, was checked by horizontal gel electrophoresis. Two prominent bands can be seen in Figure 48 representing 23S rRNA (~2500 bp), and 16S rRNA (~1400 bp). Total RNA was used for cDNA synthesis in follow-up studies.

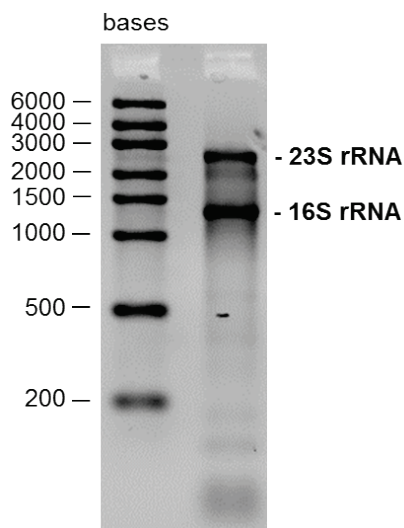


Figure 48: Agarose gel of extracted total RNA. The quality of extracted RNA from *I. hospitalis* was checked on a 1 % agarose gel.

3.3.3 Gene expression studies by qRT-PCR

3.3.3.1 Test of experimental setup

The gene expression of *I. hospitalis* was tested under varying experimental conditions by using qRT-PCR. qRT-PCR is based on real time measurements of products generated and accumulated during each cycle of the PCR process by plotting the products' fluorescent signal as a function of cycle number. Two different types of qRT-PCR analysis can be used. There is "relative quantitation" by comparing the gene of interest to that of a control gene within a sample. And "standard-curve quantitation" meaning an unknown sample can be quantified by deriving the value from a standard curve generated with a known sample (Ginzinger, 2002).

To test whether the experimental set up itself worked, and to see whether a change in RNA transcription levels can be detected, RNA from untreated and from X-ray exposed samples (1500 Gy), which were additionally incubated at 90 °C after exposure, was extracted as described in 2.5.2. As an example, the fluorescence data graph obtained using the sequence specific *recB* primer can be seen in Figure 49. Stationary phase cultures were exposed to 1500 Gy, and the repair conducted at 90°C for 5, 15, 30 min, following RNA extraction. The RNA from untreated stationary phase cells (N_0) was extracted as well.

Treated samples showed lower C_t values (cycle number at which the fluorescence signal intersects the threshold line) compared to the untreated sample (Figure 49). The smaller the C_t value the more mRNA transcripts of the gene of interest are present within the

sample. An upregulation in the case of *recB* can be seen in comparison to the untreated stationary phase culture sample (N_0). The overall experimental set up did not change in the following. Only experimental parameters in terms of exposure, and cultivation were varied.

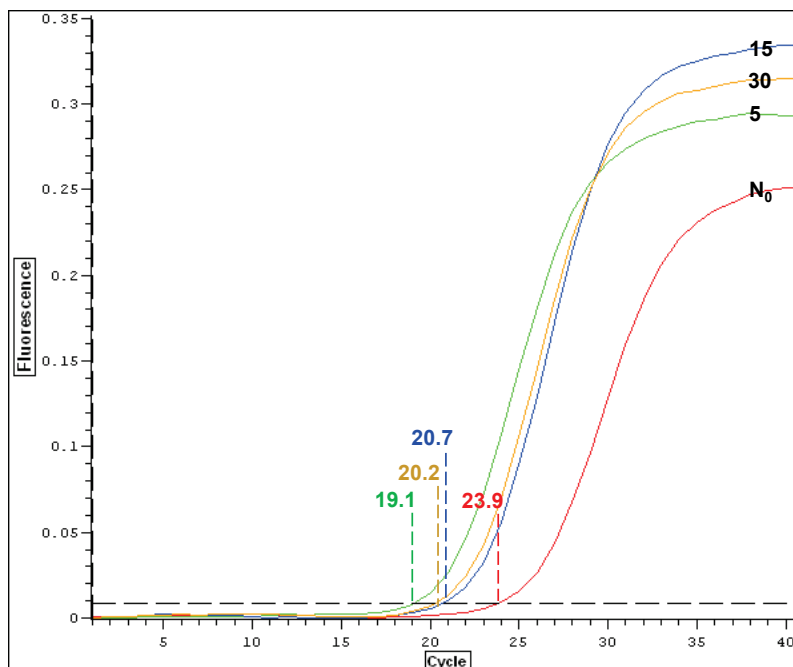


Figure 49: qRT-PCR of X-ray (1500 Gy) exposed *I. hospitalis* cells using the sequence specific *recB* primer. The cells were exposed to ionizing radiation, followed by incubated at 90 °C to repair radiation induced DNA damages. Fluorescence intensity is plotted over cycle number. The cDNA amount used for each reaction was 5 ng. The manually set threshold line can be seen as dashed line with respective C_t values. Abbreviations: 5, 15 and 30 correspond to the incubation time in min, N_0 (untreated cells; no X-ray exposure, no incubation). The PCR reactions were conducted with $n=1$.

3.3.3.2 RNA transcription levels of potential housekeeping genes tested under various experimental conditions

To be able to analyze the obtained qRT-PCR results by relative quantitation, the following experiments were conducted to find a putative “housekeeping gene”, a gene whose expression is unaffected by varying experimental conditions. The sequences of the tested primers are also listed in Table 3.

RNA transcription levels of the tested housekeeping gene candidates varied among the tested experimental conditions. Differences in transcription levels were detected comparing treated to untreated samples (Table 24).

Recorded melting curves can be seen for all housekeeping gene candidates tested under condition A (Table 24, light gray), resulting in a prominent sharp peak (temperature at which amplicon melts) for the respective specific primer (Figure 50). The amplicon was additionally visualized on a 2 % agarose gel. The best result in terms of a sharp band was

obtained for Pol E'. Primers specific for Mips, and Thermosome did not result in a satisfying amplicon although a sharp peak was present in the melting curve record. The 16S rRNA primer was used for further analysis due to the sharpest peak received during melting curve analysis. Sharp bands were obtained with this primer during later experiments as well (data not shown).

Table 24: RNA transcription levels of tested housekeeping genes listed as absolute C_t values for different experimental conditions. Abbreviations: Th (manually set threshold), Cond. (experimental conditions), [Gy] (X-ray exposure), + (X-ray exposure), - (unexposed). The PCR reactions were conducted with n=3. The corresponding experimental conditions for letters A-E are described in Figure 51/table.

Primer	Repair [min]								Th	Cond.	[Gy]
	5		15		30		90				
	-	+	-	+	-	+	-	+			
16S rRNA	8.9	10.8	9.8	9.4	9.0	10.0	9.3	9.3	0.013	A	1500
Pol E´	19.3	18.9	18.6	19.9	19.9	18.6	32.7	18.5	0.020		
Mips	18.4	19.1	18.8	18.5	19.6	19.3	18.0	28.1	0.020		
Thermosome	15.6	15.6	15.6	16.0	16.5	16.4	15.0	15.9	0.020		
Pol E´	17.5	18.0	17.1	17.0	17.3	17.0	17.4	17.3	0.013	B	3000
16S rRNA	8.2	8.5	8.4	7.8	8.3	9.7	7.7	8.1	0.013		
Pol E´	22.0	23.3	21.4	21.9	21.4	21.5	24.6	20.6	0.015	C	3000
16S rRNA	10.7	16.5	12.1	12.6	12.1	13.0	16.0	9.2	0.023		
16S rRNA	9.2	7.6	9.3	7.6	9.4	9.5	7.6	12.3	0.016	D	3000
16S rRNA	8.7	10.4	9.1	12.4	11.6	15.8	12.0	10.7	0.012	E	3000

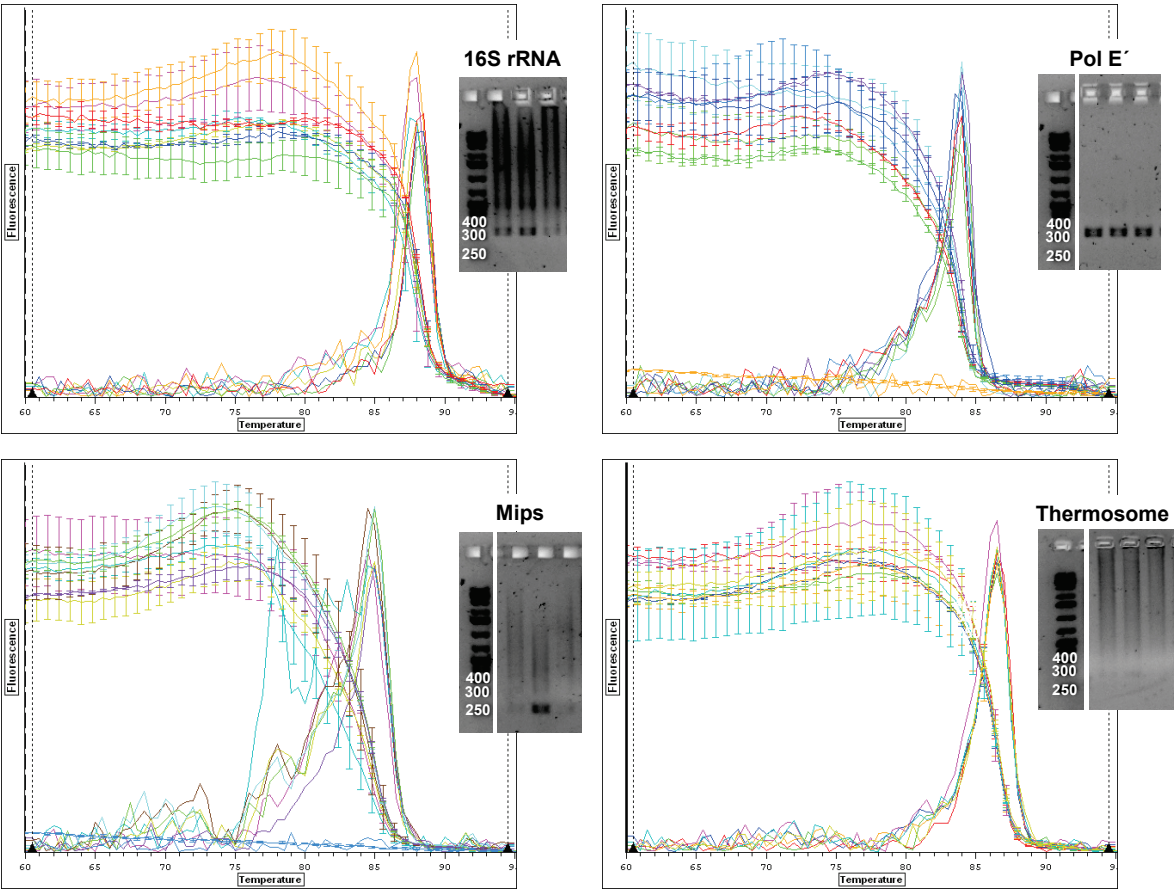


Figure 50: Recorded melting curves for gene specific primers (16S rRNA, Pol E', Mips, Thermosome) using cDNA from experimental condition A (Figure 51). Melting curves were recorded to indicate a specific amplicon. The amplicon was additionally analyzed on an agarose gel.

3.3.3.3 RNA transcription levels of DNA damage repair genes tested under various experimental conditions

Several gene specific primers were designed (rad2, rad50, recB, radA) to see whether *I. hospitalis* up- or down-regulates these genes of interest after X-ray exposure. To narrow down the choice of primers to be tested for different experimental conditions, recB and rad50 were selected due to their clear amplicon band on agarose gels (data not shown). The primer for 16S rRNA was amplified as well. The absolute C_t values obtained for every tested primer were used to determine the ratio between the C_t value for a treated sample (N), and the C_t value for the corresponding untreated sample (N_0). The ratios were plotted against the repair at 90 °C.

The following descriptions refer to Figure 51.

A) *I. hospitalis* stationary phase cultures were prepared for X-ray exposure. The cells were exposed to 1500 Gy to induce DNA damages but to inactivate the culture by less than one order of magnitude. The experiments for increasing periods of repair were conducted each of them individually to familiarize with the experimental set up. As shown in Figure 51A, the RNA transcription levels for none of the tested genes/primers were impacted by the applied X-ray dose. To induce more DNA damages, the X-ray dose was increased to 3000 Gy in the following.

B) The experiment was conducted for all four repair points in parallel. The stationary phase cultures of *I. hospitalis* were exposed to 3000 Gy. A similar result was obtained for this experimental set up compared to the results obtained for experimental condition A (see above).

C) To test whether the cultivation at 90 °C naturally increases the expression of recB and rad50, *I. hospitalis* cultures were cultivated at 75 °C ($<T_{opt}$) for 2 days to obtain cells in their stationary phase (prolonged growth). Experiments were conducted in parallel. The ratios for all tested genes vary equally by ~ 0.1 .

D) Due to low total RNA concentrations obtained following a two days incubation at 75 °C, *I. hospitalis* cells were incubated at 75 °C for 4 days to increase the cell concentration/density. The X-ray exposure, followed by repair at 90 °C occurred in parallel. Almost no differences in C_t ratios were detected independent from later incubation times at 90 °C.

E) Previous experiments were conducted with cells in their stationary phase in which they already reached their needed protein level. Therefore, *I. hospitalis* cells were incubated for 8 hours at 90 °C to investigate their RNA transcription levels during exponential phase.

The cells were exposed to 3000 Gy, and all four repair points conducted in parallel. The ratios for 16S rRNA fluctuated with increasing duration for repair, whereas the ratios of recB and rad50 stayed constant.

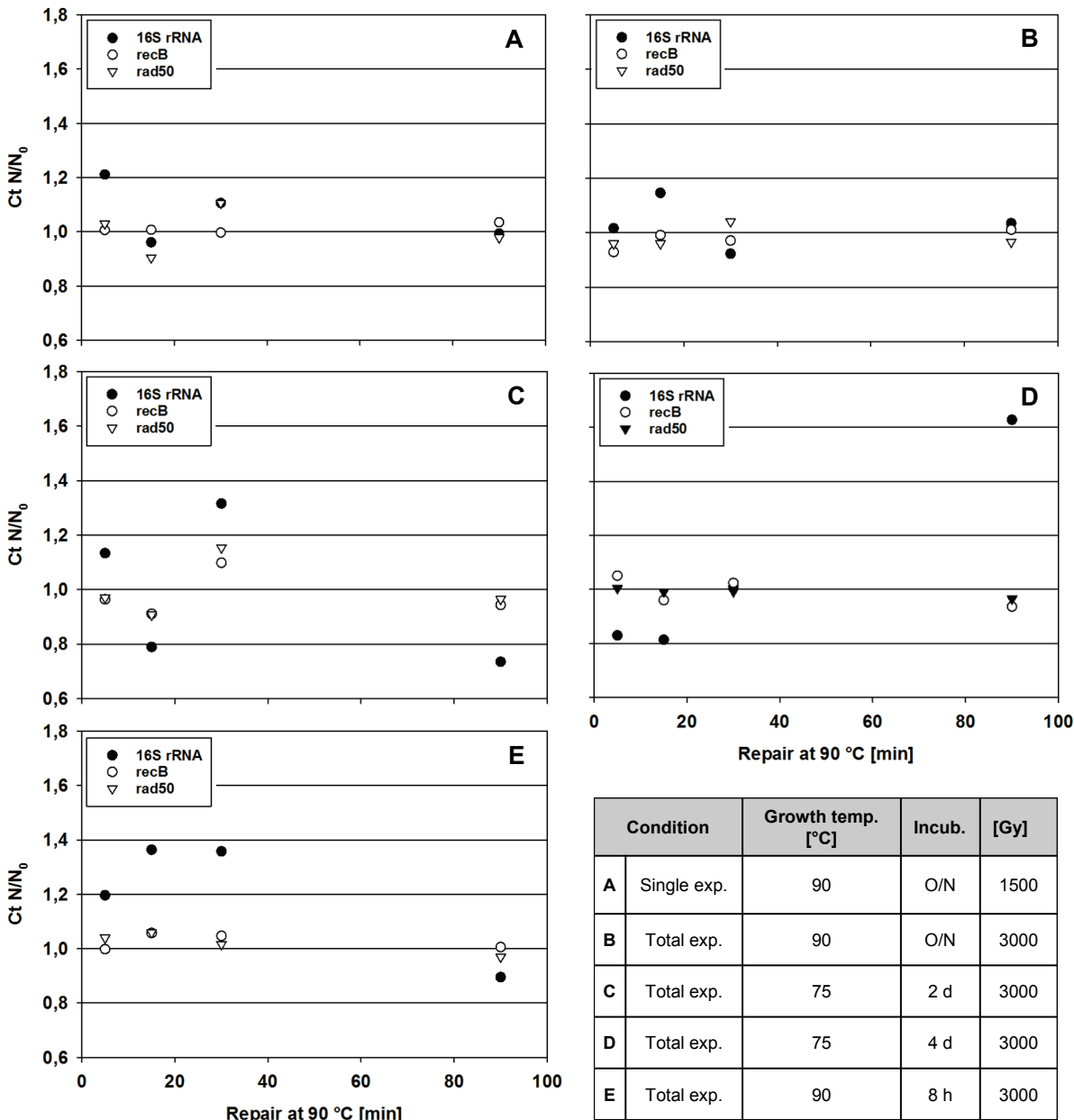


Figure 51: RNA transcription levels represented by absolute C_t values for different experimental conditions. The gene specific primers 16S rRNA, recB, and rad50 were tested. The ratio between the C_t value for a treated sample (N), and the C_t value for the corresponding untreated sample (N_0) was plotted against the repair at 90 °C. The PCR reactions were conducted with $n=3$.

3.3.3.4 Determination of molecule numbers of putative DNA damage repair genes

The molecule numbers were determined for the four DNA damage repair genes (*rad2*, *rad50*, *recB*, *radA*) tested under condition F (see 2.4.2.6).

The following description refers to Figure 52 and Figure 53.

F) *I. hospitalis* cells were incubated at 90 °C for only 4.5 hours. The dose was reduced to 1500 Gy, and the repair for every point in timer conducted in parallel.

Before calculating the molecule numbers, primer specific standard curves were generated to calculate the PCR efficiencies. Therefore, genomic DNA of *I. hospitalis* was 4-5 fold diluted with 1:10 dilution steps. The resulting efficiencies for the genes of interest were between 101-106 %; an efficiency between 90 % and 110 % corresponds to a slope between -3.58 and -3.10 and is assumed to be a good reaction (Real-time PCR handbook (2015), ThermoFisher Scientific). The standard curve shown in Figure 52 is exemplary for all other primer specific standard curves (data not shown).

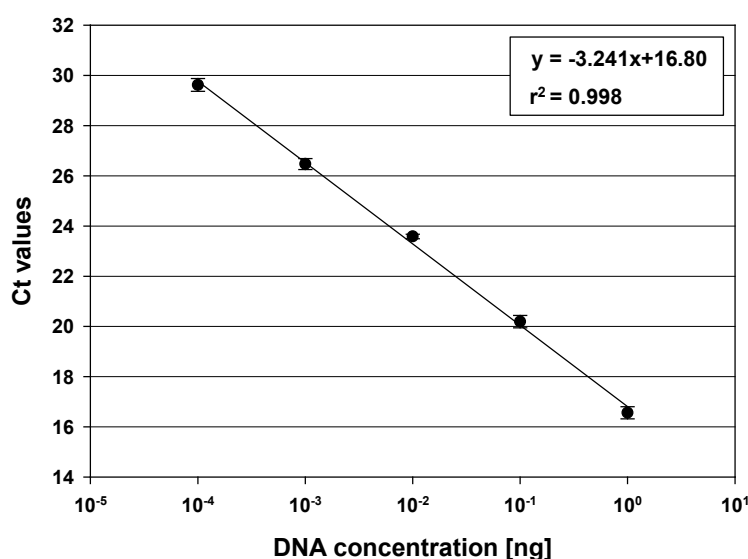


Figure 52: Standard curve generated with genomic DNA of *I. hospitalis* using the gene specific primer *recB*. Genomic DNA (1 ng) was five times diluted in 1:10 dilution steps. The slope was used to determine the PCR efficiency. The PCR efficiency of *recB* was 103 %.

The molecule numbers or copy numbers were calculated for *rad2*, *rad50*, *recB*, and *radA* and are the average of results obtained from one experiment performed in triplicates. Both, results obtained for unexposed and exposed samples were plotted against the repair (min) (Figure 53). The highest copy numbers were obtained for *radA*. By comparing the copy number of unexposed sample to the number of X-ray exposed sample after 90 min of repair one can easily see that the latter one exceeds it by $\sim 20 \times 10^8$. The overall

tendency shown for all four tested repair genes is a slight upregulation upon irradiation with an overall maximum after 90 min of repair.

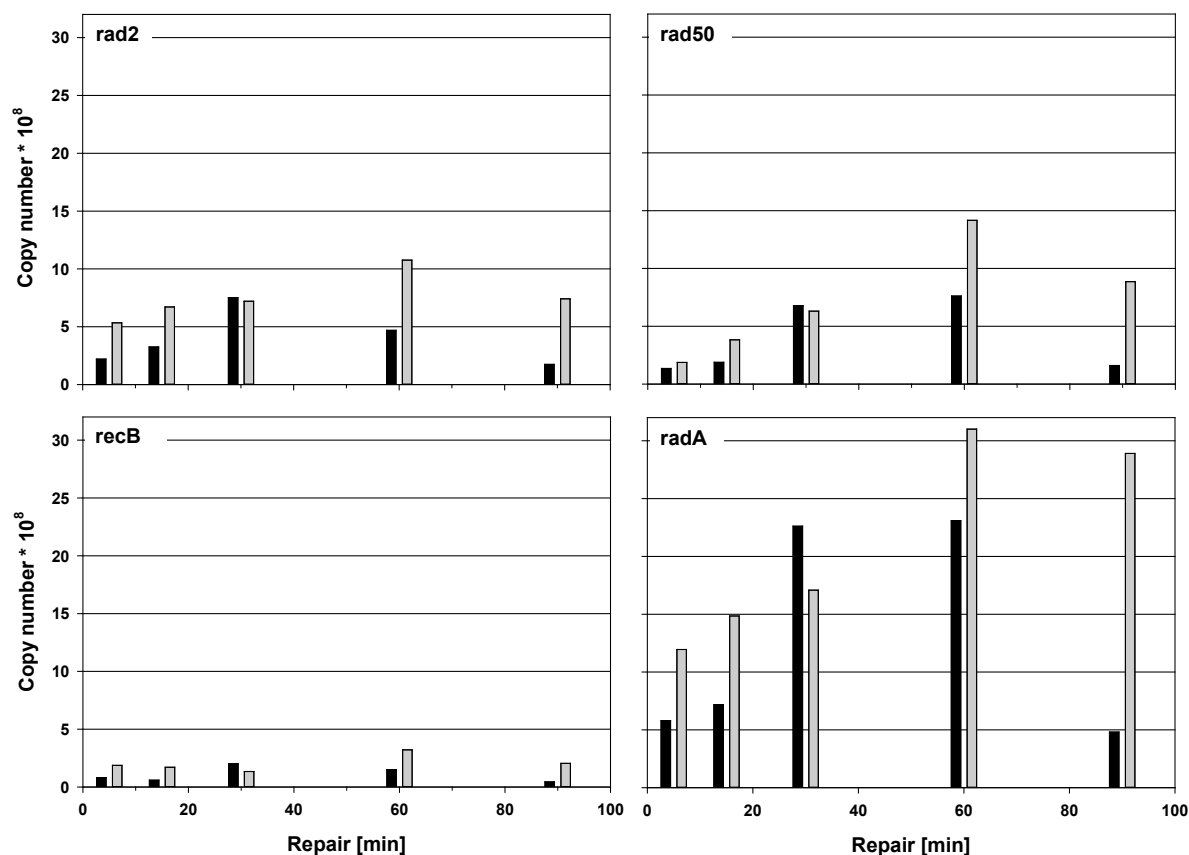


Figure 53: Calculated molecule or copy numbers for *rad2*, *rad50*, *recB*, and *radA*. Black bar: Unexposed samples. Gray bar: Samples exposed to 1500 Gy. The gene specific primers used for copy number determination are shown in the upper left corner. The experiment was conducted with n=1.

3.3.3.5 RNA transcription levels of genes involved in DNA replication

Götz *et al.* suggested in 2007 that two tested *Sulfolobus* species constitutively express genes involved in the repair of UV radiation induced damages, and observed a repression of genes involved in DNA replication and chromatin proteins, resulting in the inhibition of DNA replication. The researchers proposed that this allows the repair to take place (Götz *et al.*, 2007). To see whether a comparable effect can be seen for *I. hospitalis* after X-ray exposure, cells were exposed to 3000 Gy in their exponential phase (experimental condition E, 2.4.2.6). The repair occurred at 90 °C for increasing periods of time (Figure 54). Primers were designed for qRT-PCR studies referring to Götz *et al.*, 2007.

The following primers were tested:

ccrB	chromosome condensation protein CcrB
cdc6	cell division control protein Cdc
cdc6-orc1	ORC complex protein Cdc6/Orc1

dbp1	DNA binding protein
ber	base excision DNA repair protein
poll	DNA polymerase I
mcm	replicative DNA helicase Mcm
tfb	transcription initiation factor IIB
fen-1	endonuclease
rg	reverse gyrase

The absolute C_t values obtained for every tested primer were used to determine the ratio between the C_t value for a treated sample (N), and the C_t value for the corresponding untreated sample (N_0). The ratios were plotted against the repair at 90 °C. As shown in Figure 54 the ratios for all genes vary by ~0.1 comparing the ratio after 5 min to 90 min of repair. No up- or down-regulation was detected.

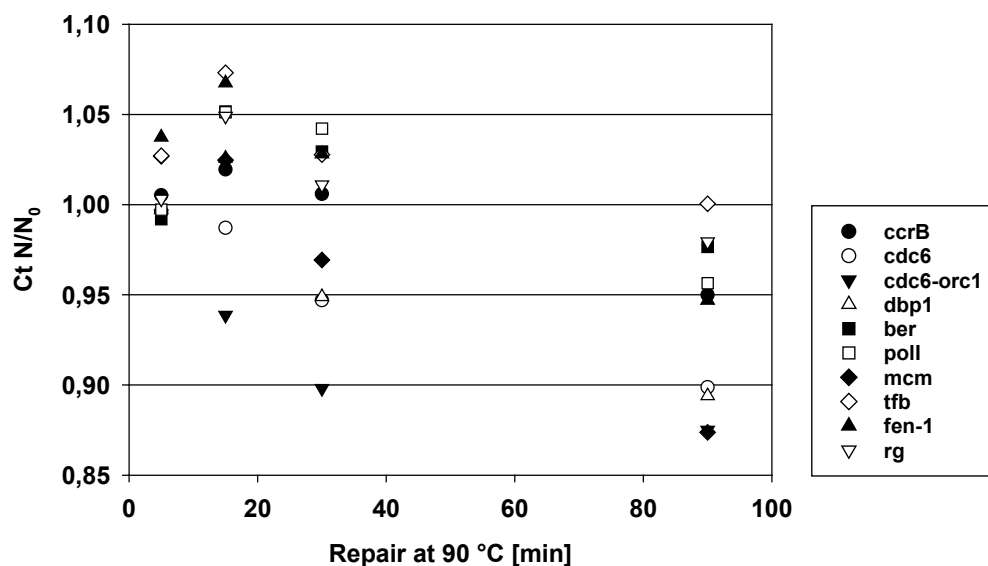


Figure 54: RNA transcription levels for genes involved in replication are represented by absolute C_t values using cDNA from experimental condition E. The ratio between the C_t value for a treated sample (N), and the C_t value for the corresponding untreated sample (N_0) was plotted against the repair at 90 °C. The gene specific primers are listed in the box. The PCR reactions were conducted with $n=1$.

3.3.3.6 DNA damage repair by photoreactivation

Photoreactivation, meaning the repair of UV-C induced DNA damages by the enzyme photolyase is known for e.g. the halophilic archaeon *Halococcus hamelinensis* (Leuko *et al.*, 2011). To test whether *I. hospitalis* expresses a light-induced photolyase able to repair non-ionizing radiation induced DNA damages, the following experiment was conducted:

I. hospitalis stationary phase cultures were anaerobically exposed to 150 J/m² monochromatic UV-C in UV-transmissible quartz cuvettes. The reference sample (no irradiation) was treated the same. Two of three cuvettes, namely “Darkness” and the

unexposed sample ("No UV-C") were wrapped in aluminum foil directly after UV-C exposure to avoid the activation of a potential photolyase by polychromatic light. All samples were transferred to preheated $\frac{1}{2}$ SME+S⁰ medium, and were incubated at 90 °C for up to 90 min under white light exposure (polychromatic light) (Figure 15). Total RNA was extracted afterwards for qRT-PCR analysis to see whether a potential photolyase was activated by UV-C induced DNA damages.

Resulting RNA transcription levels are listed in Table 25. Pol E' was used as potential housekeeping gene. The absolute C_t values vary within one data set (e.g. 5 min repair at 90 °C). No coherent up- / down-regulation can be seen for the potential photolyase.

Table 25: RNA transcription levels of Pol E' (potential housekeeping gene), and photolyase listed as absolute C_t values. Abbreviations: No UV-C (no UV-C, wrapped in aluminum foil), Light (150 J/m², and white light), Darkness (150 J/m², wrapped in aluminum foil). The PCR reactions were conducted with n=3.

Repair [min]	Pol E'			Photolyase		
	No UV-C	Light	Darkness	No UV-C	Light	Darkness
5	21.3	20.0	18.3	20.3	19.5	17.2
15	19.7	18.8	19.8	18.3	18.2	18.8
30	19.1	19.3	18.8	18.1	18.9	18.3
90	19.2	22.0	19.5	17.8	21.3	18.5

Summary:

- Experiments dealing with DNA repair and qRT-PCR were based on the information given by RAPD (Figure 47), and corresponding gray-levels. The uppermost band of the unexposed sample had a gray-level of 1655.5, whereas the value of the X-ray exposed sample was 124.8. The repair for 60 min at 90 °C resulted in a gray-level of 1178.9, which is comparable to the value obtained for the unexposed sample (Table 23). Following experiments were conducted with incubations at 90 °C for 5, 15, 30, (60) and 90 minutes after X-ray exposure.
- The first qRT-PCR experiment was designed to test whether the experimental set up itself worked to be able to detect changes in RNA transcription levels. An upregulation in the case of *recB* can be seen in comparison to the untreated stationary phase culture sample (N₀, no incubation at 90 °C) (Figure 49).
- It was tried to analyze obtained qRT-PCR results by relative quantitation. Different experiments were conducted to find a putative "housekeeping gene". The RNA transcription levels of tested housekeeping candidates varied among differing experimental conditions (Table 24). No reliable housekeeping gene was found; data analysis by relative quantitation was not possible.

- Several gene specific primers were designed for genes involved in DNA damage repair in *I. hospitalis*. None of the tested genes/primers were influenced by the applied X-ray dose (see conditions A-E); no clear up- or down-regulation was observed (Figure 51). In the case of condition F, the overall tendency shown for all four tested repair genes (*rad2*, *rad50*, *recB*, and *radA*) was a slight upregulation of *radA* upon irradiation with an overall maximum after 90 min of repair (Figure 53).
- Primers were designed for genes involved in replication processes. *I. hospitalis* cells, being in their exponential phase, were exposed to 1500 Gy. The ratios for all genes tested varied by ~0.1 comparing the ratios after 5 min to 90 min. No up- or down-regulation was detected (Figure 54).
- Finally, it was tested whether *I. hospitalis* expresses a light-induced photolyase being able to repair non-ionizing radiation induced DNA damages; no coherent up- or down-regulation was seen for the gene encoding a putative photolyase (Table 25).

4 Discussion

4.1 Non-ionizing radiation

The lack of an UV-absorbing ozone layer during the Archaean enabled the whole solar ultraviolet radiation spectrum to penetrate Earth's surface increasing the overall UV stress on the surface (Cockell & Horneck, 2001; Margulis *et al.*, 1976). When thinking of *Ignicoccus* being a potential candidate for an early Earth inhabitant, one has to consider its radiation tolerance, especially for non-ionizing radiation.

To start elucidating the radiation resistance within the genus *Ignicoccus*, the UV-C tolerance of all four representatives was investigated. One common feature is, besides the shoulder region seen in the range of 0-300 J/m², that an irradiation with 1500 J/m² and also 3000 J/m² did not further reduce the survival, rather resulted in a “tail” as described by Coohill & Sagripanti and depicted in Figure 55 (according to Coohill & Sagripanti, 2008).

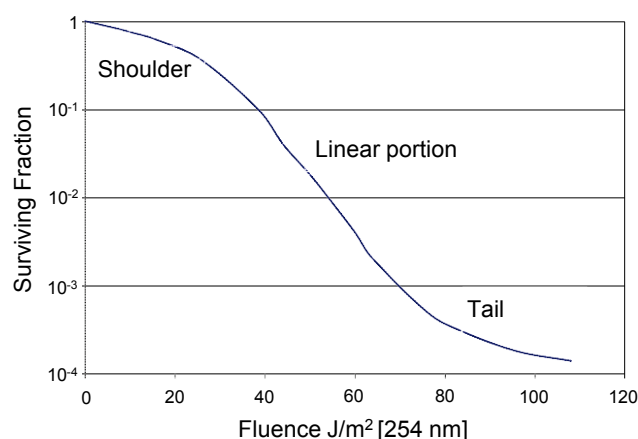


Figure 55: Bacterial survival curve after UV-C exposure. The fraction of surviving bacterial cells (here: measured in colony forming units (CFU)) is plotted against the fluence (modified from Coohill & Sagripanti, 2008; Coohill, 1994).

This so called “tailing” limited the linear portion of the survival curve to the 10⁻³ log level which ended at around ~1000 J/m². Previous research ascribed this tail to experimental conditions like self-shading of the bacterial cells, which can be avoided by a sufficient dilution of the bacterial suspension prior to experimentation and constantly stirring during the irradiation process (according to Coohill & Sagripanti, 2008; Morowitz, 1950). Vigorous stirring, non-absorbing sulfur-free medium, and an appropriate cell concentration (1 x 10⁶ cells/ml) of *Ignicoccus* minimized the shadowing effects allowing exposure to the same amount of UV-C; however, the tailing was still observed. To exclude that this effect may be ascribed to *Ignicoccus* itself, the survival of the radiation sensitive *Escherichia coli*

was investigated under similar experimental conditions. When exposed in an open petri dish, *E. coli* cells showed strongest inactivation, whereas irradiation in a UV-transmissible quartz cuvette, also used to expose *Ignicoccus*, resulted in less inactivation and the same “tailing” tendency was observed. However, none of the F_{10} -values resulting from these two differing experimental set ups ($\sim 150 \text{ J/m}^2$, petri dish; $\sim 250 \text{ J/m}^2$, cuvette; see Figure 25) coincide with the F_{10} -value (40 J/m^2) published by Arrage *et al.* in 1993. Arrage *et al.* conducted the experiments under red light to avoid any photoreaction by *E. coli*, potentially resulting in this reduced UV-C tolerance. However, it has to be taken into account that the experiments in the underlying work were conducted with higher cell concentrations of *E. coli* (1×10^7 cells/ml) in comparison to e.g. *Ignicoccus hospitalis* (1×10^6 cells/ml), so that shading effects cannot be excluded. The temperature at which all UV-C experiments were conducted may also play an important role. *I. hospitalis*, with a T_{opt} at 90°C , was irradiated at room temperature. This is a very low temperature for hyperthermophilic organisms, preventing any metabolic activity e.g. DNA repair during exposure. Therefore, damages caused by UV-C accumulated with increasing radiation periods, allowing the determination of survival depending on the exposure to defined fluence intensities. *E. coli* on the other hand has a T_{opt} at 37°C (e.g. Doyle & Schoeni, 1984) and is not completely inactivated at room temperature; repair processes may have taken place during exposure at room temperature. Nevertheless, both *Ignicoccus* and *E. coli* showed the “tailing” when exposed in quartz cuvettes.

The observed tailing may be seen as artefact ascribed to the indispensable use of quartz cuvettes to ensure anoxic conditions during irradiation, with the result that a reduction in *Ignicoccus* cell survivability can exclusively be ascribed to UV-C irradiation. Most important, the tailing region has not been taken into account to define the fluence needed to inactivate the population by 90 %, which was determined by linear regression from the linear parts of the semi-logarithmically plotted survival curves and recommended by Coohill & Sagripanti (2008). The ability of all four tested *Ignicoccus* representatives to tolerate such high fluence intensity, indicated by F_{10} -values in the range of 245 J/m^2 to 400 J/m^2 , is quite impressive as they are never exposed to UV-C radiation in their natural habitat deep-sea. Interestingly, the tolerance to radiation seems to be a widespread phenomenon among extremophilic microorganisms as previously described, although great variations between distinct strains have clearly been demonstrated (Beblo *et al.*, 2011). Of great interest are variations between different hyperthermophilic strains like *Sulfolobus* (reduced tolerance), and *Archaeoglobus* (similar tolerance) in comparison to *Ignicoccus* due to the fact that these organisms thrive at temperatures above 85°C (Marguet & Forterre, 1994; according to Stetter *et al.*, 1990), a temperature that greatly

destabilizes the primary structure of DNA (Wood *et al.*, 1997). All inhabitants of these hot environments need to be well adapted to high temperatures to maintain the double-helical structure of their DNA (Marguet & Forterre, 1994). The DNA topology of hyperthermophiles is distinguished by its unique positive supercoiling in contrast to the negatively supercoiled bacterial DNA. These positive superturns are introduced into the DNA at the expense of ATP by the enzyme reverse gyrase (according to Forterre *et al.*, 1996) which has exclusively been found in all hyperthermophiles including Bacteria (e.g. Bouthier de la Tour *et al.*, 1998) and Archaea (e.g. Napoli *et al.*, 2004). Marguet and Forterre investigated the DNA stability of plasmids *in vitro* at temperatures in the range of 95-107 °C, which is relevant for a hyperthermophilic lifestyle. The experiment pointed to a similar thermodegradation of either positively or negatively supercoiled plasmid DNA *in vitro* (Marguet & Forterre, 1994). But the presence of an active reverse gyrase in hyperthermophilic archaea (Forterre *et al.*, 1996; Kikuchi & Asai, 1984) does not only contribute to positive supercoiling of DNA, this enzyme may also be relevant to organismic radiation tolerance *in vivo* (Beblo *et al.*, 2011). As an example, it has been shown for the hyperthermophilic archaeon *Sulfolobus solfataricus* that its reverse gyrase was recruited to DNA after UV irradiation and may participate directly or indirectly in the cell response to UV light-induced DNA damage (Napoli *et al.*, 2004). The presence of this peculiar enzyme in hyperthermophilic archaea (Forterre *et al.*, 1996) living either aerobic or anaerobic seems to be crucial for their heat adaptation and allows the comparison of their radiation tolerance among themselves.

In comparison to *Ignicoccus*, *Sulfolobus* representatives occupy terrestrial hot springs with temperatures ranging from 70 °C to 95 °C which are exposed to UV radiation, and additional DNA damages are caused by reactive oxygen species (ROS) due to its aerobic lifestyle (Rolsmeier *et al.*, 2010). It has been shown for *Sulfolobus solfataricus* that cellular sensitivity to UV irradiation and spontaneous mutation rates are very similar to those of *E. coli* (Jacobs & Grogan, 1997; Wood *et al.*, 1997). Both organisms have comparable F_{10} -values with 37 J/m² for *S. solfataricus* (Beblo *et al.*, 2011) and 40 J/m² in the case of *E. coli* (Arrage *et al.*, 1993), whereas *I. hospitalis* showed an approximately 10-fold higher UV tolerance (F_{10} -value: 337 J/m²) although never exposed to UV radiation in its natural habitat. *Archaeoglobus fulgidus*, a hyperthermophilic obligate anaerobic archaeon (Stetter, 1988), showed a comparable tendency in terms of UV tolerance (F_{10} -value: 108 J/m²; Beblo *et al.*, 2011) as seen for *I. hospitalis*. One possible explanation for the high radiation tolerance of *I. hospitalis* may be the presence of a light-driven photolyase. For example, *S. solfataricus* and *E. coli* do express a photolyase, the enzyme responsible for a light-driven photoreactivation mechanism (Sakofsky *et al.*, 2011; Sancar

et al., 1984). The complete genome of *I. hospitalis* available as NCBI Reference Sequence NC_009776.1, and the complete genome of *A. fulgidus* (Klenk *et al.*, 1997), however, point towards the lack of a classical photolyase enzyme as shown for e.g. *S. solfataricus* (Sakofsky *et al.*, 2011), *E. coli* (Sancar *et al.*, 1984), or *Halobacterium salinarum* (Baliga *et al.*, 2004). The only putative proteins found within the genomes of *I. hospitalis* and *A. fulgidus* can be defined as radical SAM proteins. The widespread radical S-adenosyl-L-methionine (SAM) superfamily of enzymes (Sofia *et al.*, 2001) is involved in a wide variety of biological processes (according to Frey *et al.*, 2008). It has been shown that the light-independent Spore Photoproduct lyase (SP lyase) in *Bacillus subtilis* spores belong to this superfamily and repairs specific UV-induced DNA lesions, the spore photoproduct, by a radical-based mechanism (Benjdia *et al.*, 2012; Donnellan *et al.*, 1968), resulting in a remarkable UV tolerance (F_{10} -value: 100 J/m²; Riesenman *et al.*, 2000). Primers specific for this radical SAM protein in *I. hospitalis* (here: putative photolyase) were designed, but no up-/down-regulation of this putative photolyase gene were detectable after UV-C treatment (Table 25). One explanation may be that the chosen fluence intensity (150 J/m², 50% less than the F_{10} -value) was too high as previously seen for *H. salinarum*; only mild UV irradiation (30-70 J/m²) resulted in a detectable increase of genes involved in DNA damage repair (McCready *et al.*, 2005).

Still, *I. hospitalis* is significantly more UV-tolerant, even without classical photoreactivation. The presence of a radical SAM protein may indicate a light-independent repair as shown for *B. subtilis* spores although no up-regulation upon UV irradiation was observed. Further, it points out that increased ROS production by UV exposure can be circumvented by hyperthermophiles living anaerobically, therefore decreasing the overall ROS production to a minimum. It seems that an aerobic lifestyle has a dramatic effect on an organisms' radiation tolerance at least for the hyperthermophilic archaeon *S. solfataricus* mentioned above. The expression of the putative photolyase or better the radical SAM protein may possibly play an important role in scavenging UV induced ROS production in *I. hospitalis* cells and may point to an efficient DNA damage repair mechanism.

On the molecular level, RAPD band pattern profiles clearly indicated that the genomic DNA integrity of *I. hospitalis* was severely impacted by non-ionizing radiation. DNA damages induced by UV-C exposure resulted in a strong loss of high molecular weight bands with fluence intensities >500 J/m² and a complete loss of bands with 3000 J/m² (Figure 27). Besides this reduced genome integrity, increasing amounts of DNA lesions per 1.3 kb fragment were detected by qPCR. This result demonstrated that DNA damages accumulate upon UV-C exposure, hence decreases genomic DNA integrity as shown by the changed RAPD band pattern profile (Figure 27). Fröls and colleagues however

demonstrated that UV-induced DNA aberrations can be successfully analyzed by pulse-field gel electrophoresis in *S. solfataricus*. They analyzed the formation and extend of DNA double-strand breaks by using this method. An accumulation of chromosomal fragments of smaller size (100-600 kb in size) compared to the control samples were observed as smear after 2 hours post-UV treatment, whereas bigger fragments were compressed in the upper part of the gel. Additionally, no genomic DNA variations (here: dsDNA breaks) were observed at time zero (cells were directly harvested after irradiation) potentially indicating that dsDNA formation in *S. solfataricus* was not a direct result of UV exposure rather a result of subsequent cellular processes (Fröls *et al.*, 2007). In contrast, RAPD analysis clearly indicated that a UV treatment caused dramatically changed band profiles (here loss of bands), although determining the type of aberrations is not possible with this method. In contrast to RAPD, it was neither possible to see any changes within the DNA of UV-C exposed *S. solfataricus* cells directly after treatment using PFGE (compare to Fröls *et al.*, 2007) nor to follow the damage within the whole genome due to the compression of fragments >600 kb. Therefore, the PCR-based RAPD analysis can be recommended for getting an impression of the genomic DNA integrity after a specific treatment. Still, it is impressive that the survival of all four *Ignicoccus* representatives was only reduced by ~3 orders of magnitude after irradiating them with a fluence of ~1000 J/m², compared to the amount of lesions and the highly reduced genomic DNA integrity exemplarily shown for *I. hospitalis*. This phenomenon points out that e.g. efficient repair mechanisms may take place to successfully maintain *Ignicoccus* genome integrity even under high UV-C exposure.

4.2 Ionizing radiation tolerance

Ionizing radiation is known to be an exogenous source of free radicals (ROS), which are produced via the radiolysis of water (Kottemann *et al.*, 2005). These ROS account for >80 % of introduced DNA damages, and >20 % is the result of direct effects of γ -photons (Riley, 1994). As previously observed by Beblo *et al.* (2011), *I. hospitalis* is able to survive high doses of ionizing radiation (⁶⁰Co radiation). The underlying work was prompted by this observation, and raised the question whether this high radiation tolerance may uniquely be ascribed to *I. hospitalis* or whether other representatives from the same genus (here: "*I. morulus*") would also be able to tolerate comparable doses. First of all, it was possible to show that *I. hospitalis* ionizing radiation tolerance was within the same range after either X-ray or γ -ray exposure, although γ -rays are usually higher in energy (Ashbaugh III, 1988). The fact that both types of radiation result in the same dose-dependent decline in survival allows for inter-experimental comparison while using distinct

ionizing radiation sources. Both, *I. hospitalis* and "*I. morulus*" showed comparable D_{10} -values after ^{60}Co radiation exposure (*I. hospitalis*: D_{10} -value: 4.7 kGy; "*I. morulus*" D_{10} -value: 4.5 kGy), which fourfold exceeds the D_{10} -value of *A. fulgidus* (D_{10} -value: 1.1 kGy; Beblo *et al.*, 2011). In contrast, the radiation sensitive *E. coli* has a D_{10} -value of only 0.25 kGy (Clavero *et al.*, 1994), which is three times lower in comparison to the D_{10} -value of the (space-approved) *Bacillus subtilis* spore (D_{10} -value: 0.84 kGy; Möller *et al.*, 2007); only the extremely radiation-tolerant *Deinococcus radiodurans* exceeds the D_{10} -value of *I. hospitalis* twice (10 kGy; Daly, 2009). Most interestingly, a varying D_{10} -value was determined for *I. hospitalis* (~1.5 kGy) by Beblo *et al.* (2011) in comparison to the almost fourfold increased value presented in this work. In the work of Beblo *et al.*, the D_{10} -value is the mean of the results obtained for *I. hospitalis* cells (grown culture) exposed to ^{60}Co radiation, and cells which were serial diluted prior to irradiation (personal communication Dr. K. Beblo-Vranesevic). As shown in this work, huge differences in the radioresistance of *I. hospitalis* were observed using both experimental conditions resulting in a lowered D_{10} -value; the D_{10} -value in the underlying work was exclusively determined from stationary phase cultures which were not diluted prior to exposure. Nevertheless, the tolerance of *I. hospitalis* to radiation exceeded the tolerance of most tested organisms listed above and has independently been demonstrated. The possible reasons for this unusual high ionizing radiation tolerance are still not known.

This lack of knowledge and unanswered questions were the starting point for further experimental investigations. One question was whether the pre-incubation temperature, deflecting from its T_{opt} , may impact the radiation tolerance of *I. hospitalis*. Is there a positive, negative or no effect at all? To test this hypothesis, cells were grown below (75 °C), at (90 °C), and above (95 °C) their T_{opt} to stationary phase, followed by exposure to increasing doses of X-ray and recovery at 90 °C. It was shown that the ionizing radiation tolerance of *I. hospitalis* seemed to be unaffected by changes in growth temperature (Figure 45); an exposure to 9 kGy reduced the survival by ~2 orders of magnitude independently from pre-cultivation temperature. In contrast, it has been shown for *E. coli* that its pre-cultivation temperature influences its tolerance to heat, pulsed electric field (PEF) and hydrogen peroxide (H_2O_2). Cells grown above their T_{opt} were more resistant to heat whereas cells grown below the optimal growth temperature had increased tolerance to PEF and H_2O_2 (Cebrián *et al.*, 2008). It may be speculated that these different pre-cultivation temperatures had an influence on the overall protein composition of *I. hospitalis*; further experiments are warranted to investigate if a different protein composition may result from varying pre-incubation temperatures.

Besides the effect that pre-incubation temperature does not impact the overall resistance of *I. hospitalis* to ionizing radiation, the influence of active enzymatic repair was investigated with the “hot exposure” experiment. Three different questions should be answered. First, does a hot exposure increase the tolerance of *I. hospitalis* to ionizing radiation compared to an exposure at room temperature, because the cells are able to actively repair incoming damages? Second, is *I. hospitalis* less tolerant to ionizing radiation and is its survival decreased due to simultaneous induction of DNA damages by radiation and temperature. Or thirdly, can no differences be detected at all. The latter one seems to be true for *I. hospitalis*. The survival of hot exposed cells was almost identical to the survival of cells exposed at RT; no significant differences were detectable. Incubation at T_{opt} during ionizing radiation exposure does not influence the X-ray tolerance of *I. hospitalis* pointing to very efficient DNA repair following exposure.

The surprisingly high ionizing radiation tolerance of *I. hospitalis*, which is both unaffected by pre-cultivation temperature and active enzymatic repair during exposure, may be explained by an imaginable polyploidy, seen for other radiotolerant Archaea like *H. salinarum* (Kottemann *et al.*, 2005). Alternatively, post-translational modifications of already existing repair proteins may be postulated as well. The advantages of post-translational modifications will be described and discussed in Section 4.3. Several advantages of polyploidy are discussed by Hildenbrand *et al.* (2011) including a potentially enhanced resistance against DNA-damaging conditions especially conditions inducing dsDNA breaks such as high doses of ionizing radiation (artificial) or resistance against desiccation due to environmental changes (natural). Good examples are the extremely radioresistant and desiccation tolerant Bacterium *D. radiodurans* (Mattimore & Battista, 1996) and the Euryarchaeon *H. salinarum* (Kottemann *et al.*, 2005). One additional advantage would be global regulation of gene expression via regulation of the genome copy number in e.g. response to changes in the environment that may influence growth rates. Besides that, gene redundancy may allow the possibility to mutate the genome under unfavored conditions while keeping the wild-type information in another copy (Hildenbrand *et al.*, 2011). Thus, polyploidy found in almost all euryarchaeal species offers several possible evolutionary advantages (Spaans *et al.*, 2015; Hildenbrand *et al.*, 2011), and possibly also for Crenarchaeota although not yet observed for species of four different crenarchaeal genera tested so far (reviewed in Hildenbrand *et al.*, 2011; Bernander & Poplawski, 1997; Lundgren *et al.*, 2008).

Besides an advantageous polyploidy, Spans *et al.* (2015) speculated that the presence of histones may also play an important role in enabling polyploidy in Archaea. Archaeal homologs of histone proteins have been found in almost all Euryarchaeota, and also in

Nanoarchaeota (*Nanoarchaeum equitans*) but are generally not encoded in Crenarchaeota (e.g. Spaans et al., 2015; Čuboňová et al., 2005). But, archaeal histone-encoding genes have been identified in marine Crenarchaea by Čuboňová et al. in 2005. Up to now nothing is known about the presence of histones in *I. hospitalis*. The same accounts for its ploidy. It has been shown that Crenarchaeota may be able to express histones, and assuming that histone expression may correlate with polyploidy, it would be more than worth to investigate *I. hospitalis* in terms of its genome copy number. A potentially increased copy number may correlate with an extremely high radiation tolerance, although no remarkably desiccation tolerance was observed (Beblo et al., 2009).

This remarkable radiotolerance, although never exposed to it in its natural habitat, and its hot lifestyle give rise to the question for the boundaries and capabilities of life as we know it. To test that, *I. hospitalis* was exposed to high doses of ^{60}Co radiation (~6-120 kGy) to determine the boundaries for its survival. The results obtained during the first radiation campaign (DbR #1) join the ranks of the second (DbR #2) (Figure 31). A D_{10} -value of ~5 kGy was obtained which coincides and supports the result obtained after X-ray exposure as already described above; the same accounts for "*I. morulus*". The comparison to other microorganisms which were exposed to ionizing radiation has already been made. The most surprising result regarding ^{60}Co radiation exposure of *I. hospitalis* was, that a successful discrimination between its survival in terms of reproduction and its metabolic activity was shown. This phenomenon allowed, for the first time, the postulation of a VBNC state in the domain of Archaea, and supports this hypothesis empirically by experimentation.

The viable but nonculturable state (VBNC) of Bacteria is generally described as the stage of existence in which cells are alive but no longer be able to grow in medium they would normally grow in, while maintaining their metabolic activity (according to Oliver, 2000). This phenomenon was first described by Xu et al. in 1982 for *E. coli* and *Vibrio cholera* cells. The reversal of metabolic and physiologic processes that caused this nonculturability of an organism has been defined by the expression of resuscitation. Cells that are able to be resuscitated gain back their ability to grow on media they usually prefer (Oliver, 1993). Against the assumption that regrowth is caused by undetected residual culturable cells within a VBNC culture and occurs after removal of the inducing stress, Whitesides and Oliver showed in their study with *Vibrio vulnificus* that a real resuscitation from the VBNC state is possible (Whitesides & Oliver, 1997). In 2000, Lleò and colleagues have shown that it was also possible to resuscitate *Enterococcus faecalis* from their VBNC state by monitoring the production of mRNA molecules (Lleò et al., 2000).

They considered the description of a “dead cell” as a cell being unable to multiply is insufficient, and defined it as a cell being unable to express genes and/or the loss of a cell’s ability to return to the culturable state (Lleò *et al.*, 2000). The importance of VBNC in terms of human bacterial pathogens has extensively been described in the review of Li *et al.*, 2014. It is known since three decades that Bacteria are able to enter the viable but nonculturable state, and that resuscitation is possible for at least some of them. But knowledge in terms of Archaea is still lacking (Moissl-Eichinger, 2011). So, what is the definition of survivability by the example of *I. hospitalis*? It was possible to discriminate between the viable/culturable, and VBNC state of *I. hospitalis* after ^{60}Co radiation exposure. A dose of <19.0 kGy reduced the survival of *I. hospitalis* by ~3 orders of magnitude (Figure 32), and can be seen as viable and culturable. An applied dose in the range of 19.0-27.2 kGy was defined as transition state. The ability of reproduction/cell division ended with an applied dose >27.2 kGy, when no cells were detected with a 1000-fold magnification, while the metabolic activity was monitored on lead acetate paper. This state was described as VBNC. The VBNC state for *I. hospitalis* was shown for the first time and allows to speculate that this state exists in hyperthermophilic archaea as well. The detection of metabolically produced H_2S may also be important as biosignature gas which will be discussed in the last Section. The discrimination between reproducibility and metabolic activity helps us to better understand an organisms’ tolerance and response to a given stressor.

The propagation of life in an unfavorable environment may benefit from cellular responses and interactions between single cells. Quorum sensing, meaning the production, release, and detection of signaling molecules, and the subsequent response to them at high cell population densities, is known for Gram-negative, and Gram-positive Bacteria (according to Bassler, 2002). To draw conclusion whether quorum sensing does also exist for hyperthermophilic archaea, it was tested whether *I. hospitalis* stationary phase cultures are able to rescue *I. hospitalis* cells which were exposed to high doses of ^{60}Co radiation. Thus, to test whether secreted compounds in the supernatant of an *I. hospitalis* stationary phase culture may rescue ^{60}Co radiation exposed cells, several untreated cultures were sterile filtered to obtain a cell-free supernatant; however, the sterile filtration process was unsatisfying, because of its filterability although two different attempts were tested. In that regard, filterability means an organism’s ability to pass through micropore membrane filters. Wang *et al.* described in 2008 that besides the bacterial cell volume its overall shape including its flexibility determines its filterability. Various shapes have been reported to be filterable e.g. cocci, short rods to spirilla (Wang *et al.*, 2008; Hahn, 2004; Wang *et al.*, 2007; according to Young, 2006). Isaac and Ware reported already in 1974 that

Spirillum species were stretched up to three-times their original length without breaking under stretching-tension in glycerol-gelatin. After tension-release both, cell wall and cell content were able to return to their original size and shape (Isaac & Ware, 1974; Wang *et al.*, 2008). Wang and colleagues showed that it was possible for *Hylemonella gracilis* (*Spirillum* species) to pass through the filter pore channels with only a pore size of 0.1 μm . They assumed that their flexibility may allow this filterability. In 2004, Hahn suggested that the number of bacterial taxa isolated from 0.2 μm -filtered fresh water and the great diversity of 0.2 μm -filterable species demonstrated an underestimation of the bacterial diversity that are able to pass through this pore size without losing any viability. A similar result was obtained for *I. hospitalis*. Cells were able to pass through 0.2 μm Whatman[®] filter units (cellulose acetate membrane) (see Figure 56A; example of cellulose acetate membrane (Sterlitech Corporation)). In a second approach, Whatman[®] Nuclepore[™] Track-Etched Membranes with 0.1 μm pore size (polycarbonate membranes) (see Figure 56B; example of track-etched membrane (Sterlitech Corporation)) were used to sterile filter a stationary phase culture to obtain a cell-free supernatant. The same result was obtained. “Sterile” filtered stationary phase cultures inoculated with $\frac{1}{2}$ SME+S⁰ medium (negative control samples) gave positive signals on lead acetate paper, and cells were detected by microscopic observation (Figure 38, 39). The experiments were repeated using Whatman[®] Nuclepore[™] Track-Etched Membranes with 0.1 μm pore size. Similar results were obtained for the negative controls; therefore it was concluded that a sterile filtration was not possible. Having a closer look on the exemplarily depicted membranes in Figure 56, the cellulose acetate membrane (left side) shows a mesh-like structure, whereas the polycarbonate track-etched membrane shows a more or less defined perforation. It is imaginable that *I. hospitalis* cells are able to pass through this mesh, because the cells do not have any rigid cell wall (Rachel *et al.*, 2002). It is even more surprising that these cells were also able to pass through track-etched membranes with a putative pore size of 0.1 μm . But as shown in Figure 56B, it is very likely that the heavy ions penetrating the membranes for perforation may hit the polycarbonate surface in such a close proximity, that bigger pores are formed with a clearly increased pore size. The filterability of *I. hospitalis* seems to be influenced not only by its cell volume and shape, the lack of a rigid cell wall and the presence of two membranes may promote its flexibility, thus filterability. A sterile filtration was not possible regardless the pore size of the filter units. A definite statement cannot be made whether *I. hospitalis* secretes compounds which are able to rescue cells exposed to high doses of ionizing radiation.

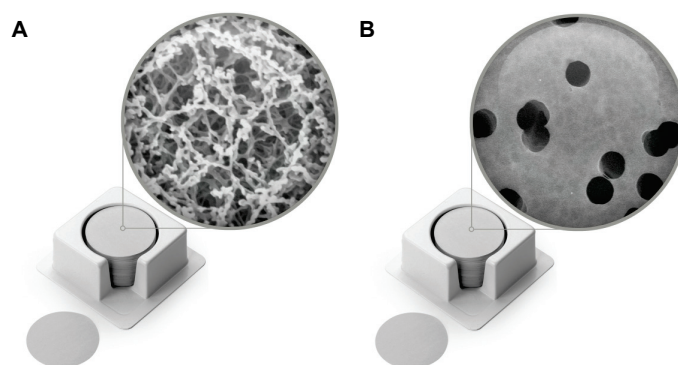


Figure 56: Different types of membranes used for sterile filtration. (A) Cellulose acetate membrane (28.04.16: http://media.sterlitech.com/catalog/product/cache/resized/CA_Main__1_h0_w600.jpg). **(B)** Polycarbonate track-etch membrane (28.04.16: <http://www.sterlitech.com/filters/membrane-disc-filters/polycarbonate-membranes.html>). Pore sizes were not stated for the single images.

The question whether the environment itself plays a role in radiation tolerance and cell survivability of an organism should also been taken into consideration. It has been presented in this work that *I. hospitalis* showed reduced tolerance to ionizing radiation (^{60}Co radiation) when serial diluted in $\frac{1}{2}$ SME+S⁰ medium prior to exposure compared to stationary phase cultures which were serial diluted in $\frac{1}{2}$ SME+S⁰ medium after exposure (DbR #1; Figure 35). To test whether the environment (here: $\frac{1}{2}$ SME+S⁰ medium) itself has a negative or inhibitory effect on cell survivability, $\frac{1}{2}$ SME+S⁰ medium was exposed to ^{60}Co radiation (DbR #2), and used for serial dilutions with untreated *I. hospitalis* cells. Surprisingly, the exposed $\frac{1}{2}$ SME+S⁰ medium showed a comparable inhibitory effect on cell survivability as shown for cells which were serial diluted prior to exposure.

To further investigate this inhibitory effect it was tried to mimic this radiation exposed medium by the irradiation of single substances; a dose specific medium was prepared later on. As shown in Figure 57 (see also Figure 37 and Appendix), the strongest color change was achieved for NaCl, NaBr, NaHCO₃ and Na₂S x 9 H₂O after exposure to 117.1 kGy.

NaCl	NaBr	KI	NaHCO ₃	Na ₂ S x 9 H ₂ O
117.1 kGy				

Figure 57: Chemical substances with strongest color change after ^{60}Co radiation exposure (117.1 kGy).

A potential explanation for this color change caused by high energy ionizing radiation (here ^{60}Co radiation) is that this radiation has enough energy to disrupt and dislodge electrons (Ashbaugh III, 1988). This process has often been seen within a gem crystal and is used by laboratory irradiation to enhance the color of different gemstones. During this process, the radiation passes through the gemstone, this imparts the energy to the crystal while creating color centers (F-centers) (Ashbaugh III, 1988; Fritsch & Rossman, 1988). The process has also been present during *I. hospitalis* ^{60}Co radiation exposure, when the exposed serum bottles turned from colorless/clear to a dark brown due to quartz (SiO_2) used for borosilicate glass production (see also Figure 43/HPLC-vial after X-ray exposure).

Similar processes took place during ^{60}Co radiation exposure of dry substances resulting in F-center formation hence strong color changes in all halide compounds (NaCl , NaBr , KI), NaHCO_3 and $\text{Na}_2\text{S} \times 9 \text{ H}_2\text{O}$. The solubility was not affected and no inhibitory effect on cellular survivability was observed in $\frac{1}{2}$ SME medium prepared from these substances. In contrast, exposed $\frac{1}{2}$ $\text{SME}+\text{S}^0$ and $\frac{1}{2}$ $\text{SME}-\text{S}^0$ medium dramatically decreased the survivability of untreated *I. hospitalis* cells. Why does irradiated $\frac{1}{2}$ $\text{SME}+\text{S}^0$ medium have a negative effect on survivability as well as $\frac{1}{2}$ $\text{SME}-\text{S}^0$ medium? Both showed comparable inactivation tendencies. It seems that the medium composition itself has a negative effect on the survival of *I. hospitalis* after ^{60}Co radiation exposure. Saran and Bors discussed in 1997 that cells suspended in physiological saline (here: PBS) were exposed to irradiation, concomitantly to varying concentrations of hydrogen peroxide (H_2O_2), hypochlorite (HOCl) and the hypochlorite radical anion which were formed in PBS during irradiation. They further described that these species react in the bulk solution to yield the physiologically harmless products chloride and ground-state oxygen. But, the chemical half-life of H_2O_2 and HOCl during this process is in the order of seconds. They proposed that this may be enough time to damage the cells substantially (Saran & Bors, 1997). The production of these cytotoxic agents is also possible during irradiation of $\frac{1}{2}$ SME medium ($+\text{S}^0/-\text{S}^0$) due to high amounts of NaCl , KCl and KH_2PO_4 , substances used also for PBS preparation. But as already mentioned by Saran and Bors, the half-life of H_2O_2 and HOCl is in the range of seconds, it may be unlikely that these cytotoxic agents are still present after weeks. Further experiments are warranted to investigate. The question whether sulfur may play a separated role is still under debate, because sulfur is the main electron acceptor used by *I. hospitalis*, and may undergo conformational changes upon irradiation; it was tried to separately investigate accompanying effects on the survivability of *I. hospitalis*. Based on that, it has to be taken into consideration that elemental sulfur which was exposed in $\frac{1}{2}$ SME medium may have changed its natural conformation (S_8)

upon irradiation hence diminishing its bioavailability. A changed conformation could also be the reason for the observed turbidity and may also have negative effects on cell survivability.

Due to sulfur's low solubility in water, experiments in homogenous systems is prevented. The sulfur radiolysis work in aqueous media has been limited to colloidal and bulk heterogeneous systems (e.g. Donaldson & Johnston, 1968). Bulk heterogeneous mixtures of sulfur and water (colloidal sulfur solubilized in aqueous media) in de-aerated systems resulted in the formation of sulfuric acid upon absorption of ionizing radiation (Della Guardia & Johnston, 1980; Donaldson & Johnston, 1968); the reaction may be initiated by OH-radicals from water that are additionally involved in subsequent steps as well. At ordinary temperatures, the dominating form of sulfur is a S_8 conformation, both in liquid and solid phase. Radiolysis may cause a ring-breakage forming an $-S-OH$ bond; subsequent steps would lead to the formation of sulfuric acid (Della Guardia & Johnston, 1980). Thus, elemental sulfur may act as "sink" for OH-radicals, formed upon irradiation of aqueous systems, which may be an important factor in radioprotection by colloidal sulfur and by sulfur-containing compounds (Della Guardia & Johnston, 1980). Based on the observations of ^{60}Co radiation exposed sulfur-containing $\frac{1}{2}$ SME medium, the same turbidity was obtained as shown for colloidal sulfur in water (produced by the reaction of sodium thiosulfate with hydrochloric acid, or purchased colloidal sulfur in water) (Figure 58). Based on pH determination using pH-indicator paper, no pH shift (acidification) was detectable upon exposure. Nevertheless, ^{60}Co radiation exposure of sulfur-containing $\frac{1}{2}$ SME medium has an inhibitory effect on *I. hospitalis*.

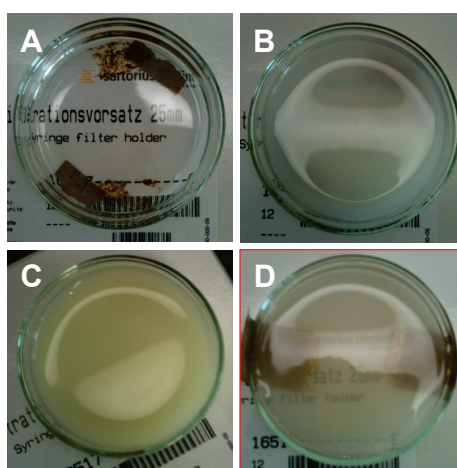


Figure 58: Colloidal sulfur. (A) 10 ml of 0.125 M sodium thiosulfate in a glass petri dish. (B) Addition of 1 ml 5 M HCl. The turbidity starts to increase. (C) The formation of colloidal sulfur at its end. (D) Colloidal sulfur purchased by Sigma-Aldrich in ~10 ml dH_2O .

The clear solution of sodium thiosulfate (Figure 58A) turned to opaque after ~1 min of incubation at RT (Figure 58B, C). Figure 58D shows that the same effect was obtained for

colloidal sulfur (reddish brown color) in dH₂O. These optical results can be compared to the increasing turbidity of ⁶⁰Co radiation exposed sulfur-containing ½ SME medium as shown in Figure 29. It was tested whether this colloidal sulfur may serve as potential sulfur source for *I. hospitalis*. It has already been shown for the anaerobic hyperthermophilic crenarchaeon *Staphylothermus marinus* that colloidal sulfur can serve as electron acceptor needed for growth (Hao & Ma, 2003). As a result, *I. hospitalis* was able to grow to the 10⁻² dilution step which is comparable to the results obtained for ⁶⁰Co radiation exposed ½ SME+S⁰ medium or the exposed sulfur-free ½ SME medium (regardless of the sulfur supplementation) (Figure 36). In summary, elemental sulfur seems to undergo a conformational change upon ⁶⁰Co radiation exposure. This conformational change can directly be seen in terms of increasing turbidity with increasing radiation dose. No significant amount of sulfuric acid was produced, hence no pH shift was detectable. The conformation of the sulfur could not be clarified. Based on current experiments it cannot be concluded whether a S₈ conformation was changed into a S₆ conformation (typical conformation of colloidal sulfur). Additionally, *I. hospitalis* seems to be able to use colloidal sulfur as electron acceptor. Surprisingly, sulfur-free ½ SME medium exposed to ⁶⁰Co radiation resulted in a comparable inactivation of *I. hospitalis* regardless the sulfur supplementation; no pH shift was observed, too. Exposed sulfur seems to play a secondary role. Based on these results, one has to think about the environment itself (here sulfur-free ½ SME medium) that can undergo unfavored changes upon external impacts such as radiation exposure, inhibiting life to propagate. These results reveal a new way of thinking combining an organisms' response with the independent environmental response to external stimuli, which may result in a potential additional stress for microbial life.

4.3 DNA integrity and DNA repair of *I. hospitalis* after ionizing radiation exposure

To investigate the DNA integrity of *Ignicoccus* after irradiation, and to monitor its DNA repair and gene expression, nucleic acids have to be extracted in the highest possible quality. Hence, two different protocols were used for nucleic acid extraction being specific for either DNA or RNA. These protocols have extensively been tested with Cyanobacteria but good results were also obtained for other microorganisms such as Archaea (Leuko *et al.*, 2008). The genomic DNA of *I. hospitalis* was extracted according to the protocol of Tillet and Neilan published in 2000. They have obtained high-quality nucleic acids from cyanobacterial strains, and also for the archaeal methanogen *Methanococcoides burtonii*. Therefore, to investigate the molecular damage caused by radiation (non- and ionizing radiation), genomic DNA from either "*I. morulus*" or *I. hospitalis* cells was extracted before

and after stress exposure according to this (slightly improved) method. The extracted genomic DNA was subjected to RAPD or qPCR analysis. The question concerning the impact of ionizing radiation on the genome integrity of *I. hospitalis* and its ability to repair radiation induced DNA damages will be discussed in the following. DNA integrity after heavy ion exposure will initially be conferred, followed by DNA lesions induced by radiation of the electromagnetic spectrum (X-ray, γ -rays). The discussion about the repair of X-ray induced DNA damages will conclude this Section, and serves as transition to gene expression studies.

I. hospitalis and "*I. morulus*" genome integrity was analyzed by RAPD after exposure to different types of ionizing radiation (X-ray, γ -ray and heavy ion), all representing a major part of the galactic radiation spectrum. As a result, the genomic DNA integrity of *I. hospitalis* was not affected by heavy ion exposure (Figure 28) regardless of the dose (0-1000 Gy) and appearance (He, Fe, Ar). No gain or loss of bands was detected in comparison to the untreated sample (0 Gy). It seems that the doses applied were too low to induce severe changes, making detection by RAPD band pattern analysis impossible. In comparison, the overall RAPD band pattern profile of both specimens was severely impacted by X-ray and γ -radiation exposure compared to untreated control samples indicating that numerous DNA damages (e.g. strand breaks) were induced by these types of radiation and severely reduced the genomic DNA integrity. To get an impression on the relative amounts of DNA lesion, qPCR was performed resulting in a decreased amplification rate with increasing radiation dose compared to the untreated transport control. With the use of a ~1.3 kb DNA fragment encoding the 16S rRNA sequence it was estimated how many damages were introduced within this small fragment after radiation exposure. An exposure of *I. hospitalis* to 117.1 kGy prevented amplification, whereas the amplification of "*I. morulus*" was already inhibited at doses above 55.8 kGy. Similar results were obtained for DNA damages induced by X-rays (data not shown). No predictions concerning unspecific changes in other targets like proteins can be made by both PCR-based methods (PCR, RAPD). Nevertheless, comparing the enormous impact of ionizing radiation especially after such high doses as were applied during DbR, it is surprising that *I. hospitalis* is able to survive (here: able to reproduce) doses of up to ~19 kGy.

The fundamental repair mechanisms present in *I. hospitalis* are supposed to be very efficient and fast to quickly respond to induced damages allowing the maintenance of genome integrity, as shown by RAPD analysis (Figure 47). The band with a size of ~5000 bp was obviously absent after X-ray exposure compared to the untreated control sample (0 Gy). This band was exemplarily used to track the DNA repair of *I. hospitalis* at 90 °C over time. The determined gray-levels (Table 23) indicated that 60 min of repair was

sufficient to regain almost the same band intensity (60 min at 90 °C: 1178.8) shown for the untreated control sample (0 Gy: 1655.5). The increase in band intensity (~5000 bp) can directly be followed on the agarose gel itself (Figure 47). In 1997, DiRuggiero and colleagues followed the DNA repair of the hyperthermophilic archaeon *Pyrococcus furiosus* after ^{60}Co radiation exposure by using pulsed field gel electrophoresis (PFGE). They were able to show that *P. furiosus* was able to repair its DNA damages induced by 2.5 kGy after incubating the exposed cells for 20 hours at 95 °C. Almost the same band intensity was obtained for the ~2.0 Mbp large chromosomal DNA band compared to the untreated control sample (DiRuggiero *et al.*, 1997). Based on RAPD analysis, the method of choice in this work, it seemed that *I. hospitalis* was able to repair its radiation induced DNA damages faster. A potential explanation would be the differing experimental set up. Here, cells were exposed at room temperature, whereas previously reported exposures were conducted on ice. Besides DiRuggiero *et al.* (1997), Williams and colleagues exposed *Pyrococcus furiosus* on ice as well and reported that it took 20 min to reach the incubation temperature of 90 °C following irradiation (Williams *et al.*, 2007). This lag phase may be one imaginable reason for the different repair rates (Williams *et al.*, 2007; DiRuggiero, 1997). The experiments concerning repair kinetics were conducted with *I. hospitalis* stationary phase cells, therefore it may be speculated that a similar process as previously observed is occurring in stationary phase cultures of *I. hospitalis* as well. In the case of *Thermococcus gammatolerans* it has been shown that the growth phase does not influence its radioresistance under optimal growth conditions, but stationary phase cells were able to reconstitute the shattered chromosome faster than exponentially growing cells (Tapias *et al.*, 2009). Whether *I. hospitalis* is more or less radioresistance in its exponential phase has not been investigated. In this work it was shown that the ionizing radiation tolerance of *I. hospitalis* is unaffected by cultivation temperature and the temperature during exposure. Thus, whether *I. hospitalis* differently behave to radiation under varying growth phases is an interesting point for future experiments.

To further investigate the repair potential of *I. hospitalis*, gene-regulation studies during repair were conducted employing quantitative Reverse-Transcription (qRT)-PCR. The first qRT-PCR experiment was designed to test whether the experimental set up itself worked out to be able to detect changes in RNA transcription levels. An upregulation in the case of *recB* has been observed in comparison to the untreated stationary phase culture sample (N_0 , no incubation at 90 °C) (Figure 49). To be able to analyze the obtained qRT-PCR results by relative quantitation, different experiments were conducted to find a putative “housekeeping gene”; however, no reliable housekeeping gene was found. Data

analysis by relative quantitation was not possible therefore it was decided to analyze the obtained data by absolute quantification as previously described (see 2.5.6.1).

Several gene specific primers were designed, for genes involved in DNA damage repair, to see whether *I. hospitalis* up- or down-regulates these genes of interest after X-ray exposure. Only *I. hospitalis* cells being in their early exponential phase (see condition F, 2.4.2.6) showed a slight upregulation of all tested genes upon irradiation with an overall maximum after 90 min of repair (Figure 53). Comparing the relative copy number of *radA* to all other tested genes, *radA* showed highest expression (Figure 53). This moderate increase in the mRNA levels of this recombinase RadA is in agreement with previous studies of other mesophilic and hyperthermophilic archaea (Williams *et al.*, 2007; Baliga *et al.*, 2004; Komori *et al.*, 2000, Reich *et al.*, 2001). In contrast to *E. coli*, *recA* expression was increased up to 10-fold following exposure to DNA damaging events (Courcelle *et al.*, 2001; Liu *et al.*, 2003). The studies of Williams and colleagues with *P. furiosus* and other microorganisms (e.g. Baliga *et al.*, 2004) suggest that DNA repair proteins are constitutively expressed and that they may be present in the cell at a level sufficient to maintain the integrity of the cell's material (Williams *et al.*, 2007; Kottemann *et al.*, 2005); this may also be the case for *I. hospitalis*. Whole-genome studies with *P. furiosus* (Williams *et al.*, 2007) or the halophilic archaeon *H. salinarum* NRC-1 (Baliga *et al.*, 2004; Whitehead *et al.*, 2006) suggest that the transcriptional response to DNA damage in Archaea differs from bacterial response. It is known that several stress response systems are inducible in mesophiles, and may be constitutively expressed in hyperthermophiles (Williams *et al.*, 2007; Gerard *et al.*, 2001; Jolivet *et al.*, 2003; Kottemann *et al.*, 2005). A constitutive expression of genes relevant for DNA damage repair in *I. hospitalis*, and a constant supply of repair enzymes may be supported by the results of the "hot exposure" experiment. An additional heat stress during exposure did not result in reduced survivability compared to cells exposed to ionizing radiation at room temperature.

Whether the protein composition within the cell has changed upon irradiation has not yet been investigated. Assuming a constant supply of repair enzymes, their activity may be regulated after their translation. Post-translational modifications (PTM) of proteins are widespread in the three domains of life and take place in Archaea as well (e.g. Kish *et al.*, 2016). With these modifications it is possible to modulate and alter a protein's physicochemical and biological properties including effects that influence its activity, function, the subcellular localization, oligomerization, folding and also its turnover without the necessity of being synthesized *de novo* (according to Eichler & Adams, 2005; Oberle & Blattner, 2010). PTMs may help an organism to overcome the challenges by their environment e.g. temperature, because the properties of a protein can quickly be changed

without the need to transcribe damaged DNA which may be hindered by induced lesions resulting in potentially non-functional protein products. The addition or removal of small chemical groups allows the modification of the target protein's characteristic (according to Oberle & Blattner, 2010). However, most modifications of archaeal proteins remain unclear (according to Eichler & Adams, 2005). Assuming that *I. hospitalis* constantly express genes involved in DNA damage repair, it is less surprising that neither up- nor down-regulation of interesting genes e.g. *rad50*, *recB*, *rad2* or *radA* was observed in e.g. stationary phase cells. Whether *I. hospitalis* post-translationally modifies its proteins has not been investigated yet. Post-translational modifications however would be on the one hand a completely new way of thinking in terms of its radiation tolerance and on the other hand a promising assumption in terms of constantly expressed genes and potentially high levels of repair proteins present due to its hot lifestyle. Additional exposure to ionizing radiation without a reduced survivability may be feasible as seen during the "hot exposure" experiment.

A constitutive expression of genes involved in the repair of UV-C radiation induced damages in two exponentially growing *Sulfolobus* species, and a coherent repression of genes involved in DNA replication and chromatin proteins, resulting in the inhibition of DNA replication, was suggested by Götz *et al.*, (2007). The researchers proposed that this allows the repair to take place. To see whether a comparable effect can be seen for *I. hospitalis* after X-ray exposure, cells were exposed to 3 kGy in their exponential phase (experimental condition E, Figure 51/table). Primers for genes involved in replication processes were designed referring to Götz *et al.*, 2007 including *ccrB* (chromosome condensation protein CcrB), *cdc6* (cell division control protein Cdc6), *cdc6-orc1* (ORC complex protein Cdc6/Orc1), *dbp1* (DNA-binding protein), *ber* (base excision DNA repair protein), *poll* (DNA polymerase I), *mcm* (replicative DNA helicase Mcm), *tfb* (transcription initiation factor IIB), *fen-1* (endonuclease), *rg* (reverse gyrase). The ratios for all genes tested varied by ~0.1 comparing the ratios after 5 min to 90 min of repair. No up- or down-regulation was detected (Figure 54). Although it was not possible to describe a similar effect for *I. hospitalis* cells, as described by Götz *et al.* for *Sulfolobus*, an upregulation of genes involved in DNA repair processes was demonstrated in this work; this promising result highly encourages to continue and expand gene expression studies with *I. hospitalis*.

5 Conclusion and Outlook

Besides optimal organismic adaptation to the natural habitat, the propagation of life in an unfavorable environment benefits from cellular responses that may also be advantageous during additional unpredictable stress exposure. The results presented in the underlying work showed that all tested representatives from the genus *Ignicoccus* have a remarkable radiotolerance (radiation tolerance) in common, which is quite surprising when thinking of their natural habitat deep-sea; the high radiation intensities (non-ionizing and ionizing radiation) chosen for experimentation may have never been present in this habitat. It was shown that all *Ignicoccus* representatives are clearly more UV-tolerant in comparison to other hyperthermophilic archaea, like e.g. the aerobic *Sulfolobus solfataricus*. An increased ROS production, due to UV exposure, can possibly be circumvented by hyperthermophiles living anaerobically, therefore decreasing the overall ROS production to a minimum. The exposure of e.g. *Ignicoccus hospitalis* to high fluences of non-ionizing radiation resulted in a severe reduction of its genomic DNA integrity concomitantly with an increased amount of DNA lesions. Nevertheless, its very high radiotolerance may point to very efficient repair mechanisms taking place to successfully maintain its genome integrity while exposed to these high radiation fluences. Furthermore, it was shown in this work, that classical light-dependent photoreactivation by the enzyme photolyase may possibly be not present in *I. hospitalis*. Instead, the presence of a radical SAM protein is speculated to play an important role in scavenging UV induced ROS in *I. hospitalis* cells; this may support the idea of correlating a high radiotolerance with an anaerobic, hyperthermophilic lifestyle.

Besides non-ionizing radiation, ionizing radiation is also known to be an exogenous source of free radicals (ROS), which are produced via the radiolysis of water and account for >80 % of introduced DNA damages, whereas only >20 % of introduced damages are ascribed to direct effects of γ -photons. By way of comparison, it was demonstrated that *I. hospitalis* is more tolerant to ionizing radiation than other organisms mentioned in this work. Cellular responses and interactions between single cells are assumed to be beneficial for life to propagate and withstand unfavored environmental conditions. It was possible to discriminate between the survival of *I. hospitalis* in terms of reproduction and its metabolic activity after exposure to extremely high doses of ^{60}Co radiation. This phenomenon allowed, for the first time, the postulation of a VBNC state in the domain of Archaea, and supports this hypothesis empirically by experimentation. The discrimination between reproducibility and metabolic activity helps us to better understand an organisms'

tolerance and response to a given stressor. The presence of a postulated VBNC state in *I. hospitalis* may be encouraging to think of quorum sensing as well. Inter-cellular communication and interaction is assumed to be very beneficial for a population allowing subsequent propagation under stress-reduced environmental conditions. A definite statement whether quorum sensing does exist for *I. hospitalis* cannot be made due to its filterability meaning the ability to pass through micropore membranes. Nevertheless, VBNC and potential quorum sensing would be extremely beneficial when unpredicted external stimuli (here: ^{60}Co radiation) change the environment in which *Ignicoccus* would normally thrive. The underlying work has shown that the environment itself (here: $\frac{1}{2} \text{SME} + \text{S}^0$ or $-\text{S}^0$) plays a role in radiation tolerance and cell survivability. Both, exposed $\frac{1}{2} \text{SME} + \text{S}^0$ and $\frac{1}{2} \text{SME} - \text{S}^0$ medium, showed comparable inhibitory effects on cell survivability. This may indicate that the composition of the medium, the environment, can undergo unfavorable changes resulting in negative effects influencing the cellular survival after ^{60}Co radiation exposure. A reduced or altered bioavailability of a substance needed for proper metabolism (here: elemental sulfur) has to be taken into account, too. It has been observed that elemental sulfur seems to undergo a conformational change upon ^{60}Co radiation exposure, seen by increasing turbidity with increasing radiation dose. It may be assumed that *I. hospitalis* is able to use colloidal sulfur as electron acceptor as well, although resulting in reduced growth. This may point to an alternative energy source which can potentially be used by the organism, even if other sources would be favored. In summary, one has to think about the environment and energy sources themselves that may undergo unfavored changes upon external impacts such as radiation exposure, inhibiting life to propagate. These results reveal a new way of thinking combining the response of an organism with the independent environmental response to external stimuli, which may result in a potential additional stress for microbial life.

Organismic adaptation to harsh environments and underlying fundamental repair mechanisms need to be very efficient and fast to quickly respond to induced damages allowing the maintenance of genome integrity. It has been shown for *I. hospitalis* that 60 min of ionizing radiation induced DNA damage repair was sufficient to regain almost the same RAPD band intensity shown for the untreated control sample. Additionally, it was presented in this work that the ionizing radiation tolerance of stationary phase cells was unaffected by cultivation temperature and the temperature during exposure. Tapias and colleagues showed in 2009 that the radioresistance of the archaeon *Thermococcus gammatolerans* was independent from its growth phase, whereas *Deinococcus radiodurans* was found to be more resistant in stationary phase (Keller and Maxcy, 1984). The ionizing radiation tolerance of *I. hospitalis*, representing all other

Ignicoccus species, was exclusively investigated with cells in stationary phase. It would be interesting to investigate whether the survival of *Ignicoccus* may also be independent from growth phase under optimal growth conditions as shown for *T. gammatolerans* (Tapias *et al.*, 2009); this is an interesting point for future experiments.

We have seen that *Ignicoccus*, here *I. hospitalis*, is able to tolerate high levels of different types of radiation, that its DNA damage repair is very fast and efficient and that its tolerance seems to be unaffected by its pre-cultivation temperature and the temperature during radiation exposure. But why and how is this organism able to withstand this radiation stress to which it is never exposed in its natural habitat? Right at the beginning, one has to think about the expression of genes playing an important role in these repair processes. Thus, experiments in terms of gene expression in *I. hospitalis* upon X-ray exposure were conducted by qRT-PCR and may point to a growth phase dependent regulation. The expression of the *radA* gene was slightly upregulated in cells being in their early exponential phase, while other tested genes involved in DNA repair (*rad50*, *recB*, *rad2*) showed a naturally occurring high base level of expression. *I. hospitalis* stationary phase cells may potentially constantly express genes involved in DNA damage repair; it is less surprising that neither up- nor down-regulation of interesting genes was observed. It was postulated for e.g. *P. furiosus* and other microorganisms that DNA repair proteins are constitutively synthesized due to harsh environmental conditions, and that they may be present in the cell at a level sufficient to maintain the integrity of the cell's material; this would also be imaginable for *I. hospitalis*. Assuming constitutive expression of genes relevant for DNA damage repair proteins and a constant supply of these repair enzymes, their activity may quickly be regulated after their translation. Post-translational modifications (PTM) of proteins are widespread in the three domains of life and are known to take place in Archaea as well. These PTMs may help organisms to overcome the challenges by their surrounding environmental conditions e.g. temperature and additional outer influences like radiation. A first impression concerning constant protein supply could be obtained by determining the relative abundance of RadA protein after ionizing radiation exposure by western blotting using a RadA specific antibody. Comparable experiments were conducted with *S. solfataricus*. Rolfsmeier and colleagues assessed in 2011 the abundance of the RadA protein in different *Sulfolobus* species with and without ionizing radiation induced damages. They have observed an alteration in transcript levels which correlates with modest changes in protein production. The less dramatic increase in RadA protein abundance and the strong transcriptional induction of the gene may suggest additional control levels through protein stability or translation (Rolfsmeier *et al.*, 2011). Whether a similar effect can be detected for *I. hospitalis* would be interesting to

investigate; high protein abundance, only slightly affected by additional stress, may possibly point to a post-translational modification activating the suitable enzyme. Whether *I. hospitalis* post-translationally modifies its proteins has not been investigated yet. PTMs, however, would be on the one hand a completely new way of thinking in terms of its radiation tolerance and on the other hand a promising assumption in terms of constantly expressed genes and potentially high levels of repair proteins present due to its hot lifestyle. In depth transcriptomic and proteomic studies with *Ignicoccus* would shine light on this currently advancing research in Archaea and would help us to better understand the origin of life on a molecular level. This may support our ideas concerning organismic abilities needed to propagate terrestrial life to the present day.

Besides very efficient DNA damage repair pathways and potential PTMs of constantly supplied repair proteins, as already mentioned, intracellular concentrations of compatible solutes or other cellular substances like manganese and iron have long been of special interest. Daly *et al.* reported in 2004 that the extremely radiation-resistant, obligate aerobic living bacterium *D. radiodurans* accumulates high amounts of intracellular manganese and low levels of iron. They proposed that Mn(II) accumulation facilitates recovery from radiation induced damages, and that aerobic living microorganisms including Archaea depend on Mn-antioxidant complexes that are responsible for the scavenging of reactive oxygen species (ROS) generated by radiation (Kish *et al.*, 2009). Whether *Ignicoccus* accumulates high amounts of manganese intracellularly like many radioresistant aerobes or whether they constitutively express detoxification systems circumventing this accumulation of Mn-antioxidant complexes, which was seen in anaerobic hyperthermophiles (Webb and DiRuggiero, 2012), has to be determined. An adequate determination of the intracellular manganese/iron ratios in *Ignicoccus* would be achieved by ICP-MS analysis.

An additional very interesting point in terms of radiation tolerance would be polyploidy. Multiple chromosomal copies may be beneficial in regard to elevated radiation exposure allowing enhanced tolerance to induced dsDNA breaks (Hildenbrand *et al.*, 2011). A potential polyploidy may give a promising explanation on *Ignicoccus* impressive radiation tolerance. This determination may be achieved by a commonly used real-time PCR method; a schematic overview can be found in Hildenbrand *et al.*, 2011. Besides a potential polyploidy, the additional plasmids, which seem to be unique to "*I. morulus*" (Figure 26), need further investigation. A sequence comparison to the chromosome of *I. hospitalis* would give information on putative genes and coherent interspecies variations.

We have seen, in the underlying work, that *I. hospitalis* and all other tested representatives showed remarkable radiation tolerance although never exposed to it in their natural habitat. This ability still supports the idea of early Earth inhabitants, when the environmental conditions were hostile with elevated radiation levels compared to present days. But which organismic abilities may have been necessary for life to propagate, besides a high radiotolerance? The present accessible Archaean geologic record point to a slowly cooling climate at the end of the Hadean, when the CO₂ greenhouse was terminated leaving an overall temperature of 50-70 °C in which only thermophiles were able to exist (according to Sleep, 2010; Gaucher *et al.*, 2008, 2010). Pace suggested already in 1991 that the molecular evolution analysis indicates that anaerobic sulfur-reducing chemosynthetic hyperthermophiles may act as the oldest recognizable prokaryotes (according to Pace, 1991; according to Miller & Lazcano, 1995). As shown in Figure 2, phylogentic trees based on 16S rRNA sequence comparison of living, cultivable organisms compare these recent organisms to each other; this may give an idea of their (recent) evolutionary distance. Whether phylogenetic trees, constructed on the basis of genomic sampling of previously unexamined environments together with already published sequences, do reflect the evolutionary development of an organism (Hug *et al.*, 2016) is under debate. Assuming that early life may have inhabited environments like present day deep-sea hydrothermal vents or terrestrial hot springs, Figure 59 shows a simple extrapolation of growth temperatures of extant hyperthermophiles to the origin of life ~3.8 Ga years ago (dashed lines). Based on a hot origin, life may have adapted to lower temperatures during evolution, but it would also be imaginable that life may have adapted to higher temperatures starting from a cold origin (solid lines). As shown for *I. hospitalis*, an adaptation and successful reproduction can occur over a wide temperature range. The optimal growth temperature is at 90 °C but growth at temperatures below (75 °C) and above (95 °C) this T_{opt} , does not result in any reduced stress tolerance (here: X-ray radiation). Therefore, an overall adaptation to a hot environment would have been beneficial to survive the last ocean-boiling asteroid impact around 3.8 Ga ago (Figure 59) independent from the environmental origin. (Hyper-) thermophilic organisms seem to be the most suitable survivors after this late heavy bombardment indicating them at least as potential candidates for early Earth inhabitants (Miller & Lazcano, 1995).

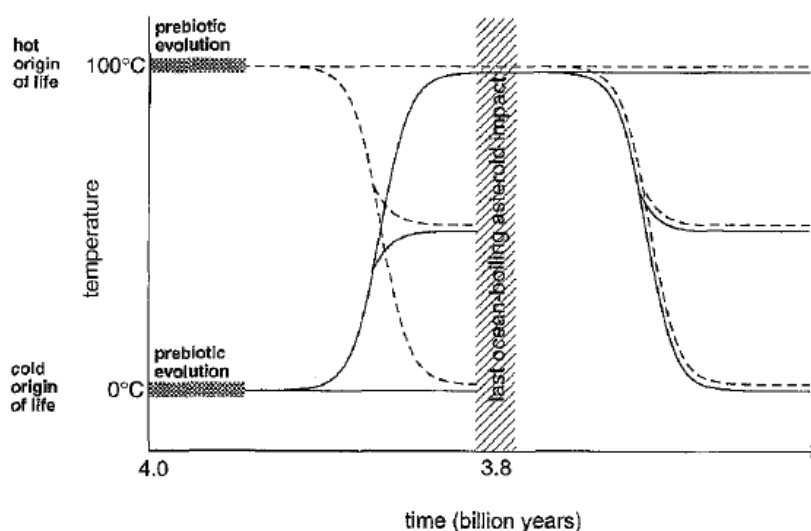


Figure 59: Potential scenario for the origin and early evolution of life. Dotted line: Hot origin of life followed by adaptation to cold temperature; hyperthermophiles would have survived asteroid impacts boiling the ocean. Solid line: Cold origin of life adapted to hot temperature; secondarily adapted hyperthermophiles would have survived asteroid collisions (according to Miller & Lazcano, 1995).

Thus, a hot origin of life is still under debate and was the starting point for my experimental work with *Ignicoccus*. It is feasible to believe that early microbial communities have lived for example around mid-ocean ridges e.g. close to hydrothermal vents (Nisbet, 2000); the area where *Ignicoccus* species were isolated in a depth ranging from hundreds to thousands of meters (see Section 1.3 and following). This habitat would have been beneficial to hide from the elevated radiation levels on the surface due to e.g. the lack of an ozone layer. Keeping in mind that an ancestor is expected to have properties that are transmitted to its descendant (Pace, 1991), it is reasonable to investigate recent organisms regarding their ability to tolerate life hostile environmental conditions as they occurred on early Earth.

To go on with this idea, i.e. assuming *Ignicoccus* is a promising candidate for an early Earth inhabitant, representatives of this genus may also be interesting candidates for potential inhabitants of other planetary bodies like the Jovian moon Europa. Europa's putative ocean has been regarded as potential habitat for life (e.g. Marion *et al.*, 2003). The lethal radiation and the low temperature on the icy surface preclude the possibility of biological activity within this region. Only at the base of this surface layer one would expect to find suitable temperatures including liquid water (Marion *et al.*, 2003). Whether *Ignicoccus* would be able to live on Europa cannot clearly be defined based on our current knowledge. One can assume that potential habitats on Europa are extreme environments compared to our clement Earth; extraterrestrial life, if exists, may be well adapted to its natural environment (Marion *et al.*, 2003). Nevertheless, we still have to think about potential (bio-) signatures that allow us to be able to even detect life. Seager and

colleagues recently proposed the concept that all stable and potentially volatile molecules should initially be considered as viable biosignature gases (Seager *et al.*, 2016), which may include thousands of different gases. However, most of Earth's atmospheric gases are not unique to life meaning that in many cases life may not be the dominant source of atmospheric gases. Some are already basic atmospheric constituents e.g. N_2 , CO_2 , and H_2O , whereas others like CH_4 and H_2S are produced by geological processes as well (Seager *et al.*, 2016). The relative rate of production of a gas by life is specific to a planet because it depends on geological and biological production rates; meaning that biology could be the primary source of a gas on other worlds in comparison to Earth (Seager *et al.*, 2016). One has to keep in mind that only a stable molecule can accumulate in a planetary atmosphere, meaning it has to be stable over days in pure entities and should be stable to hydrolysis (Seager *et al.*, 2016). The latter condition is important due to the fact that water is the key solvent for terrestrial life therefore very likely to be present on an inhabited world. According to the assumption that life is water-based, the produced volatile molecule has to diffuse out of the cell. One very interesting molecule would be metabolically produced hydrogen sulfide (H_2S). All *Ignicoccus* representatives produce H_2S from energy-requiring metabolic reactions to gain biomass. H_2S serves as by-product gas from biological energy extraction from geochemically produced energy gradients (see 1.2). This metabolically produced H_2S was used, in this study, to detect the metabolic activity of *I. hospitalis* after exposure to high doses of ionizing radiation (here: ^{60}Co). With this, it was possible to detect their presence although a microscopic observation did not support this observation. Therefore, H_2S should be taken into consideration when thinking of an interesting biosignature gas regardless its potential abiotic production. In terms of H_2S detection in pristine environments e.g. on Earth or other planets and moons in our solar system and beyond, additional experiments have to be taken into consideration to distinguish between metabolically and abiotically produced hydrogen sulfide.

Ignicoccus representatives were isolated from submarine hydrothermal systems at a depth of ~106 m and deep-sea black smokers at a depth of 2500 m. Their unusual cell biology in combination with their special lifestyle and the remarkable radiotolerance, presented in the underlying work, point to a very dramatic microbe. All these abilities enabled *Ignicoccus* to withstand early Earth's harsh, hostile and changing conditions resulting in successful terrestrial propagation to the present day. These organismic capabilities may have also been highly beneficial to thrive on other planetary bodies in our solar system and beyond; their metabolically produced H_2S may be seen as promising biosignature gas indicating their potential presence outside Earth. Up to now, the

assertion whether *Ignicoccus* inhabits extraterrestrial niches can neither be proved nor refuted.

My personal résumé after a little bit more than three years of my dependent relationship with *Ignicoccus hospitalis* is, that I can definitely agree with Beatrice the Biologist who said “Archaea live in places that scientists long thought were incapable of supporting life, like thermal vents at the bottom of the ocean and boiling acidic hot springs. So in a nutshell, archaea [particularly *Ignicoccus* species] are very strange, very dramatic microbes. They live in dramatic places and cause drama among scientists [especially astrobiologists].” (Beatrice the Biologist, September 20, 2009).

6 References

A

Arrage, A. A., Phelps, T. J., Benoit, R. E., Palumbo, A. V., White, D. C. (1993). Bacterial sensitivity to UV light as a model for ionizing radiation resistance. *Journal of Microbiological Methods* **18**:127-136.

Ashbaugh III, C. E. (1988). Gemstone irradiation and radioactivity. *Gems & Gemology* **24**:196-213.

B

Balch, W. E., Wolfe, R. S. (1976). New approach to the cultivation of methanogenic bacteria: 2-mercaptoethanesulfonic acid (HS-CoM)-dependent growth of *Methanobacterium ruminantium* in a pressurized atmosphere. *Applied and Environmental Microbiology* **32**:781-791.

Baliga, N. S., Bjork, S. J., Bonneau, R., Pan, M., Iloanusi, C., Kottmann, M. C. H., Hood, L., DiRuggiero, J. (2004). Systems level insights into the stress response to UV radiation in the halophilic archaeon *Halobacterium* NRC-1. *Genome Research* **14**:1025-1035.

Baross, J. A. & Hoffmann, S. E. (1985). Submarine hydrothermal vents and associated gradient environments as sites for the origin and evolution of life. *Origins of Life* **15**:327-345.

Bassler, B. L. (2002). Small Talk: Cell-to-Cell Communication in Bacteria. *Cell* **109**, 421-424.

Bauermeister, A., Bentschikou, E., Möller, R., Rettberg, P. (2009). Roles of PprA, IrrE, and RecA in the resistance of *Deinococcus radiodurans* to germicidal and environmentally relevant UV radiation. *Archives of Microbiology* **191**:913-918.

Baumstark-Khan, C., Facius, R. (2001). Life under conditions of ionizing radiation. In *Astrobiology: The Quest for the Conditions of Life* (ed. Horneck, G., Baumstark-Khan, C.) pp 260-283. (Springer, Berlin).

Beblo, K., Douki, T., Schmalz, G., Rachel, R., Wirth, R., Huber, H., Reitz, G., Rettberg, P. (2011). Survival of thermophilic and hyperthermophilic microorganisms after exposure to UV-C, ionizing radiation and desiccation. *Archives of Microbiology* **193**:797-809.

Beblo, K., Rabbow, E., Rachel, R., Huber, H., Rettberg, P. (2009). Tolerance of thermophilic and hyperthermophilic microorganisms to desiccation. *Extremophiles* **13**:521-531.

Benjdia, A., Heil, K., Barends, T. R. M., Carell, T., Schlichting, I. (2012). Structural insights into recognition and repair of UV-DNA damage by spore photoproduct lyase, a radical SAM enzyme. *Nucleic Acids Research* **40**:9308-9318.

Bernander, R., Poplawski, A. (1997). Cell cycle of the thermophilic archaea. *Journal of Bacteriology* **179**:4963-4969.

Bouthier de la Tour, C., Portemer, C., Kaltoum, H., Duguet, M. (1998). Reverse gyrase from the hyperthermophilic bacterium *Thermotoga maritima*: Properties and gene structure. *Journal of Bacteriology* **180**:274-281.

Brochier-Armanet, C., Boussau, B., Gribaldo, S., Forterre, P. (2008). Mesophilic crenarchaeota: proposal for a third archaeal phylum the Thaumarchaeota. *Nature Reviews* **6**:245-252.

C

Canfield, D. E., Habicht, K. S., Thamdrup, B. (2000). The archean sulfur cycle and the early history of atmospheric oxygen. *Science* **288**:658-661.

Canfield, D. E., Teske, A. (1996). Late proterozoic rise in atmospheric oxygen concentration inferred from phylogenetic and sulphur-isotope studies. *Nature* **382**:127-132.

Carell, T., Eppler, R. (1998). Repair of UV light induced DNA lesions: A comparative study with model compounds. *European Journal of Organic Chemistry* **7**:1245-1258.

Cebrián, G., Sagarzazu, N., Pagán, R., Codón, S., Manas, P. (2008). Resistance of *Escherichia coli* grown at different temperatures to various environmental stresses. *Journal of Applied Microbiology* **105**:271-278.

Clavero, M. R. S., Monk, J. D., Beuchat, L. R., Doyle, M. P., Brackett, R. E. (1994). Inactivation of *Escherichia coli* O157:H7, *Salmonellae*, and *Campylobacter jejuni* in raw ground beef by gamma irradiation. *Applied and Environmental Microbiology* **60**:2069-2075.

Cockell, C. S., Horneck, G. (2001). The history of the UV radiation climate of the earth- theoretical space-based observations. *Photochemistry and Photobiology* **73**:447-451.

Coohill, T. (1994). Exposure response curves action spectra and amplification factors. NATO ASI Series. In *Stratospheric Ozone Depletion/UV-B in the Biosphere*, Vol 118 (Edited by R. H. Biggs and M. E. B. Joyner), pp. 57-62. Springer-Verlag, Berlin, Heidelberg, Germany.

Coohill, T. P., Sagripanti, J.-L. (2008). Overview of the inactivation by 254 nm ultraviolet radiation of bacteria with particular relevance to biodefense. *Photochemistry and Photobiology* **84**:1084-1090.

Courcelle J., Khodursky, A., Peter, B., Brown, P. O., Hanawalt, P. C. (2001). Comparative gene expression profiles following UV exposure in wild-type and SOS-deficient *Escherichia coli*. *Genetics* **158**:41-64.

Čuboňová, L., Sandman, K., Hallam, S. J., DeLong, E. F., Reeve, J. N. (2005). Histones in *Crenarchaea*. *Journal of Bacteriology* **187**:4582-4585.

D

Daly, M. J. (2009). A new perspective on radiation resistance based on *Deinococcus radiodurans*. *Nature Reviews Microbiology* **7**:237-245.

Daly, M. J., Gaidamakova, E. K., Matrosova, V. Y., Vasilenko, A., Zhai, M., Venkateswaran, A., Hess, M., Omelchenko, M. V., Kostandarithes, H. M., Makarova, K. S., Wackett, L. P., Fredrickson, J. K., Ghosal, D. (2004). Accumulation of Mn(II) in *Deinococcus radiodurans* facilitates gamma-radiation resistance. *Science* **306**:1025-1028.

De Vega, M. (2013). The minimal *Bacillus subtilis* nonhomologous end joining repair machinery. *PLOS One* **8**:e64232.

Deamer, D. W. (1997). The first living systems: a bioenergetics perspective. *Microbiology and Molecular Biology Reviews* **61**:239-261.

Deamer, D. W., Georgiou, C. D. (2015). Hydrothermal conditions and the origin of cellular life. *Astrobiology* **15**:1091-1095.

Deamer, D., Weber, A. L. (2010). Bioenergetics and life's origins. *Cold Spring Harb Perspect Biol* **2**:a004929.

Della Guardia, R. A., Johnston, F. J. (1980). Radiation-induced reaction of sulfur and water. *Radiation Research* **84**:259-264.

Di Giulio, M. (2000). The universal ancestor lived in a thermophilic or hyperthermophilic environment. *Journal of Theoretical Biology* **203**:203-213.

Di Giulio, M. (2001). The universal ancestor was a thermophile or a hyperthermophile. *Gene* **281**:11-17.

Di Giulio, M. (2007). The universal ancestor and the ancestors of archaea and bacteria were anaerobes whereas the ancestor of the eukarya domain was an aerobe. *European Society for Evolutionary Biology* **20**:543-548.

Di Giulio, M. (2010). Biological evidence against the panspermia theory. *Journal of Theoretical Biology* **266**:569-572.

Di Giulio, M. (2011). The last universal common ancestor (LUCA) and the ancestors of archaea and bacteria were progenates. *Journal of Molecular Evolution* **72**:119-126.

DiRuggiero, J., Santangelo, N., Nackerdien, Z., Ravel, J., Robb, F. T. (1997). Repair of extensive ionizing-radiation DNA damage at 95 °C in the hyperthermophilic archaeon *Pyrococcus furiosus*. *Journal of Bacteriology* **179**:4643-4645.

Donaldson, D. W., Johnston, F. J. (1968). The radiolysis of colloidal sulfur. *Journal of Physical Chemistry* **72**:3552-3558.

Donnellan, J. E., Jr., Stafford, R. S. (1968). The ultraviolet photochemistry and photobiology of vegetative cells and spores of *Bacillus megaterium*. *Biophysical Journal* **8**:17-28.

Doolittle, R. F. (2000). Searching for the common ancestor. *Research in Microbiology* **151**:85-89.

Doyle, M. P., Schoeni, J. L. (1984). Survival and growth characteristics of *Escherichia coli* associated with Hemorrhagic Colitis. *Applied and Environmental Microbiology* **48**:855-856.

E

Eichler, J., Adams, M. W. W. (2005). Posttranslational protein modification in archaea. *Microbiology and Molecular Biology Reviews* **69**:393-425.

F

Forterre, P., Bergerat, A., Lopez-Garcia, P. (1996). The unique DNA topology and DNA topoisomerase of hyperthermophilic archaea. *FEMS Microbiological Reviews* **18**:237-248.

Franson, M. A. H. (1985). Standard methods for the examination of water and wastewater, 16th edition (ed. Greenberg, A. E., Trussell, R. R., Clesceri, L. S.) *American Public Health Association*, Washington DC (USA).

Frey, P. A., Hegeman, A. D., Ruzicka, F. J. (2008). The radical SAM superfamily. *Critical Reviews in Biochemistry and Molecular Biology* **43**:63-88.

Friedberg, E. C., Walker, G. C., Siede, W. (1995). DNA repair and mutagenesis. *ASM Press*, Washington DC (USA).

Fritsch, E., Rossman, G. R. (1988). An update on color in gems. Part 2: Colors involving multiple atoms and color centers. *Gems & Gemology* **24**:3-15.

Fröls, S., Gordon, P. M. K., Panlilio, M. A., Duggin, I. G., Bell, S. D., Sensen, C. W., Schleper, C. (2007). Response of the hyperthermophilic archaeon *Sulfolobus solfataricus* to UV damage. *Journal of Bacteriology* **189**:8708-8718.

G

Galtier, N., Tourasse, N., Gouy, M. (1999). A nonhyperthermophilic common ancestor to extant life forms. *Science* **283**:220-221.

Gaucher, E. A., Govindarajan, S., Ganesh, O. K. (2008). Palaeotemperature trend for precambrian life inferred from resurrected proteins. *Nature* **451**:704-708.

Gaucher, E. A., Kratzer, J. T., Randall, R. N. (2010). Deep phylogeny-how a tree can help characterize early life on earth. *Cold Spring Harb Perspect Biology* **2**:a002238.

Gérard, E., Jolivet, E., Prieur, D., Forterre, P. (2001). DNA protection mechanisms are not involved in the radioresistance of the hyperthermophilic archaea *Pyrococcus abyssi* and *P. furiosus*. *Molecular Genetics and Genomics* **266**:72-78.

Ginzinger, D. G. (2002). Gene quantification using real-time quantitative PCR: An emerging technology hits the mainstream. *Experimental Hematology* **30**:503-512.

Goodhead, D. T. (1999). Mechanisms for the biological effectiveness of high-LET radiations. *Journal of Radiation Research* **40**:1-13.

Götz, D., Paytubi, S., Munro, S., Lundgren, M., Bernander, R., White, M. F. (2007). Responses of hyperthermophilic crenarchaea to UV irradiation. *Genome Biology* **8**:R220.1-18.

Graham, D. E., Overbeek, R., Olsen, G. J., Woese, C. R. (2000). An archaeal genomic signature. *Proceedings of the National Academy of Sciences* **97**:3304-3308.

Grassineau, N.V., Nisbet, E. G., Bickle, M. J., Fowler, C. M. R., Lowry, D., Matthey, D. P., Abell, P., Martin, A. (2001). Antiquity of the biological sulphur cycle: evidence from sulphur and carbon isotopes in 2700 million-year-old rocks of the Belingwe Belt, Zimbabwe. *Proceedings of the Royal Society of London B* **268**:113-119.

Grenfell, J. L., Rauer, H., Selsis, F., Kaltenegger, L., Beichman, C., Danchi, W., Eiroa, C., Fridlund, M., Henning, T., Herbst, T., Lammer, H., Léger, A., Liseau, R., Lunine, J., Paresce, F., Penny, A., Quirrenbach, A., Röttgering, H., Schneider, J., Stam, D., Tinetti, G., White, G. J. (2010). Co-evolution of atmosphere, life, and climate. *Astrobiology* **10**:77-88.

Grogan, D. W. (1998). Hyperthermophiles and the problem of DNA stability. *Molecular Microbiology* **28**:1043-1049.

Grogan, D. W. (2000). The question of DNA repair in hyperthermophilic archaea. *Trends in Microbiology* **8**:180-185.

Grogan, D. W. (2004). Stability and repair of DNA in hyperthermophilic Archaea. *Current Issues in Molecular Biology* **6**:137-144.

Grogan, D. W. (2015). Understanding DNA repair in hyperthermophilic archaea: Persistent gaps and other reasons to focus on the fork. *Achaea* **2015**: 942605.

H

Habicht, K. S., Canfield, D. E. (1996). Sulphur isotope fractionation in modern microbial mats and the evolution of the sulphur cycle. *Nature* **382**:342-343.

Hahn, M. W. (2004). Broad diversity of viable bacteria in 'sterile' (0.2 µm) filtered water. *Research in Microbiology* **155**:688-691.

Hao, X., Ma, K. (2003). Minimal sulfur requirement for growth and sulfur-dependent metabolism of the hyperthermophilic archaeon *Staphylothermus marinus*. *Archaea* **1**:191-197.

Haymon, R. M. (1983). Growth history of hydrothermal black smoker chimneys. *Nature* **301**:695-698.

Heimerl, T. (2014). *Ignicoccus* und *Nanoarchaeum*: 3D-Struktur und Proteom. *Dissertation, University Regensburg, Germany*.

Hildenbrand, C., Stock, T., Lange, C., Rother, M., Soppa, J. (2011). Genome copy numbers and gene conversion in methanogenic archaea. *Journal of Bacteriology* **193**:734-743.

Holland, H. D. (1994). Early proterozoic atmospheric change. In *Early life on Earth. Proceedings of Nobel Symposium No. 84* (ed. Bengtson, S.) pp. 237-244. (Columbia University Press, New York).

Holland, H. D. (1999). When did the Earth's atmosphere become oxic? A reply. *The Geochemical News* **100**:20-22.

Horneck, G., Klaus, D. M., Mancinelli, R. L. (2010). Space Microbiology. *Microbiology and Molecular Biology Reviews* **74**:121-156.

Huber, H. & Stetter, K. O. (2001). Order II. *Desulfurococcales* ord. nov. In *Bergey's Manual of Systematic Bacteriology*, 2nd edition, Volume 1 (ed. Garrity, G., Boone, D. R., Castenholz, R. W.) pp. 179-180. (Springer, New York).

Huber, H., Burggraf, S., Mayer, T., Wyschkony, I., Rachel, R., Stetter, K. O. (2000). *Ignicoccus* gen. nov., a novel genus of hyperthermophilic, chemolithoautotrophic Archaea, represented by two new species, *Ignicoccus islandicus* sp. nov. and *Ignicoccus pacificus* sp. nov. *International Journal of Systematic and Evolutionary Microbiology* **50**:2093-2100.

Huber, H., Hohn, M. J., Rachel, R., Fuchs, T., Wimmer, V. C., Stetter, K. O. (2002). A new phylum of Archaea represented by a nanosized hyperthermophilic symbiont. *Nature* **417**:63-67.

Huber, H., Hohn, M. J., Rachel, R., Stetter, K. O. (2006). *Nanoarchaeota*. In *The Prokaryotes: a handbook on the Biology of Bacteria*, 3rd edition, Volume 3, *Archaea. Bacteria: Firmicutes, Actinomycetes* (ed. Dworkin, M., Falkow, S., Rosenber, E., Schleifer, K. H., Stackebrandt, E.) pp. 274-280. (Springer, New York).

Huber, H., Hohn, M. J., Stetter, K. O., Rachel, R. (2003). The phylum Nanoarchaeota: present knowledge and future perspectives of a unique form of life. *Research in Microbiology* **154**:165-171.

Huber, H., Küper, U., Daxer, S., Rachel, R. (2012). The unusual cell biology of the hyperthermophilic Crenarchaeon *Ignicoccus hospitalis*. *Antonie van Leeuwenhoek* **102**:203-219.

Hug, L. A., Baker, B. J., Anantharaman, K., Brown, C. T., Probst, A. J., Castelle, C. J., Butterfield, C. N., Hermsdorf, A. W., Amano, Y., Ise, K., Suzuki, Y., Dudek, N., Relman, D. A., Finstad, K. M., Amundson, R., Thomas, B. C., Banfield, J. F. (2016). A new view of the tree of life. *Nature Microbiology* 1:16048.

Hungate, R.E (1950). The anaerobic mesophilic cellulolytic bacteria. *Bacteriological Reviews* 14:1-49.

Hunter S. E., Jung D., Di Giulio R. T., Meyer J. N. (2010). The QPCR assay for analysis of mitochondrial DNA damage, repair, and relative copy number. *Methods* 51:444-451.

I

Isaac, L., Ware, G. C. (1974). The flexibility of bacterial cell walls. *Journal of Applied Bacteriology* 37:335-339.

J

Jacobs, K. L., Grogan, D. W. (1997). Rates of spontaneous mutation in an archaeon from geothermal environments. *Journal of Bacteriology* 179:3298-3303.

Jagger, J. (1967). Introduction to research in ultraviolet photobiology (ed. Smith, K. C.) (Prentice-Hall, Inc., Englewood Cliffs, NJ.).

Jahn, U., Gallenberger, M., Paper, W., Junglas, B., Eisenreich, W., Stetter, K. O., Rachel, R., Huber, H. (2008). *Nanoarchaeum equitans* and *Ignicoccus hospitalis*: New insights into a unique, intimate association of two archaea. *Journal of Bacteriology* 190:1743-1750.

Jahn, U., Huber, H., Eisenreich, W., Hügler, M., Fuchs, G. (2007). Insights into the autotrophic CO₂ fixation pathway of the archaeon *Ignicoccus hospitalis*: Comprehensive analysis of the central carbon metabolism. *Journal of Bacteriology* 189:4108-4119.

Jolivet, E., Matsunaga, F., Ishino, Y., Forterre, P., Prieur, D., Myllykallio, H. (2003). Physiological responses of the hyperthermophilic archaeon "*Pyrococcus abyssi*" to DNA damage caused by ionizing radiation. *Journal of Bacteriology* 185:3958-3961.

Jones, G. D. D., Boswell, T. V., Lee, J., Milligan, J. R., Wards, J. F., Weinfeld, M. (1994). A comparison of DNA damages produced under conditions of direct and indirect action of radiation. *International Journal of Radiation Biology* 66:441-445.

K

Karam, P. A., Leslie, S. A. (1999). Calculations of background beta-gamma radiation dose through geologic time. *Health Physics Society* 77:662-667.

Karam, P.A., Leslie, S. A., Anbar, A. (2001). The effects of changing atmospheric oxygen concentrations and background radiation levels on radiogenic DNA damage rates. *Health Physics Society* 81:545-553.

Kasting, J. F. (1993). Earth's early atmosphere. *Science* 259:920-926.

- Keller, L. C., Maxcy, R. B. (1984).** Effect of physiological age on radiation resistance of some bacteria that are highly radiation resistant. *Applied and Environmental Microbiology* **47**:915-918.
- Kelley, D. S., Baross, J. A., Delaney, J. R. (2002).** Volcanoes, fluids, and life at mid-ocean ridge spreading centers. *Annual Review of Earth and Planetary Science* **30**:385-491.
- Kelman, Z., White, M. F. (2005).** Archaeal DNA replication and repair. *Current Opinion in Microbiology* **8**:669-676.
- Kiefer, J. (1990).** Biological Radiation Effects. (Springer, New York, Berlin).
- Kikuchi, A., Asai, K. (1984).** Reverse gyrase-a topoisomerase which introduces positive superhelical turn into DNA. *Nature* **309**:677-681.
- Kiontke, S., Geisselbrecht, Y., Pokorny, R., Carell, T., Batschauer, A., Essen, L.-O. (2011).** Crystal structure of an archaeal class II DNA photolyase and its complex with UV-damaged duplex DNA. *The EMBO Journal* **30**:4437-4449.
- Kish, A., Gaillard, J.-C., Armengaud, J., Elie, C. (2016).** Post-translational methylation of the archaeal Mre11:Rad50 complex throughout the DNA damage response. *Molecular Microbiology* **100**:362-378.
- Kish, A., Kirkali, G., Robinson, C., Rosenblatt, R., Jaruga, P., Dizdaroglu, M., DiRuggiero, J. (2009).** Salt shield: intracellular salts provide cellular protection against ionizing radiation in the halophilic archaeon, *Halobacterium salinarum* NRC-1. *Environmental Microbiology* **11**:1066-1078.
- Klenk, H.-P., Clayton, R. A., Tomb, J.-F., White, O., Nelson, K. E., Ketchum, K. A., Dodson, R. J., Gwinn, M., Hickey, E. K., Peterson, J. D., Richardson, D. L., Kerlavage, A. R., Graham, D. E., Kyrpides, N. C., Fleischmann, R. D., Quackenbush, J., Lee, N. H., Sutton, G. G., Gill, S., Kirkness, E. F., Dougherty, B. A., McKenney, K., Adams, M. D., Loftus, B., Peterson, S., Reich, C. I., McNeil, L. K., Badger, J. H., Glodek, A., Zhou, L., Overbeek, R., Gocayne, J. D., Weidman, J. F., McDonald, L., Utterback, T., Cotton, M. D., Spriggs, T., Artiach, P., Kaine, B. P., Sykes, S. M., Sadow, P. W., D'Andrea, K. P., Bowman, C., Fujii, C., Garland, S. A., Mason, T. M., Olsen, G. J., Fraser, C. M., Smith, H. O., Woese, C. R., Venter, J. C. (1997).** The complete genome sequence of the hyperthermophilic, sulphate-reducing archaeon *Archaeoglobus fulgidus*. *Nature* **390**:364-370.
- Komori, K., Miyata, T., DiRuggiero, J., Holley-Shanks, R., Hayashi, I., Cann, I. K. O., Mayanagi, K., Shinagawa, H., Ishino, Y. (2000).** Both RadA and RadB are involved in homologous recombination in *Pyrococcus furiosus*. *The Journal of Biological Chemistry* **275**:33782-33790.
- Kottmann, M., Kish, A., Iloanusi, C., Bjork, S., DiRuggiero, J. (2005).** Physiological responses of the halophilic archaeon *Halobacterium* sp. strain NRC1 to desiccation and gamma irradiation. *Extremophiles* **9**:219-227.
- Küper, U., Meyer, C., Müller, V., Rachel, R., Huber, H. (2010).** Energized outer membrane and spatial separation of metabolic processes in the hyperthermophilic Archaeon *Ignicoccus hospitalis*. *Proceedings of the National Academy of Sciences* **107**:3152-3156.
- L**
- Lepage, E., Marguet, E., Geslin, C., Matte-Tailliez, O., Zillig, W., Forterre, P., Tailliez, P. (2004).** Molecular diversity of new *Thermococcales* isolates from a single area of hydrothermal

deep-sea vents as revealed by randomly amplified polymorphic DNA fingerprinting and 16S rRNA gene sequence analysis. *Applied and Environmental Microbiology* **70**:1277-1286.

Leuko, S., Goh, F., Ibáñez-Peral, R. Burns, B. P., Walter, M. R., Neilan, B. A. (2008). Lysis efficiency of standard DNA extraction methods for *Halococcus* spp. in an organic rich environment. *Extremophiles* **12**:301-308.

Leuko, S., Neilan, B. A., Burns, B. P., Walter, M. R., Rothschild, L. J. (2011). Molecular assessment of UVC radiation-induced DNA damage repair in the stromatolitic halophilic archaeon, *Halococcus hamelinensis*. *Journal of Photochemistry and Photobiology B: Biology* **102**:140-145.

Li, L., Mendis, N., Trigui, H., Oliver, J. D., Faucher, S. P. (2014). The importance of the viable but non-culturable state in human bacterial pathogens. *Frontiers in Microbiology* **5**:258.

Lindahl, T., Wood, R. D. (1999). Quality control by DNA repair. *Science* **286**:1897-1905.

Liu, Y., Zhou, J., Omelchenko, M. V., Beliaev, A. S., Venkateswaran, A., Stair, J., Wu, L., Thompson, D. K., Xu, D., Rogozin, I. B., Gaidamakova, E. K., Zhai, M., Makarova, K. S., Koonin, E. V., Daly, M. J. (2003). Transcriptome dynamics of *Deinococcus radiodurans* recovering from ionizing radiation. *Proceedings of the National Academy of Sciences* **100**:4191-4196.

Lleò, M. M., Pierobon, S., Tafi, M. C., Signoretto C., Canepari, P. (2000). mRNA detection by reverse transcription-PCR for monitoring viability over time in an *Enterococcus faecalis* viable but nonculturable population maintained in a laboratory microcosm. *Applied and Environmental Microbiology* **66**:4564-4567.

Lundgren, M., Malandrin, L., Eriksson, S., Huber, H., Bernander, R. (2008). Cell cycle characteristics of *Crenarchaeota*: Unity among diversity. *Journal of Bacteriology* **190**:5362-5367.

M

Mackinodan, T., James, S.J. (1990). T cell potentiation by low dose ionizing radiation: Possible mechanisms. *Health Physics* **59**:29-34

Madronich, S., McKenzie, R. L., Björn, L. O., Caldwell, M. M. (1998). Changes in biologically active ultraviolet radiation reaching the Earth's surface. *Journal of Photochemistry and Photobiology B: Biology* **46**:5-19.

Marguet, E., Forterre, P. (1994). DNA stability at temperatures typical for hyperthermophiles. *Nucleic Acids Research* **22**:1681-1686.

Margulis, L. (1971) Symbiosis and evolution. *Scientific American* **225**:48-57.

Margulis, L. (1976). Genetic and evolutionary consequences of symbiosis. *Experimental Parasitology* **39**:277-349.

Margulis, L., Walker, J. C. G., Rambler, M. (1976). Reassessment of roles of oxygen and ultraviolet light in precambrian evolution. *Nature* **264**: 620-624.

Marion, G. M., Fritsen, C. H., Eicken, H., Payne, M. C. (2003). The search for life on Europa: Limiting environmental factors, potential habitats, and Earth analogues. *Astrobiology* **3**:785-811.

Martin, W., Baross, J., Kelley, D., Russell, M. J. (2008). Hydrothermal vents and the origin of life. *Nature Review Microbiology* **6**:805-814.

- Mattimore, V., Battista, J. R. (1996).** Radioresistance of *Deinococcus radiodurans*: Functions necessary to survive ionizing radiation are also necessary to survive prolonged desiccation. *Journal of Bacteriology* **178**:633-637.
- McCollom, T. M., Shock, E. L. (1997).** Geochemical constraints on chemolithoautotrophic metabolism by microorganisms in seafloor hydrothermal systems. *Geochimica et Cosmochimica Acta* **61**:4375-4391.
- McCready, S., Müller, J. A., Boubriak, I., Berquist, B. R., Ng, W. L., DasSarma, S. (2005).** UV irradiation induces homologous recombination genes in the model archaeon, *Halobacterium* sp. NRC-1. *Saline Systems* **1**:3.
- Mewaldt, R. A. (1994).** Galactic cosmic ray composition and energy spectra. *Advances in Space Research* **14**:737-747.
- Michaels, H. B., Hunt, J. W. (1978).** A model for radiation damage in cells by direct effect and by indirect effect: A radiation chemistry approach. *Radiation Research* **74**:23-34.
- Miller, S. L., Lazcano, A. (1995).** The origin of life-did it occur at high temperatures? *Journal of Molecular Evolution* **41**:689-692.
- Miller, T. L., Wolin, M. J. (1974).** A serum bottle modification of the Hungate technique for cultivating obligate anaerobes. *Applied Microbiology* **27**:985-987.
- Moissl-Eichinger, C. (2011).** Archaea in artificial environments: Their presence in global spacecraft clean rooms and impact on planetary protection. *The ISME Journal* **5**:209-219.
- Möller, R., Reitz, G., Berger, T., Okayasu, R., Nicholson, W. L., Horneck, G. (2010).** Astrobiological aspects of the mutagenesis of cosmic radiation on bacterial spores. *Astrobiology* **10**:509-521.
- Möller, R., Stackebrandt, E., Reitz, G., Berger, T., Rettberg, P., Doherty, A. J., Horneck, G., Nicholson, W. L. (2007).** Role of DNA repair by nonhomologous-end joining in *Bacillus subtilis* spore resistance to extreme dryness, mono- and polychromatic UV, and ionizing radiation. *Journal of Bacteriology* **189**:3306-3311.
- Morowitz, H. J. (1950).** Absorption effects in volume irradiation of microorganisms. *Science* **111**:229-230.
- N**
- Napoli, A., Valenti, A., Salerno, V., Nadal, M., Garniers, F., Rossi, M., Ciaramella, M. (2004).** Reverse gyrase recruitment to DNA after UV light irradiation in *Sulfolobus solfataricus*. *The Journal of Biological Chemistry* **279**:33192-33198.
- Näther, D. J., Rachel, R. (2004).** The outer membrane of the hyperthermophilic archaeon *Ignicoccus*: dynamics, ultrastructure and composition. *Biochemical Society Transactions* **32**:199-203.
- Newcombe, D. A., Schuerger, A. C., Benardini, J. N., Dickinson, D., Tanner, R., Venkateswaran, K. (2005).** Survival of spacecraft-associated microorganisms under simulated martian UV irradiation. *Applied and Environmental Microbiology* **71**:8147-8156.
- Nisbet, E. (2000).** The realms of archaean life. *Nature* **405**:625-626.

Nisbet, E. G., Sleep N. H. (2001). The habitat and nature of early life. *Nature* **409**:1083-1091.

O

Oberle C., Blattner, C. (2010). Regulation of the DNA damage response to DSBs by post-translational modifications. *Current Genomics* **11**:184-198.

Oliver, J. D. (1993). Formation of viable but nonculturable cells. In *Starvation in bacteria* (ed. Kjelleberg, S.) pp. 239-272. (Plenum Press, New York, N. Y.).

Oliver, J. D. (2000). The public health significance of viable but nonculturable bacteria. In *Nonculturable Microorganisms in the Environment* (ed. Colwell, R.R., Grimes, D.J.) pp. 277-299. (ASM Press, Washington DC).

P

Pace, N. R. (1991). Origin of life-facing up to the physical setting. *Cell* **65**:531-533.

Pagé, A., Tivey, M. K., Stakes, D. S., Reysenbach, A-L. (2008). Temporal and spatial archaeal colonization of hydrothermal vent deposits. *Environmental Microbiology* **10**:874-884.

Paper, W., Jahn, U., Hohn, M. J., Kronner, M., Näther, D. J., Burghardt, T., Rachel, R., Stetter, K. O., Huber, H. (2007). *Ignicoccus hospitalis* sp. nov., the host of '*Nanoarchaeum equitans*'. *International Journal of Systematic and Evolutionary Microbiology* **57**:803-808.

Pfeifer, G. P. (1997). Formation and processing of UV photoproducts: Effects of DNA sequence and chromatin environment. *Photochemistry and Photobiology* **65**:270-283.

Pinto, F. L., Thapper, A., Sontheim, W., Lindblad, P. (2009). Analysis of current and alternative phenol based RNA extraction methodologies for cyanobacteria. *BMC Molecular Biology* **10**:79.

Pley, U., Schipka, J., Gambacorta, A., Jannasch, H. W., Fricke, H., Rachel, R. & Stetter, K. O. (1991). *Pyrodictium abyssi* sp. nov. represents a novel heterotrophic marine archaeal hyperthermophile growing at 110°C. *Systematic and Applied Microbiology* **14**:245-253.

Powell, C. F. (1959). The study of elementary particles by the photographic method: an account of the principal techniques and discoveries, illustrated by an atlas of photomicrographs (ed. Fowler, P. H., Perkins, D. H.). (Pergamon Press, London, New York).

R

Rachel, R., Meyer, C., Klingl, A., Gürster, S., Heimerl, T., Wasserburger, N., Burghardt, T., Küper, U., Bellack, A., Schopf, S., Wirth, R., Huber, H., Wanner, G. (2010). Analysis of the ultrastructure of Archaea by electron microscopy. *Methods in Cell Biology* **96**:47-69.

Rachel, R., Wyschkony, I., Riehl, S., Huber, H. (2002). The ultrastructure of *Ignicoccus*: Evidence for a novel outer membrane and for intracellular vesicle budding in an archaeon. *Archaea* **1**:9-18.

Radonić, A., Thulke, S., Mackay, I. M., Landt, O., Siegert, W., Nitsche, A. (2004). Guideline to reference gene selection for quantitative real-time PCR. *Biochemical and Biophysical Research Communications* **313**:856-862.

Rasmussen, B. (2000). Filamentous microfossils in a 3,235-million-year-old volcanogenic massive sulphide deposit. *Nature* **405**:676-679.

Rastogi, R. P., Richa, Kumar, A., Tyagi, M. B., Sinha, R. P. (2010). Molecular mechanisms of ultraviolet radiation-induced DNA damage repair. *Journal of Nucleic acids* **2010**:592980.

Reich, C. I., McNeil, L. K., Brace, J. L., Brucker, J. K., Olsen, G. J. (2001). Archaeal RecA homologues: different response to DANN-damaging agents in mesophilic and thermophilic archaea. *Extremophiles* **5**:265-275.

Riesenman, P. J., Nicholson, W. L. (2000). Role of the spore coat layers in *Bacillus subtilis* spore resistance to hydrogen peroxide, artificial UV-C, UV-B, and solar UV radiation. *Applied and Environmental Microbiology* **66**:620-626.

Riley, P. A. (1994). Free radicals in biology: oxidative stress and the effects of ionizing radiation. *International Journal of Radiation Biology* **65**:27-33.

Rolfsmeier, M. L., Laughery, M. F., Haseltine, C. A. (2010). Repair of DNA double-strand breaks following UV damage in three *Sulfolobus solfataricus* strains. *Journal of Bacteriology* **192**:4954-4962.

Rolfsmeier, M. L., Laughery, M. F., Haseltine, C. A. (2011). Repair of DNA double-strand breaks by ionizing radiation damage correlates with upregulation of homologous recombination genes in *Sulfolobus solfataricus*. *Journal of Molecular Biology* **414**:485-498.

Rupert, C. S., Goodgal, S. H., Herriott, R. M. (1958). Photoreactivation in vitro of ultraviolet inactivated hemophilus influenzae transforming factor. *Journal of General Physiology* **41**:451-471.

S

Sage, E. (1993). Distributions and repair of photolesions in DNA: Genetic consequences and the role of sequence context. *Photochemistry and Photobiology* **57**:163-174.

Sakofsky, C. J., Runck, L. A., Grogan, D. W. (2011). *Sulfolobus* mutants, generated via PCR products, which lack putative enzymes of UV photoproduct repair. *Archaea* **2011**:864015.

Sancar, A. (1996). DNA excision repair. *Annual Reviews of Biochemistry* **65**:43-81.

Sancar, A. (2003). Structure and function of DNA photolyase and cryptochrome blue-light photoreceptors. *Chemical Reviews* **103**:2203-2237.

Sancar, A., Franklin, K. A., Sancar, G. B. (1984). *Escherichia coli* DNA photolyase stimulates uvrABC excision nuclease *in vitro*. *Proceedings of the National Academy of Sciences USA* **81**:7397-7401.

Saran, M., Bors, W. (1997). Radiation chemistry of physiological saline reinvestigated: Evidence that chloride-derived intermediates play a key role in cytotoxicity. *Radiation Research* **147**:70-77.

Schrenk, M. O., Kelley, D. S., Delaney, J. R., Baross, J. A. (2003). Incidence and diversity of microorganisms within the walls of an active deep-sea sulfide chimney. *Applied and Environmental Microbiology* **69**:3580-3592.

Seager, S., Bains, W., Petkowski, J. J. (2016). Towards a list of molecules as potential biosignature gases for the search for life on exoplanets and applications to terrestrial biochemistry. *Astrobiology* **16**:1-21.

Seitz, E. M., Haseltine, C. A., Kowalczykowski, S. C. (2001). DNA recombination and repair in archaea. *Advances in Applied Microbiology* **50**:101-169.

Sessions, A. L., Doughty, D. M., Welander, P. V., Summons, R. E., Newman, D. K. (2009). The continuing puzzle of the Great Oxidation Event. *Current Biology* **19**:R567-R574.

Sinha, R. P., Häder, D.-P. (2002). UV-induced DNA damage and repair: a review. *Photochemical and Photobiological Sciences* **1**:225-236.

Sleep, N. H., (2010). The hadean-archaeon environment. *Cold Spring Harbor Perspectives in Biology* **2**:a002527.

Sofia, H. J., Chen, G., Hetzler, B. G., Reyes-Spindola, J. F., Miller, N. E. (2001). Radical SAM, a novel protein superfamily linking unresolved steps in familiar biosynthetic pathways with radical mechanisms: functional characterization using new analysis and information visualization methods. *Nucleic Acids Research* **29**:1097-1106.

Spaans, S. K., van der Oost, J., Kengen, S. W. M. (2015). The chromosome copy number of the hyperthermophilic archaeon *Thermococcus kodakarensis* KOD1. *Extremophiles* **19**:741-750.

Spang, A., Saw, J. H., Jørgensen, S. L., Zaremba-Niedzwiedzka, K., Martijn, J., Lind, A. E., van Eijk, R., Schleper, C., Guy, L., Ettema, T. J. G. (2015). Complex archaea that bridge the gap between prokaryotes and eukaryotes. *Nature* **521**:173-179.

Stetter, K. O. (1988). *Archaeoglobus fulgidus* gen. nov.: a new taxon of extremely thermophilic archaeobacteria. *Systematic and Applied Microbiology* **10**:172-173.

Stetter, K. O. (1996). Hyperthermophiles in the history of life. In *Evolution of Hydrothermal Ecosystems on Earth (and Mars?)* (ed. Bock, G. R., Goode, J. A.) pp. 1-18. (CIBA Foundation Symposium 202) (Wiley, Chichester).

Stetter, K. O. (2006). Hyperthermophiles in the history life. *Philosophical Transactions of the Royal Society B: Biology* **361**:1837-1843.

Stetter, K. O., Fiala, G., Huber, G., Huber, R., Segerer, A. (1990). Hyperthermophilic microorganisms. *FEMS Microbiology Reviews* **75**:117-124.

Stetter, K. O., König, H. & Stackebrandt, E. (1983). *Pyrodictium* gen. nov., a new genus of submarine disc-shaped sulphur reducing archaeobacteria growing optimally at 105°C. *Systematic and Applied Microbiology* **4**:535-551.

T

Taghipour, F. (2004). Ultraviolet and ionizing radiation for microorganism inactivation. *Water Research* **38**:3940-3948.

Tapias, A., Leplat, C., Confalonieri, F. (2009). Recovery of ionizing-radiation damage after high doses of gamma ray in the hyperthermophilic archaeon *Thermococcus gammatolerans*. *Extremophiles* **13**:333-343.

Tillett D., Neilan B. A. (2000). Xanthogenate nucleic acid isolation from cultured and environmental cyanobacteria. *Journal of Phycology* **36**:254-258.

V

Von Damm, K. L. (online 2013). Controls on the chemistry and temporal variability of seafloor hydrothermal fluids. In *Seafloor Hydrothermal Systems- physical, chemical, biological, and geological interactions* (ed. Humphris, S. E., Zierenberg, R. A., Mullineaux, L. S., Thomson, R. E.) pp. 222-247. (American Geophysical Union, Washington DC, 1995).

Von Damm, K. L., Lilley, M. D., Shanks III, W. C., Brockington, M., Bray, A. M., O'Grady, K. M., Olson, E., Graham, A., Proskurowski, G. (2003). Extraordinary phase separation and segregation in vent fluids from the southern East Pacific Rise. *Earth and Planetary Science Letters* **206**:265-378.

W

Wang, Y., Hammes, F., Boon, N., Egli, T. (2007). Quantification of the filterability of freshwater bacteria through 0.45, 0.22, and 0.1 µm pore size filters and shape-dependent enrichment of filterable bacterial communities. *Environmental Science and Technology* **41**:7080-7086.

Wang, Y., Hammes, F., Düggelin, M., Egli, T. (2008). Influence of size, shape, and flexibility on bacterial passage through micropore membrane filters. *Environmental Science and Technology* **42**:6749-6754.

Waters, E., Hohn, M. J., Ahel, I., Graham, D. E., Adams, M. D., Barnstead, M., Beeson, K. Y., Bibbs, L., Bolanos, R., Keller, M., Kretz, K., Lin, X., Mathur, E., Ni, J., Podar, M., Richardson, T., Sutton, G. G., Simon, M., Söll, D., Stetter, K. O., Short, J. M., Noordewier, M. (2003). The genome of *Nanoarchaeum equitans*: Insights into early archaeal evolution and derived parasitism. *Proceedings of the National Academy of Sciences* **100**:12984-12988.

Webb, K. M., DiRuggiero, J. (2012). Role of Mn²⁺ and compatible solutes in the radiation resistance of thermophilic bacteria and archaea. *Archaea* **2012**:845756.

Whelan, J. A., Russel, N. B., Whelan, M. A. (2003). A method for the absolute quantification of cDNA using real-time PCR. *Journal of Immunological Methods* **278**:261-269.

Whitehead, K., Kish, A., Pan, M., Kaur, A., Reiss, D. J., King, N., Hohmann, L., DiRuggiero, J., Baliga, N. S. (2006). An integrated systems approach for understanding cellular response to gamma radiation. *Molecular Systems Biology* **2**:47.

Whitesides, M. D., Oliver J. D. (1997). Resuscitation of *Vibrio vulnificus* from the viable but nonculturable state. *Applied and Environmental Microbiology*. **63**:1002-1005.

Williams, E., Lowe, T. M., Savas, J., DiRuggiero, J. (2007). Microarray analysis of the hyperthermophilic archaeon *Pyrococcus furiosus* exposed to gamma irradiation. *Extremophiles* **11**:19-29.

Woese, C. R. (1987). Bacterial evolution. *Microbiological Reviews* **51**:221-271.

Woese, C. R. (1998). The universal ancestor. *Proceedings of the National Academy of Sciences* **95**:6854-6859.

Woese, C. R., Fox, G. E. (1977). The concept of cellular evolution. *Journal of Molecular Evolution* **10**:1-6.

Woese, C. R., Kandler, O., Wheelis, M. L. (1990). Towards a natural system of organisms: Proposal for the domains archaea, bacteria, eucarya. *Proceedings of the National Academy of Sciences* **87**:4576-4579.

Woese, C. R., Magrum, L. J., Fox, G. E. (1978). Archaeobacteria. *Journal of Molecular Evolution* **11**:245-252.

Wood, E. R., Ghané, F., Grogan, D. W. (1997). Genetic response of the thermophilic archaeon *Sulfolobus acidocaldarius* to short-wavelength UV light. *Journal of Bacteriology* **179**:5693-5698.

X

Xu, H-S, Roberts, N., Singleton, F. L., Attwell, R. W., Grimes, D. J. (1982). Survival and viability of nonculturable *Escherichia coli* and *Vibrio cholera* in the estuarine and marine environment. *Microbial Ecology* **8**:313-323.

Y

Yoon, J.-H., Lee, C.-S., O'Connor, T. R., Yasui, A., Pfeifer, G. P. (2000). The DNA damage spectrum produced by simulated sunlight. *Journal of Molecular Biology* **299**:681-693.

Young, K. D. (2006). The selective value of bacterial shape. *Microbiology and Molecular Biology Reviews* **70**:660-703.

Z

Zuckerkandl, E., Pauling, L. (1965). Molecules as documents of evolutionary history. *Journal of Theoretical Biology* **8**:357-366.

7 Appendix

Primer design

➤ qRT-PCR primers specific for potential housekeeping genes

16S rRNA

IGNI_RS04235 16S ribosomal RNA [*Ignicoccus hospitalis* KIN4/I]

Gene ID: 5562932, updated on 20-Aug-2015

Gene symbol: IGNI_RS04235
 Gene description: 16S ribosomal RNA
 Locus tag: IGNI_RS04235
 Sequence: NC_009776.1 (728379..729800)

Showing 1.42kb region from base 728379 to 729800.

Ignicoccus hospitalis KIN4/I, complete genome

NCBI Reference Sequence: NC_009776.1

```
>gi|156936795:728379-729800 Ignicoccus hospitalis KIN4/I, complete genome
CGGACCCGACCGCTATCGGGGTAAGGCTAAGCCATGGGAGTCGAACGCCCGCCGCCGCGGGCGTGCGGGA
CGGCTGAGTAACACGTGGCTAACCTACCCTCGGGAGGGGGATAACACCGGGAAACTGGTGCTAATCCCCC
ATAGGGGCGGAGGCCTGGAAGGGTTCCGCCCCGAAAGGGGCTCGGGGGGAACGCCCCGAGTCCGCCCCGA
GGATGGGGCCGCGCCCCATCAGGTAGTTGGCGGGGTAATGGCCCCGCAAGCCGAAGACGGGTAGGGGCCG
TGGGAGCGGGAGCCCCAGATGGGCACTGAGACAAGGGCCCAGGCCCTACGGGGCGCACCAGGCGCGAAA
ACTCCGCAATGCGGGCAACCGTGACGGGGTTACCCCGAGTGCCCCCTCTCCGGGGGCTTTTCCCCGCTGT
AAACAGGCGGGGGTAATAAGCGGGGGCAAGTCTGGTGTGACGCCCGCGGTAATACCAGCCCCGCGAGT
GGTCGGGACGATTATTGGGCCTAAAGCGCCCGTAGCCGGCCTGGTGGCCCCCTCCTAAAGCCCCGGGCT
CAACCCGGGGACTGGAGGGGGTAGCGCCAGGCTAGGGGGCGGGAGAGGCCGAGGGTACTCCCGGGGTAGG
GGCGAAATCCGATAATCCCGGGAGGACCGCCAGTGGCGAAGGCGCTCGGCTGGAACGCGCCCGACGGTGA
GGGGCGAAAGCCGGGGGAGCAAACCGGATTAGATAACCCGGTAGTCCCGGCTGTAAACGATGCGGGCTAG
GTGTTGGGCGGGCTTCGAGCCCCGCCAGTGCCGCAAGGAAGCCGTTAAGCCCGCCGCTGGGGAGTACGG
CCGCAAGGCTGAACTTAAAGGAATTGGCGGGGAGCACCACAAGGGGTGGAGCCTGCGGCTTAATTGGA
GTCAACGCCGGAACCTTACCGGGGGCGACAGCAGGATGAAGGTGAGGCTGAAGACCTTACCTGACGCGC
TGAGAGGAGGTGCATGGCCGTCGCCAGCTCGTGCCGTGAGGTGTCCGGTTAAGTCCGGCAACGAGCGAGA
CCCCCGTCCCCAGTTGCTACCCGGGGCTCCGGCCCCGGGGCACACTGGGGAGACTGCCGCCGTATAAGGC
GGAGGAAGGAGGGGGCTATGGCAGGTGAGCATGCCCCGAAACCCCCGGGCTGCACGCGGGCTACAATGGC
GGGGACAGCGGGTTGCGACCCCCGAAAGGGGGAGCCAATCCCTGAAACCCCCGCGAGGTTGGGATCGAGGG
CTGCAACTCGCCCTCGTGAACGCGGAATCCCTAGTAACCGCGCGTTAGCATCGCGCGGTGAACACGTCCC
TGCTCCTTGACACACACCGCCCGTCGCTCCACCCGAGGGGGGAGAAGTCGTAACAAGGTAGCCGTAGGGGA
ACCTGCGGCTGGATCACCTCCC
```

Mips**IGNI_RS04495 myo-inositol-1-phosphate synthase [Ignicoccus hospitalis KIN4/I]**

Gene ID: 5562327, updated on 23-Aug-2015

Gene symbol: IGNI_RS04495
 Gene description: myo-inositol-1-phosphate synthase
 Locus tag: IGNI_RS04495
 Sequence: NC_009776.1 (771144..772307, complement)

NCBI Reference Sequence: NC_009776.1

>gi|156936795:c772307-771144 Ignicoccus hospitalis KIN4/I, complete genome

TTGATAAGGGTCGCTGTGGTGGGTGCCGGAAGTTCGAGGAGCCACTACGCGGCAGGCCTCCAGAGGTAA
 AAAGGGCCGAAATCGAGCCCTACGGGGTCCCCCTGGCCAAGTTCAGGTAATAAAAGACTACGTAGAGGA
 GGAGGTGGTCTCCGCGTACGACGTAGACGCCAACAGGTGGGAAAGCCCCCTCTCTGAGGTAGTGAAGAGG
 CAGCTGGAAGGAGTTGTCCCGGTGCCCCCGGACGTCCCCGACTTCGAGGTCAGGGAAGGGGTCTCGCCT
 CCTCCGGGGCCGGAAGTGTTCCTCCGTAAGGGGGAGGGATCAGAAGCTCCCCTTAAAGGAAGC
 CGTAGAAGAGATAGCGAAGGAGTTTAAGAGTGACAACGTCAACGTGGTTTTGAACTTGATCTCCACCGAG
 CCCGCGGAGCCCTTCGGGGACGAGGGGAAGCTCGCAAAGGCCTTGAGAGGGGCGAGGTGAGCGCCGGCC
 AAGCCTACGCGTTTGCAGCTTACTTGCCGCCAAAGACTCCGGCAAGCCAGTGGCGTTCATAAACTTAAT
 ACCCACGCCCTTGCCCAATGACCCGGCCTTCGTCAAACCTTTACGAAGACGCTAACTCCCTCGTACTGGGG
 GACGACGGGGCCACCGGGGTACGCCGCTGACCGCAGACTTGTGGAGCACCTAGCGGAGAGGAACAGAA
 AGGTCCGGTACATCGTCCAGTTCAACATAGGTGGCAACACCGACTTCTTAGCGTTGACTATACCTGAGAG
 GAACTTGATGAAGGAGAAGACGAAGTCCAGCGTGGTGGAAAGATATCCTAGGCTACGACGCCCCCCTAC
 ATAAAGCCGACGGGCTACGTGGAAGCTATAGGGGACAGGAAGTTCGTAGCTATGGACATAGAGTGGATAA
 CCTTCAACGGCTTGGTGGACGAACCTATAGTTAACATGAGGATTAATGACTCGCCCCGCGTTGGCGGGCCT
 CGCCGTGGACTTGGTCAGGCTTGCTGCGGCTCTGCTAGAAAAGGGCGTTAAGGGCACATTCTACGACGTC
 AACGCCTTCTTCATGAAGAACCCTGGTCCGAAGGAGGCTAGGAACAAAGCTAGAATAAAGGCGTACTATG
 ACATGATCTCGGCCCTGAGGGAGCTCGGGGTAATAGTCGAGTGA

Thermosome**IGNI_RS00515 thermosome subunit [Ignicoccus hospitalis KIN4/I]**

Gene ID: 5563019, updated on 23-Aug-2015

Gene symbol: IGNI_RS00515
 Gene description: thermosome subunit
 Locus tag: IGNI_RS00515
 Sequence: NC_009776.1 (89714..91390)

NCBI Reference Sequence: NC_009776.1

>gi|156936795:89714-91390 Ignicoccus hospitalis KIN4/I, complete genome
 ATGGCGCCGGTGTACCGGTTCTGATACTCAAGGAGGGCGCCACCAGGACCTACGGCAGGGAGGCTCTGA
 GGAGCAACATACTAGCCGCTAGGATAATTGCCGAAGCGTTGAAGACCAGCTTGGGTCCCAGAGGAATGGA
 CAAGATGATAGTTGACGCCTTCGGAGACATCACTGTAACCAACGACGGTGTAAACCATACTCAAGGAGATG
 GACGTCCAGCACCCCTGCCGCCAAGTTGATCGTGGAGACCGCCAAGGCTCAAGATGCGGAGGTGGGCGACG
 GCACTACCAGCGTCGTCGTTGGCCGGCAGCTTGCTGGAAGAGGCCGAGCCCCCTGCTCGACCAGAACAT
 CCACCCAGCATAATAATCGAAGGATACAAGAAGGCGATGGAGAAGGCTCTAGAGGAGCTCAGCAACATA

GCCGTTAAGATAAACCCCAAGGACAAGGAGTATATGAGGAAGCTAGTATACACCACCTCAGCAGCAAGT
 TCGTCGGCCAGGAGGCCGAGGAGATAAGGAACAAGCTGCTAGACATGATAATCGAGGCCGCTACACCGT
 GGCCGTCGAGCAGCCTGACGGCACTCTGAGGATGAGCCTCGACGACATAAAGATAGAAAAGAAGAGGC
 GGAAGCTTGCTCGACAGCCAGCTGGTAAAGGGCATAGTGCTGGACAAGGAAGTGGTCCACCCGGGCATGC
 CGAAGAGGGTGGAGAACGCGAAGATACTGGTCCTCGACGCCCCGCTGGAGGTCGAGAAGCCCCGACATAAC
 TGCCAAGATAAACATAACTGACCCAGGCAGATAGAGGCGTTCTTGAGGAGCAGACCAAGATACTCAAG
 GAGATGGTAGACAAGATCGCCGAGACCGGCCAACGTAAGTATGATAACTCAGAAGGGCATCGACGACGTCG
 CCGCTCACTTCTTGCGAAGAAGGGCATAATGGCCGTTAGGAGGGTGAAGAGGAGCGACATAGAGAAGGT
 GGCCAAGGCTACCGGAGCCAAGGTGGTGACCAGCATAAAGGACGTGAGCCCCGAGGTGTTGGGCGAGGCC
 AAGCTAGTGAGGAGAGGAGGGTAGGCAAGGACAAGATGGTCTTCATCGAGGGCGCCAAGAACCCGAGGG
 CGGTACCATACTGCTGAGGGGTGCCAGCGACATGGCGCTGGACGAGGCTGAGAAGAACATAACCGACGC
 TCTCCACGTGCTGAGGAACATATTCATGAAGCCCATGATAGTGGGCGGCGGAGGGGCGGTGGAGGTAGAG
 CTCGCCGAGCGCTTGAGGAAGTTCGCTTCCACCGTGGGCGGCAAGGAGCAGCTGGCGATAGAGGCTTACG
 CCGAGGCACTCGAAGAGATACCGGTAGTGTTGGCCGACACCGCGGTATGGACACCCTCGAAGCGCTCAT
 GGAAGTGAAGGAGCTCCACAGGGAAGGCAAGATCTGGGCTGGCGTCAACGTAGTCGAGGGCAAGATAGAG
 GAGGACATGACCAAGCTCGGAGTAGTGAGGCGGTGAGGGTGAAGGAGCAAGTGCTCAAGAGCGCCACCG
 AGGCAGCTAACGCCTTGCTGAAGATCGACGACGTGATTGCGGCCGCCCGCCGAAGGAGGGCAAGAAGGG
 CAAGAAGGAAGAGGGCGGAGAGGAGGAAGAGGAAGGCGGCTCCAGCAAGTTCGGAAGCGAGTTCTAA

znuC

IGNI_RS00620 hypothetical protein [*Ignicoccus hospitalis* KIN4/I]

Gene ID: 5561999, updated on 12-Dec-2015

Gene symbol: IGNI_RS00620
 Gene description: hypothetical protein
 Locus tag: IGNI_RS00620
 Sequence: NC_009776.1 (107253..108068, complement)

NCBI Reference Sequence: NC_009776.1

>gi|156936795:c107996-107253 *Ignicoccus hospitalis* KIN4/I, complete genome

GTGAAGTACGGAGACACGTACGCGCTCGAAGGGGTGACGCTAGACGTACCCAAGGGGGACTTCCTAGCGA
 TCATGGGGCCTAACGGGGCCGGGAAGAGCACGCTCTTGAAACAATCCTAGGCTTGCCCCCCTAGTGAG
 GGGAAGCGTCAGAGTTTTTGGAAAGGACCCCTACAAGCAGAGGAGCGAAATTGCGAAGAAGATCGGCTAC
 GTCCCGCAGAGGGAGAACGTCAACGACGAGGTCCCTTAAGGGCGATAGACGTAGTGATGATGGGCCTCA
 TAGAGGGCATGAGGCCACAGAGGGAGGAAGCCCTCATGGACAAAGCCTTGAAAGCTTTAGAGGAAGTAGG
 TCTTGTGGACGTAGCATAACAAGACCTATAGGGAGCTGTCCGAGGACAAAAGCAGAGGGGTGCTGATAGCG
 AGAGCCATAGTCTCTAAACCCGAGCTCTTGCTCTTGGACGAACCCTTCTCCGCGCTCGACGCGCAGAGCT
 CAAGGACCGTCGCCCCACTCTTGAAGAAGTATAATGATGAGGGGACTACTATAATTCTAGTAACACGA
 CATCACACCTATCGAAACGACGTAAAGAGGGTAGCGTTATTGAATAAGAAGCTAATAGCCGTGGGCGAG
 CCTTTAAAGATATTCACTAAAGAGAACTTGTGAAAACCTACGGGGTAGAGGTCCCGGTGCTCGTGCAAG
 GAAGACTCTGCATACCGCTGATAGGTGATCAACATGGACGTTAG

pol E'**IGNI_RS00455 DNA-directed RNA polymerase subunit E' [Ignicoccus hospitalis KIN4/I]**

Gene ID: 5562132, updated on 23-Aug-2015

Gene symbol: IGNI_RS00455
 Gene description: DNA-directed RNA polymerase subunit E'
 Locus tag: IGNI_RS00455
 Sequence: NC_009776.1 (81589..82122, complement)

NCBI Reference Sequence: NC_009776.1

```
>gi|156936795:c82122-81589 Ignicoccus hospitalis KIN4/I, complete genome
TTGTACAGGATCTACCGCTTCAAAGACATGGTTAGAATACCGCCCCGAGAGGTTTCGGCGAGGACTTGAAGA
AGGTCGCTCTCGAACTCCTCAGGGAGGAGTACGAGGGCGTGATAGACGAGGAGCTCGGCATAATTCTGAC
AGTAACTGACGTGGACATCTCCCCGAGGGCTACATAGTGCCGGGCGACGGAGGCACCTACCACGAGGCC
ACCTTCACTTTGCTCGCCTTCAAGCCCTTGAGGAACGAGGTAGTTGAGGGCATAGTAGTTAACGTTACCA
AGAACGGGATATACGTTAACTAGGCCCCATAGACGGTATGGTGCACAAGGCCAGCTCGGCGACGAGCG
TTTCGAGTACGACCGCGACCGGGAGCATGGTAGGCACCAGCACGAAAACGGTCATAAAGAGGGGAGAC
CTCGTTAGGGCTAGGATAGTACAGATTTGACACCAGGAGGGGCCTCAAGGTGGGTATGAGTATGAAAGGCC
CGTACTTGGGTAAAATTAAGGACGCGGAGGAGGTCAAGCAATGA
```

➤ **qRT-PCR primers specific for genes involved in DNA repair****rad2****IGNI_RS03580 endonuclease [Ignicoccus hospitalis KIN4/I]**

Gene ID: 5562892, updated on 23-Aug-2015

Gene symbol: IGNI_RS03580
 Gene description: endonuclease
 Locus tag: IGNI_RS03580
 Sequence: NC_009776.1 (624002..625054, complement)

NCBI Reference Sequence: NC_009776.1

```
>gi|156936795:c625054-624002 Ignicoccus hospitalis KIN4/I, complete
genome
TTGGGCGTTACAGCCCTAAGGGAACATCCCCAGCAAGTGCAAGAAGACCTTAGAGCTAAAGTCCTTGT
CGAACAAGAGCGTGCCCTCGACGCTTACAACACCTTGTATCAGTTCTTAGCTGCCATAAGGGGCGAAGA
CGGCAGGCCCCCTCATGGAATCCAAAGGGCGCGTGACCAGCCACCTCTCCGACTTTTCTACAGAACAATC
AACATGTTGGAAAACGGAATAAAGGTAGCCTACGTCTTCGACGGCGCCCCCTCCAAGCTCAAGACGCGCG
AGATAGAGAGGAGGCAGAACTCAAGCAAGAGGCCGAGAAGAAGTACGAGGAGGCAGTTAGGAGGGGGGA
CGTCGAGGAAGCTAGGAAGTACGCCAGATGAGCGCAAAGCTGACGAAGGAGATGGTAGAAGAAGCTAAG
AGGTTGCTCGAGGCTATGGGGGTCCCGTGCGGTACAAGCCCCAGCGAGGGAGAGGCCCAAGCGGCCTACA
TGGCCGCTAAGGGAGACGTCTGGGCGTCTGCTAGTCAAGATTACGACTCCTTGCTCTTCGGCTCTCTCG
CTTGGTTAGGAACTTGGCCGTGAGTGGGCGCAGGAAGCTCCCTAACAAGAAGCTGTACGTCAAGTGAAG
CCCGAGGAAATAACTTTGAAGTGTGTGCTGGAGGAGTTGGGCATAACCCGAGAGCAGCTCGTTGCAATAG
CCGTCTTGATAGGGACCGACTACACGCCCGGGGTGAAGGGCGTCGGGCCGAAGACCGCCTTAAGGTACGT
GAAGAGCTATGGTGACTTAGAGAGGGTGCTTACTGCCCTAGGCGTCGATGACAAGGAGTTGTACTTGGAG
GCGTATAATTTCTTCTTGAACCCCCAGGTGACCGACGACTACGAGCTCGTGTGGAGGAGGCCCGACCCCC
```

AAAAGATAATTGAAATCCTAGTGTACGAACACGACTTCAACGAGGAGCGCGTGAGAAAAGGCGATAGAGCG
CTTAATGAAGGCCTGGAAGGAAAAGCTCAGCACTAAGCAGAGCACGTTGGACATGTTCTTTAAAAAGCGT
TGA

rad50

IGNI_RS07180 hypothetical protein [*Ignicoccus hospitalis* KIN4/I]

Gene ID: 5562064, updated on 12-Dec-2015

Gene symbol: IGNI_RS07180
Gene description: hypothetical protein
Locus tag: IGNI_RS07180
Sequence: NC_009776.1 (1245174..1247795)

NCBI Reference Sequence: NC_009776.1

>gi|156936795:1245174-1247795 *Ignicoccus hospitalis* KIN4/I, complete genome

TTGAAGCTAGAGTTAAGAACTTCCTTTTCGTACGAGAACTTAGAAGTGCGCATACCGGAAGGCGTGGTAG
TCGTAGTGGGTCCCAACGGCGCTGGTAAGAGCAGCTTTGTGGACGCCATAGCCTACGCCCTGACGAGCGC
CGCGGTGAGCCGAAAGGTCACCAACAAGGAGCTGATTAATTACGGCGCCAAGAGCGCCGAGGTGGTCCCTT
ACCTTCTCCGCGTCAAATAAGGTATACGAAGTGAAGAGGGCTATAGGAGTTGGAACTCTGTACAAGCCG
TCCTAAAGGAGGGCGGCAAACTATACGCCTCGGGCTCTCAAGCCGTAAACAAAGCCATAGCTTCCTTATT
GGGATTTCGAGACGTCAAAGCGCTGCGTGAAACCGTCTTCGTACCCAGGGAAAATTGACGAGTTGGTG
GAGTTGAGTCCTTCGGAATTGAAGAACAAGGTTCTAGAGTTGCTGGGAGTTAGAGACAAGGAAGCCGTCG
AAGCTTCTCTGAGAGAAATAATAAACTACTATAAGGGCACCGCATCCAACCTTGGTGAACGTTCAAAGGAC
GTATGAAAAGTATAAGAAAGAGTTGAATAGCGAAATGAACAGGATAAAGGAATTACAAGAGAAGCTGCCG
TTGCTCAAGGAAGAGCTCCGCATGGTCGAGGACAACTGAACGACTTAAGGTCTGAACTTAACGAGCTTA
AAGAGAAGAAGGCCAAATACCAAAGGTTAAGGCCCACTAATGAAAGTCCAAGAGGAGTTGAGGACGCT
AATTGGAGAACTTGAAGCTCTTAGCGACCTCGACGAAGCTGAGCTAACTTGCTGAGGTCCAAGCTAGTT
AAGGTTAAGGACCTAAGCCTGATTAAAGAGCGCCTCGAAAACGAACTGAAAGCCATAAAGAGTAAGAAAG
AGCTCTTAGCCAAAAGAGAGGCGGTTAAATCCGAGCTGCGCAAGCTCAAGGACTTGGAGAGGAGAAGGGA
TGAGCTTTCAAAGAAGTTAGACGAAATGTTGGAAAGGCGTCAATTACTCGTCATGAAGTTGGGAACGCTT
GAAAAGAGGTGGAGGAAATAGAGAAAGAAATCAAAAGGATTGAGAAGAACTATGTGCTGTTGGAGAGGG
AGTTGGACGGCCTTACGATCAGCGACCTCGAGCAACGGGTTACAGAGCTCGAAAAGATGTACGAGAACGT
CAAGAAAGAGCTAGAGGAGGTCCTAACGAGAGAAGGCTCGTCAAGTAATGTTGGACGAAAGGCGCCGC
GCAATAGAGATGCTAAGGGGGAGGGACTCCTGCCCGGTCTGCGGGTCCCCACTCCCTCCCGAAAGGCGGG
AGTCCCTCATAAGGCGCTACGCCGAGGAAGTCGCGAAGTTTGAAGAAAAGCTGACCGAGTTGAAAGCTAG
AGAGAAGAGGTTGGAAACGGAAGCACGGCTCTTGGAGTCTAGGCTAGAGAAGCTCAAGAGGGCTTTGGAC
AAGGCGCGCGCCGATTGGAGAGCCTAGGCTTCGAAGACCTAGACGCATTAGGACTTTATTTAGCTGACT
TGAAAAGAGGTTTAACGAACTGAAAGAACAATTATCGCGAACTAGGGCTTCGGTCGAGCATTACGACAA
GCTGGTCAAAGAAGTTAAGGAAGAGCTAAGCGCCGTGACGGCCCACTAGAGGAGCTAAAAAGGAAGGAG
GGGATGCTCAGACAAATAGAACATCAGCTAGAAGAGCTACGAGGAGTAGACGCAAGCAAAGAAGAAGAGG
TAGAGAAGCGCTTGAGCGAAATAAAGAAAGAGTTGGAAGTGCTTGGCTCACCAGAAGAGCTCGAAAAGGAG
AATAGCGGAGCTGGAGAGGTTAGCCTCCAAGAAAAAGGAGCTAAGCGCCGCAGCAGAGCTCAAGAGGAGA
GAGGAGGCTGAGCTGAAGAGAGAGTTAGCCTCGCTGGGCTTCGACGAAGCCTCATTAGAACGGCTAGCGC
GAGAGGTGAGGCCTTGGAAAGGAAGAGGGACGCCCTCCTCCGCAACATATCAGAAACGGAGGCAAAAAT

AATGGAAACTAGGCGGAACGTAGCGAAGCTGAGAGAGGAGCTAAACAGGTACCAGAATGAGATAGAAAAG
 CTTAGGGCGTACGAACAATACGCCATCTTCCTTGAGGAGTTCAGAAAAACCTTCTCCACCGTCATTATAG
 ACAAAGTACTGAGAGCTTCAGAAAGGCGTGGGAGGAGGAAGCGAACAGAATATTAGATATGTTTCGACCT
 TAACGTAAAGAAGGTGGAGATAAAGGAGATAATTGAAAAGAGGAAGAAGGGGTGGACGATAAGGGCGGTA
 CTAGACGGCGGCGCGAGGGTGACCGTGGACTCCCTCTCCGGAGGCGAGAGGGTCGGGGTCGCCCTTGGCTC
 TGAGGCTCTCGTTAGCGAAGCTCCTCTCTCGCGGGAGGATATCCTTCTTGATAATGGACGAGCCAACAGC
 CTACTTGGACTCCGAAAGGAGGCAAGCTTTGAAGAAGATAATCTCGTACGCCGTCGGCCCCCTCTTTGACC
 CAAATGATAGTTGTGACTCACGACAGAGAGATGATGGATATTGCCGACTCCGCATGTCACGTTAGAAGGA
 CCCCCAAGGGTTCTACGATTACGTGCGAATGA

recB

IGNI_RS02490 recombinase B [*Ignicoccus hospitalis* KIN4/I]

Gene ID: 5562880, updated on 23-Aug-2015

Gene symbol: IGNI_RS02490
 Gene description: recombinase B
 Locus tag: IGNI_RS02490
 Sequence: NC_009776.1 (430537..431124)

NCBI Reference Sequence: NC_009776.1

>gi|156936795:430537-431124 *Ignicoccus hospitalis* KIN4/I, complete genome
 TTGAGGAGGGCGAGGAGCGAGAGGTTGGCGGAGGAGGTGCTCCGATCCATGGGCTTCGAGGTGGTGAGCG
 TCAACGCGCCGGTAAAGGTCGGGGACAAAGAGGTGGCGGAGGTGGACTTGTGTGGTCAAGCCCCCTCCCGG
 GCCCCCTCGCGGTAGAGGTCAAGTCCGGAAAAAGTGGACGTGAGCGCCGTCAGACAAGCGTACGCCAACGCG
 AAGGCCATAGGGGCGGAGCCTATGGTCATGGGCTCGGGGTGGGCCAACGAAGAAGCCAAGCTATTGGCAG
 ACAAGTTGGGCGTCAAGTACCTCATGTTTCGAGGACGTGATGGTAGCTAGCAAGGAAGAGCTCTACGACGT
 AGTCAAGGGGGCGGTACAGAGGTTTGTAGTGGTTTCATAAACTCCTTGTACCCGGACGAACGCGCGTGC
 GTCATAGCGGAAGCGGGAAGCTTGGAGGAGGCAGAAAAAGCGTTGGGTAAGGAGGAGTTAAGGAAATTAT
 TAAAGAGAATGGGCAGAGCGGGCGGCTCGGAGGCCGTGCTCGCCGCGGCGAGGCTCTCGTGTCTGTGTGTG
 GAAGCTCTTGAAGGGGGGTGAAAGGTTGA

radA

IGNI_RS05180 DNA repair and recombination protein RadA [*Ignicoccus hospitalis* KIN4/I]

Gene ID: 5563025, updated on 23-Aug-2015

Gene symbol: IGNI_RS05180
 Gene description: DNA repair and recombination protein RadA
 Locus tag: IGNI_RS05180
 Sequence: NC_009776.1 (896102..897085, complement)

NCBI Reference Sequence: NC_009776.1

>gi|156936795:c897085-896102 *Ignicoccus hospitalis* KIN4/I, complete
 genome
 GTGGGTCAAGTGGCCACTGAGGAGAAGAGGCCGACGTCCGTGGCGGAGCTCCCCGGCGTGGGGCCCTCCA
 CCGCGGCCAAGCTGATAGACGCCGGCTACGGCACCATAGAGGCGCTGGCCGTCGCCACGCCGGAGGAGCT
 CGTAGCGATAGGCATACCCCTCACTACGGCCCAGAAGATCATCAGAGCCGCGAGGCAGATGCTGGACATA
 AGGTTTCAGGACGGCAAAAGAGGTAAAGCTAGAAAAGGATGAACTTAAGGAAGATAACCACCGGCTCTAAGA
 ACTTGACGACTTGCTGGGAGGCGGTATAGAGACCAAAACCATAACCGAATTCTTCGGCGAGTTCGGGAG

CGGCAAGAGCCAGCTCTGCCACCAAGCGAGCGTCAACGTCCAACCTCCCCTTGGAGCAAGGGGGCTTGAGC
 GAGGGCGACAAGGTCGCGAAGGCCGTCTACGTAGACACCGAGGGCACCTTCAGGTGGGAGAGGATAGAAC
 AAATGGCCAAGTGCTTGGGCCTCGACCCGGACCAAGTAATGGACAACATATACTACATCAGGGCAGTTAA
 CAGCGACCACCAGATGGCCATCGTAGAGGAGCTCTTCAACTTGGTACCCAAGGAAAACGTGAAACTAATA
 GTGGTCGACTCGGTGACCAGCCACTTCAGGGCGGAGTACCCCGGCCGGGAGAACTTGGCGGTAAGGCAAC
 AGAAGTTGAATAAGCACCTACACCAGCTGGGCAAGCTGGCGGAAGTTTACAACACCCGCAGTCATAATTAC
 AAACCAAGTAATGGCGAGGCCAGACGTGTTCTACGGCGACCCACCCAAGCGGTGGGCGGCCACGTACTC
 TACCACGCCCCGGGCGTGAGGGTGCAGCTGAAGAAGGCGAGGGGCACAAGAGGATAGCGAGGGTTGTAG
 ATGCTCCCCACTTGCCGGAGGCGGAGGCTGTCTTCGCGATAACGGACTGCGGAATAAGGGACCCGGAGGA
 CTAA

Photolyase

IGNI_RS04065 radical SAM protein [*Ignicoccus hospitalis* KIN4/I]

Gene ID: 5561934, updated on 23-Aug-2015

Gene symbol: IGNI_RS04065
 Gene description: radical SAM protein
 Locus tag: IGNI_RS04065
 Sequence: NC_009776.1 (699797..700654)

NCBI Reference Sequence: NC_009776.1

>gi|156936795:699797-700654 *Ignicoccus hospitalis* KIN4/I, complete genome
 GTGAGGTTTCGAGGTACTGAGGGAGTTCGACCCGTGGAACGGGGCCCTTGTGCACGTGTCCTAGGAAGTACA
 GCCTCCAACCGTATACCGGTTGTCCGTTTTCTGCCTTTACTGTTACGCGACGTCTATATAGGGAAGAA
 GTTCTACCCCAAAAAGAACTTCTTGGAGAGGCTCGAGTGCAGACTTGAGGAAGGCCGATAGATCAAAGGTG
 ATAAACGTGTCTACTTCCAGCGACCCCTACCCGCCTATAGAGGAGAGGCTGGAGCTCACCAGGGGAGCGT
 TGAAACTCATCAGGGACTACGGCTTCAAGGTCCTCATAACGACGAAGGGGGTGCTCTTCGAGAGGGACGC
 GGATTTAATTGAAGGGATCGGGGCGATAATGGTTACGATAACTACCTTGGACGAGGAGTTGGCCAGAGTT
 ATGGAGCCGGGCGCCCCCTCCCCCTGGAGAGGCTCGAGGCCATCAAGAGGGTCTCGCACAGAGTTCCGG
 TAGGGGTGAGAATAGACCCGGTGGTCCCCGGGGTAAACGACTCGGAGGACGACATCAAAGAGATGTTGAA
 GTTGTGAAAAACGCTGGCGTAAAACACGTGACGACGTCAACTTACAAGGCGAAGCCGGACAACCTGAAA
 AGGATGACTAAGGCCTTCCCGCATTTGAAGGAGTTGTACAAGAGCGCCGTAAAGGTTGGGGGTACCTCT
 ACTTGCCCCGAGGAGCTCAGACGTGAGCTCTTGAGGCCCGTGGCCGAGGGGGCCAAGAGGTTGGGCATGAG
 CTATGCTTTCTGTAGGGAAGGTTTCCCTTCGAGGCGCCCTCTTGCGACGGCTCTCACTTGATACCTAGC
 AAGCACTTGCCCTCGTAG

➤ qRT-PCR primers specific for genes involved in replication

ccrB

IGNI_RS04740 chromosome condensation protein CcrB [*Ignicoccus hospitalis* KIN4/I]

Gene ID: 5562546, updated on 23-Aug-2015

Gene symbol: IGNI_RS04740
 Gene description: chromosome condensation protein CcrB
 Locus tag: IGNI_RS04740
 Sequence: NC_009776.1 (816604..816975)

NCBI Reference Sequence: NC_009776.1

>gi|156936795:816604-816975 *Ignicoccus hospitalis* KIN4/I, complete genome
 TTGAAGGCGCTGGTCTGGGTCGCGCTAGGGGCGCTCTGGGAGCCATAGTGAGGTACTTCTTCTACAAGT
 TCGTCCCCCAGGTCTATGACTTCCCCCTAGCCACCTTTTTGGTAAACGTAGTTGCGAGCTTTTGTCTCGG
 CTTTCATTATCGGCGCGTTTCGAGGCCAAGCCTTGGGGACAGCAGCTGAAGCTCGCCCTCGCCACAGGCTTC
 TCGGGGCGTTGAGCACCTTC**TCCACCTTCGCTGCTGATA**ACTACATCTTATTGAGGAGTTCCAAGTACA
 TAACTGCCTTCGTTTACACTGCGGTCAGCGTGGGCTTGGGC**ATAGTCTCGGTCGCTCTGGGGGAGGACTT**
 GGCTCAGCGCTTGCTCAAGTAG

cdc6**IGNI_RS01295 cell division control protein Cdc6** [*Ignicoccus hospitalis* KIN4/I]

Gene ID: 5561949, updated on 23-Aug-2015

Gene symbol: IGNI_RS01295
 Gene description: cell division control protein Cdc6
 Locus tag: IGNI_RS01295
 Sequence: NC_009776.1 (216447..217658)

NCBI Reference Sequence: NC_009776.1

>gi|156936795:216447-217658 *Ignicoccus hospitalis* KIN4/I, complete genome
 GTGCTGACCGCGACCTCGACGACATACTCGACGACGTCTTCGAACGGGTGACCAGCTCGAGGATATTCA
 AGAACAGGGACGTGCTGCTGCCGATTACTTGCCTAACAAGCTTCCCCATAGAGAAGAACAATAAGGAA
 GGTGGCCAGCGTCCTAGCCCAAGCCCTCAAGGGCTACAAGCCGAACAACCTTGTTTCATATATGGCCTCACG
 GGCACCGGTAAGACAGCGGTCGTAAAGCTGGTAGTCAAGAAGTTAAGTGAGAAAGCCGTCGAGAAGGGAG
 TTAAATTGAAAATAACCTTCATCAACACCAAGAGGGACGATACCCC**GTATAGGGTGCTAGCGAGGAT**GCCT
 GGAGGACATAGGGATAAGGGTACCCCCGACGGGAGTGCGCAGCGCGGAGCTCTACTCGAGGTTCAAGAAG
 TTCTTGACAAAGAAGGGAACCTTTGATGATACTCGTGTTAGACGAGATAGACTATCACGTAAAGAAGTACG
 GCGACGACTTGCTCTACAAGCTG**ACCAGGATAAACGAGGAGCT**CCAAAGGTCCAAGGTATCCTTGGTGCG
 AATAACGAACGACGTCAACTTCACCAGCTGGCTCGACCCTAGGGTAAAGTCTCTCTTGGGCGAGGAGGAG
 CTCGTGTTCCCCCGTACACGGCCGAGCAGCTGAGGGACATATTGAAGGACAGGGCGGAGATGGCGTTTCG
 TAGAGGGGGTGCTGGGGGAGGGAGTGATAGAGCTCTGCGCGGCCTTGCTGCTAGGGAAAACGGGGACGC
 TAGGAAGGCCCTCGACTTGTTGAGGATATCCGGCGAAATAGCCGAGAGGAGCGGCTCCTCGAAGGTTACC
 GTAGAGCACGTCAGGAGGGCTTGGGAGCAGATGGAGAAGGACAGGGTGGTGGAGATAGTGAAGAGCTTGC
 CCTTACACAGCAAGTTGATACTGTATTCCATACTCCTCTTGACGAAGGGCGGGAAGACCACCTACACCGG
 CGAGGTGTACCGCAAGTACAAGGAGCTGACCGCGGAGCTCGGGATAGAGACCCTAACGCTTAGGAGGGTC
 GGCGACTTGATTTTCGAGTTAGACATGTTGGGGCTCATCTCCACCGAGGTGGTGAGCAGGGGGAGGAGGG
 GGCTCACTCGAGTGATCAGCTTGAGAGCGACCCAGAGGCTATAAGAAAGGGGCTGCTCGTGGACCCAC
 GGTGGCCGAGGTCGCCGTTAG

cdc6-orc1**IGNI_RS06675 ORC complex protein Cdc6/Orc1** [*Ignicoccus hospitalis* KIN4/I]

Gene ID: 5561959, updated on 23-Aug-2015

Gene symbol: IGNI_RS06675
 Gene description: ORC complex protein Cdc6/Orc1
 Locus tag: IGNI_RS06675

Sequence: NC_009776.1 (1150318..1151592)

NCBI Reference Sequence: NC_009776.1

>gi|156936795:1150318-1151592 *Ignicoccus hospitalis* KIN4/I, complete genome

GTGAGCAGCGAGCTCTTCGACGAAATATACTCGGGGGGTACAGGGTCATAAAGAACGAGGAGCTCCTGC
 ACCCGGACACAGTGCCCCCTAGAATGCCCCACAGGGAGGAGGAAGTCAAGAAGTTGGCCTACCTCTTCAT
 GTCCTTGGTTAAGGAACCCGGAGAGACCTTCAACTTCGCGGTTATATCGGGGAAGCAAGGGGTAGGCAAG
 ACCCACTCCACAATCTTCTTCTACGAGCACGGACTCGCTAAACATTTAAAAGAGAAACAAGGAAAAGAGA
 TAATACTGGCCCATGTGAACTGCTTCAAGAACAGCACTTTGAACTCCATCTTGGCCACGGTATTAAACAG
 CATGCTGAGGGTCCCTCAGCCCCCGGGGGGTCTCGCCCAAGGAGCAGCTGGACATAATTATGAATAGA
 TTAGAGAGGAAGGATCGCTACATGCTCTTGGTCTCGACGACTTCCACGTGGCCCTCCAGAGGCAAGGCG
 AGTCCTTGACCAACTTCTTCGTCCGCATGTACGAGGACTCCGAGTACAAGAAGAAGAGGGTCCACGTCGT
 TTTCATAGTTAGAGATTTTGATGTTATGGAGAGGTACTTAAGCGATCAAAAGGCTAAACTTAACTTGAAG
 AGTCGCCACATACACTTCGACCCCTACACGAGCTCTCAACTCTTCGACATTCTGGAAGACAGGGCGAAGC
 TTGCCCTCTACGAGAGCTCTTACGACGAAGAAGTACTGTGGGAGATCTCTAGGATGATAGGTTACGACGT
 GAACCCCACTTTGCCCGACTCCGGGAGCGCGCGGTTCGCTATAGAGATGTTATACTACGCCGCGAGGAAC
 GCAGAAGAGCACGGGAGGAGTCAAATAACGATTGACGACGTTAGGGTCGCTTGGGGGGTCTTGAGCGAGA
 GGGGAGGGGACTTGATTAGGATAAGCGAGGCGTTGGAAGACCTTAACGACCACCAGCTCTTGCTGCTCCT
 CTCCCTGTTGAACTTGTTGAAGCTGGACCCCGAGGGGGTGCCCATAGGTAGGATAGAGGAGGAGTACAGG
 GAGGTGTGCGAAGTGGCGGGCGTGAGCCTAGGAAGCACACCCAAGTCTACCAGTACGTGACGGACATGG
 AGAAGAAAGGCATCGTAGACAGGATCGTGGGTAAGGTGAAGAACTCAAAGGGGAGGTCTCCATAATAAG
 CGTGAGGTACCCTCCGGACGCCATGAGGAGGAGAGTCTCGAGATACTTAAGAGGAGGGGGGTACAACGTT
 GCGCATCTCGCGTGA

dbp1

IGNI_RS00915 DNA-binding protein [*Ignicoccus hospitalis* KIN4/I]

Gene ID: 5562396, updated on 23-Aug-2015

Gene symbol: IGNI_RS00915
 Gene description: DNA-binding protein
 Locus tag: IGNI_RS00915
 Sequence: NC_009776.1 (156959..157252)

NCBI Reference Sequence: NC_009776.1

>gi|156936795:156959-157252 *Ignicoccus hospitalis* KIN4/I, complete genome
 GTGGCCGCTCAGATACCCCAAAGCAACGAGGTAGGGTCGGTAAGAAGCCCGTCATGAACTACGTGCTGG
 CGACCCTGACCCTCCTGAACCAGGGTGTGGACAGGATAGAGATAAAGGCCAGGGGTAGGGCCATAAGCAA
 GGCGGTAGACACCGTGGAGATAGTGAGGAACAGGTTCTGCCCCGCCAAGTGAGGGTTCGCTGAGATAAGG
 ATCGGCAGCCAGACCGTGACCAGCGCCGACGGCAGGCAGAGCAGGATAAGCACCATAGACATAGTCTTGG
 AGAGGGTCAAGTAA

ber

IGNI_RS04460 base excision DNA repair protein [*Ignicoccus hospitalis* KIN4/I]

Gene ID: 5562416, updated on 23-Aug-2015

Gene symbol: IGNI_RS04460
 Gene description: base excision DNA repair protein
 Locus tag: IGNI_RS04460
 Sequence: NC_009776.1 (765361..765999, complement)

NCBI Reference Sequence: NC_009776.1

```
>gi|156936795:c765999-765361 Ignicoccus hospitalis KIN4/I, complete
genome
TTGAGGAGGCTGAGGGAAGTCTTCGGCGACTTGGACGACTACGAGAACGAGTTCATCGCGTACTACGTGT
ACAAGAGGTACAAAGACCCCTTCGCCGTGCTCGTGGCGACCGTACTGTCCCAGAACACCACAGAGAAGAA
CGCCTTCGCGGCTTGGAGGAACCTAGAGGAGGCGTTGGGGAGGGTCACTCCCGAGGCGGTCTCTCGCTC
GGAACGAGAGGTTGAAGGAGCTCATAAGGCCCGCAGGGCTCCAAGAGCAGAAGGCCCTCCGCCATCGTGG
AGGCTGCCCCGCAAGTGGGAAGAGGTAAAGAAGGCCATAGAAAAGGGAGACAAAGGCGTCTTAAC TAGGAT
AAAGGGCATAGGCGAGAAAACGGCCGATGTCTGTGTTGATGAGCTTCGGACACGAGGAGTTCCCCGTAGAC
ACGCACGTGAAGAGGGTTCGTAAGAGGCTGGGGCTGGTCGACGAAACGCTTACAAGGAGGTCTCGTCCC
GGCTCAAGGAGCTCTTCAAGGGTAGGACGAGGGAGGCGCACATGTACCTAATACTGCTCGGGAGGAAGTA
CTGTAAGGCTAAAAAGCCTCTGTGCTCGGAGTGCCCGCTCTCCGACCTCTGCCCTAAGCGGGGGGTTTCG
GCACGATGA
```

poll

IGNI_RS03575 DNA polymerase I [Ignicoccus hospitalis KIN4/I]

Gene ID: 5562872, updated on 23-Aug-2015

Gene symbol: IGNI_RS03575
 Gene description: DNA polymerase I
 Locus tag: IGNI_RS03575
 Sequence: NC_009776.1 (621184..623928, complement)

NCBI Reference Sequence: NC_009776.1

```
>gi|156936795:c623928-621184 Ignicoccus hospitalis KIN4/I, complete
genome
GTGAAGAAACCCGAAGGGGACCGACGCTCCTAGACTTCCTCAAGCAGAAACAAGCCAACGACGGGTCTA
AGGCCTTAAAGGCCCCCAAGCCAGTAGAGGAGAAGGCTCCGAAGAGGCCCTTGAGGGCGCGGAGAAGAT
AGAAAAACAAGATAGTCAATCTAATCGTCTCGAAGAAGGTAGATCCACAGTTCCAGAAGTTCGTCAACTCC
GGAGACCGGAGGTACGCGGCGCTGGCGCAGCCTAGACGGGAGGCCGGGGACGGCGAGTACTACCTACTGC
AAGTGGTCTACGACGGTAAGAGGAACAAGGCTGTCTCTTGTATATGACGAGGAACGCCACGAGGTCTGT
GGAGTGGGTAGATGCCTTCGGTCAACAAGCCGTACTTCCTAACCAACTTGACCCAGAGGAGATCAGGAAG
CTGGGGCTGCACAAGCACCAGAACTTCGCGGGGATGGAGGTGGTCTACCGCTACGACTTACTCCATTTTG
AGAATAGGAAGTTGACGAAGATCTACACGACAGACCCCTGGCGGTGAGGGAACCTCAGGGAGAAGGTGCC
CAAGGCTTGGGAGGCCAAGATAAAGTACCACGACAACTACACTTACGACATAGGCCTAGTCCCCACCTTG
AAGTACAAAATTAAGAATAACAAGCTCTTCCCGTTTCCTTACAAGGTCAGCGAGGGAGAAGTGAGAAAGG
TATTAAAGGCCTTCGAGGAGGAGAGCGACGAGTTCAAGCGCCTAGCCATATCTTGGATACCCATCTTCGA
GGCCCCGCCTCCGACGGTCAAAGCGATAGCAATAGACATAGAGGTGTTTACGCCCGCCATAGGCAGGATA
CCGGACCCCGAGACCGCTCAGTACCCGGTCATCTCGGTGGCCCTCTCCTCTAACGACGGCCTTAAGAAAG
TCCTCGTACTAATTAGAGAAAACCTTAAGCTCACCGAAGATCAGCTCAAGGAGCTCGCCGAAGAGGACTA
CGAGGTGGAGTTCTACGACTCTGAGAAAAGTATGTTGATAGAGGTTATGAGAATTATAAGGGATTACCCG
```

GTACTGCTCACTTACAACGGCGACAACCTTCGACCTCGCCTACCTTTACAACAGGGCGCTCAAGCTCGGAA
TACCCAAGGAGATGATAATATTTAAGAAGGGTTCTGACAAGTTCGAGATAAAACACGGAATACACATAGA
CCTCTACCGCTTCTACGACATAGCGGCGATAAAGACCTACGCATTTCGGGAACAAGTATAAGGAAGTTAAC
TTGGACGCCGTCGCGGGCGCGCTCCTCGGCGAGCACAAGGTCCAAGTGACCAAGTCGATAAGCGAGCTTA
ACTATTACGAGCTGGCCCATTACAACCTCCGCGACGCCAACCTCACGCTGAAACTCTTCACCTTTAACGA
CTACTTGCCGTGGAAGTTGATGGTACTGATAGCCGAATTTCCAAGCTCGGGATAGAAGACCTAACTAGG
AAGCAAGTGTCCGCGTGGATCAAGAACTTGTTCTTCTGGGAGCACCGCAGGAGGAAGTACCTCATCCCTA
ACAAAGAGGATATAATTTTCGATGAAAGGGACCGTGAAGAGTTCGGCGATAATAAAGGGGAAGAGCTACCA
AGGAGCCTTCGTCTTCGAGCCCAGCGCCGGTATATTCTTCAATGTAGTTGTATTGGACTTCGCGTCGCTG
TATCCAACCATAATTAAGCAATATAACATAAGTTACGAGACGGTGAACGCCCCGAAGTGTAAGAACTACT
ACGAGGTTCCGGAGGTGGGGCACAGGATATGCAAGGACGTCGAGGGCATAACCTCCCAGATAGTCGGGTT
GTTAAGAGATTACAGAGTTAAAATATACAAGAAAAAGCGAAGGACAAAAGCTTGGACGACAAGATGAAA
ATGTGGTACGACACCGTTCAGTCAGCAATGAAGGTATACATAAACCGCTCCTACGGCGTCTTGCGCGCGG
AGAGCTTCGAGCTTTACTGCCCTCCGGCGGCCGAGAGCATCACCGCTTACGGGAGGTTCCGCATAAAGAG
TACTATGGATTATGCTAAGAAAAACAAGATCGCCGTTCTATACGGAGATACCGACTCGATGTTCCCTTGG
GACCCTCCGCAGAACTTGTTAGACGACATCATAGAGTGGGTCAAGAACAACCTTCGGCTTAGAAATAGAAA
TAGATAAGACCTATAGGTTTCGTAGCGTTCACAGGTCTAAAGAAGAACTACATAGGTGTGTACCCGGGAGG
GGAGATAGACGTCAAGGGTTGTTGGGGAAGAAGAGGAATACCCCGCAGTTTCGTCAAAGAGGCGTTCATA
AAAATGATAGAAATGATCAGGAACCTCCAGAGCCCGGAAGAGGTAGTGAAGACGCGCGAAGAAGTCAAGA
ACTTAGTGAAAGAGTTGTATATGAACCTCAAGAGGCAGTACTACGACTTGGACGAGTTGGCGTTCCACAT
GCAACTTACTAAGCCCATAGAGTCTTACACTAAGAACATGCCGAGCACGTGAAGGCGGCGAAGATGCTA
GCCAAGTTCGGCATAACGTCACCAAGGTGACGTGGTATCCTTCGTTAAGGTGAAGGGCGCAGAAGGCG
TGAAGCCCGTGCAGCTGGCCAAGCTACCGGAGGTCGACGTGGAGAAGTACTACGAAGCGATAGAGTCCAC
GCTAGGACAGATACTGAAGGCGTTCAGCTTGGACGCGGCTTCATTGAGCGGGACGACCAAGTTGATGGCG
TTCTTGAACAAATAA

mcm

IGNI_RS06685 replicative DNA helicase Mcm [*Ignicoccus hospitalis* KIN4/I]

Gene ID: 5562624, updated on 23-Aug-2015

Gene symbol: IGNI_RS06685
Gene description: replicative DNA helicase Mcm
Locus tag: IGNI_RS06685
Sequence: NC_009776.1 (1151795..1153864, complement)

NCBI Reference Sequence: NC_009776.1

>gi|156936795:c1153864-1151795 *Ignicoccus hospitalis* KIN4/I, complete genome

GTGAGTGAGGCGGGCTTCCTCGAGGAGAAGTTACCGGTCGAGGAGCGGTTTCAGAGAGTTCTTGAGTCCT
ACGAAGTAAACGGGAGAGTGAAGTACAAGGACGAAATAAGGAACGCCGTGGCCGAGAGGAGGGCGAGCGT
AGTAGTCGACTTCACCGACGTAATAGAGTTTGACCAAGAGTTGGCCGAAGAGATAGTCGAGAACCCGCTG
GAAACGTTAGATAAACTGGATCAAGTAGTTACAGAAATAGCAAGCGGTTTGCAAACAAAAAGTACCCGA
TGAGAGTTTCGCTTACCAACTTGCCGAGAGAAGGTGAGGCTCAGAGACCTTAGAGAGAGGTACGTCGGCAA
GTTAGTGGCGTTTCGACGGGATAGTTACGAAGGCGACCAACGTAAAGGGCAAGCCGAAGAAGCTCTACTTC
CGGTGCGAGGCGTGCGGGACGGTGTTCCTCGGTCGAGCAGAGGGGAAAGTACTACCAAGCCCTACCGTCT

GTCCCAACCCGAGTGTCTAAGAAGACCGGCCCTTTCACCTTGTTAGAGAACCACCCCAAGAACGAGTA
 CGTGGAAGTATAGTGGAGGGCAAGGACCTCGTCGACGTAGCGCGCCCCGAGATAGGGTTACAGTAATAG
 ATAGAAGTTATAGTGGAGGGCAAGGACCTCGTCGACGTAGCGCGCCCCGAGATAGGGTTACAGTAATAG
 GCGTCTTGGAGGCGGTTCCTAACAGAGTGCCCAAGAGAGGTTCCATGGTGGTTTTCGACTTCAAGATGAT
 AGCCAACAACATAGAGGTTTCGCAGAAGGTGTTGGAAGACGTCCACTTGAGTCCGGAGGACGTCGAAAGA
 ATAAAGGAGCTCTCGAAAGACCCCTGGATCCACAAGAGCATAATCTTGAGCATAGCCCCGGCTATATACG
 GCCACTGGGACATAAAGGAGGCGATAGCCTTCGCGCTCTTCGGAGGGGTACCGAAGGAGCTGGAGGACGG
 AACTAGGATAAGGGGCGACATCCACGTCTTGATAATAGGGGACCCGGGCACGGCCAAGTCCCAGCTCTTG
 CAGTACGCAGCTAGGATAGCGCCGAGGAGCGTTTACACGACCGCAAGGGGAGCACCGCGGCGGGCCCTCA
 CGGCTGCAGTAGTTAGGGACAACATAACCGGCGAATACTACCTAGAGGCCGGCGCCTTAGTGTTGGCGGA
 CGGCGGAGTGCGGTTCATAGACGAGATAGACAAGATGAGGGAGGAGGACCGGTTCGGCCATACACGAAGCT
 ATGGAGCAGCAGACGGTCTCCATAGCTAAGGCGGGAATAGTGGCCAAGCTCAACGCCCCGCTGCGCGGTGC
 TCGCGGCGGGCAACCCCCGTACGGCCGCTACGTGCCCCGAGAGTCCGTGGCGGAGAACATAAACTTGCC
 CCCGAGCATACTCTCGAGGTTCGACCTAATATTCGTCTTGAGGGACGTCCCTGACCCGAAGAGGGATAGG
 AGGTTAGTAAGGTACATATTGAACGTACACAAGGAGGCCGACAAGATAGTCCCGGAGATACCGGCGGACT
 TGCTGAAGAAGTACATAGCCTACGCGCGGAAGAGCGTGAAGCCCAAGCTCTCGGAGGCCGCGGCGAGGAT
 AATCGAGAAGTCTTCGTAGACTTGAGGAAGACCGCGGCCGAGAACCCGAGATGGGCGTCCCCATAACA
 GCGAGGCAGCTGGAAGCTCTGGTCAGGATGAGCGAGGCCACGCGAAGATGGCCCTCAGAAGCGTGGTGG
 AGGAGGCCGACGCGATAGAGGCTGTCCGCATGATGCTCGCATTTCTTAAGTACGGCTGGGGTCGACGTAGA
 GACCGGCAGGATAGACATAGATACCATATACGTGGGCGTTTCCAAGAGCAACCGCCAAAAGAGGCTGATA
 TTGAAGGACATAATCAAAAGAGAAGTTTAAGGAGAAGGGGACTTGTGTGCACTTGAAGGAGGTAGTCAGGG
 AGGCGAGGAAGAGGGGTCTGAACGAGGAAGAGATAGAGCAAATACTGACCCAGATGGTCAACCAAGGCGA
 GATATACGAGCCCAAGACCGCTGTTACTCCCCGCTATAG

tfb

IGNI_RS07105 transcription initiation factor IIB [*Ignicoccus hospitalis* KIN4/I]
 Gene ID: 5562291, updated on 23-Aug-2015

Gene symbol: IGNI_RS07105
 Gene description: transcription initiation factor IIB
 Locus tag: IGNI_RS07105
 Sequence: NC_009776.1 (1227915..1228865, complement)

NCBI Reference Sequence: NC_009776.1

>gi|156936795:c1228865-1227915 *Ignicoccus hospitalis* KIN4/I, complete
 genome
 TTGCCCCAACAGGAGGCTTTTAGGCTCCGTTGCCCCGTGTGCGGGAGCACCGACATAGTCTTCAACGAGG
 AGACCGGGGAGTACGTGTGCGCCCGTTGCGGTACCATAGTGCTGGACCGGTACGTGGACCAAGGCCCCGA
 GTGGAGGGCCTTCACCCCCGAGGAGAGGGAAAGGAGGGGTAGGACCGGCGCCCCCTCTCTCCACCCCTC
 CACGACCACGGCTTGTTCCACGGTTATAGATCATAGGGATCGGGACGCGTTAGGGAAGCGCTAAGCCCTA
 GGAAGAGGCAAGAAGTCCAGAGGCTTAGGAAGTGGCAGCTCAGGGCGCGCATCCAGACGGGTATGGATAG
 GAACCTAACTATAGCTATGAACGAGCTCGACAGGATGGCAAACCTCTTGAACCTCCCGAAACAGATCAAG
 GAAGAGGCGGCGGTAATCTATAGGAAGGCCGTGGAGAAGGGCCTCGTTAGGGGGAGGAGCATAGAGTCCG
 TAGTAGCGGCTGTAATATATGCCGCTTGTAGGATCCACCACCAACCGCGCACCTTGACGAGATAGCTAA
 GAAGTTGGAGGTGAATAGGAAAGAAGTGGCCAGGTGTTACAGGCTTATAACTAAAGAGCTCAAACCTAAAG

GTGCCCATCGCCGACGCAATGGACCACATACCCAGAATAGGCGAGGCCCTCAAGCTCAGGGGCGATATAA
 TAGAATACGCCATGAAGATCATGGAAAAGATAAAGGGGCACCCGATAACCGCCGAAAGGACCCCGCGGG
 CATAGCGGCGGCAGTGATATACATAGCTGTTCATGCAGAAGGGCGAAAGGAGGACGCAGAAGGAGATAGCG
 AACGTTGCCGAGTAACCGAGGTCACTGTGAGAAACAGGTACAAGGAGATAATGAAGGTCCTCAACGAGA
 TGGACTTAGAGGAGATCGAGAAAGAGGTCTCAAAGAAGTAG

fen-1

IGNI_RS03580 endonuclease [*Ignicoccus hospitalis* KIN4/I]

Gene ID: 5562892, updated on 23-Aug-2015

Gene symbol: IGNI_RS03580
 Gene description: endonuclease
 Locus tag: IGNI_RS03580
 Sequence: NC_009776.1 (624002..625054, complement)

NCBI Reference Sequence: NC_009776.1

>gi|156936795:c625054-624002 *Ignicoccus hospitalis* KIN4/I, complete genome
 TTGGGCGTTACAGCCCTAAGGGAACCTCATCCCCAGCAAGTGCAAGAAGACCTTAGAGCTAAAGTCCTTGT
 CGAACAAGAGCGTGCCCTCGACGCTTACAACACCTTGTATCAGTTCTTAGCTGCCATAAGGGGCGAAGA
 CGGCAGGCCCTCATGGACTCCAAAGGGCGCGTGACCAGCCACCTCTCCGGACTTTTCTACAGAACAATC
 AACATGTTGGAAAACGGAATAAAGGTAGCCTACGTCTTCGACGGCGCCCTCCCAAGCTCAAGACGCGCG
 AGATAGAGAGGAGGCAGAACTCAAGCAAGAGGCCGAGAAGAAGTACGAGGAGGCAGTTAGGAGGGGGGA
 CGTCGAGGAAGCTAGGAAGTACGCCAGATGAGCGCAAAGCTGACGAAGGAGATGGTAGAAGAAGCTAAG
 AGGTTGCTCGAGGCTATGGGGGTCCCGTGGGTACAAGCCCCCAGCGAGGGAGAGGCCCAAGCGGCCTACA
 TGGCCGCTAAGGGAGACGTCTGGGCGTCTGCTAGTCAAGATTACGACTCCTTGCTCTTCGGCTCTCCTCG
 CTTGTTAGGAACCTGGCCGTGAGTGGGCGCAGGAAGCTCCCTAACAAGAACGTGTACGTCGAAGTGAAG
 CCCGAGGAAATAACTTTGAAGTGTGTGCTGGAGGAGTTGGGCATAACCCGAGAGCAGCTCGTTGCAATAG
 CCGTCTTGATAGGGACCGACTACACGCCCCGGGTGAAGGGCGTCGGGCCGAAGACCGCCTTAAGGTACGT
 GAAGAGCTATGGTGACTTAGAGAGGGTGCTTACTGCCCTAGGCGTCGATGACAAGGAGTTGTACTTGAG
 GCGTATAATTTCTTCTGAACCCCCAGGTGACCGACGACTACGAGCTCGTGTGGAGGAGGCCCGACCCCC
 AAAAGATAATTGAAATCCTAGTGTACGAACACGACTTCAACGAGGAGCGCGTGAGAAAGGCGATAGAGCG
 CTTAATGAAGGCCTGGAAGGAAAAGCTCAGCACTAAGCAGAGCACGTTGGACATGTTCTTTAAAAAGCGT
 TGA

rg

IGNI_RS02665 reverse gyrase [*Ignicoccus hospitalis* KIN4/I]

Gene ID: 5562369, updated on 23-Aug-2015

Gene symbol: IGNI_RS02665
 Gene description: reverse gyrase
 Locus tag: IGNI_RS02665
 Sequence: NC_009776.1 (457134..460913)

NCBI Reference Sequence: NC_009776.1

>gi|156936795:457134-460913 *Ignicoccus hospitalis* KIN4/I, complete genome
 TTGTACGCTTCTACCGACGCTCGTGCCCTCGTGCGGAGGGGAAATAGAGGACGTCAACTTGTCCTTGG

GCTTGCCTTGCGACAAGTGCTTGAGGGTTGTGGGCTTAGAGAGCTTGAAGTTAGACCCTTCTAAGAAGGA
 CTCGCCCTCCGTCCGGAGGAGGCTGATAGAACTAGGGGGGCCCTTAGGGGAAAGCTTGAAGCTCGAAGAG
 GAGCTGGAGTCCCTTGAGAGAAGGTGTTCCAAGAAGTCTTGGGAGCCCCATGTGGAGCGCCCAGAGGGCTT
 GGGCCCTGAGGGCCCTGAGGGGGGAGAGCTTCTCCATAGTGGCCCCGACGGGCATGGGCAAGAGCACCTT
 GGGTGCGCTCCTTTCTGTGTATCTGAGCCACAAAAAGAAGAAGAGCTACATTATAGTCCCCACCACG
 CCGCTCGTAGATATGATGTTTCAAAAAGGTCTCCGCCCTTCGCGGAGGCCTTCGGCGTCCGGGCGGTTTACT
 TCCACTCCAAGATGTGCCCCCTCAGAGGAAGGAAATGAAGGAGAGGCTCCTCTCTGGGGACTTCGACGT
 ACTCATTACTACCTCCAGATTTCTAATAAATAATTTAGACTTACTGAAGAATTACGAGTTCGGATTTCGTC
 TTCGTCGACGACGTGATTTCAGTCTTGAAGAGTCCCCAAAACGTGGACAGGATATTAATGGTGTAGGCC
 TCCAAGAGTCAGACGTCAAAGGCTGGAGGAGGTAGACAAGGAGCTCTCTAGGAAAGCACAAGTGTAAAC
 GAAGCTTCAAGATTTGCAGAAGAGATACCAACTCTTAAAGGAGATGAGAGAGCTAGAGGAAGAATTGGAA
 GATTTGAAGAGGAAAGTTAAGGGGAAGTTGATAGTAAGCTCTGCTACGGGGAGAGCGAAAGGGAATAGGG
 TAAGGCTCTTCACGCGCTTGTGGGCTTCACCCCGGGCGGCGTCGGAGAAGGGTAAGGAACGTGGTCGA
 CTCTACTCCCGCTCTCGGACGTGTTGAAGTGGTCAAGAAGCTGGGCAAGGGAGGGCTGGTCTTCGTC
 CCCGCCGACTTGGGAGCCAAGGGAGCCGAGGAAGTCGCGGAGGCCTTGAAGGCCGCCGGGTTGCAGCTG
 AGGTCGCGACCTCGGAGAGGATCGGCGTCATTAAAGACTTTGAGGAAGGGAGGGTTGAAGTCTTGGTGGG
 CGTGGCCACCCACTACGGGGTGTGGTGAGGGGCATAGACTTGCCCCACGTGGTGCGCTACGCCGTCTTC
 GTAGGCGTGCCCCGGTTCAAGTTCAAGCTGAAGCTGGAAGAGCCCTCGCCCATGACCATTTATAGGCTCT
 GCTCGTTGGCGGCCAGGTTCTTCGAGGAGTGTGCCTCCCTCTACGCCAAGCTGCGCAAGTGGGTCCAGAG
 GCTGGGGCCCCCGGGGCTTCAAAGCGTAGAGGAGGCCTTGAAGGAGGGAAGCGCTCCACCCCGGCCCTCT
 AAGGACTTCATGGAAGCTTATACCAAAGTGAAGAGATAATAGAAAAAACGGATTTTATTGAAAACTCA
 AGGAGTCCGGCGAAGTGGACGTGGTAGCGGAGGACTCTCTGTACGTCTTGATTCCCGACGCCGCCACCTA
 CTTACAAGCCTCCGGGAGGACGTCCAGGCTTTACGCGGGAGGCGTCACCAAGGGCTTGTCCGTAGTACTG
 GTGGACTCGGAGCCCCCTCTCAGAGGCCTCAAGAAGAGGTTGGCGTGGGTGGTGGAGGAGTGAAGGAGT
 TCGAGTCCTTGAAGTTGAGTGAGCTGCTCAAGGAGATAGACGAGGATAGGAAGAAGGTCTTAAAGGTCAT
 CAGGGGGGAGCTAAAGGTTGAAGAAGTTCGAGACCTCATGAAGACCGTACTAATGATAGTTGAGTCGCCC
 AACAAAGCTAGGACGATAACGAGCTTCTTCGGGCGCCCCAGCGTGAGACAAGTGAAGGGCGTGAAGGTTT
 ACGAGGTACCTTGGGGGACAAGCTCTTGTACGTGGCCGCCAGCGGAGGCCACGTGTACGACCTAGTCGA
 AGAGGCCGACCTTGTAACGAGGAGCCTTGCATGCTCTTCGGCATAAGGGTAAAGGACGTGCCGGAGGAG
 GTGCTGAGCTCCATAAAGCGGTGCGCCGTGTGCGGCCACCAGTTCTCGGGGGACGTGAAGGAGTGCCCGA
 GGTGCGGCTCGCCCTTCATAAAGGACGCCAAGGACGTGGTGGACGGGTAAAGGGAGCTCGCCCAAGAAGT
 GGACGAGGTCTAATCGGCACGGACCCCGACACGGAGGGGGAGAAGATAGGCTGGGACTTGAAGAACCTA
 ATATCCCCGTTTCGCGAAGAAGATAAGGAGGGCCGAGTTCCACGAAATAACGAAGAAGGCAATATTGAAG
 CGTTGGAGAACCCAAGGGACTTCGACATGGGGTACGTTTGGTCCCAGATGGTCCGGAGGGCCGAGGACAG
 GCTGACAGGCTTCACCTTGAGCCCGAAGCTCTGGTTCGAACTGTGGCCGACGCTGTGCGAGGTCCTCCAA
 GAAATGAAGAAGAAGCTGCTCGGGTGTCCGCTCACTAGGAAGTTGTCCGCCGGAAGGGTCCAGACCCCG
 TCCTCGGGTGGGTAAATACAGAGGTACGAGGAATACGCCAAGTCCAAGAAGAAGTTCTACATAATAAGGTT
 CGACGGACGCGAGCTCGAGTTCTCCGAGGACGAGTTGAGAGGCTTCTCCAAAAAGCTCGCAATAGACGGG
 AAGGTCAAAAATACTCAAGGTAGAGGAGGAGGTAGAGGAGCTCAAGCCCTTGCCCCCTACACCACAGACA
 CCATGCTCGAGGACGCCTCCAAGCTGGGGCTGGACCCCTCGAGAGCTATGAGGGTAGCCCAAGACTTGTT
 CGAGATGGGGTTCATAACTTACCACAGGACGGACTCCACCAGGGTGTGCGACGCGGGCATAGCGGTGGCG
 AGGGAGTGGATAACCTCCAAGTTCGAGGGCTTGTTTCGCGCCAGGAGGTGGGGGGAGGGAGGGGCCACG
 AGGCGATAAGGGCCACGAGGCCGTGAGCGCGGAGGACCTCAAGAGGTTAATAGAGGAGGGCATGATAAC
 GCCCCCTAGGGAGCTCAGCAAGCAACACTTCATGTTGTACGACATGATATTTAGGAGGTTTATGGCAAGC

CAGATGAAGGAGGCGAAGGTTAAGAAAGCGGTGTACGAAATAACGGTTGAGGAGGGAGGTGCGGTAGTAG
 GCAAGAAGGTTTTTGGAGAAATACGTAGAAAGGGTG**TTCGACGGCTTCCTCTTAGT**ATACCCTATAGTCAA
 GATAGAGAGCCTCCCCGAGGGGGAGTACGAGGTTAAGGAGGTTAGGGCCGTCTCCCCGCCACACGGTGCCC
 TTGTACACCCAAGCCGACCTCATAAGGCTCATGAAGGAGAGGGGGCTCGGCAGGCCGAGCACCTACGCGA
 AGATAGTTAGTACCTTGCTCGAGAGGAGGT**ACGTAACCTCTGAGCAAGGTGGG**CAAGAACTCGTCCCCAC
 GGTTAGGGGCTACGCTGTGTACTCGTACCTCACCGGGAAGGTAGTGGGCGCCGGCTGGGTTAGGAAGGCG
 CTGGAGGTCATCATAAATCCCGAGGGCAAGTCTAAGTACTTCCAAAAGCTGGTGGAAGAAGAGGCCACTA
 GGAGGTTGGAGAAGGTCATGGACGAGATAGCGGAGAAGAAGGACGAGAAGATGTATATTAACGTACTCAA
 GGATATCATAGAGGAGACCAAGGTTATTCTTTTCTTAAGCGACAAGGGCGCTCAGCCCAGCCTCCGGTAG

➤ **qPCR primers for DNA damage detection after ⁶⁰Co radiation exposure**

DbR

IGNI_RS04235 16S ribosomal RNA [Ignicoccus hospitalis KIN4/I]

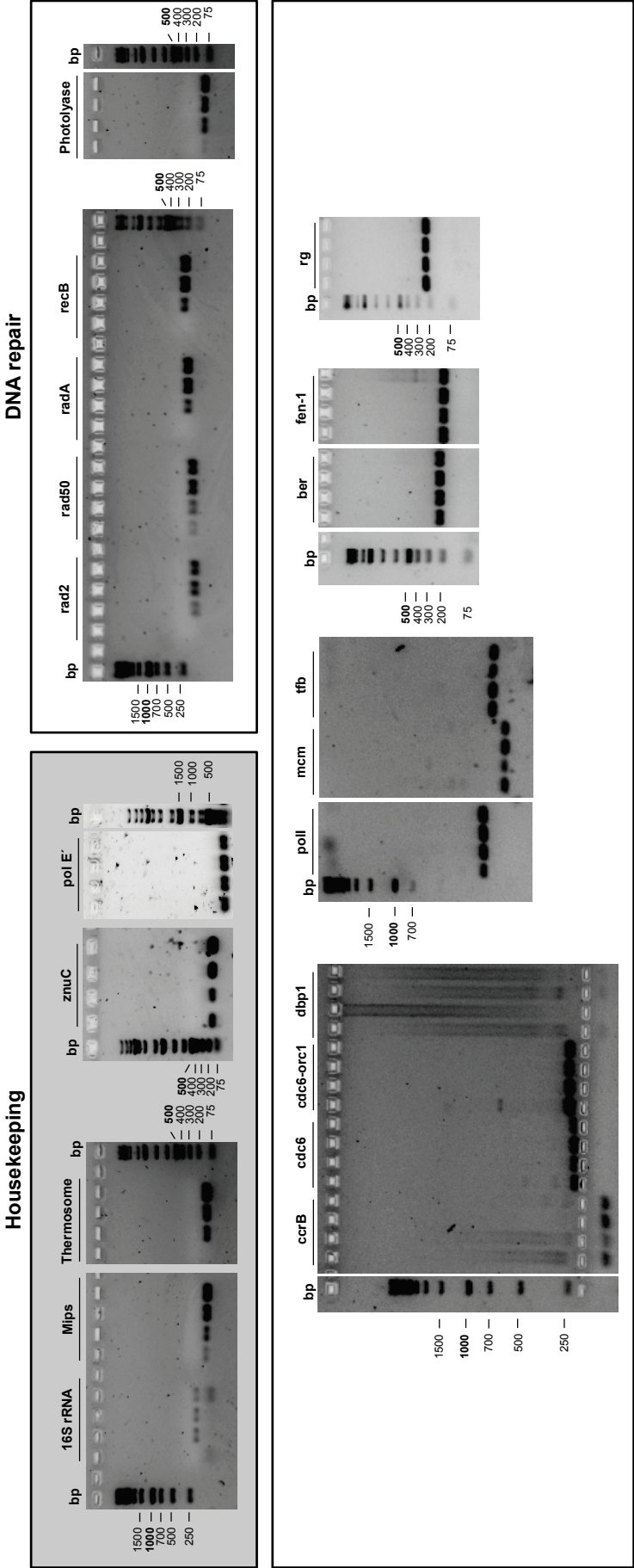
Gene ID: 5562932, updated on 20-Aug-2015

Gene symbol: IGNI_RS04235
 Gene description: 16S ribosomal RNA
 Locus tag: IGNI_RS04235
 Sequence: NC_009776.1 (728379..729802)

Showing 1.42kb region from base 728379 to 729800.

NCBI Reference Sequence: NC_009776.1

>gi|156936795:728379-729800 Ignicoccus hospitalis KIN4/I, complete genome
 CGGACCCGACCGCTATCGGGTAAGG**TAAGCCATGGGAGTCGAAC**GCCCCGCCGCCGGGCGTGCGGA
 CGGCTGAGTAACACGTGGCTAACCTACCCTCGGGAGGGGGATAACACCGGGAAACTGGTGCTAATCCCC
 ATAGGGGCGGAGGCCTGGAAGGGTTCCGCCCCGAAAGGGGGCTCGGGGGGAACGCCCCGAGTCCGCCCCG
 GGATGGGGCCGCGCCCCATCAGGTAGTTGGCGGGTAATGGCCCCCAAGCCGAAGACGGGTAGGGGCCG
 TGGGAGCGGGAGCCCCAGATGGGCACTGAGACAAGGGCCCAGGCCCTACGGGGCGCACCAGGCGCGAAA
 ACTCCGCAATGCGGGCAACCGTGACGGGGTTACCCCGAGTGCCCCCTCTCCGGGGGCTTTTCCCCGCTGT
 AAACAGGCGGGGGTAATAAGCGGGGGCAAGTCTGGTGTGACGCCCGCGGTAATACCAGCCCCGCGAGT
 GGTGCGGACGATTATTGGGCCTAAAGCGCCCGTAGCCGGCCTGGTGGCCCCCTCCTAAAGCCCCGGGCT
 CAACCCGGGGACTGGAGGGGGTAGCGCCAGGCTAGGGGGCGGGAGAGGCCGAGGGTACTCCCGGGGTAGG
 GGCGAATCCGATAATCCCGGGAGGACCGCCAGTGGCGAAGGCGCTCGGCTGGAACGCGCCCCGACGGTGA
 GGGGCGAAAGCCGGGGGAGCAAACCGGATTAGATACCCGGGTAGTCCCGGCTGTAAACGATGCGGGCTAG
 GTGTTGGGCGGGCTTCGAGCCCGCCCAGTGCCGCAGGGAAGCCGTTAAGCCCGCCGCTGGGGAGTACGG
 CCGCAAGGCTGAACTTAAAGGAATTGGCGGGGAGCACCACAAGGGGTGGAGCCTGCGGCTTAATTGGA
 GTCAACGCCGGGAACCTTACCGGGGGCGACAGCAGGATGAAGGTCAGGCTGAAGACCTTACCTGACGCGC
 TGAGAGGAGGTGCATGGCCGTCGCCAGCTCGTGCCGTGAGGTGTCCGGTTAAGTCCGGCAACGAGCGAGA
 CCCCCGTCCCCAGTTGCTACCCGGGGCTCCGGCCCCGGGGCACACTGGGGAGACTGCCGCCGTATAAGGC
 GGAGGAAGGAGGGGGCTATGGCAGGTGAGCATGCCCCGAAACCCCCGGGCTGCACGCGGGCTACAATGGC
 GGGGACAGCGGGTTGCGACCCCCGAAAGGGGGAGCCAATCCCTGAAACCCCCCGGAGGTTGGGATCGAGGG
 CTGCAACTCGCCCTCGTGAACGCGGAATCCCTAGTAACCGCGCGTTAGCATCGCGCGGTGAACACGTCCC
 TGCTCCTTGACACACCCGCCCCGTCGCTCCACCCGAGGGGGGAGA**AGTCGTAACAAGGTAGCCGT**AGGGGA
 ACCTGCGGCTGGATCACCTCCC



Metabolic activity of “*I. morulus*” after ⁶⁰Co radiation exposure

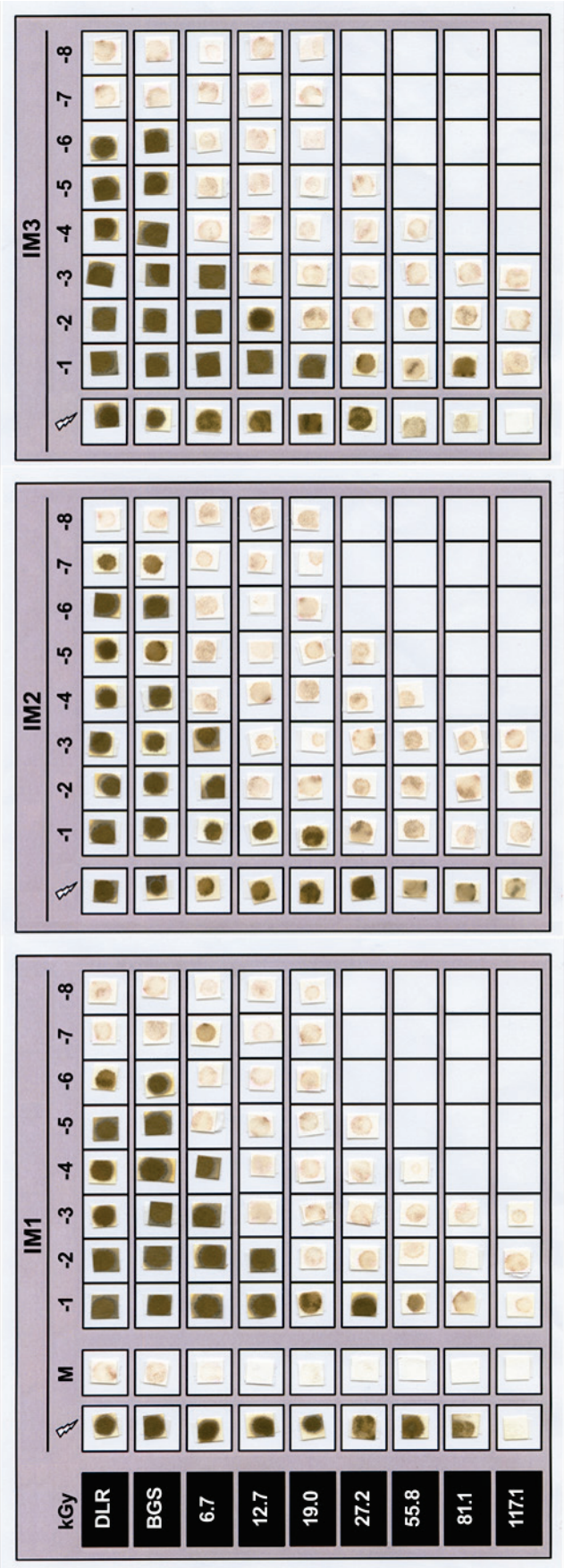


Figure 61: Metabolic activity of “*I. morulus*” (IH1, IH2, IH3) after ⁶⁰Co radiation exposure monitored on lead acetate paper. The metabolically produced H₂S reacts with lead acetate to lead sulfide, visible as dark brown spots. Abbreviations: Flash (⁶⁰Co exposed stationary phase cultures), M (½ SME+S⁰ medium incubated at 90 °C for up to six days), DLR (lab control), BGS (transport control). Serial dilutions with 1:10 dilution steps (10⁻¹ to 10⁻⁸) are represented by the exponent (-1 to -8).

^{60}Co irradiation of single $\frac{1}{2}$ SME medium compounds

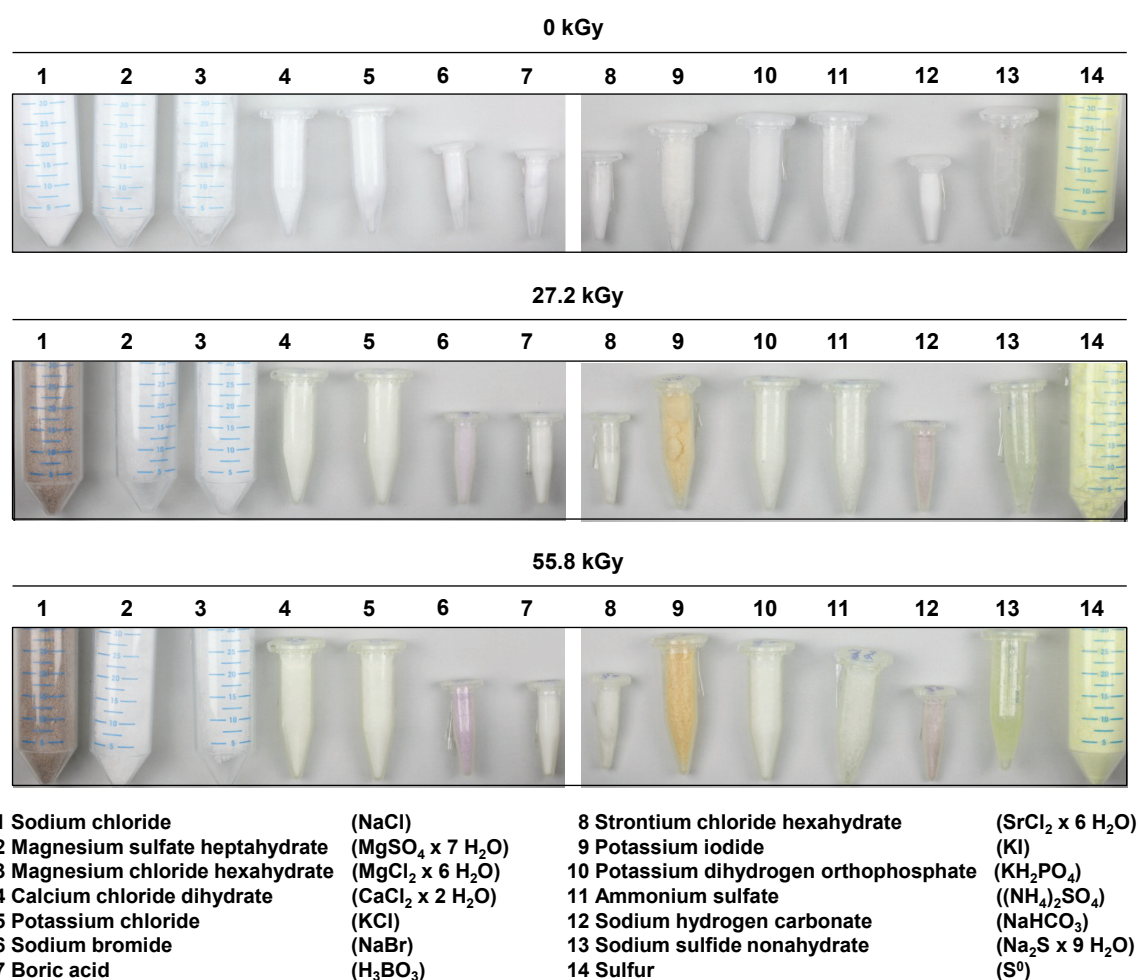


Figure 62: Aliquots of substances needed for $\frac{1}{2}$ SME-S⁰ medium preparations. The exposure was conducted in either Falcon® or Eppendorf Tubes®. Pictures were taken before (0 kGy) and after ^{60}Co radiation exposure (27.2 kGy, 55.8 kGy).

Certified dosimetry data for DbR #1, #2, #3


<h1>Zertifikat</h1>		BGS
		IDEEN PLUS ENERGIE
<p>BGS Fritz-Kotz-Straße 16 51574 Wühl DLR e.V. Inst.f. Luft- und Raumfahrtmedizin Strahlenbiologie Linder Höhe 51147 Köln</p>		
<p>BGS-Auftrags-Nr.: 25049</p>		<p>Ihre Lieferschein-Nr.: X/316/67207221 Kunden-Nr.: 101235 Datum: 05.12.2014</p>
		<p>Zertifikat Nr.: 76767 Serie: 1 / 1</p>
<p>BGS-Chargen-Nr./Spill Nr.: 14031870/0</p>		
Bestrahlte Menge:	7 Karton(s)	
Ihr Artikel:	Forschungsproben	
BGS Materialnummer:	043550	
Strahlenart:	Gamma	
Erforderlicher Dosisbereich [kGy]:	6,00 – 102 kGy	
Bestrahlt am:	28.11.2014 - 05.12.2014	
Gemessene Außendosis Probe 1 [kGy]:	6,25	
Gemessene Innendosis Probe 1 [kGy]:	6,16	
Gemessene Außendosis Probe 2 [kGy]:	12,05	
Gemessene Innendosis Probe 2 [kGy]:	11,13	
Gemessene Außendosis Probe 3 [kGy]:	17,76	
Gemessene Innendosis Probe 3 [kGy]:	17,25	
Gemessene Außendosis Probe 4 [kGy]:	23,99	
Gemessene Innendosis Probe 4 [kGy]:	23,85	
Gemessene Außendosis Probe 5 [kGy]:	47,87	
Gemessene Innendosis Probe 5 [kGy]:	45,88	
Gemessene Außendosis Probe 6 [kGy]:	72,58	
Gemessene Innendosis Probe 6 [kGy]:	71,74	
Gemessene Außendosis Probe 7 [kGy]:	114,4	
Gemessene Innendosis Probe 7 [kGy]:	112,1	
<p>Dieses Dokument ist ohne Unterschrift gültig, da es mit einem validierten System erzeugt wurde, das die Anforderungen von FDA 21 CFR Part 11 erfüllt.</p>		
<p>BGS Beta-Gamma-Service GmbH & Co. KG · Sitz Wühl · Registergericht Köln HRA 14938 · Ust.-IdNr. DE 122 533 721 PhG BGS Beteiligungs GmbH · Sitz Wühl · Registergericht Köln HRB 38648 · Geschäftsführer: Dr. Andreas Ostrowicz</p>		
		 EN ISO 9001 EN ISO 13485

Figure 63: Certificate of irradiation for DbR #1.

Zertifikat

BGS

IDEEN PLUS ENERGIE

BGS Fritz-Kolz-Straße 15 51674 Wiehl
 DLR e.V.
 Inst.f. Luft- und
 Raumfahrtmedizin
 Strahlenbiologie
 Linder Höhe
 51147 Köln

BGS-Auftrags-Nr.: 45688

Ihre Lieferschein-Nr.: DE 121965658
 Ihre Bestellung: X/316/67216928
 Kunden-Nr.: 101235
 Datum: 03.07.2015

Zertifikat Nr.: 141921/V1
 Seite: 1 / 1

BGS-Chargen-Nr./Split Nr.: 15025188/0

Bestrahlte Menge:	1 Palette(n), 7 Karton(s)
Ihr Artikel:	Forschungsproben
BGS Materialnummer:	043550
Strahlenart:	Gamma
Dosisbereich [kGy]:	6 – 102
Bestrahlt am:	02.07.2015

Probe 1	
Gemessene Oberflächendosis [kGy]:	6,79
Ermittelte Minimaldosis [kGy]:	6,52
Probe 2	
Gemessene Oberflächendosis [kGy]:	12,98
Ermittelte Minimaldosis [kGy]:	12,46
Probe 3	
Gemessene Oberflächendosis [kGy]:	19,43
Ermittelte Minimaldosis [kGy]:	18,65
Probe 4	
Gemessene Oberflächendosis [kGy]:	27,70
Ermittelte Minimaldosis [kGy]:	26,59
Probe 5	
Gemessene Oberflächendosis [kGy]:	56,96
Ermittelte Minimaldosis [kGy]:	54,66
Probe 6	
Gemessene Oberflächendosis [kGy]:	82,78
Ermittelte Minimaldosis [kGy]:	79,44
Probe 7	
Gemessene Oberflächendosis [kGy]:	120,50
Ermittelte Minimaldosis [kGy]:	115,63

Dieses Dokument ist ohne Unterschrift gültig.

BGS Beta-Gamma-Service GmbH & Co. KG · Sitz Wiehl · Registergericht Köln HRA 16938 · Ust-IdNr.: DE 122 533 721
 PhG BGS Beteiligungs GmbH · Sitz Wiehl · Registergericht Köln HRB 36648 · Geschäftsführer: Dr. Andreas Ostrowski

EN ISO 9001
EN ISO 13485

Bestrahlungszertifikat - Certificate of irradiation - Certificat d'irradiation
 BGS IDEEN PLUS ENERGIE BGS IDEEN PLUS ENERGIE BGS IDEEN PLUS ENERGIE

Figure 64: Certificate of irradiation for DbR #2.

Zertifikat

BGS

IDEEN PLUS ENERGIE

BGS Fritz-Katz-Straße 16 51674 Wühl

DLR e.V.
 Inst.f. Luft- und
 Raumfahrtmedizin
 Strahlenbiologie
 Linder Höhe
 51147 Köln

BGS-Auftrags-Nr.: 71607

Ihre Bestellung: D/316/67227297
 Kunden-Nr.: 101235
 Datum: 29.03.2016

Zertifikat Nr.: 226971
 Seite: 1 / 2

BGS-Chargen-Nr./Split Nr.: 16011654/0

Bestrahlte Menge:	1 Karton(s)
Ihr Artikel:	Forschungsproben
BGS Materialnummer:	046391
Strahlenart:	Gamma
Bestrahlt am:	23.03.2016
Gemessener Dosiswert [kGy]:	6,54
Chargen-Freigabe:	Harnisch Hella, 29.03.2016, 11:50


BGS-Chargen-Nr./Split Nr.: 16011655/0

Bestrahlte Menge:	1 Karton(s)
Ihr Artikel:	Forschungsproben
BGS Materialnummer:	046391
Strahlenart:	Gamma
Bestrahlt am:	23.03.2016
Gemessener Dosiswert [kGy]:	24,23

BGS Beta-Gamma-Service GmbH & Co. KG · Sitz Wühl · Registergericht Köln HRA 16938 · Ust-IdNr.: DE 122 533 721
 PhG BGS Beteiligung GmbH · Sitz Wühl · Registergericht Köln HRB 38648 · Geschäftsführer: Dr. Andreas Ostrowski

Bestrahlungszertifikat - Certificate of irradiation - Certificat d'irradiation

BGS IDEEN PLUS ENERGIE BGS IDEEN PLUS ENERGIE BGS IDEEN PLUS ENERGIE



EN ISO 9001
EN ISO 13485

Figure 65: Certificate of irradiation for DbR #3.

Zertifikat

BGS

IDEEN PLUS ENERGIE

BGS-Auftrags-Nr.: 71607

Chargen-Freigabe:

Zertifikat Nr.: 226871
Seite: 2 / 2

Hamisch Hella, 29.03.2016, 11:50

BGS-Chargen-Nr./Split Nr.: 16011656/0

Bestrahlte Menge:	1 Karton(s)
Ihr Artikel:	Forschungsproben
BGS Materialnummer:	046391
Strahlenart:	Gamma
Bestrahlt am:	23.03.2016
Gemessener Dosiswert [kGy]:	50,27
Chargen-Freigabe:	Hamisch Hella, 29.03.2016, 11:50

BGS-Chargen-Nr./Split Nr.: 16011657/0

Bestrahlte Menge:	1 Karton(s)
Ihr Artikel:	Forschungsproben
BGS Materialnummer:	046391
Strahlenart:	Gamma
Bestrahlt am:	22.03.2016
Gemessener Dosiswert [kGy]:	114,30
Chargen-Freigabe:	Hamisch Hella, 29.03.2016, 11:50

BGS-Chargen-Nr./Split Nr.: 16011660/0


Bestrahlte Menge:	1 Karton(s)
Ihr Artikel:	Forschungsproben
BGS Materialnummer:	046391
Strahlenart:	Gamma
Bestrahlt am:	23.03.2016
Gemessener Dosiswert [kGy]:	250,10
Chargen-Freigabe:	Hamisch Hella, 29.03.2016, 11:50

Dieses Dokument ist ohne Unterschrift gültig.

BGS Beta-Gamma-Service GmbH & Co. KG • Sitz Wahl • Registergericht Köln HRB 16938 • Ust-IdNr. DE 122 533 721
 P/G BGS Beteiligungs GmbH • Sitz Wahl • Registergericht Köln HRB 38648 • Geschäftsführer: Dr. Andreas Ostrowski

Bestrahlungszertifikat - Certificate of irradiation - Certificat d'irradiation

BGS IDEEN PLUS ENERGIE BGS IDEEN PLUS ENERGIE BGS IDEEN PLUS ENERGIE



EN ISO 9001
EN ISO 13485

Figure 65: Certificate of irradiation for DbR #3 (continued).

Acknowledgement

I would like to express my gratitude to Prof. Dr. Reinhard Wirth for his supervision, continuous support and critical discussions about my work and my results throughout the years (and for one or another bet). I would particularly like to thank Dr. Harald Huber for his help and advice and his enthusiasm for my work with *Ignicoccus*. Many thanks also to Prof. Dr. Reinhard Rachel for his critical remarks, which helped to improve the quality of the thesis.

Additionally, I am thankful to PD Dr. Ruth Hemmersbach for her encouragement and her willingness to be available as a second referee and being my SpaceLife mentor.

I would like to give thanks to Dr. Günther Reitz and PD Dr. Christine Hellweg for giving me the opportunity to work in the Radiation Biology Department, to present my work at several international conferences and to attend several summer schools.

Further on, I would particularly like to thank Dr. Petra Rettberg, who gave me the chance to gain an insight into the great topic of Astrobiology with its exciting issues, problems and possibilities. I am also grateful for her growing interest in my work and her increasing support with every year. Thanks for believing in me and my dramatic microbes, even when I did not.

I owe special thanks to Dr. Stefan Leuko and Dr. Kristina Beblo-Vranesevic for continuous support in the lab, fruitful discussions and interesting ideas for new experiments. Furthermore, I would like to thank for conscientious and fast proof-reading activities. In this connection, I thank Dr. Greg Vilks for his kindly proof-reading activities, too.

For the great opportunity to attend “Death by Radiation”, I would like to thank Dr. Ralf Möller. I enjoyed your honesty and our periodical conversations about food and drink and the exchange of favorite recipes.

I additionally thank all colleagues of the Radiation Biology Department for a friendly and humorous working atmosphere throughout the years! Special thanks to Bartos Przybyla and his know-how and the “nasty” questions of a physicist. He made a big contribution in terms of design, implementation and trouble-shooting allowing the “Hot Exposure” experiment to come true.

Furthermore, I would also like to give thanks to the four “inhabitants” of Room 129, namely Simon Barczyk, Maria Bohmeier, Dr. Corinna Panitz and André Parpart. You guys helped me to see the funny side of everything in all kinds of situations.

I owe special thanks to Dr. Elke Rabbow for her open ear to all my questions and problems, and her readiness to get access to every paper I needed. I really appreciate your excitement for *Ignicoccus* and early Life on Earth.

In addition, I am very grateful to Claudia Schmitz, who always listened sympathetically, and helped in word and deed.

I would like to thank Claudia Hahn, that we were able to overcome ups and downs together, having the aim to obtain the doctoral degree always in our minds. Additional thanks goes to Bernd Henschenmacher for his contagious enthusiasm for Astrobiology and habitable planets and moons and his daily motivating words. I furthermore thank Felix “FF” Fuchs for the nice and jolly atmosphere in the office.

Further on, I would like to acknowledge the SpaceLife graduate school (Helmholtz Space Life Sciences Research School) for funding the thesis and providing insights into diverse space-relevant research. As part of SpaceLife, I am very grateful to PD Dr. Christine Hellweg, Dr. Luis Spitta, Anna-Maria Trautmann and Claudia Schmitz.

The “Regensburg International Graduate School of Life Sciences” (RIGeL) from the University Regensburg is also acknowledgement and Prof. Dr. Helga Stan-Lotter for being my RIGeL mentor.

Ich möchte Bartos dafür danken, dass er stets an den Erfolg dieser Arbeit geglaubt hat und mir in den richtigen Momenten die benötigte Unterstützung entgegengebracht hat. Ein ganz besonderer Dank geht an meine Familie und meine Freunde, die mich während dieser 3 Jahre unterstützt haben und mir immer mit gutem Rat und Tat zur Seite standen.